# UNIVERSIDAD AUTÓNOMA DE BAJA CALIFORNIA

INSTITUTO DE INVESTIGACIONES OCEANOLÓGICAS


# RESPUESTAS DE PASTOS MARINOS DE BAJA CALIFORNIA (*PHYLLOSPADIX SCOULERI* Y *PHYLLOSPADIX TORREYI*) AL ESTRÉS TÉRMICO ASOCIADO A OLAS DE CALOR MARINAS

T E S I S

QUE PARA CUBRIR PARCIALMENTE LOS REQUISITOS NECESARIOS PARA OBTENER EL GRADO DE

**DOCTOR EN MEDIO AMBIENTE Y DESARROLLO**

PRESENTA

**MANUEL VIVANCO BERCOVICH**

Ensenada, Baja California, México. Abril de 2023

**RESUMEN**

*Phyllospadix scouleri* y *Phyllospadix torreyi* (o "surfgrasses" por su nombre común en inglés) son los únicos pastos marinos que crecen en zonas expuestas de las costas del Pacífico Norteamericano, con un amplio rango de distribución latitudinal que abarca desde Canadá a Baja California Sur (México). Tienen una elevada productividad que los destaca sobre la mayoría de angiospermas marinas, y ciertas particularidades morfológicas y anatómica que les permiten crecer sobre sustratos rocosos del intermareal azotado por el fuerte hidrodinamismo. Estas especies son también las únicas representantes de pastos marinos en la Reserva de la Biosfera de las Islas del Pacífico Mexicano. Por todo ello, las praderas de *Phyllospadix* son reconocidas por sus importantes valores socio-ecológicos, desde su papel como biofiltros hasta su función como refugio y criadero de especies que sustentan importantes pesquerías. Sin embargo, y en comparación con otras especies de pastos marinos de regiones templadas, existe un gran desconocimiento acerca de su ecología y fisiología básicas, y en consecuencia, de su tolerancia/sensibilidad frente a diferentes estresores naturales o antropogénicos. Al igual que otras especies de pastos marinos en otras regiones del mundo, las praderas de *Phylloxpadix* están sujetas a estresores asociados al cambio climático, como las olas de calor marinas (OCMs). Existen evidencias claras de que las OCMs ya han tenido impactos notables en distintos hábitats costeros de esta región, incluyendo otros tipos de bosques sumergidos. Para el caso de *Phyllospadix*, los reportes son sorprendentemente escasos. Esta tesis, por tanto, tuvo como meta principal la de evaluar las respuestas de *P. scouleri* y *P. torreyi* frente a OCMs bajo distintas aproximaciones experimentales: i) la combinación de OCM con reducción de irradiancia (Capítulo 1), ii) la comparación entre los efectos de una OCM con OCMs repetidas (Capítulo 2),

y iii) la comparación entre OCMs de distinta intensidad (severas vs. extremas) (Capítulo 3). Los efectos de estrés y las respuestas de aclimatación al incremento de temperatura fueron examinados a través de distintos descriptores ecofisiológicos (fotosíntesis, respiración, propriedades bio-ópticas, estrés oxidativo, reservas de carbohidratos, tasas incorporación de nitrato, contenido de nitrógeno y $\delta^{15}N$) y del crecimiento de las hojas. Cabe destacar que la mayoría de estos descriptores fisiológicos han sido evaluados por primera vez para estas especies en este trabajo. De forma general, y en base a los resultados de los tres experimentos, se pudo concluir que i) los efectos negativos de las OCMs en *Phyllospadix* podrían ser intensificados si su ocurrencia coincide con condiciones de baja irradiancia, ii) que la exposición a OCMs consecutivas podría generar un debilitamiento fisiológico progresivo en *Phyllospadix*, iii) que *Phyllospadix* podría tolerar OCMs severas ($T_{máx}$: 25°C) sin mayores alteraciones fisiológicas, mientras que OCMs extremas ($T_{máx}$: 28°C) podrían afectar su fisiología a tal punto de comprometer su crecimiento, y iv) que la inclusión de fases experimentales de recuperación en trabajos de experimentación es crucial para obtener conocimiento robusto acerca de la termo-tolerancia de la planta.

INSTITUTO DE INVESTIGACIONES OCEANOLÓGICAS
DOCTORADO EN MEDIO AMBIENTE Y DESARROLLO

# RESPUESTAS DE PASTOS MARINOS DE BAJA CALIFORNIA (*PHYLLOSPADIX SCOULERI* Y *PHYLLOSPADIX TORREYI*) AL ESTRÉS TÉRMICO ASOCIADO A OLAS DE CALOR MARINAS

T E S I S

QUE PARA CUBRIR PARCIALMENTE LOS REQUISITOS NECESARIOS PARA OBTENER EL GRADO DE

DOCTOR EN MEDIO AMBIENTE Y DESARROLLO

Presenta

MANUEL VIVANCO BERCOVICH

Aprobada por:

Dr. Jose Miguel Sandoval Gil

Dra. Nadine Schubert
Sinodal

Dr. Lázaro Marin Guirao
Sinodal

Dr. Alejandro Cabello Pasini
Sinodal

Dra. Raquel Muñiz Salazar
Sinodal

**AGRADECIMIENTOS**

Esto solamente fue posible porque hay un montón de gente a mi lado, colaborando de distintas maneras, para dar forma, color, contenido, inspiración y alegría a este trabajo. Para empezar, yo no estaría aquí si no fuera el apoyo incondicional y eterno de mi familia, en lo que sea que decida hacer, aunque tenga que irme tan lejos y dejar de vernos por tanto tiempo, gracias Má, Pá, Juli, Gogó y Celia. Quiero agradecer a Jose, mi tutor de tesis - quien tuvo la gran idea de escribir el proyecto y conseguir fondos para el desarrollo de este proyecto - por guiarme en este camino con tanta dedicación, con paso firme, pero sin perder el humor ¡Research! También agradezco a mi comité de tesis (Lázaro, Raquel, Alejandro, Leo, Gabriele y Nadine), que con sus aportes elevaron muchísimo la calidad del trabajo. Un agradecimiento especial a Nadine, la responsable de que me enterara de esta oportunidad, y por recibirnos en Faro, Portugal. Quisiera agradecer a mi compañera Jessica, a quien conocí en una pradera de *Phyllospadix* (dice la leyenda), por compartir cada renglón escrito/borrado, cada buceo, sesión de surf, por inspirarme a seguir adelante, y darle vida a todo esto – no me imagino sin ti. Agradezco al grupo Botánica Marina con sus investigadores, trabajadores, técnicos y estudiantes, por el gran trabajo en equipo, desde las salidas de campo, los experimentos, análisis de laboratorio, y pláticas diversas a lo largo de estos años. Agradezco al Programa de Doctorado Medio Ambiente y Desarrollo, al IIO y a la UABC, con todos sus trabajadores, administrativos, estudiantes, profesores e investigadores, por mantener la "máquina" funcionando y permitir que se puedan desarrollar trabajos como este. Gracias al CONACYT, por la beca que me permitió dedicar exclusivamente al doctorado. Gracias a Ensenada, con todas sus lindas personas y lugares, por abrirme las puertas - y las olas - para lo que ya siento como una segunda casa en este mundo.

**ÍNDICE**

# INTRODUCCIÓN

## 1. Pastos marinos: características, importancia y amenazas

Los pastos marinos son un conjunto de angiospermas monocotiledóneas de naturaleza clonal, cuyos ancestros (hidrófitos terrestres) colonizaron el ambiente marino del Mar de Tetis, 60-90 millones de años atrás (Larkum et al., 2018). En su proceso adaptativo, los pastos marinos ganaron y perdieron genes relacionados con procesos metabólicos y propiedades morfológicas claves para soportar condiciones de inmersión en un medio marino, p. ej., fisiología de osmo- y fotoaclimatación (Olsen et al., 2016; Chen et al. 2021). El éxito evolutivo de estas plantas se refleja en su amplia distribución mundial a lo largo de biorregiones templadas y tropicales (den Hartog, 1970; Short et al., 2007). Actualmente se conocen aproximadamente 65 especies de pastos marinos, las cuales están agrupadas en por lo menos 12 géneros y forman un grupo polifilético dentro del orden Alismatales (den Hartog & Kuo, 2006).

A pesar de que tengan origen en distintas ramas evolutivas, los pastos marinos convergen en un fenotipo relativamente similar, moldeado por las condicionantes ambientales de su hábitat marino (p. ej., de los Santos et al., 2016). La mayor parte de los pastos marinos posee hojas acintadas (cilíndricas u ovaladas, en algunos casos), finas, delgadas y flexibles, las cuales crecen verticalmente y albergan las estructuras fotosintéticas (Kuo & den Hartog, 2006). Estas se extienden a partir de nodos del rizoma, órgano responsable por integrar la estructura clonal de la planta y almacenar la mayor parte de su reserva energética (Kuo & den Hartog, 2006). Las raíces comparten con las hojas la función de asimilar nutrientes, y junto con el rizoma, forman una estructura de anclaje al sustrato (Kuo & den Hartog, 2006). Las flores son pequeñas y la

polinización es hidrófila (Kendrick et al., 2016). Aunque la mayoría de las especies de pastos marinos son dioicas, también hay ejemplares monoicos (p. ej., *Halophila*) y hermafroditas (p. ej., *Posidonia*) (Ackerman, 2006). Además, crecen y se reproducen de manera clonal por medio de la extensión y fragmentación de sus rizomas (Hemminga & Duarte, 2000). Un único clon puede alcanzar dimensiones extraordinarias (centenas de quilómetros cuadrados) y altísima longevidad (miles de años) (p. ej., *Posidonia australis*, Edgeloe et al., 2022).

Los pastos marinos típicamente crecen sobre sustratos arenosos en aguas calmas, sean salinas o salobres. Sin embargo, también existen especies adaptadas a vivir expuestas al intenso oleaje y sobre sustratos rocosos (p. ej., género *Phyllospadix*). Difícilmente son encontrados a profundidades mayores que 50 metros (Esteban et al., 2018), ya que el principal factor limitante para su crecimiento es la disponibilidad de luz (Ralph et al., 2007). Al otro extremo batimétrico, su límite de distribución es el intermareal medio, donde algunas especies logran resistir los periodos de emersión a través de distintas estrategias fisiológicas (p. ej., Ruiz-Montoya et al., 2021).

Las praderas conformadas por pastos marinos son consideradas como sistemas bioingenieros. Estos bosques sumergidos pueden alcanzar enormes extensiones (p. ej., hasta 92.000 $km^2$, Gallagher et al., 2022), y son reconocidas entre los hábitats costeros más valiosos del planeta por los importantes servicios ecosistémicos que proporcionan (Costanza et al., 2014; Unsworth et al., 2022). Entre ellos, se destaca la capacidad que tienen en secuestrar carbono (conocido por "Carbono Azul"), lo que les confiere gran importancia en el contexto del cambio climático (Fourqurean et al., 2012; Macreadie et al., 2021). Además, las praderas de pastos marinos actúan como biofiltros de nutrientes, controlan la erosión costera y sirven de refugio para una variedad

de organismos, inclusive algunos de gran importancia comercial (Barbier et al., 2011; de los Santos et al., 2020).

Por otro lado, hay especies de pastos marinos en riesgo de extinción (Short et al., 2011) y estos ecosistemas están entre los más amenazados del mundo debido a los múltiples estresores a los que están expuestos, tanto en escala local como global (Orth et al., 2006; Waycott et al., 2009). Se estima que aproximadamente el 20% de la cobertura global de pastos marinos se ha perdido en el transcurso del último siglo (Dunic et al., 2021). En gran parte, esto se atribuye a las actividades que impactan directamente a las praderas a través del desarrollo urbano (p. ej., dragados, estructuras portuarias, Erftemeijer & Lewis, 2006), y deterioran la calidad del agua y la disponibilidad de luz (Burkholder et al., 2007; Ralph et al., 2007). A nivel global, el preocupante calentamiento de los océanos se suma a esos estresores (Doney et al. 2012; Nguyen et al., 2021). Particularmente, eventos extremos de aumento regional en la temperatura del agua (olas de calor marinas, OCM) han demostrado tener un impacto muy negativo en praderas de pastos marinos y demás ecosistemas marinos (Smith et al., 2023).

## 2. Efectos de estrés térmico y olas de calor en pastos marinos

### *Respuestas generales de pastos marinos al estrés térmico*

La temperatura es una de las variables ambientales que determinan las dinámicas biológicas/ecológicas de los pastos marinos, e incluso su distribución (Jayathilake & Costello, 2018). Los pastos marinos presentan distintos grados de plasticidad fenotípica frente a las variaciones de la temperatura del agua de mar (Bennet et al., 2021; Pazzaglia et al., 2021). Se sabe que las capacidades de aclimatación y los umbrales de tolerancia (i.e. termo-resistencia)

varían entre especies, pero también de manera intraespecífica, entre poblaciones (ecotipos/genotipos) de distintos regímenes/nichos térmicos (p. ej., Bennet et al., 2022; Dubois et al., 2022). Sin embargo, hay ciertas respuestas que son relativamente comunes en pastos marinos expuestos al calentamiento, las cuales han sido revisadas en la última década por distintos autores (Koch et al., 2013; Duarte et al., 2018; Nguyen et al., 2021).

Por ejemplo, bajo condiciones de estrés térmico, se ha reportado la activación de mecanismos de disipación de energía en forma de calor (por medio del ciclo de deepoxidación de las xantofilas, cuantificada como apagamiento no fotoquímico, o NPQ, por su nomenclatura en inglés), y el empleo de sumideros de electrones alternativos al flujo entre fotosistemas (Repolho et al., 2017; Pazzaglia et al., 2022), lo cual favorece la protección de su maquinaria fotosintética, aparentemente susceptible al daño térmico (Mathur et al., 2014). Por otra parte, como estrategias para minimizar el potencial daño oxidativo causado por estrés térmico, se ha observado en algunos pastos la regulación de la fluidez de las sus membranas celulares mediante la alteración de su composición lipídica, y la eliminación de especies reactivas de oxígeno (EROs) con agentes enzimáticos y no enzimáticos (Tutar et al., 2017). Aspectos claves en la aclimatación a temperaturas elevadas incluyen el uso de estrategias para equilibrar las ganancias y pérdidas de carbono, como la estabilización respiratoria, la mejora del desempeño fotosintético, la movilización de reservas de carbono y los ajustes en la distribución de la biomasa (Marín-Guirao et al., 2018). De forma general, se ha demostrado que incrementos de temperatura pueden estimular la respiración, mientras que la fotosíntesis solo lo hace hasta un umbral específico a partir del cual se inhibe progresivamente (Lee et al., 2007). Ya sea mediante el aumento de la respiración o mediante la disminución de la fotosíntesis, el calentamiento puede reducir la productividad neta de las plantas, induciendo el consumo de reservas de almacenamiento y la

reducción del crecimiento (Collier et al., 2017; Beca-Carretero et al., 2021). Temperaturas elevadas a un nivel extremo, o por periodos prolongados, pueden resultar en desequilibrios severos en el balance metabólico de carbono y, en consecuencia, mortalidad (Collier & Waycott, 2014).

***Olas de calor marinas: proyecciones y potencial de impacto en pastos marinos***

La temperatura superficial del agua de mar podría elevarse gradualmente hasta 4°C para el año 2100, dependiendo de las trayectorias socioeconómicas que seguirán las sociedades futuras (Fox-Kemper et al., 2021). A la par de esta tendencia, se proyecta que la intensidad y frecuencia de ocurrencia de OCMs aumenten drásticamente en las próximas décadas (Oliver et al., 2019; Marin et al., 2021). Las OCMs se definen como eventos de calentamiento anómalo del agua del mar, con por lo menos cinco días de duración, en que la temperatura excede el 90º percentil con respecto a la climatología local de los últimos treinta años (Hobday et al., 2016). Son pocas las OCMs que han alcanzado la categoría "extrema" durante el último siglo, (según la categorización de Hobday et al. (2018)), pero éstas podrían representar hasta el 70% de todas las OCMs a nivel mundial para el año 2100, dependiendo de los escenarios de emisiones (Oliver et al., 2019). Así, las OCMs que ocurrían una sola vez cada cientos o miles de años en el periodo preindustrial podrían convertirse en eventos anuales (Laufkötter et al., 2020). Estas predicciones son alarmantes, ya que las OCMs han causado grandes alteraciones en la estructura y el funcionamiento de las praderas de pastos marinos, e incluso eventos de mortalidad masiva en diversas partes del mundo (Serrano et al., 2021; Smith et al., 2023). El impacto recurrente de OCMs en el Mar Mediterráneo ha sido relacionado con importantes eventos de mortandad en praderas de *Posidonia oceanica*, favoreciendo incluso la expansión de macrófitos exóticos

(Marbà & Duarte 2010; Jordà et al., 2012; Marbà et al., 2014). Este tipo de efectos también se ha documentado en praderas de *Zostera marina* y *Thalassia testudinum* en bahías de California y Florida, en EE. UU. (Johnson et al., 2003; Carlson et al., 2018). Además, los efectos de las OCMs pueden actuar sinérgicamente con otro tipo de estresores, bióticos y abióticos (McMahon et al., 2022). Por ejemplo, la combinación de OCMs con reducciones en la transparencia de la columna de agua indujo el colapso de más de 1000 $km^2$ de praderas de *Amphibolis antartica* y *Posidonia australis* en la costa oeste australiana en 2011 (Hyndes et al., 2016; Kendrick et al. 2019), y pérdidas de hasta un 29% de las praderas de *Z. marina* en Chesapeake Bay, EE. UU. (Moore et al., 2014; Lefcheck et al. 2017).

## 3. Aproximaciones experimentales para el estudio del estrés térmico en pastos marinos

Diversos estudios han examinado las respuestas de pastos marinos al estrés térmico en condiciones experimentales controladas (Tabla 1), la mayoría centrados en plantas adultas de las especies *Zostera marina*, *Posidonia oceanica* y *Cymodocea nodosa*. Algunos han comparado las respuestas al estrés térmico entre especies (p. ej., Campbell et al., 2006; Collier & Waycott, 2014), entre poblaciones con diferentes nichos térmicos (p. ej., diferentes profundidades, Marín-Guirao et al., 2016; diferentes latitudes, Bergmann et al., 2010; Beca-Carretero et al., 2018), o entre tejidos (p. ej., hojas maduras vs. hojas nuevas, Ruocco et al., 2019). Otros autores han examinado la combinación del estrés térmico con otras fuentes de estrés, como eutrofización (p. ej., Mvungi & Pillay, 2019; Ontoria et al., 2019; Pazzaglia et al., 2020), acidificación (p. ej., Egea et al., 2018) o reducción de luz (p. ej., Collier et al., 2011; Costa et al. 2021), o incluso los efectos de la temperatura en la reproducción (p. ej., Marín-Guirao et al., 2019) o en individuos juveniles (p. ej., Niu et al., 2012; Artika et al., 2020). Estudios recientes han explorado el potencial de

generación de memoria de estrés en pastos marinos al ser expuestos a repetidos eventos de calentamiento (p. ej., Nguyen et al., 2020; Pazzaglia et al., 2022).

Los tratamientos experimentales de calentamiento son altamente variables entre estudios. Algunos se han basado en pulsos diarios de alta temperatura con duración de 3h (simulando condiciones de intermareal; Massa et al., 2009), mientras otros han aplicado hasta 90 días de exposición continua (Hernán et al., 2017). En general, estudios enfocados en poblaciones del intermareal aplican tratamientos con temperaturas más elevadas (p. ej., hasta 50°C, Pedersen et al., 2016). La simulación experimental de OCMs se ha realizado de acuerdo con registros de temperatura de las praderas naturales objeto de estudio (p. ej., Franssen et al., 2014), o acorde a proyecciones futuras (p. ej., Ontoria et al., 2019). Aunque escasos, resultan muy interesantes los trabajos que recientemente han discutido la exposición repetida a olas de calor sucesivas en pastos marinos (p. ej., DuBois et al., 2020; Nguyen et al., 2020; Saha et al., 2020; Pazzaglia et al., 2022). Algunos estudios evalúan las respuestas biológicas únicamente durante el tratamiento térmico (p. ej., Chartrand et al., 2018), mientras otros también incluyen un periodo de recuperación en su análisis (Marín-Guirao et al., 2016).

**Tabla I.** Resumen de trabajos que evaluaron las respuestas de pastos frente a incrementos de temperatura en condiciones de laboratorio. La tabla presenta los atributos principales de las praderas donadoras (sitios de colecta) y de los diseños experimentales. Los estudios que incluyen múltiples especies, o poblaciones, fueron divididos en múltiples líneas para resaltar los regímenes térmicos específicos de cada población y los parámetros experimentales.

| Donor meadow´s characteristics | | | | Experimental settings | | | | References |
|---|---|---|---|---|---|---|---|---|
| **Species** | **Location** | **Depth (m)** | **Field reference temperature (°C)** | **Acclimation temperature (°C)** | **Control temperature (°C)** | **Warming treatments (°C)** | **Exposure duration** | |
| *Cymodocea nodosa* | Ria Formosa (Portugal) | Shallow subtidal | Range (Spring): 18 - 30<br>Maximun (Summer): 35 | - | 20 | 40 | 4 d | Costa et al., 2021 |
| *Cymodocea nodosa* | Ria Formosa (Portugal) | ~ 2 | Range (Spring): 18 - 30<br>Maximun (Summer): 35 | 20 | 20 | 28 | 7 d | Deguette et al., 2022 |
| *Cymodocea nodosa* | Isla Grosa (Spain) | 5 | Field condition: 24<br>Maximun (Summer): 28 | 24 | 24 | 32 | 5 d | Marín-Guirao et al., 2016; 2017<br>Tutar et al., 2017 |
| *Cymodocea nodosa* | Isla Grosa (Spain) | 1 - 2 | Field condition: 23<br>Mean (Summer): 25 | 24 | 24 | 28 | 45 d | Marín-Guirao et al., 2018; 2019<br>Beca-Carretero et al., 2018b |
| *Cymodocea nodosa* | Ebro Delta (Spain) | 1 - 2 | Field condition: 25<br>Mean (Summer): 30 | 25 | 25 | 29 | 45 d | Marín-Guirao et al., 2018; 2019<br>Beca-Carretero et al., 2018b |
| *Cymodocea nodosa* | Gulf of Naples (Italy) | 8-10 | Field condition: ~26<br>Range (Annual): 13 - 28 | 26 | 26 | 32 | 12 d | Nguyen et al., 2021 |
| *Cymodocea nodosa* | Alfacs Bay (Spain) | 0.5 | Field condition: 19.5<br>Maximum (Summer): 33 | 20 | 20 | 30 and 35 | 15 d | Ontoria et al., 2019b |
| *Cymodocea nodosa* | Alfacs Bay (Spain) | 0.5 | Field condition: 19.5<br>Maximum (Summer): 33 | 20 | 20 | 30 and 35 | 7 d | Ontoria et al., 2019b |
| *Cymodocea nodosa* | Cadiz (Spain) | 1 - 2 | - | 20 | 22 | 26 | 28 d | Egea et al., 2018 |
| *Cymodocea rotundata* | Fantome Island (Australia) | Intertidal | Range (Annual): 20 - 35<br>Low tide spikes: < 43 | - | 20.9 - 22.7 | 35, 40 and 43 | 6 d<br>(2.5 h daily heat shocks) | Collier & Waycott, 2014 |
| *Cymodocea rotundata* | Green Island (Australia) | Mid-intertidal - shallow subtidal | Field condition: 26 | 26 | 26 | 35, 40 and 45 | 5 d (4h daily heat shocks) | Campbell et al., 2006 |
| *Cymodocea serrulata* | Changuu Island (Tanzania) | 0.5 - 4 | Field condition: 26.4 - 28.4 | 26 | 26 | 31 | 32 d | Viana et al., 2020 |
| *Cymodocea serrulata* | Green Island (Australia) | Shallow subtidal | Field condition: 26 | 26 | 26 | 35, 40 and 45 | 5 d (4h daily heat shocks) | Campbell et al., 2006 |
| *Enhalus acoroides* | Kimberley (Australia) | Intertidal (Macro-tidal region) | Field condition: 27- 37<br>Maximum (Springtide): 40 | 25 | - | 25, 30, 35, 40, 45 and 50 | 2 - 3 h | Pedersen et al., 2016 |
| *Enhalus acoroides (seedlings)* | Barrang Lompo Island (Indonesia) | 1 - 3 | Range (Annual): 26 - 32 | - | 26 | 31 | 32 d | Artika et al., 2020 |
| *Halodule uninervis* | Magnetic Island (Australia) | Intertidal | Field condition: 27<br>Maximun (Summer): ~30 | 27 | 27 | 30 and 33 | 34 d | Collier et al., 2011 |
| *Halodule uninervis* | Fantome Island (Australia) | Intertidal | Range (Annual): 20 - 35<br>Low tide spikes: < 43 | - | 20.9 - 22.7 | 35, 40 and 43 | 6 d<br>(2.5 h daily heat shocks) | Collier & Waycott, 2014 |
| *Halodule uninervis* | Green Island (Australia) | Mid-intertidal - shallow subtidal | Field condition: 26 | 26 | 26 | 35, 40 and 45 | 5 d (4h daily heat shocks) | Campbell et al., 2006 |
| *Halodule wrightii* | Porjoe Key (USA) | - | Field condition: 28 - 29 | - | - | 28-29, 30-31, 32-33 and 34-35 | 38 d | Koch et al., 2007 |
| *Halophila decipiens* | Green Island (Australia) | 17 | Field condition (Spring): 26 | 26 | 26 | 30 | 28 d | Chartrand et al., 2018 |
| *Halophila ovalis* | Fantome Island (Australia) | Intertidal | Range (Annual): 20 - 35<br>Low tide spikes: < 43 | - | 20.9 - 22.7 | 35, 40 and 43 | 6 d<br>(2.5 h daily heat shocks) | Collier & Waycott, 2014 |
| *Halophila ovalis* | Swan-Canning Estuary (Australia) | < 2 | Field condition: 23<br>Range (Summer): 22 - 24 | - | - | 20, 24, 28, 31 and 34 | 1 d | Ontoria et al., 2020 |
| *Halophila ovalis* | Peel Harvey Estuary (Australia) | < 0.5 | Field condition: 20<br>Range (Summer): 21 - 23 | - | 24 | 30 | 13 d | Ontoria et al., 2020 |
| *Halophila ovalis* | Green Island (Australia) | Upper intertidal - deep subtidal | Field condition: 26 | 26 | 26 | 35, 40 and 45 | 5 d (4h daily heat shocks) | Campbell et al., 2006 |

| | | | | | | | | |
|---|---|---|---|---|---|---|---|---|
| *Halophila spinulosa* | Bowen (Australia) | 10 | Field condition (Spring): 26 | 26 | 26 | 30 | 28 d | Chartrand et al., 2018 |
| *Halophila stipulacea* | Changuu Island (Tanzania) | 0.5 - 4 | Field condition: 26.4 - 28.4 | 26 | 26 | 31 | 32 d | Viana et al., 2020 |
| *Nanozostera noltii* | Hals (Denmark) | - | Field condition: 14<br>Range (Summer): 13 - 22 | 14 - 19 | 19 | 26 | 21 d | Franssen et al., 2014 |
| *Nanozostera noltii* | Gabicce Mare (Italy) | - | Field condition: 14<br>Range (Summer): 21 - 29 | 14 - 19 | 19 | 26 | 21 d | Franssen et al., 2014 |
| *Phyllospadix scouleri* | Isla Todos Santos (Mexico) | 5 | Field condition: 18<br>Range (Annual): 15 - 21 | 18 | 18 | 24 + 24 | 7 + 7 d | This study (Experiment 2) |
| *Phyllospadix scouleri* | San Juanico (Mexico) | - | Field condition: 22 | 22 | - | 20, 22, 24, 26 and 28 | 15 d | Venegas, 2019 |
| *Phyllospadix scouleri* | Bahía Magdalena (Mexico) | - | Field condition: 22 | 22 | - | 20, 22, 24, 26 and 28 | 15 d | Venegas, 2019 |
| *Phyllospadix scouleri* | Conquista Agraria (Mexico) | - | Field condition: 22 | 22 | - | 20, 22, 24, 26 and 28 | 15 d | Venegas, 2019 |
| *Phyllospadix scouleri* | Isla Todos Santos (Mexico) | 5 | Field condition: 18.5<br>Range (Annual): 15 - 21<br>Past MHWs: 25 | 18 ± 1.5 | 18 ± 1.5 | 23.5 ± 1.5 and 26.5 ± 1.5 | 7 d | This study (Experiment 3) |
| *Phyllospadix torreyi* | Ensenada (Mexico) | 5 | Field condition: 16<br>Range (Annual): 15 - 21 | 16 | 16 | 25 | 7 d | This study (Experiment 1) |
| *Phyllospadix torreyi* | Ensenada (Mexico) | 4 - 5 | Field condition: 18<br>Range (Annual): 15 - 21 | 18 | 18 | 40 | 3 h | Ruiz-Montoya et al.,2021 |
| *Posidonia australis* | Port Stephens (Australia) | 0.7 | Field condition: 25<br>Range (Annual): 17 - 26 | 26 | 26 | 29 + 32 | 6 + 9 d | Nguyen et al., 2020 |
| *Posidonia australis* | Port Stephens (Australia) | 0.7 | Field condition: 25<br>Range (Annual): 17 - 26 | 26 | 26 | 32 | 9 d | Nguyen et al., 2020, 2021 |
| *Posidonia oceanica* | Bay of Palma (Spain) | - | Field condition: 24 - 25<br>Maximun (Summer): 28 | - | 25 | 30 | 21 d | Hendriks et al., 2017 |
| *Posidonia oceanica* | Isla Grosa (Spain) | 5 | Field condition: 24<br>Maximun (Summer): 28 | 24 | 24 | 32 | 5 d | Marín-Guirao et al., 2016; 2017<br>Tutar et al., 2017 |
| *Posidonia oceanica* | Isla Grosa (Spain) | 25 | Field condition: 24<br>Maximun (Summer): 27 | 24 | 24 | 32 | 5 d | Marín-Guirao et al., 2016; 2017<br>Tutar et al., 2017 |
| *Posidonia oceanica* | Cala Montgó (Spain) | 5 - 7 | Field condition: 19.5<br>Mean (Summer): 23 | 23 | 23 | 27 | 45 d | Marín-Guirao et al., 2018; 2019<br>Beca-Carretero et al., 2018b |
| *Posidonia oceanica* | Isla Grosa (Spain) | 5 - 7 | Field condition: 23<br>Mean (Summer): 25 | 25 | 25 | 29 | 45 d | Marín-Guirao et al., 2018; 2019<br>Beca-Carretero et al., 2018b |
| *Posidonia oceanica* | Gulf of Naples (Italy) | 5-6 | Field condition: ~26<br>Range (Annual): 13 - 28 | 26 | 26 | 32 | 12 d | Nguyen et al., 2021 |
| *Posidonia oceanica* | Cala Montgo (Spain) | 8 | Field condition: ~20<br>Range (Annual): 12-25<br>Past MHWs: 28 | 20 | 20 | 30 and 35 | 5 d | Ontoria et al., 2019a |
| *Posidonia oceanica* | Gulf of Pozzuoli (Italy) | 7 - 9 | Field condition: 21<br>Maximun (Summer): 28-30<br>Average (Summer): 24-25 | 21 | 24 | 30 | 35 d | Pazzaglia et al., 2020; 2022a |
| *Posidonia oceanica* | Island of Ischia (Italy) | 7 - 9 | Field condition: 21<br>Maximun (Summer): 28-30<br>Average (Summer): 24-25 | 21 | 24 | 30 | 35 d | Pazzaglia et al., 2020; 2022a |
| *Posidonia oceanica* | Gulf of Naples (Italy) | 8 - 10 | Field condition: 25<br>Range (Annual): 14 - 29 | 25 | 25 | 34 | 7 d | Ruocco et al., 2019 |
| *Posidonia oceanica* | Isla Grosa (Spain) | 5 | Field condition: 18<br>Range (Annual): 14 - 26 | 18 - 20 | 20 | 24, 28 and 32 | 28 d | Traboni et al., 2018 |
| *Posidonia oceanica* | Cala Millor (Spain) | 6 - 7 | Field condition: 23 | 23 | - | 26, 27, 28.5, 30, 31.2 and 31.8 | 50 d | García et al., 2012 |
| *Posidonia oceanica (seedlings)* | Mazarrón Bay (Spain) | - | Maximun (Summer): 27-29 | 21 | - | 27, 29, 31 and 33 | 3 h | Guerrero-Meseguer et al., 2017 |

| | | | | | | | | |
|---|---|---|---|---|---|---|---|---|
| *Posidonia oceanica (seedlings)* | Mazarrón Bay (Spain) | - | Maximun (Summer): 27-29 | 21 | - | 27, 29, 31 and 33 | 30 d | Guerrero-Meseguer et al., 2017 |
| *Posidonia oceanica (seedlings)* | Marsala (Italy) | - | Range (Summer): 24 - 26 | 26 | 26 | 30.5 + 32 | 11 + 14 d | Pazzaglia et al., 2022b |
| *Posidonia oceanica (seedlings)* | Marsala (Italy) | - | Range (Summer): 24 - 26 | 26 | 26 | 32 | 14 d | Pazzaglia et al., 2022b |
| *Posidonia oceanica (seedlings)* | Palma Bay (Spain) | - | Average (Summer): 25 | 21 | 25 | 27 and 29 | 90 d | Hernán et al., 2017 |
| *Posidonia oceanica (seedlings)* | Mallorca (Spain) | - | Average (Summer): 25 | 20 | 25 | 27 and 29 | 90 d | Pereda-Briones et al., 2019 |
| *Syringodium isoetifolium* | Green Island (Australia) | Shallow - deep subtidal | Field condition: 26 | 26 | 26 | 35, 40 and 45 | 5 d (4h daily heat shocks) | Campbell et al., 2006 |
| *Thalassia hemprichii* | Kimberley (Australia) | Intertidal (Macro-tidal region) | Field condition: 27- 37<br>Maximum (Springtide): 40 | 25 | - | 25, 30, 35, 40, 45 and 50 | 2 - 3 h | Pedersen et al., 2016 |
| *Thalassia hemprichii* | Changuu Island (Tanzania) | 0.5 - 4 | Field condition: 26.4 - 28.4 | 26 | 26 | 31 | 32 d | Viana et al., 2020 |
| *Thalassia hemprichii* | Green Island (Australia) | Mid-intertidal - shallow subtidal | Field condition: 26 | 26 | 26 | 35, 40 and 45 | 5 d (4h daily heat shocks) | Campbell et al., 2006 |
| *Thalassia hemprichii* | Fantome Island (Australia) | Intertidal | Range (Annual): 20 - 35<br>Low tide spikes: < 43 | - | 20.9 - 22.7 | 35, 40 and 43 | 6 d<br>(2.5 h daily heat shocks) | Collier & Waycott, 2014 |
| *Thalassia testudinum* | Green Mangrove Key (USA) | - | Field condition: 28 - 29 | - | - | 28-29, 30-31, 32-33 and 34-35 | 38 d | Koch et al., 2007 |
| *Zostera capensis* | Langebaan Lagoon (South Africa) | - | Field condition: 18 | 15.5 | 18 | 24 and 30 | 35 d | Mvungi & Pillay, 2019 |
| *Zostera capensis* | Langebaan Lagoon (South Africa) | - | Average (Summer): 24<br>Maximum (Summer): 30 | 20 | 24 | 30 | 28 d | Lawrence & Bolton, 2022 |
| *Zostera capricorni* | Cairns Harbour (Australia) | Upper intertidal - shallow subtidal | Field condition: 26 | 26 | 26 | 35, 40 and 45 | 5 d (4h daily heat shocks) | Campbell et al., 2006 |
| *Zostera japonica* | Changdao (China) | 1 2 | Field condition: 20 | 20 | - | 20, 24, 28 and 32 | 4 h | Zhang et al., 2017 |
| *Zostera marina* | Kobbe Fjord (Greenland) | 2 - 3 | Range (Summer): 8.5 - 10 | 5 | - | 10, 15, 20, 25 and 28 | 14 - 15 d | Beca-Carretero et al., 2018 |
| *Zostera marina* | Kapisillit (Greenland) | 2 - 3 | Range (Summer): 11.6 - 15 | 5 | - | 10, 15, 20, 25 and 28 | 14 - 15 d | Beca-Carretero et al., 2018 |
| *Zostera marina* | Århus Bay (Dennmark) | 1 | Range (Summer): 18 - 22 | 15 | - | 10, 15, 20, 25 and 28 | 14 - 15 d | Beca-Carretero et al., 2018 |
| *Zostera marina* | Finavarra (Ireland) | 2 - 3 | Field condition (Spring): 11 | 11 | - | 6, 12, 16, 20, and 24 | 15 - 16 d | Beca-Carretero et al., 2021 |
| *Zostera marina* | Finavarra (Ireland) | 2 - 3 | Field condition (Summer): 17 | 17 | - | 6, 12, 16, 20, and 24 | 15 - 16 d | Beca-Carretero et al., 2021 |
| *Zostera marina* | Finavarra (Ireland) | 2 - 3 | Field condition (Autumm): 11 | 11 | - | 6, 12, 16, 20, and 24 | 15 - 16 d | Beca-Carretero et al., 2021 |
| *Zostera marina* | Finavarra (Ireland) | 2 - 3 | Field conditions (Winter): 6 | 6 | - | 6, 12, 16, 20, and 24 | 15 - 16 d | Beca-Carretero et al., 2021 |
| *Zostera marina* | Doverodde (Denmark) | 1.5 - 3 | Field condition (Spring): 14<br>Maximun (Summer): < 26 | 19 | 19 | 26 | 30 d | Bergmann et al., 2010 |
| *Zostera marina* | Ebeltoft (Denmark) | 1.5 - 3 | Field condition (Spring): 14<br>Maximun (Summer): < 26 | 19 | 19 | 26 | 30 d | Bergmann et al., 2010 |
| *Zostera marina* | Gabicce Mare (Italy) | 1.5 - 3 | Field condition (Spring): 14<br>Maximun (Summer): > 26 | 19 | 19 | 26 | 30 d | Bergmann et al., 2010 |
| *Zostera marina* | Bodega Harbor (USA) | 0.25 | Average (Summer): 13<br>Past MHWs: 14.9 - 17.4 | - | 13.7 + 13.5 | 15.4 + 16.7 | 45 + 40 d | Dubois et al., 2020 |

| | | | | | | | | |
|---|---|---|---|---|---|---|---|---|
| *Zostera marina* | Bodega Harbor (USA) | 0.25 | Average (Summer): 13<br>Past MHWs: 14.9 - 17.4 | - | 13.5 | 16.7 | 40 d | Dubois et al., 2020 |
| *Zostera marina* | Hals (Denmark) | - | Field condition: 14<br>Range (Summer): 13 - 22 | 14 - 19 | 19 | 26 | 21 d | Franssen et al., 2014 |
| *Zostera marina* | Gabicce Mare (Italy) | - | Field condition: 14<br>Range (Summer): 21 - 29 | 14 - 19 | 19 | 26 | 21 d | Franssen et al., 2014 |
| *Zostera marina* | Gals Klint (Denmark) | 1.5 | Field condition: 8.4 -15.7<br>Mean (Summer): 18 | - | 18 | 21, 27 | 21 d | Höffle et al., 2011 |
| *Zostera marina* | Bodega Bay (USA) | - | Range (Summer): 14 - 15<br>Maximum (Summer): 17 - 18 | ~ 13 - 17 | ~ 12 - 20 | ~ 18 - 25 | 35 d | Reynolds et al., 2016 |
| *Zostera marina* | Changdao (China) | 1 | Maximum (Summer): 25 | 18 | 25 | 30 | 3 h | Yang et al., 2018 |
| *Zostera marina* | Doverodde (Denmark) | 1.5 - 3 | Field condition: 12 - 16<br>Average (Summer): 19<br>Past MHW: 25 | 14 - 19 | 19 | 25 | 21 d | Winters et al., 2011 |
| *Zostera marina* | Ebeltoft (Denmark) | 1.5 - 3 | Field condition: 12 - 16<br>Average (Summer): 19<br>Past MHW: 25 | 14 - 19 | 19 | 25 | 21 d | Winters et al., 2011 |
| *Zostera marina* | Gabicce Mare (Italy) | 1.5 - 3 | Field condition: 12 - 16<br>Average (Summer): 19<br>Past MHW: 25 | 14 - 19 | 19 | 25 | 21 d | Winters et al., 2011 |
| *Zostera marina* | Sanggou Bay (China) | - | Field condition: 15 | 15 | 20 | 26, 28, 30, 31 and 32 | 7 d | Gao et al., 2017 |
| *Zostera marina* | Sanggou Bay (China) | 1 2 | Field condition: 16 | 16 | 16 | 32 | 2 d | Gao et al., 2019 |
| *Zostera marina (seedlings)* | Lidao Bay (China) | - | - | 20 | - | 10, 15, 20, 25 and 30 | 30 d | Niu et al., 2012 |
| *Zostera marina (seedlings)* | Lidao Bay (China) | - | - | 20 | - | 10 ± 2, 15 ± 2, 20 ± 2, 25 ± 2 and 30 ± 2 | 30 d | Niu et al., 2012 |
| *Zostera muelleri* | Magnetic Island (Australia) | Intertidal | Field condition: 27<br>Maximun (Summer): ~30 | 27 | 27 | 30 and 33 | 34 d | Collier et al., 2011 |
| *Zostera muelleri* | Church Point (Australia) | 0.7 | Field condition: 25<br>Range (Annual): 17 - 26 | 26 | 26 | 29 + 32 | 6 + 9 d | Nguyen et al., 2020 |
| *Zostera muelleri* | Church Point (Australia) | 0.7 | Field condition: 25<br>Range (Annual): 17 - 26 | 26 | 26 | 32 | 9 d | Nguyen et al., 2020, 2021 |
| *Zostera muelleri* | Lake Macquarie (Australia) | Shallow subtidal | Range (Annual): 12 - 33 | 18 - 24 | - | 24, 27, 30 and 32 | 90 d | York et al., 2013 |
| *Zostera noltii* | Ria Formosa (Portugal) | Upper intertidal | Maximun (Summer): 36 - 38 | - | - | 35, 37, 39 and 41 | 22 d<br>(3h daily heat shocks) | Massa et al., 2009 |
| *Zostera noltii* | Ria Formosa (Portugal) | Lower intertidal | Maximun (Summer): 36 - 38 | - | - | 35, 37, 39 and 41 | 22 d<br>(3h daily heat shocks) | Massa et al., 2009 |
| *Zostera noltii* | Caldeira de Tróia (Portugal) | - | Field condition: 18 | 18 | 18 | 22 | 30 d | Repolho et al., 2017 |

## 4. *Phyllospadix* spp. y olas de calor marinas en Baja California

A lo largo de la Península de Baja California, sobre los biodiversos fondos marinos rocosos de su costa expuesta al Océano Pacífico, se distinguen las extensas praderas de *Phyllospadix* (*Phyllospadix torreyi* y *Phyllospadix scouleri*) (Fig. 1A, B). Parte de las praderas queda en

emersión durante mareas vivas (Fig. 1C), pero la mayor densidad y cobertura se encuentran en el submareal, extendiéndose hasta los ~7 m de profundidad (Garcia-Pantoja et al., 2020). Se distribuyen desde Alaska (*P. torreyi* desde la Isla de Vancouver) hasta Baja California Sur (México), y son los únicos pastos marinos presentes en la Reserva de la Biósfera Islas del Pacífico de Baja California (RBIPBC) (Fig. 1H). Notables bioingenieros, estos pastos marinos regulan importantes procesos fisicoquímicos y biológicos en su hábitat (Shelton, 2010), donde diversos organismos marinos se refugian y alimentan (p. ej., Guzmán-del Proo et al., 1991; Moulton & Hacker, 2011). Destacan entre otros pastos marinos por su elevada productividad (6000 g PS $m^{-2}$, Garcia-Pantoja et al., 2020), y alta capacidad de fijación de carbono (hasta 1700 mol $CO_2$ $m^{-2}$ $dia^{-1}$, Garcia-Pantoja et al., 2020). También son los únicos pastos marinos capaces de colonizar sustratos rocosos expuestos al oleaje (Cooper & McRoy, 1988), por lo que se les adjudicó el nombre común de *surfgrass*, en inglés.

La costa de Baja California ha sido azotada por una serie de intensas OCMs en los últimos años (Bond et al., 2015; Sen Gupta et al. 2020, Wei et al. 2021), que han ocasionado grandes impactos en la biota marina (Smith et al., 2023), incluyendo bosques de macroalgas (Arafeh-Dalmau et al., 2019; Umanzor et al., 2021; Michaud et al., 2022). Un evento excepcionalmente duradero e intenso, llamado "The Blob", se registró como varias OCMs largas consecutivas (> 100 días) que aumentaron la temperatura de la superficie del mar hasta + 7°C y profundizaron la termoclina hasta más de 50 m de profundidad, lo cual desencadenó cambios biogeoquímicos y ecológicos importantes en el entorno marino costero (Zaba & Rudnick et al. 2016; Dorantes-Gilardi & Rivas 2019). Los posibles efectos en las praderas de *surfgrass* son poco conocidos. Se reportaron potenciales pérdidas cerca de su límite de distribución, en Baja California Sur, donde praderas del intermareal desaparecieron después del paso de OCMs y huracanes (Venegas, 2019; Pedraza et

al., 2021). Menge et al. (2020) detectaron una posible correlación positiva entre el crecimiento de *P. scouleri* con la temperatura del agua en el intermareal de Oregon y California (EE. UU.), pero durante un período en que no hubo registro de OCMs intensas. Los escasos estudios experimentales con *Phyllospadix* spp. sugieren que su crecimiento y supervivencia podrían verse comprometidos bajo condiciones de temperaturas elevadas (Drysdale & Barbour, 1975; Venegas, 2019).

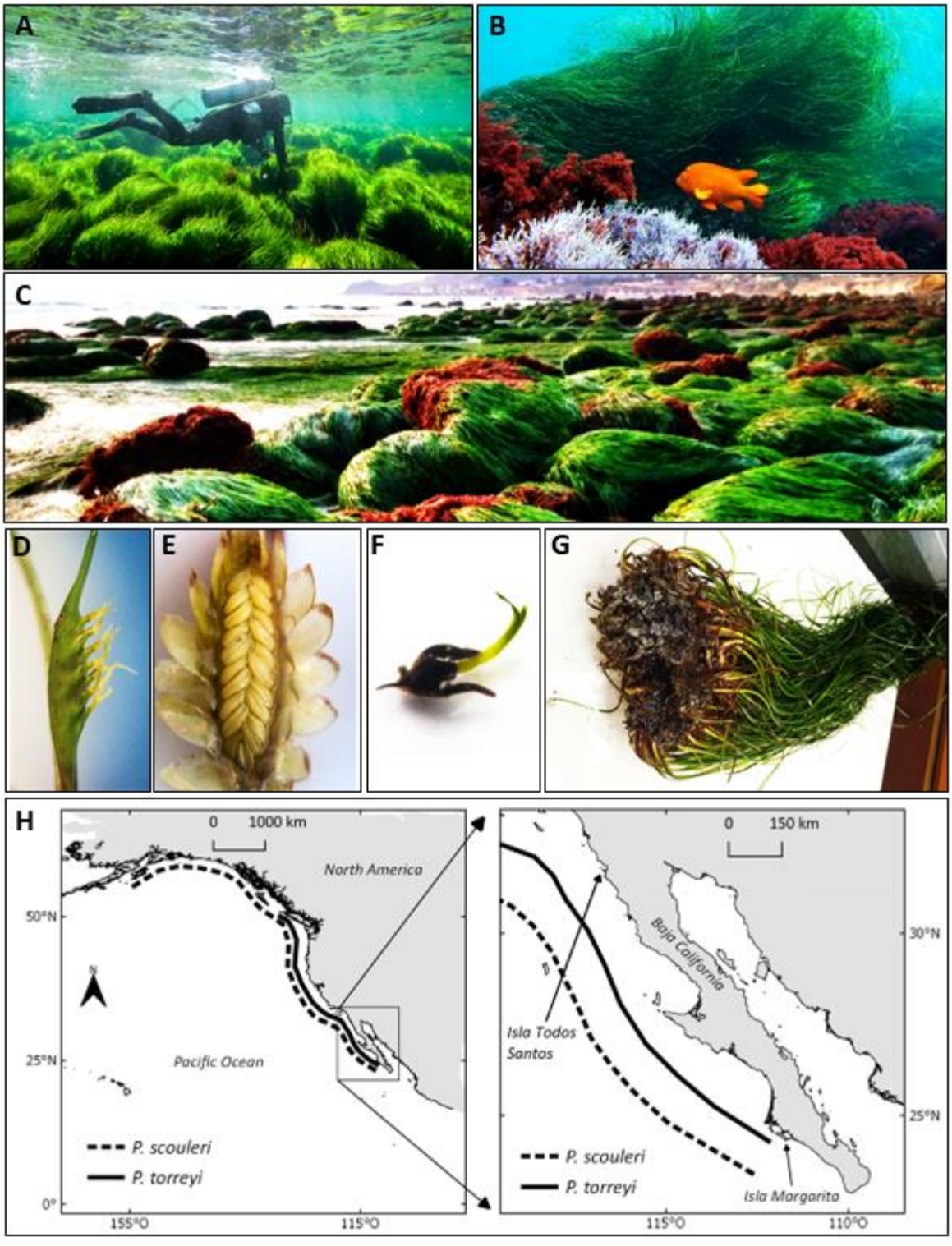
A
B
C
D
E
F
G
H
0 1000 km
North America
50°N
25°N
0°
Pacific Ocean
P. scouleri
P. torreyi
155°O
115°O
0 150 km
Baja California
30°N
25°N
Isla Todos Santos
Isla Margarita
115°O
110°O

**Figura 1.** Las praderas mixtas de *Phyllospadix torreyi* y *Phyllospadix scouleri* son importantes componentes biológicos de la zona submareal (A, B) e intermareal (C) de la costa oeste de la Península de Baja California. Son angiospermas dioicas, que producen inflorescencias femeninas (D) y masculinas (E), y semillas (F). Sus robusto sistemas rizomáticos que segregan compuestos mucilaginosos les permiten adherirse al sustrato rocoso con fuerza, y soportar el envite de las olas (G). Se distribuyen a lo largo de la costa oeste Norteamérica, incluyendo reservas marinas como el Área Natural Protegida de la Isla de Todos Santos (H). Mapa modificado de Phillips (1979) y Ramírez-García et al. (2002).

## 5. Objetivos de esta tesis

Como una de las múltiples manifestaciones del cambio climático en los océanos, la creciente frecuencia e intensidad de las olas de calor marinas está alterando la estructura y funcionalidad de los ecosistemas marinos globalmente, incluyendo a los formados por pastos marinos. Los efectos de estos fenómenos son aún desconocidos para los pastos marinos del género *Phyllospadix,* los cuales forman ecosistemas de gran valor socio-ecológico a lo largo de las costas rocosas del Pacífico Norteamericano. Por lo tanto, esta tesis tiene por objetivo general examinar los potenciales impactos de las OCMs en la fisiología y el crecimiento de *P. torreyi* y *P. scouleri*.

Para esto, se llevaron a cabo tres experimentos de mesocosmos en las instalaciones del Instituto de Investigaciones Oceanológicas de la Universidad Autónoma de Baja California (IIO/UABC, Ensenada, México). En estos experimentos se expusieron las plantas a simulaciones de OCMs con diferentes características representativas de la ocurrencia de estos eventos en Baja California (ver Tabla 2). Las respuestas de estrés térmico y/o de mecanismos de termo-aclimatación se examinaron a nivel fisiológico y vegetativo. La tesis está estructurada en tres capítulos, en

formato de artículo científico. En el **Capítulo I** se evalúan los efectos de una OCM, reducción de irradiancia, y la interacción de ambos factores sobre *Phyllospadix torreyi*. En el **Capítulo II** se comparan las respuestas de *Phyllospadix scouleri* frente a la exposición única o repetida a OCMs, incluyendo períodos de recuperación. En el **Capítulo III**, se comparan los efectos de OCMs con distintas intensidades (severas vs. extremas) en el desempeño ecofisiológico de *P. scouleri* y en su capacidad de recuperación.

**Tabla II.** Características generales y descriptores biológicos analizados en los tres experimentos que se llevaron a cabo para la elaboración de esta tesis.

| | **Experimento 1 (Capítulo 1)** | **Experimento 2 (Capítulo 2)** | **Experimento 3 (Capítulo 3)** |
|---|---|---|---|
| *Tema general* | OCM + Irradiancia reducida | OCMs consecutivas | OCMs más intensas |
| *Especie utilizada* | *P. torreyi* | *P. scouleri* | *P. scouleri* |
| *Pradera donadora* | Punta Morro,<br>3 m de profundidad | Isla Todos Santos,<br>5 m de profundidad | Isla Todos Santos,<br>5 m de profundidad |
| *Duración total del experimento* | 7 días | 39 días | 27 días |
| *Temperatura promedio de la OCM* | 25°C | 24°C | 23.5°C<br>26.5°C |
| *Temperatura máxima de la OCM* | 25°C | 24°C | 25°C<br>28°C |
| *Temperatura del control* | 16°C | 18°C | 18.5°C ± 1.5°C |
| *OCMs consecutivas* | | ✓ | |
| *Periodos de recuperación* | | ✓ | ✓ |
| *--- Descriptores analizados ---* | | | |
| *Descriptores fotosintéticos y respiración (derivados de curvas PE)* | ✓ | ✓ | ✓ |
| *Descriptores fotosintéticos derivados de la Fluorescencia de Chl* | ✓ | ✓ | ✓ |

| | | | |
|---|---|---|---|
| *a* | | | |
| *Pigmentos (Clorofilas a y b y carotenoides)* | ✓ | ✓ | ✓ |
| *Contenido e incorporación de nitrógeno* | | ✓ | |
| *Contenido total de fenoles* | ✓ | ✓ | ✓ |
| *Capacidad antioxidante total* | ✓ | ✓ | ✓ |
| *Peroxidación lipídica* | | ✓ | ✓ |
| *Contenido en carbohidratos no estructurales* | ✓ | ✓ | ✓ |
| *Productividad diaria* | ✓ | ✓ | ✓ |
| *Crecimiento foliar relativo* | ✓ | ✓ | ✓ |

## 6. Referencias

Ackerman, J., 2006. Sexual Reproduction of Seagrass: Pollination in the Marine Context, in: Seagrass: Biology, Ecology and Conservation. Springer, pp. 89–109.

Arafeh-Dalmau, N., Montaño-Moctezuma, G., Martínez, J.A., Beas-Luna, R., Schoeman, D.S., Torres-Moye, G., 2019. Extreme marine heatwaves alter kelp forest community near its equatorward distribution limit. Front. Mar. Sci. 6, 499. https://doi.org/10.3389/fmars.2019.00499

Artika, S.R., Ambo-Rappe, R., Teichberg, M., Moreira-Saporiti, A., Viana, I.G., 2020. Morphological and physiological responses of *Enhalus acoroides* seedlings under varying temperature and nutrient treatment. Front. Mar. Sci. 7.

Barbier, E.B., Hacker, S.D., Kennedy, C., Koch, E.W., Stier, A.C., Silliman, B.R., 2011. The value of estuarine and coastal ecosystem services. Ecol. Monogr. 81, 169–193. https://doi.org/10.1890/10-1510.1

Beca-Carretero, P., Azcárate-García, T., Julia-Miralles, M., Stanschewski, C.S., Guihéneuf, F., Stengel, D.B., 2021. Seasonal acclimation modulates the impacts of simulated warming and light reduction on temperate seagrass productivity and biochemical composition. Front. Mar. Sci. 8.

Beca-Carretero, Pedro, Guihéneuf, F., Marín-Guirao, L., Bernardeau-Esteller, J., García-Muñoz, R., Stengel, D.B., Ruiz, J.M., 2018. Effects of an experimental heat wave on fatty acid

composition in two Mediterranean seagrass species. Mar. Pollut. Bull., Securing a future for seagrass 134, 27–37. https://doi.org/10.1016/j.marpolbul.2017.12.057

Beca-Carretero, P., Olesen, B., Marbà, N., Krause-Jensen, D., 2018. Response to experimental warming in northern eelgrass populations: comparison across a range of temperature adaptations. Mar. Ecol. Prog. Ser. 589, 59–72. https://doi.org/10.3354/meps12439

Bennett, S., Alcoverro, T., Kletou, D., Antoniou, C., Boada, J., Buñuel, X., Cucala, L., Jorda, G., Kleitou, P., Roca, G., Santana-Garcon, J., Savva, I., Vergés, A., Marbà, N., 2022. Resilience of seagrass populations to thermal stress does not reflect regional differences in ocean climate. New Phytol. 233, 1657–1666. https://doi.org/10.1111/nph.17885

Bennett, S., Vaquer-Sunyer, R., Jorda, G., Forteza, M., Roca, G., Marbà, N., 2021. Thermal performance reflects evolutionary legacies of seaweeds and seagrasses across a regional climate gradient (preprint). In Review. https://doi.org/10.21203/rs.3.rs-228005/v1

Bergmann, N., Winters, G., Rauch, G., Eizaguirre, C., Gu, J., Nelle, P., Fricke, B., Reusch, T.B.H., 2010. Population-specificity of heat stress gene induction in northern and southern eelgrass *Zostera marina* populations under simulated global warming: *Zostera* gene expression under heat stress. Mol. Ecol. 19, 2870–2883. https://doi.org/10.1111/j.1365-294X.2010.04731.x

Bond, N.A., Cronin, M.F., Freeland, H., Mantua, N., 2015. Causes and impacts of the 2014 warm anomaly in the NE Pacific: 2014 warm anomaly in the ne pacific. Geophys. Res. Lett. 42, 3414–3420. https://doi.org/10.1002/2015GL063306

Burkholder, J.M., Tomasko, D.A., Touchette, B.W., 2007. Seagrasses and eutrophication. J. Exp. Mar. Biol. Ecol. 350, 46–72. https://doi.org/10.1016/j.jembe.2007.06.024

Campbell, S.J., McKenzie, L.J., Kerville, S.P., 2006. Photosynthetic responses of seven tropical seagrasses to elevated seawater temperature. J. Exp. Mar. Biol. Ecol. 330, 455–468. https://doi.org/10.1016/j.jembe.2005.09.017

Carlson, D.F., Yarbro, L.A., Scolaro, S., Poniatowski, M., McGee-Absten, V., Carlson, P.R., 2018. Sea surface temperatures and seagrass mortality in Florida Bay: Spatial and temporal patterns discerned from MODIS and AVHRR data. Remote Sens. Environ. 208, 171–188. https://doi.org/10.1016/j.rse.2018.02.014

Chartrand, K.M., Szabó, M., Sinutok, S., Rasheed, M.A., Ralph, P.J., 2018. Living at the margins – The response of deep-water seagrasses to light and temperature renders them susceptible to acute impacts. Mar. Environ. Res. 136, 126–138. https://doi.org/10.1016/j.marenvres.2018.02.006

Chen, L.-Y., Lu, B., Morales-Briones, D.F., Moody, M.L., Liu, F., Hu, G.-W., Huang, C.-H., Chen, J.-M., Wang, Q.-F., 2021. Integrating transcriptomes to investigate genes associated with adaptation to aquatic environments, and assess phylogenetic conflict and whole-genome duplications in Alismatales. bioRxiv 2021–11.

Collier, C.J., Ow, Y.X., Langlois, L., Uthicke, S., Johansson, C.L., O'Brien, K.R., Hrebien, V., Adams, M.P., 2017. Optimum temperatures for net primary productivity of three tropical seagrass species. Front. Plant Sci. 8, 1446.

Collier, C.J., Uthicke, S., Waycott, M., 2011. Thermal tolerance of two seagrass species at contrasting light levels: Implications for future distribution in the Great Barrier Reef. Limnol. Oceanogr. 56, 2200–2210.

Collier, C.J., Waycott, M., 2014. Temperature extremes reduce seagrass growth and induce mortality. Mar. Pollut. Bull. 83, 483–490. https://doi.org/10.1016/j.marpolbul.2014.03.050

Cooper, L.W., McRoy, C.P., 1988. Anatomical adaptations to rocky substrates and surf exposure by the seagrass genus *Phyllospadix*. Aquat. Bot. 32, 365–381. https://doi.org/10.1016/0304-3770(88)90108-8

Costa, M.M., Silva, J., Barrote, I., Santos, R., 2021. Heatwave effects on the photosynthesis and antioxidant activity of the seagrass *Cymodocea nodosa* under contrasting light regimes. Oceans 2, 448–460. https://doi.org/10.3390/oceans2030025

Costanza, R., de Groot, R., Sutton, P., van der Ploeg, S., Anderson, S.J., Kubiszewski, I., Farber, S., Turner, R.K., 2014. Changes in the global value of ecosystem services. Glob. Environ. Change 26, 152–158. https://doi.org/10.1016/j.gloenvcha.2014.04.002

de los Santos, C., Onoda, Y., Vergara, J., Pérez-Lloréns, J., Bouma, T., La Nafie, Y., Cambridge, M., Brun, F., 2016. A comprehensive analysis of mechanical and morphological traits in temperate and tropical seagrass species. Mar. Ecol. Prog. Ser. 551, 81–94. https://doi.org/10.3354/meps11717

de los Santos, C.B., Scott, A., Arias-Ortiz, A., Jones, B., Kennedy, H., Mazarrasa, I., McKenzie, L., Nordlund, L.M., de la Torre-Castro, M. de la T., Unsworth, R.K.F., Ambo-Rappe, R., 2020. Seagrass ecosystem services: assessment and scale of benefits. Blue Value Seagrasses Environ. People 19–21.

Deguette, A., Barrote, I., Silva, J., 2022. Physiological and morphological effects of a marine heatwave on the seagrass *Cymodocea nodosa*. Sci. Rep. 12, 7950. https://doi.org/10.1038/s41598-022-12102-x

Den Hartog, C., 1970. The sea-grasses of the world. N.-Holl. Amst.

Doney, S.C., Ruckelshaus, M., Emmett Duffy, J., Barry, J.P., Chan, F., English, C.A., Galindo, H.M., Grebmeier, J.M., Hollowed, A.B., Knowlton, N., 2012. Climate change impacts on marine ecosystems. Annu. Rev. Mar. Sci. 4, 11–37.

Dorantes-Gilardi, M., Rivas, D., 2019. Effects of the 2013–2016 Northeast Pacific warm anomaly on physical and biogeochemical variables off northwestern Baja California, derived

from a numerical NPZD ocean model. Deep Sea Res. Part II Top. Stud. Oceanogr. 169–170, 104668. https://doi.org/10.1016/j.dsr2.2019.104668

Drysdale, F.R., Barbour, M.G., 1975. Response of the marine angiosperm *Phyllospadix torreyi* to certain environmental variables: A preliminary study. Aquat. Bot. 1, 97–106. https://doi.org/10.1016/0304-3770(75)90015-7

Duarte, B., Martins, I., Rosa, R., Matos, A.R., Roleda, M.Y., Reusch, T.B.H., Engelen, A.H., Serrão, E.A., Pearson, G.A., Marques, J.C., Caçador, I., Duarte, C.M., Jueterbock, A., 2018. Climate change impacts on seagrass meadows and macroalgal forests: an integrative perspective on acclimation and adaptation potential. Front. Mar. Sci. 5, 190. https://doi.org/10.3389/fmars.2018.00190

DuBois, K., Pollard, K., Kauffman, B., Williams, S., Stachowicz, J., 2022. Local adaptation in a marine foundation species: Implications for resilience to future global change. Glob. Change Biol. 28. https://doi.org/10.1111/gcb.16080

DuBois, K., Williams, S.L., Stachowicz, J.J., 2020. Previous exposure mediates the response of eelgrass to future warming via clonal transgenerational plasticity. Ecology 101. https://doi.org/10.1002/ecy.3169

Dunic, J.C., Brown, C.J., Connolly, R.M., Turschwell, M.P., Côté, I.M., 2021. Long-term declines and recovery of meadow area across the world's seagrass bioregions. Glob. Change Biol. 27, 4096–4109. https://doi.org/10.1111/gcb.15684

Edgeloe, J.M., Severn-Ellis, A.A., Bayer, P.E., Mehravi, S., Breed, M.F., Krauss, S.L., Batley, J., Kendrick, G.A., Sinclair, E.A., 2022. Extensive polyploid clonality was a successful strategy for seagrass to expand into a newly submerged environment. Proc. R. Soc. B Biol. Sci. 289, 20220538. https://doi.org/10.1098/rspb.2022.0538

Egea, L.G., Jiménez-Ramos, R., Vergara, J.J., Hernández, I., Brun, F.G., 2018. Interactive effect of temperature, acidification and ammonium enrichment on the seagrass *Cymodocea nodosa*. Mar. Pollut. Bull., Securing a future for seagrass 134, 14–26. https://doi.org/10.1016/j.marpolbul.2018.02.029

Erftemeijer, P.L.A., Robin Lewis, R.R., 2006. Environmental impacts of dredging on seagrasses: A review. Mar. Pollut. Bull. 52, 1553–1572. https://doi.org/10.1016/j.marpolbul.2006.09.006

Esteban, N., Unsworth, R.K.F., Gourlay, J.B.Q., Hays, G.C., 2018. The discovery of deep-water seagrass meadows in a pristine Indian Ocean wilderness revealed by tracking green turtles. Mar. Pollut. Bull., Securing a future for seagrass 134, 99–105. https://doi.org/10.1016/j.marpolbul.2018.03.018

Fourqurean, J.W., Duarte, C.M., Kennedy, H., Marbà, N., Holmer, M., Mateo, M.A., Apostolaki, E.T., Kendrick, G.A., Krause-Jensen, D., McGlathery, K.J., Serrano, O., 2012. Seagrass

ecosystems as a globally significant carbon stock. Nat. Geosci. 5, 505–509. https://doi.org/10.1038/ngeo1477

Fox-Kemper, B., 2021. Ocean, Cryosphere and Sea Level Change (Ch. 9 of Climate Change 2021: The Physical Science Basis). Contrib. Work. Group Sixth Assess. Rep. Intergov. Panel Clim. Change.

Franssen, S.U., Gu, J., Winters, G., Huylmans, A.-K., Wienpahl, I., Sparwel, M., Coyer, J.A., Olsen, J.L., Reusch, T.B.H., Bornberg-Bauer, E., 2014. Genome-wide transcriptomic responses of the seagrasses *Zostera marina* and *Nanozostera noltii* under a simulated heatwave confirm functional types. Mar. Genomics 15, 65–73. https://doi.org/10.1016/j.margen.2014.03.004

Gallagher, A.J., Brownscombe, J.W., Alsudairy, N.A., Casagrande, A.B., Fu, C., Harding, L., Harris, S.D., Hammerschlag, N., Howe, W., Huertas, A.D., Kattan, S., Kough, A.S., Musgrove, A., Payne, N.L., Phillips, A., Shea, B.D., Shipley, O.N., Sumaila, U.R., Hossain, M.S., Duarte, C.M., 2022. Tiger sharks support the characterization of the world's largest seagrass ecosystem. Nat. Commun. 13, 6328. https://doi.org/10.1038/s41467-022-33926-1

Gao, Y., Fang, Jianguang, Du, M., Fang, Jinghui, Jiang, W., Jiang, Z., 2017. Response of the eelgrass (*Zostera marina* L.) to the combined effects of high temperatures and the herbicide, atrazine. Aquat. Bot. 142, 41–47. https://doi.org/10.1016/j.aquabot.2017.06.005

Gao, Y., Jiang, Z., Du, M., Fang, Jinghui, Jiang, W., Fang, Jianguang, 2019. Photosynthetic and metabolic responses of eelgrass *Zostera marina* L. to short-term high-temperature exposure. J. Oceanol. Limnol. 37, 199–209. https://doi.org/10.1007/s00343-019-7319-6

García, R., Sánchez-Camacho, M., Duarte, C.M., Marbà, N., 2012. Warming enhances sulphide stress of Mediterranean seagrass (*Posidonia oceanica*). Estuar. Coast. Shelf Sci. 113, 240–247. https://doi.org/10.1016/j.ecss.2012.08.010

García-Pantoja, J.A., Ruiz-Montoya, L., Sandoval-Gil, J.M., Vivanco-Bercovich, M.V., Ferreira-Arrieta, A., Zertuche-González, J.A., Guzmán-Calderón, J.M., Norzagaray-López Orión; Samperio-Ramos, G., Montaño-Moctezuma, G., Hernández-Ayón, M., 2020. Fijación neta de carbono por pastos marinos (*Phyllospadix* spp.) en una isla del Pacífico Mexicano, in: Estado actual del conocimiento del ciclo del carbono y sus interacciones en México: Síntesis a 2020, Síntesis Nacionales. Programa Mexicano del Carbono en colaboración con la Universidad Autónoma Metropolitana-Xochimilco, Texcoco, Estado de México, México, p. 602.

Guerrero-Meseguer, L., Marín, A., Sanz-Lázaro, C., 2017. Future heat waves due to climate change threaten the survival of *Posidonia oceanica* seedlings. Environ. Pollut. 230, 40–45. https://doi.org/10.1016/j.envpol.2017.06.039

Guzmán del Próo, S.A., Mille-Pagaza, S.R., Guadarrama-Granados, R., De la Campa-De Guzmán, S., Carrillo-Laguna, J., Pereira-Corona, A., Belmar-Pérez, J., Parra-Alcocer, M. de J., Luque-Guerrero, A.C., 1991. La comunidad bentónica de los bancos de abulón (*Haliotis* spp.)

Mollusca: gastropoda en Bahía Tortugas, Baja California Sur, México. An. Esc. Nac. Cienc. Biológicas 36, 27–59.

Hartog, C. den, Kuo, J., 2006. Taxonomy and biogeography of seagrasses, in: Seagrasses: biology, ecology and conservation. Springer Netherlands, Dordrecht, pp. 1–23. https://doi.org/10.1007/978-1-4020-2983-7_1

Hemminga, M.A., Duarte, C.M., 2000. Seagrass ecology. Cambridge University Press, Cambridge, UK ; New York, NY.

Hendriks, I.E., Olsen, Y.S., Duarte, C.M., 2017. Light availability and temperature, not increased $CO_2$, will structure future meadows of *Posidonia oceanica*. Aquat. Bot. 139, 32–36. https://doi.org/10.1016/j.aquabot.2017.02.004

Hernán, G., Ortega, M.J., Gándara, A.M., Castejón, I., Terrados, J., Tomas, F., 2017. Future warmer seas: increased stress and susceptibility to grazing in seedlings of a marine habitat-forming species. Glob. Change Biol. 23, 4530–4543. https://doi.org/10.1111/gcb.13768

Hobday, A.J., Alexander, L.V., Perkins, S.E., Smale, D.A., Straub, S.C., Oliver, E.C.J., Benthuysen, J.A., Burrows, M.T., Donat, M.G., Feng, M., Holbrook, N.J., Moore, P.J., Scannell, H.A., Sen Gupta, A., Wernberg, T., 2016. A hierarchical approach to defining marine heatwaves. Prog. Oceanogr. 141, 227–238. https://doi.org/10.1016/j.pocean.2015.12.014

Hobday, A.J., Oliver, E.C., Gupta, A.S., Benthuysen, J.A., Burrows, M.T., Donat, M.G., Holbrook, N.J., Moore, P.J., Thomsen, M.S., Wernberg, T., 2018. Categorizing and naming marine heatwaves. Oceanography 31, 162–173.

Höffle, H., Thomsen, M.S., Holmer, M., 2011. High mortality of *Zostera marina* under high temperature regimes but minor effects of the invasive macroalgae *Gracilaria vermiculophylla*. Estuar. Coast. Shelf Sci. 92, 35–46. https://doi.org/10.1016/j.ecss.2010.12.017

Hyndes, G.A., Heck, K.L., Vergés, A., Harvey, E.S., Kendrick, G.A., Lavery, P.S., McMahon, K., Orth, R.J., Pearce, A., Vanderklift, M., Wernberg, T., Whiting, S., Wilson, S., 2016. Accelerating tropicalization and the transformation of temperate seagrass meadows. BioScience 66, 938–948. https://doi.org/10.1093/biosci/biw111

Jayathilake, D.R.M., Costello, M.J., 2018. A modelled global distribution of the seagrass biome. Biol. Conserv. 226, 120–126. https://doi.org/10.1016/j.biocon.2018.07.009

Johnson, M.R., Williams, S.L., Lieberman, C.H., Solbak, A., 2003. Changes in the abundance of the seagrasses *Zostera marina* L.(eelgrass) and *Ruppia maritima* L.(widgeongrass) in San Diego, California, following and El Niño Event. Estuaries 26, 106–115.

Jordà, G., Marbà, N., Duarte, C.M., 2012. Mediterranean seagrass vulnerable to regional climate warming. Nat. Clim. Change 2, 821–824. https://doi.org/10.1038/nclimate1533

Kendrick, G.A., Nowicki, R.J., Olsen, Y.S., Strydom, S., Fraser, M.W., Sinclair, E.A., Statton, J., Hovey, R.K., Thomson, J.A., Burkholder, D.A., McMahon, K.M., Kilminster, K., Hetzel, Y., Fourqurean, J.W., Heithaus, M.R., Orth, R.J., 2019. A systematic review of how multiple stressors from an extreme event drove ecosystem-wide loss of resilience in an iconic seagrass community. Front. Mar. Sci. 6, 455. https://doi.org/10.3389/fmars.2019.00455

Kendrick, G.A., Orth, R.J., Statton, J., Hovey, R., Ruiz Montoya, L., Lowe, R.J., Krauss, S.L., Sinclair, E.A., 2017. Demographic and genetic connectivity: the role and consequences of reproduction, dispersal and recruitment in seagrasses. Biol. Rev. 92, 921–938. https://doi.org/10.1111/brv.12261

Koch, M., Bowes, G., Ross, C., Zhang, X.-H., 2013. Climate change and ocean acidification effects on seagrasses and marine macroalgae. Glob. Change Biol. 19, 103–132. https://doi.org/10.1111/j.1365-2486.2012.02791.x

Koch, M.S., Schopmeyer, S., Kyhn-Hansen, C., Madden, C.J., 2007. Synergistic effects of high temperature and sulfide on tropical seagrass. J. Exp. Mar. Biol. Ecol. 341, 91–101. https://doi.org/10.1016/j.jembe.2006.10.004

Kuo, J., Hartog, C. den, 2006. Seagrass Morphology, anatomy, and ultrastructure, in: Larkum, A.W.D., Orth, R.J., Duarte, C.M. (Eds.), Seagrasses: biology, ecology and conservation. Springer Netherlands, Dordrecht, pp. 51–87. https://doi.org/10.1007/978-1-4020-2983-7_3

Larkum, A.W.D., Waycott, M., Conran, J.G., 2018. Evolution and Biogeography of Seagrasses, in: Larkum, A.W.D., Kendrick, G.A., Ralph, P.J. (Eds.), Seagrasses of Australia: Structure, Ecology and Conservation. Springer International Publishing, Cham, pp. 3–29. https://doi.org/10.1007/978-3-319-71354-0_1

Laufkötter, C., Zscheischler, J., Frölicher, T.L., 2020. High-impact marine heatwaves attributable to human-induced global warming. Science. https://doi.org/10.1126/science.aba0690

Lawrence, C.M., Bolton, J.J., 2022. Experimental effects of warming and epiphyte grazing on the ecophysiology of two seagrass morphotypes. J. Exp. Mar. Biol. Ecol. 151834. https://doi.org/10.1016/j.jembe.2022.151834

Lee, K.-S., Park, S.R., Kim, Y.K., 2007. Effects of irradiance, temperature, and nutrients on growth dynamics of seagrasses: A review. J. Exp. Mar. Biol. Ecol. 350, 144–175. https://doi.org/10.1016/j.jembe.2007.06.016

Lefcheck, J.S., Wilcox, D.J., Murphy, R.R., Marion, S.R., Orth, R.J., 2017. Multiple stressors threaten the imperiled coastal foundation species eelgrass (*Zostera marina*) in Chesapeake Bay, USA. Glob. Change Biol. 23, 3474–3483. https://doi.org/10.1111/gcb.13623

Macreadie, P.I., Costa, M.D.P., Atwood, T.B., Friess, D.A., Kelleway, J.J., Kennedy, H., Lovelock, C.E., Serrano, O., Duarte, C.M., 2021. Blue carbon as a natural climate solution. Nat. Rev. Earth Environ. 2, 826–839. https://doi.org/10.1038/s43017-021-00224-1

Marbà, N., Díaz-Almela, E., Duarte, C.M., 2014. Mediterranean seagrass (*Posidonia oceanica*) loss between 1842 and 2009. Biol. Conserv. 176, 183–190. https://doi.org/10.1016/j.biocon.2014.05.024

Marbà, N., Duarte, C.M., 2010. Mediterranean warming triggers seagrass (*Posidonia oceanica*) shoot mortality. Glob. Change Biol. 16, 2366–2375. https://doi.org/10.1111/j.1365-2486.2009.02130.x

Marin, M., Feng, M., Phillips, H.E., Bindoff, N.L., 2021. A global, multiproduct analysis of coastal marine heatwaves: distribution, characteristics, and long-term trends. J. Geophys. Res. Oceans 126, e2020JC016708. https://doi.org/10.1029/2020JC016708

Marín-Guirao, L., Bernardeau-Esteller, J., García-Muñoz, R., Ramos, A., Ontoria, Y., Romero, J., Pérez, M., Ruiz, J.M., Procaccini, G., 2018. Carbon economy of Mediterranean seagrasses in response to thermal stress. Mar. Pollut. Bull. 135, 617–629. https://doi.org/10.1016/j.marpolbul.2018.07.050

Marín-Guirao, L., Entrambasaguas, L., Dattolo, E., Ruiz, J.M., Procaccini, G., 2017. Molecular mechanisms behind the physiological resistance to intense transient warming in an iconic marine plant. Front. Plant Sci. 8, 1142. https://doi.org/10.3389/fpls.2017.01142

Marín-Guirao, L., Entrambasaguas, L., Ruiz, J.M., Procaccini, G., 2019. Heat-stress induced flowering can be a potential adaptive response to ocean warming for the iconic seagrass *Posidonia oceanica*. Mol. Ecol. 28, 2486–2501. https://doi.org/10.1111/mec.15089

Marín-Guirao, L., Ruiz, J.M., Dattolo, E., Garcia-Munoz, R., Procaccini, G., 2016. Physiological and molecular evidence of differential short-term heat tolerance in Mediterranean seagrasses. Sci. Rep. 6, 28615. https://doi.org/10.1038/srep28615

Massa, S.I., Arnaud-Haond, S., Pearson, G.A., Serrão, E.A., 2009. Temperature tolerance and survival of intertidal populations of the seagrass *Zostera noltii* (Hornemann) in Southern Europe (Ria Formosa, Portugal). Hydrobiologia 619, 195–201. https://doi.org/10.1007/s10750-008-9609-4

Mathur, S., Agrawal, D., Jajoo, A., 2014. Photosynthesis: Response to high temperature stress. J. Photochem. Photobiol. B, Stress and Photosynthesis 137, 116–126. https://doi.org/10.1016/j.jphotobiol.2014.01.010

McMahon, K., Kilminster, K., Canto, R., Roelfsema, C., Lyons, M., Kendrick, G.A., Waycott, M., Udy, J., 2022. The risk of multiple anthropogenic and climate change threats must be considered for continental scale conservation and management of seagrass habitat. Front. Mar. Sci. 9.

Menge, B.A., Close, S.L., Hacker, S.D., Nielsen, K.J., Chan, F., 2020. Biogeography of macrophyte productivity: Effects of oceanic and climatic regimes across spatiotemporal scales. Limnol. Oceanogr. lno.11635. https://doi.org/10.1002/lno.11635

Michaud, K.M., Reed, D.C., Miller, R.J., 2022. The Blob marine heatwave transforms California kelp forest ecosystems. Commun. Biol. 5, 1–8. https://doi.org/10.1038/s42003-022-04107-z

Moore, K.A., Shields, E.C., Parrish, D.B., 2014. Impacts of varying estuarine temperature and light conditions on *Zostera marina* (eelgrass) and its interactions with *Ruppia maritima* (widgeongrass). Estuaries Coasts 37, 20–30. https://doi.org/10.1007/s12237-013-9667-3

Moulton, O.M., Hacker, S.D., 2011. Congeneric variation in surfgrasses and ocean conditions influence macroinvertebrate community structure. Mar. Ecol. Prog. Ser. 433, 53–63. https://doi.org/10.3354/meps09180

Mvungi, E.F., Pillay, D., 2019. Eutrophication overrides warming as a stressor for a temperate African seagrass (*Zostera capensis*). PLOS ONE 14, e0215129. https://doi.org/10.1371/journal.pone.0215129

Nguyen, H.M., Bulleri, F., Marín-Guirao, L., Pernice, M., Procaccini, G., 2021a. Photo-physiology and morphology reveal divergent warming responses in northern and southern hemisphere seagrasses. Mar. Biol. 168, 129. https://doi.org/10.1007/s00227-021-03940-w

Nguyen, H.M., Kim, M., Ralph, P.J., Marín-Guirao, L., Pernice, M., Procaccini, G., 2020. Stress memory in seagrasses: first insight into the effects of thermal priming and the role of epigenetic modifications. Front. Plant Sci. 11, 494. https://doi.org/10.3389/fpls.2020.00494

Nguyen, H.M., Ralph, P.J., Marín-Guirao, L., Pernice, M., Procaccini, G., 2021b. Seagrasses in an era of ocean warming: a review. Biol. Rev. 96, 2009–2030. https://doi.org/10.1111/brv.12736

Niu, S., Zhang, P., Liu, J., Guo, D., Zhang, X., 2012. The effect of temperature on the survival, growth, photosynthesis, and respiration of young seedlings of eelgrass *Zostera marina* L. Aquaculture 350–353, 98–108. https://doi.org/10.1016/j.aquaculture.2012.04.010

Oliver, E.C.J., Burrows, M.T., Donat, M.G., Sen Gupta, A., Alexander, L.V., Perkins-Kirkpatrick, S.E., Benthuysen, J.A., Hobday, A.J., Holbrook, N.J., Moore, P.J., Thomsen, M.S., Wernberg, T., Smale, D.A., 2019. Projected Marine Heatwaves in the 21st Century and the Potential for Ecological Impact. Front. Mar. Sci. 6.

Olsen, J.L., Rouzé, P., Verhelst, B., Lin, Y.-C., Bayer, T., Collen, J., Dattolo, E., De Paoli, E., Dittami, S., Maumus, F., 2016. The genome of the seagrass *Zostera marina* reveals angiosperm adaptation to the sea. Nature 530, 331–335.

Ontoria, Y., Cuesta-Gracia, A., Ruiz, J.M., Romero, J., Pérez, M., 2019a. The negative effects of short-term extreme thermal events on the seagrass *Posidonia oceanica* are exacerbated by ammonium additions. PLOS ONE 14, e0222798. https://doi.org/10.1371/journal.pone.0222798

Ontoria, Y., Gonzalez-Guedes, E., Sanmartí, N., Bernardeau-Esteller, J., Ruiz, J.M., Romero, J., Pérez, M., 2019b. Interactive effects of global warming and eutrophication on a fast-growing

Mediterranean seagrass. Mar. Environ. Res. 145, 27–38. https://doi.org/10.1016/j.marenvres.2019.02.002

Ontoria, Y., Webster, C., Said, N., Ruiz, J.M., Pérez, M., Romero, J., McMahon, K., 2020. Positive effects of high salinity can buffer the negative effects of experimental warming on functional traits of the seagrass *Halophila ovalis*. Mar. Pollut. Bull. 158, 111404. https://doi.org/10.1016/j.marpolbul.2020.111404

Orth, R.J., Carruthers, T.J.B., Dennison, W.C., Duarte, C.M., Fourqurean, J.W., Heck, K.L., Hughes, A.R., Kendrick, G.A., Kenworthy, W.J., Olyarnik, S., Short, F.T., Waycott, M., Williams, S.L., 2006. A Global Crisis for Seagrass Ecosystems. BioScience 56, 987. https://doi.org/10.1641/0006-3568(2006)56[987:AGCFSE]2.0.CO;2

Pazzaglia, J., Badalamenti, F., Bernardeau-Esteller, J., Ruiz, J.M., Giacalone, V.M., Procaccini, G., Marín-Guirao, L., 2022a. Thermo-priming increases heat-stress tolerance in seedlings of the Mediterranean seagrass *P. oceanica*. Mar. Pollut. Bull. 174, 113164. https://doi.org/10.1016/j.marpolbul.2021.113164

Pazzaglia, J., Reusch, T.B.H., Terlizzi, A., Marín-Guirao, L., Procaccini, G., 2021. Phenotypic plasticity under rapid global changes: The intrinsic force for future seagrasses survival. Evol. Appl. 14, 1181–1201. https://doi.org/10.1111/eva.13212

Pazzaglia, J., Santillán-Sarmiento, A., Helber, S.B., Ruocco, M., Terlizzi, A., Marín-Guirao, L., Procaccini, G., 2020. Does Warming Enhance the Effects of Eutrophication in the Seagrass *Posidonia oceanica*? Front. Mar. Sci. 7. https://doi.org/10.3389/fmars.2020.564805

Pazzaglia, J., Santillán-Sarmiento, A., Ruocco, M., Dattolo, E., Ambrosino, L., Marín-Guirao, L., Procaccini, G., 2022b. Local environment modulates whole-transcriptome expression in the seagrass *Posidonia oceanica* under warming and nutrients excess. Environ. Pollut. 303, 119077. https://doi.org/10.1016/j.envpol.2022.119077

Pedersen, O., Colmer, T.D., Borum, J., Zavala-Perez, A., Kendrick, G.A., 2016. Heat stress of two tropical seagrass species during low tides – impact on underwater net photosynthesis, dark respiration and diel in situ internal aeration. New Phytol. 210, 1207–1218. https://doi.org/10.1111/nph.13900

Pedraza, K., Cadena-Roa, M.A., León-Cisneros, K., López-Vivas, J.M., Muñiz-Salazar, R., Terrados, J., 2021. Anomalías positivas de temperatura del 2014-2016 en Bahía Magdalena: el caso de *Phyllospadix scouleri*.

Pereda-Briones, L., Terrados, J., Tomas, F., 2019. Negative effects of warming on seagrass seedlings are not exacerbated by invasive algae. Mar. Pollut. Bull. 141, 36–45. https://doi.org/10.1016/j.marpolbul.2019.01.049

Phillips, R.C., 1979. Ecological notes on *Phyllospadix* (potamogetonaceae) in the Northeast Pacific. Aquat. Bot. 6, 159–170. https://doi.org/10.1016/0304-3770(79)90059-7

Ralph, P.J., Durako, M.J., Enríquez, S., Collier, C.J., Doblin, M.A., 2007. Impact of light limitation on seagrasses. J. Exp. Mar. Biol. Ecol. 350, 176–193. https://doi.org/10.1016/j.jembe.2007.06.017

Ramírez-García, P., Terrados, J., Ramos, F., Lot, A., Ocaña, D., Duarte, C.M., 2002. Distribution and nutrient limitation of surfgrass, *Phyllospadix scouleri* and *Phyllospadix torreyi*, along the Pacific coast of Baja California (México). Aquat. Bot. 74, 121–131. https://doi.org/10.1016/S0304-3770(02)00050-5

Repolho, T., Duarte, B., Dionísio, G., Paula, J.R., Lopes, A.R., Rosa, I.C., Grilo, T.F., Caçador, I., Calado, R., Rosa, R., 2017. Seagrass ecophysiological performance under ocean warming and acidification. Sci. Rep. 7, 41443. https://doi.org/10.1038/srep41443

Reynolds, L.K., DuBois, K., Abbott, J.M., Williams, S.L., Stachowicz, J.J., 2016. Response of a habitat-forming marine plant to a simulated warming event is delayed, genotype specific, and varies with phenology. PLOS ONE 11, e0154532. https://doi.org/10.1371/journal.pone.0154532

Ruiz-Montoya, L., Sandoval-Gil, J.M., Belando-Torrentes, M.D., Vivanco-Bercovich, M., Cabello-Pasini, A., Rangel-Mendoza, L.K., Maldonado-Gutiérrez, A., Ferrerira-Arrieta, A., Guzmán-Calderón, J.M., 2021. Ecophysiological responses and self-protective canopy effects of surfgrass (*Phyllospadix torreyi*) in the intertidal. Mar. Environ. Res. 172, 105501. https://doi.org/10.1016/j.marenvres.2021.105501

Ruocco, M., De Luca, P., Marín-Guirao, L., Procaccini, G., 2019. Differential leaf age-dependent thermal plasticity in the keystone seagrass *Posidonia oceanica*. Front. Plant Sci. 10, 1556. https://doi.org/10.3389/fpls.2019.01556

Saha, M., Barboza, F.R., Somerfield, P.J., Al-Janabi, B., Beck, M., Brakel, J., Ito, M., Pansch, C., Nascimento-Schulze, J.C., Jakobsson Thor, S., Weinberger, F., Sawall, Y., 2020. Response of foundation macrophytes to near-natural simulated marine heatwaves. Glob. Change Biol. 26, 417–430. https://doi.org/10.1111/gcb.14801

Sen Gupta, A., Thomsen, M., Benthuysen, J.A., Hobday, A.J., Oliver, E., Alexander, L.V., Burrows, M.T., Donat, M.G., Feng, M., Holbrook, N.J., Perkins-Kirkpatrick, S., Moore, P.J., Rodrigues, R.R., Scannell, H.A., Taschetto, A.S., Ummenhofer, C.C., Wernberg, T., Smale, D.A., 2020. Drivers and impacts of the most extreme marine heatwave events. Sci. Rep. 10, 19359. https://doi.org/10.1038/s41598-020-75445-3

Serrano, O., Arias-Ortiz, A., Duarte, C.M., Kendrick, G.A., Lavery, P.S., 2021. Impact of marine heatwaves on seagrass ecosystems, in: Ecosystem Collapse and Climate Change. Springer, pp. 345–364.

Shelton, A.O., 2010. Temperature and community consequences of the loss of foundation species: Surfgrass (*Phyllospadix* spp., Hooker) in tidepools. J. Exp. Mar. Biol. Ecol. 391, 35–42. https://doi.org/10.1016/j.jembe.2010.06.003

Short, F., Carruthers, T., Dennison, W., Waycott, M., 2007. Global seagrass distribution and diversity: A bioregional model. J. Exp. Mar. Biol. Ecol. 350, 3–20. https://doi.org/10.1016/j.jembe.2007.06.012

Short, F.T., Polidoro, B., Livingstone, S.R., Carpenter, K.E., Bandeira, S., Bujang, J.S., Calumpong, H.P., Carruthers, T.J.B., Coles, R.G., Dennison, W.C., Erftemeijer, P.L.A., Fortes, M.D., Freeman, A.S., Jagtap, T.G., Kamal, A.H.M., Kendrick, G.A., Judson Kenworthy, W., La Nafie, Y.A., Nasution, I.M., Orth, R.J., Prathep, A., Sanciangco, J.C., Tussenbroek, B. van, Vergara, S.G., Waycott, M., Zieman, J.C., 2011. Extinction risk assessment of the world's seagrass species. Biol. Conserv. 144, 1961–1971. https://doi.org/10.1016/j.biocon.2011.04.010

Smith, K.E., Burrows, M.T., Hobday, A.J., King, N.G., Moore, P.J., Sen Gupta, A., Thomsen, M.S., Wernberg, T., Smale, D.A., 2023. Biological Impacts of Marine Heatwaves. Annu. Rev. Mar. Sci. 15, null. https://doi.org/10.1146/annurev-marine-032122-121437

Traboni, C., Mammola, S.D., Ruocco, M., Ontoria, Y., Ruiz, J.M., Procaccini, G., Marín-Guirao, L., 2018. Investigating cellular stress response to heat stress in the seagrass *Posidonia oceanica* in a global change scenario. Mar. Environ. Res. 141, 12–23. https://doi.org/10.1016/j.marenvres.2018.07.007

Tutar, O., Marín-Guirao, L., Ruiz, J.M., Procaccini, G., 2017. Antioxidant response to heat stress in seagrasses. A gene expression study. Mar. Environ. Res. 132, 94–102. https://doi.org/10.1016/j.marenvres.2017.10.011

Umanzor, S., Sandoval-Gil, J., Sánchez-Barredo, M., Ladah, L.B., Ramírez-García, M.-M., Zertuche-González, J.A., 2021. Short-term stress responses and recovery of giant kelp (*Macrocystis pyrifera*, Laminariales, Phaeophyceae) juvenile sporophytes to a simulated marine heatwave and nitrate scarcity1. J. Phycol. 57, 1604–1618. https://doi.org/10.1111/jpy.13189

Unsworth, R.K., Cullen-Unsworth, L.C., Jones, B.L., Lilley, R.J., 2022. The planetary role of seagrass conservation. Science 377, 609–613.

Venegas, K., 2019. Distribución espacio-temporal y efecto de la temperatura en praderas de *Phyllospadix scouleri* en tres localidades de B.C.S. Tesis de Doctorado. Universidad Autónoma de Baja California Sur.

Viana, I.G., Moreira-Saporiti, A., Teichberg, M., 2020. Species-specific trait responses of three tropical seagrasses to multiple stressors: the case of increasing temperature and nutrient enrichment. Front. Plant Sci. 11.

Vivanco-Bercovich, M., Belando-Torrentes, M.D., Figueroa-Burgos, M.F., Ferreira-Arrieta, A., Macías-Carranza, V., García-Pantoja, J.A., Cabello-Pasini, A., Samperio-Ramos, G., Cruz-López, R., Sandoval-Gil, J.M., 2022. Combined effects of marine heatwaves and reduced light on the physiology and growth of the surfgrass *Phyllospadix torreyi* from Baja California, Mexico. Aquat. Bot. 178, 103488. https://doi.org/10.1016/j.aquabot.2021.103488

Waycott, M., Duarte, C.M., Carruthers, T.J.B., Orth, R.J., Dennison, W.C., Olyarnik, S., Calladine, A., Fourqurean, J.W., Heck, K.L., Hughes, A.R., Kendrick, G.A., Kenworthy, W.J., Short, F.T., Williams, S.L., 2009. Accelerating loss of seagrasses across the globe threatens coastal ecosystems. Proc. Natl. Acad. Sci. 106, 12377–12381. https://doi.org/10.1073/pnas.0905620106

Wei, X., Li, K., Kilpatrick, T., Wang, M., Xie, S., 2021. Large-scale conditions for the record-setting southern California marine heatwave of August 2018. Geophys. Res. Lett. 48. https://doi.org/10.1029/2020GL091803

Winters, G., Nelle, P., Fricke, B., Rauch, G., Reusch, T., 2011. Effects of a simulated heat wave on photophysiology and gene expression of high- and low-latitude populations of *Zostera marina*. Mar. Ecol. Prog. Ser. 435, 83–95. https://doi.org/10.3354/meps09213

Yang, X.Q., Zhang, Q.S., Zhang, D., Feng, J.X., Zhao, W., Liu, Z., Tan, Y., 2018. Interaction of high seawater temperature and light intensity on photosynthetic electron transport of eelgrass (*Zostera marina* L.). Plant Physiol. Biochem. 132, 453–464. https://doi.org/10.1016/j.plaphy.2018.09.032

York, P.H., Gruber, R.K., Hill, R., Ralph, P.J., Booth, D.J., Macreadie, P.I., 2013. Physiological and morphological responses of the temperate Seagrass *Zostera muelleri* to multiple stressors: investigating the interactive effects of light and temperature. PLoS ONE 8, e76377. https://doi.org/10.1371/journal.pone.0076377

Zaba, K.D., Rudnick, D.L., 2016. The 2014–2015 warming anomaly in the Southern California Current System observed by underwater gliders. Geophys. Res. Lett. 43, 1241–1248. https://doi.org/10.1002/2015GL067550

Zhang, D., Zhang, Q.S., Yang, X.Q., 2017. Adaptive strategies of *Zostera japonica* photosynthetic electron transport in response to thermal stress. Mar. Biol. 164, 35. https://doi.org/10.1007/s00227-016-3064-y

**CAPÍTULO I - Combinación de estrés térmico y reducción de irradiancia en la ecofisiología y crecimiento del pasto marino *Phyllospadix torreyi***

(Artículo 1, publicación original)

*Disponible en:*

*https://doi.org/10.1016/j.aquabot.2021.103488*

Aquatic Botany 178 (2022) 103488

Contents lists available at ScienceDirect

Aquatic Botany

journal homepage: www.elsevier.com/locate/aquabot

# Combined effects of marine heatwaves and reduced light on the physiology and growth of the surfgrass *Phyllospadix torreyi* from Baja California, Mexico

Manuel Vivanco-Bercovich [a,1], María Dolores Belando-Torrentes [b,1], María Fernanda Figueroa-Burgos [a], Alejandra Ferreira-Arrieta [a], Víctor Macías-Carranza [a], Jessica Anayansi García-Pantoja [a], Alejandro Cabello-Pasini [a], Guillermo Samperio-Ramos [a], Ricardo Cruz-López [a], Jose Miguel Sandoval-Gil [a,*,1,2]

[a] Universidad Autónoma de Baja California (UABC), Instituto de Investigaciones Oceanológicas (IIO), Marine Botany Research Group, Ensenada, Baja California, México

[b] Instituto Español de Oceanografía (IEO), Centro Oceanográfico de Murcia, Seagrass Ecology Group, C/Varadero s/n, 30740 San Pedro del Pinatar, Murcia, Spain

ARTICLE INFO

*Keywords:*
Marine heatwaves
Low light
Seagrass ecophysiology
Climate change
Surfgrass

ABSTRACT

This study aimed to elucidate for the first time the combined effects of marine heatwaves (MHWs) and light limitation simulated in mesocosm on critical physiological descriptors of the surfgrass *Phyllospadix torreyi*, which constitutes highly productive meadows along the intertidal and subtidal rocky shores of the Pacific coast of North America. Our results revealed that short-term exposure (~7 days) to extreme thermal anomalies of + 9 °C had positive effects on the photosynthetic capacities of *P. torreyi*, as indicated by increments in maximum photosynthetic rates, photosynthetic efficiency (α), maximum electron transport rate, and effective quantum yield. Despite that its photosynthetic performance was enhanced, exposure to warming caused a decrease in its internal carbon reserves (i.e. energy status), likely as a consequence of carbon mobilization/utilization to activate heat-stress responses. Plants exposed to light limitation (i.e. sub-saturating irradiance of 30 μmol photon $m^{-2}$ $s^{-1}$) generally exhibited an increase in α and/or a decrease in respiration, which ultimately allowed for a reduction in plant compensation irradiance. The combination of low light and seawater warming resulted in a decrease in non-structural carbohydrates content, daily net-productivity, and leaf growth rates. Gross photosynthetic rates at control saturating irradiance exhibited higher activation energy and, thus, greater responsiveness to seawater warming than plants kept under light limitation. While our results indicated that unusual warming events might favor the photosynthetic performance of *P. torreyi*, combining this condition with a drastic light reduction can lead to internal carbon depletion and potentially compromise plant survival in the long term.

## 1. Introduction

Under a changing climate scenario, ocean warming is considered a major threat to submerged vegetation worldwide (Serrano et al., 2021). Global sea surface temperature is projected to rise between 0.5 °C and 1.5 °C by the end of the 21st century, as human activities intensify the release of $CO_2$ into the atmosphere (Collins et al., 2013). Furthermore, the increased frequency and intensity of discrete events of extreme/-anomalous regional warming such as marine heatwaves (MHWs) has lead to deleterious effects on seagrass meadows vitality and community

*Abbreviations:* MHW, Marine heatwaves; Net-$P_{max}$, Net photosynthetic rate; Gross-$P_{max}$, Gross photosynthetic rate; R, Respiration rate; α, Photosynthetic efficiency; $E_c$, Compensation Irradiance; NSCs, Non-structural carbohydrates; $ETR_{max}$, Maximum electron transport rate; $\Phi_{PSII}$, Effective quantum yield; NPQ, Non-photochemical quenching; $F_v/F_m$, Maximum quantum yield; RGR, Relative growth rate.

* Correspondence to: Universidad Autónoma de Baja California (UABC), Instituto de Investigaciones Oceanológicas, Carretera Ensenada-Tijuana No. 3917, Fraccionamiento Playitas C.P. 22860 en Ensenada, Baja California, México.

*E-mail address:* jmsandovalgil@gmail.com (J.M. Sandoval-Gil).

[1] These authors contributed equally to the manuscript.

[2] Orchid ID: 0000–0001-8973–0306

https://doi.org/10.1016/j.aquabot.2021.103488

Available online 30 December 2021

structure worldwide (Marbà and Duarte, 2010; Serrano et al., 2021). Depending on their duration and intensity (see Hobday et al., 2016), MHWs can drive changes in the whole seagrass habitats' structure and threaten their capacity for providing ecological goods and services (Smale et al., 2019). Widespread seagrass dieback events have also been attributed to the combination of MHWs with other environmental forcing limiting plant productivity (e.g., increased turbidity; Kendrick et al., 2019).

There are considerable evidences about the ecophysiological acclimation and stress responses of seagrasses to increasing temperature (Koch et al., 2013, and references therein), documented at different biological levels (Marín-Guirao et al., 2017; Nguyen et al., 2021). At metabolic/physiological level, the enhancement of respiration rate can potentially lead to an overall carbon deficit (Bulthuis, 1987; Collier et al., 2011). Conversely, the stimulation of carbon uptake and assimilation via photosynthesis, the utilization of internal carbon reserves, or increasing the above to below ground biomass ratio are strategies documented to counterbalance respiratory carbon losses (Marín-Guirao et al., 2016, 2018). If warming events exceed plants' thermal tolerance thresholds, they can cause a decline in photosynthetic rates and depletion of carbon reserves, ultimately affecting plant growth and survival (Collier and Waycott, 2014). Although temperate seagrasses generally seem to be more vulnerable to warming than tropical species (Collier and Waycott, 2014), upper thermal limits and acclimation responses vary among and within species according to the adaptation of ecotypes/genotypes to different environmental conditions (Bennett et al., 2021).

The metabolic theory of ecology (MTE), as applied to plant science at the individual level, suggests a temperature dependence of biological processes and the functional properties of metabolically active organelles (Brown et al., 2004; Price et al., 2010). Furthermore, MTE can facilitate the parameterization of thermal physiological responses to predict adaptive shifts in metabolic traits when the environmental resources change (Padfield, 2017). For instance, according to the MTE, numerous physiological functions of seagrasses (e.g., photosynthesis and respiration) undergo exponential temperature-associated changes. This uniformity facilitates comparisons about the plant metabolic sensitivity to warming events, which is expressed as the activation energy causing a given percent variation in the process rate (Brown et al., 2004; Price et al., 2010; Beca-Carretero et al., 2018).

The effects of seawater warming might be influenced by concurrent environmental stressors, such as limited light availability (Collier et al., 2011; Beca-Carretero et al., 2018; Kim et al., 2020), which may decrease seagrass capacity to acclimate and recover from warming events. Sediment resuspension due to coastal engineering (Erftemeijer and Robin Lewis, 2006), storms (Cabello-Pasini et al., 2002), terrestrial runoff (Fraser et al., 2014), high epiphyte loading on seagrass leaves, and phytoplankton/macroalgae blooms triggered by eutrophic conditions (Burkholder et al., 2007), can dramatically reduce light availability. To counteract a decrease in plant energy status under light-limitation, seagrasses must activate a series of photo-acclimation mechanisms at multiple organizational levels (Ralph et al., 2007). Some studies have documented short-term changes in leaf pigments to improve light harvesting and photosynthetic efficiency (Collier et al., 2009; Olivé et al., 2013). At longer temporal (and spatial) scales, adjustments in shoot morphology (e.g., reduction in leaf length) and canopy structure (e.g., decrease in shoot density) can reduce self-shading of plant tissues and respiratory demand at the whole-plant level (Collier et al., 2009). The photoacclimatory responses may vary among species (Statton et al., 2018), ecotypes (e.g., depth, Procaccini et al., 2017), ramets (Ruocco et al., 2019), and leaf sections (Olivé et al., 2013).

The concurrence of seawater warming and light deprivation is a common scenario in seagrass meadows globally (Stockbridge et al., 2020). Some field monitoring studies have attributed massive mortality events in seagrass meadows to the overlapped effects of both stressors (Kendrick et al., 2019). Shallow and deep Mediterranean seagrasses have exhibited divergent resistance and acclimation mechanisms to MHWs, likely due to adaptive properties developed at different light and thermal regimes through the bathymetric gradient (Marbà and Duarte, 2010; Marín-Guirao et al., 2016). Synergistic effects of warming and shading may cause a decline in photosynthetic productivity and a stimulates respiratory activity, which may result in carbon deficit (Collier et al., 2011; Beca-Carretero et al., 2018; Kim et al., 2020), and other detrimental effects in the photosynthetic apparatus (Collier and Waycott, 2014). In contrast, other experimental studies did not detect significant interactions between thermal stress and light limitation, yet observed individual effects (York et al., 2013; Chartrand et al., 2018; Costa et al., 2021).

Surfgrasses (including Phyllospadix scouleri) also play an important role regulating physico-chemical and biological processes in the intertidal and shallow subtidal, and represent a significant source of food and shelter for various marine organisms (Shelton, 2010; Moulton and Hacker, 2011). Furthermore, surfgrasses are the unique seagrasses able to colonize wave exposed rocky substrates, owing to a series of ultrastructural, physiological, and anatomical adaptations (Cooper and McRoy, 1988, Ramírez-García et al., 1998). The surfgrass Phyllospadix torreyi S. Watson constitutes large and highly productive (up to ~8000 g DW m-2 year-1) meadows along the Pacific coast of North America, from Vancouver Island (Canada) to Baja California Sur in Mexico (Den Hartog, 1970; Ramírez-García et al., 2002). Since P. torreyi grows in shallow waters (intertidal to ~5 m depth), it is commonly exposed to drastic changes in environmental conditions, such as light, temperature and nutrient availability (Ramírez-García et al., 1998). Although few studies have examined some aspects of its physiology (e.g. photosynthesis, nitrogen acquisition, osmoregulation; Drew, 1979, Terrados and Williams, 1997, Ruiz-Montoya et al., 2021), knowledge about its ecophysiological plasticity and resilience under such extreme environmental conditions continues to be scarce and intriguing, especially in a climate change scenario.

Extensive climate change impacts have been documented for marine ecosystems in the Northeastern Pacific coast (Smale et al., 2019), a region where several MHWs have occurred during the last decade (Sen Gupta et al., 2020; Wei et al., 2021). An excepcionally long and intense event, named "The Blob", was registered as several consecutive long MHWs (>100 days) which increased sea surface temperature up to + 7 °C, triggering major biogeochemical and ecological changes in the coastal marine environment (Dorantes-Gilardi and Rivas, 2019). In addition, diminished light availability associated with sediment resuspension and phytoplanktonic blooms have led to severe detrimental effects in eelgrass and seaweeds populations in the Northeastern Pacific coast (Dean, 1985; Cabello-Pasini et al., 2002). Regarding the genera Phyllospadix, Drysdale and Barbour (1975) reported negative effects on leaf growth rate under independent treatments of warming and reduced light. Venegas (2019) demonstrated that seawater warming associated with intense MHWs and ENSO events reduced the vegetative productivity of *P. scouleri.* Conversely, Menge et al. (2020) stated that seawater warming could be correlated with the stimulation of *P. scouleri* growth. However, the physiological acclimation mechanisms and stress responses behind the sensitivity and/or resistance of *Phyllospadix* to seawater warming and light limitation remain largely unknown.

The present study aimed, for the first time, to elucidate the potential effects of a simulated MHW in combination with reduced irradiance on photobiological descriptors, oxidative stress and nutrient status of *P. torreyi.* Experimental treatments were simulated under laboratory

conditions assessing the effects on the plant performance by integrating those critical ecophysiological traits. Additionally, the temperature-dependence of such descriptors and its relation with acclimation/stress responses was analized by determining their activation energy.

## 2. Materials & methods

### 2.1. Plant collection and experimental design

*Phyllospadix torreyi* shoot clumps maintaining clonal integrity (i.e., keeping the connection among ramets) were collected in a healthy and dense meadow from Baja California (Punta Morro, Ensenada, México, 31°51' 42.9" N 116° 39' 55" W) in May 2018. The donor meadow was located at the infralittoral zone (~5 m below MHWL) of a rocky and wave-exposed shore, where annual seawater temperature ranges between 15 and 21 °C (Delgadillo-Hinojosa et al., 2020).

Plants were transported in coolers (within 1 h) to the facilities at the Instituto de Investigaciones Oceanológicas (University of Baja California). To obtain field reference values of plant biological status (Table 1), photobiological descriptors were measured in four individuals, and leaf tissues of other 10 individuals were kept frozen (−80 °C) to perform pigment and non-structural carbohydrate analysis. In addition, shoot clumps were placed (within 2 h) in the indoor experimental system for acclimation during three days prior to the experiment. The acclimation conditions corresponded to averaged field temperature (16 °C) and maximum PAR irradiance measured in the field (200 μmol photon $m^{-2}$ $s^{-1}$), which were monitored one month prior to the plant collection by using submersible light/temperature sensors (Onset-HOBO MX2202), previously calibrated against a 2π cosine corrected quantum sensor (LI-COR, LI-192).

A factorial design was conducted to test temperature and light's individual and interactive effects on *P. torreyi*. The light treatments consisted of two irradiance levels: saturating-irradiance (200 μmol photon $m^{-2}$ $s^{-1}$), referred hereafter as control (C); and sub-saturating irradiance (near compensation irradiance, 30 μmol photon $m^{-2}$ $s^{-1}$), referred hereafter as low irradiance (L). Irradiance values were selected based on the photosynthetic capacities of *P. torreyi* examined by P-E curves (see methods below). The two light levels were combined with two temperatures (16 °C and 25 °C) to obtain four different treatments: 16 C, 16 L, 25 C and 25 L. 16 °C treatment simulated the average field temperature in the meadow, monitored three weeks before the beginning of the experiment. The warm treatment (25 °C) corresponded to the region's maximum temperature recorded for MHWs (Arafeh-Dalmau et al., 2019). The experiment lasted seven days, simulating the duration of an ordinary MHW in the region (Schlegel, 2020).

The experimental system consisted of 16 independent aquaria (80 L), each considered as the experimental unit (EU). Four aquaria were disposed for each treatment (n = 4). Each EU contained approximately 200 connected shoots attached to the bottom of the aquaria by plastic grids. Each EU had fluorescent lamps with a neutral (12:12) photoperiod. The temperature was controlled by chillers and submersible quartz heaters. Temperature was increased at a rate of three °C per day in the 25 °C treatments (25 C and 25 L), which is close to the daily variation of seawater surface temperature for the region (NOAA-ESRL Physical Sciences Laboratory, https://psl.noaa.gov/thredds/catalog/Datasets/noaa.oisst.v2.highres/catalog.html). Submersible pumps were installed in EU to improve water circulation and avoid temperature gradients. Seawater was partially replaced (50%) every two days with filtered (1 μm)-UV treated water to maintain water quality. Salinity (34.3–35.2) and pH (7.9–8.1) conditions were kept similar to those at the sampling site. Water temperature, salinity and pH were monitored using a multiparameter submersible probe (HACH HQd, YSI Professional Plus).

**Table 1**
Physiological characterization of *P. torreyi* plants after collection, prior the beginning of the experiment. The number of samples (n), unit, the minimum (Min.), maximum (Max.) and mean values and the standard error (SE) are shown for each descriptor. Net-$P_{max}$: Net maximum photosynthetic rate, Gross-$P_{max}$: Gross maximum photosynthetic rate, α: Photosynthetic efficiency, $E_c$: Compensation irradiance, $E_k$: Saturation irradiance, R: Respiration rate, $F_v/F_m$: Maximum quantum yield, NSCs: Non-structural carbohydrates content.

| Descriptors | n | Units | Reference values of *P. torreyi* | | |
|---|---|---|---|---|---|
| | | | Min. | Max. | Mean ± SE |
| Net-$P_{max}$ | 4 | μmol $O_2$ $g^{-1}$ DW $h^{-1}$ | 77.6 | 87.3 | 82.5 ± 1.9 |
| Gross-$P_{max}$ | 4 | μmol $O_2$ $g^{-1}$ DW $h^{-1}$ | 107.1 | 112.8 | 109.9 ± 2.4 |
| α | 4 | μmol $O_2$ $g^{-1}$ DW $h^{-1}$/ μmol quanta $m^{-2}$ $s^{-1}$ | 1.3 | 1.4 | 1.3 ± 0.02 |
| $E_c$ | 4 | μmol quanta $m^{-2}$ $s^{-1}$ | 26.5 | 29.3 | 28.2 ± 0.6 |
| $E_k$ | 4 | μmol quanta $m^{-2}$ $s^{-1}$ | 92.1 | 181.7 | 135.5 ± 24.4 |
| R | 4 | μmol $O_2$ $g^{-1}$ DW $h^{-1}$ | -51.2 | -38.4 | -46.1 ± 2.8 |
| $F_v/F_m$ | 4 | – | 0.7 | 0.75 | 0.72 ± 0.01 |
| Chlorophyll a | 10 | μg $g^{-1}$ FW | 23.1 | 454.6 | 251.6 ± 75.6 |
| Chlorophyll b | 10 | μg $g^{-1}$ FW | 15.7 | 183.6 | 99.1 ± 27.1 |
| Carotenoids | 10 | μg $g^{-1}$ FW | 119.8 | 292.5 | 199.4 ± 26.7 |
| NSCs | 10 | mg $g^{-1}$ DW | 325 | 401.5 | 346.3 ± 11.6 |

### 2.2. Physiological traits and growth

At the end of the experiment, random shoots from the EUs were sampled for the physiological analysis and growth determination. For each descriptor, measurements were averaged for two plants per EU to obtain the true replicate (n = 4 per treatment), except for P-E curves, which were performed in only one shoot per EU. All samples were taken from the middle section of the second mature leaf to reduce the variability of biological descriptors within/among leaves.

#### 2.2.1. Photosynthesis and respiration (P vs. E curves)

Photosynthesis (P) and respiration (R) rates were determined in leaf segments using a respirometer. This respirometer consisted of 200 mL borosilicate jacketed chambers connected to a controlled temperature circulating bath and surrounded by four light sources (LED 10 W) automatically controlled by customized software. Oxygen evolution was measured by optodes (dipping probe DP-PSt3, PreSens, Germany) connected to a fiber-optic oxygen meter (OXY4 SMA, PreSens, Germany) controlled by software (Measurement Studio 2, PreSens, Germany). A ratio of plant biomass/seawater volume of about 0.03–0.05 g DW $L^{-1}$ was used to ensure accurate measurements of photosynthetic rates, avoiding the underestimation of photosynthesis due to oxygen oversaturation and carbon limitation. Leaf segments were initially incubated in darkness for 15 min to determine R. Subsequently, tissues were exposed to increasing PAR irradiance levels (E, 0 – 1635 μmol photon $m^{-2}$ $s^{-1}$) for 6 min at each irradiance level. Light intensities within the chamber were previously calibrated using a spherical (4π) quantum sensor (Biospherical Instruments; California, USA). Maximum net photosynthetic rate (net-$P_{max}$; μmol $O_2$ $g^{-1}$ DW $h^{-1}$) was determined by averaging the maximum values above the saturating irradiance ($E_k$ = net-$P_{max}$/ α; μmol photon $m^{-2}$ $s^{-1}$). Maximum gross photosynthesis (gross-$P_{max}$; μmol $O_2$ $g^{-1}$ DW $h^{-1}$) was calculated as the sum of net-$P_{max}$ and R. Photosynthetic efficiency (α) was calculated as the slope of the regression line fitted to the initial linear part of the P vs. E curve. The compensation irradiance ($E_c$; μmol photon $m^{-2}$ $s^{-1}$) was determined as the intercept of the initial linear part of the curve on the X-axis. A proxy of daily net-productivity (or daily carbon balance) was calculated, considering specific light conditions of each treatment; since the

selected photoperiod was 12:12, for plants under low irradiance (L) was calculated as [(net-$P_{30}$ x 12) - (R x 12)], where net-$P_{30}$ is the net photosynthesis corresponding to the irradiance at 30 μmol photon $m^{-2}$ $s^{-1}$ of P-E curves. Similarly, daily net-productivity for plants under control-saturating irradiance (C) was calculated as [(net-$P_{200}$ x 12) - (R x 12)], where net-$P_{200}$ is the net photosynthesis corresponding to the irradiance at 200 μmol photon $m^{-2}$ $s^{-1}$.

### 2.2.2. Chlorophyll a fluorescence

The chlorophyll-*a* fluorescence emission of PSII was measured using a portable Diving-PAM fluorometer (Walz, Germany). The leaf surface was carefully cleaned off epiphytes, and held in the fluorometer DCL-8 leaf-clip holder to assure a constant distance between the tissue and the fiber optic of the fluorometer. To standardize data collection among plants, photochemistry measurements were performed in the middle section of the leaf where maximum values of maximum quantum yield ($F_v/F_m$) were measured in previous trials. Rapid Light Curves (RLCs) and $F_v/F_m$ were obtained from plants maintained in darkness overnight. For RLCs the clipped segments were exposed to nine consecutive periods of actinic-light (1 min each, when photosynthetic steady-state is reached) with increasing intensity ranging from 5 to 406 μmol photon $m^{-2}$ $s^{-1}$, preceded by saturating pulses of ~ 5000 μmol photon $m^{-2}$ $s^{-1}$ for 0.8 s. Maximum electron transport rate ($ETR_{max}$), Effective Quantum Yield ($\Phi_{PSII}$), and Non-photochemical quenching (NPQ) were calculated for every actinic-light intensity. Absolute $ETR_{max}$ was calculated as $ETR_{max} = \Phi_{PSII} \cdot E \cdot A \cdot 0.5$, where E is the intensity of each actinic light pulse, A is the leaf absorptance averaged in the PAR region (see below), and 0.5 is a constant assuming that half of the incident photons go through PSII (Beer et al., 2014). Finally, the NPQ was calculated as $(F_m\text{-}F_{m'})/F_{m'}$, where $F_m$ is the maximum fluorescence obtained in plants adapted to darkness overnight, and $F_{m'}$ the fluorescence measured under different intensities of the actinic light.

### 2.2.3. Leaf absorptance

Leaf absorbance (O.D.) was measured spectrophotometrically (Shimadzu UV-1800) using the opal glass technique developed by Shibata (1959). A bleached leaf was used as a reference and absorbance was measured in the PAR range (400–700 nm). The proportion of light captured by leaf tissues was expressed as absorptance ($A = 1\text{–}10^{-D}$) (see further details in Vásquez-Elizondo et al., 2017). Values of $A_{400–700}$ corresponded to averaged absorptance in the PAR region, while $A_{680}$ corresponded to absorptance values at the chlorophyll *a* (Chl*a*) peak of 680 nm.

### 2.2.4. Pigment content

Leaf pigments were extracted from 0.8 $cm^2$ leaf segments homogenized in 80% acetone, with $MgCO_3$ solution added to prevent acidification of the extract (Dennison, 1990). Extracts were stored at 4 °C in the dark for 24 h. After centrifugation (1000 x g, 10 min) absorbance was measured spectrophotometrically at 470, 646, and 663 nm, using 1 mL cuvettes. The Chl *a*, *b,* and total carotenoid concentration were calculated using the equations described by Lichtenthaler and Wellburn (1983) and expressed as μg $g^{-1}$ FW.

### 2.2.5. Non-structural carbohydrates

Total soluble non-structural carbohydrates (free sugars and starch) were determined using the colorimetric phenol-sulfuric acid method (Dubois et al., 1956) using glucose as standard. Leaf tissues were oven-dried at 60 °C until constant weight and ground to a fine powder. The powder was digested in 0.2 M HCl (60° C, 3 h), centrifuged (1000 x g, 5 min), and the supernatant mixed with 3% phenol and concentrated sulphuric acid. Absorbance was measured spectrophotometrically at 490 nm. Non-structural carbohydrates content (NSCs) was expressed in mg $g^{-1}$ DW.

### 2.2.6. Total phenolic content and antioxidant capacity

Phenolic and antioxidant compounds were extracted from dried ground leaf tissue (0.03 g DW) in 0.75 mL 80% methanol in darkness for 24 h. The extract was then centrifuged at 10,000 rpm for 10 min. The methanolic extracts were used to quantify phenolic compounds and antioxidant capacity. The phenolic compound content was determined according to a modification of the Folin–Ciocalteu assay using gallic acid as standard (Singleton and Rossi, 1965). The methanolic extract (0.025 mL) was diluted in 1 mL distilled water ($dH_2O$), 0.1 mL Folin–Ciocalteu reagent, and 0.3 mL $dH_2O$ saturated with $NaCO_3$. This mixture was homogenized, heated (40 °C for 3 min), and its absorbance read spectrophotometrically at 765 nm. Total phenolic content was expressed as gallic acid equivalents (mg Eq. GA $g^{-1}$ DW). The same methanolic extracts were used to quantify the radical scavenging activity according to Sabeena Farvin, Jacobsen (2013); the reaction mixture was prepared with 0.1 mL of diluted extract (1:4 with 80% methanol) and 1 mL of 30 μM 2,2-diphenyl-1-picrylhydrazyl (DPPH) dissolved in 90% methanol. The absorbance was measured at 517 nm 30 min after DPPH addition. The total antioxidant capacity was expressed as ascorbic acid equivalents (mg Eq. AA $g^{-1}$ DW).

### 2.2.7. Relative leaf growth rate

At the beginning of the experimental period, leaves were marked following the punching hole method adapted from Zieman (1974). At the end of the experimental period, all marked shoots were harvested, and leaf segments below the mark (i.e., newly formed tissue) were dried and weighted for all leaves of each shoot. Shoot growth was expressed as relative to the total shoot biomass or relative leaf growth rate (RGR; mg $g^{-1}$ DW $day^{-1}$).

## 2.3. Activation Energy

The Boltzmann–Arrhenius model, incorporated into the metabolic theory of ecology (Gillooly et al., 2001), was used to quantify the temperature-associated changes on physiological rates of *P. torreyi* and to compare their thermal sensitivity under both experimental irradiance conditions. Because the responses of the biological processes describe a unimodal function as the whole temperature range operates (Dell et al., 2011), the activation energy calculated here can represent a rise or fall component of the thermal studied breadth uniquely (Samperio-Ramos et al., 2015). The activation energy was estimated using the following equation:

$$R = R_0 \cdot e^{(-E_a/KT)}$$

where R is the biological parameter (i.e. RGR, gross-$P_{max}$, respiration rate, $ETR_{max}$), $R_0$ is a scaling coefficient dependent on the organism, $E_a$ is the activation energy (eV), K is Boltzmann's constant ($8.62 * 10^{-5}$ eV $K^{-1}$) and T is the absolute temperature (in Kelvin).

## 2.4. Statistical analysis

Multivariate analyses were performed with the normalized data of all response variables and a ranked triangular similarity matrix constructed using Euclidean distances. A two-way PERMANOVA crossed design was performed (9999 permutations) to test for temperature (two levels: 16 vs. 25 °C), light (two levels: C vs. L) and their interactive effects on all biological traits (Net and Gross $P_{max}$, $E_k$, $E_c$, α, Respiration rate, Daily productivity, NSCs, $F_v/F_m$, $\Phi_{PSII}$, $ETR_{max}$, NPQ, Absorptance, *Chl a* and *b*, Carotenoids, Chl b/a, Phenolic content, Antioxidant capacity and RGR). Significant differences in the pair-wise posteriori comparison were tested using Monte Carlo p-values, due to the restricted number of possible permutations. Similarity percentage analysis (SIMPER) analysis was performed to test average distance between each pair of treatments using PRIMER 6 & PERMANOVA+ v.1.0.2 software package (Anderson et al., 2008). To display multivariate patterns of samples and to explore

its relationships with the different biological descriptors, a principal components analysis (PCA) was performed using PAST software (Hammer, 2001).

The significant effects of irradiance and temperature, separately and in combination, on each analyzed plant variable were analyzed using two-way ANOVA. *Post hoc* Tukey tests were performed to test for posterior pair wise comparisons among all treatments. Data were square root or log transformed when normality was not met (Shapiro-Wilk normality test). Regression analysis on log-transformed parameters was used to calculate the activation energy of physiological rates in each light treatment. Differences in activation energy between irradiance levels were tested using two sample t-test or Welch's t-test for unequal variances. Model checking included a visual inspection of the variance-to-mean relationship and linearity of predictors. If homocedasticity and normality of model residuals were not met, a more conservative approach was applied using pair wised post hoc analyses with Bonferroni correction (Underwood et al., 1997; Rutherford, 2001). For all statistical analyses, a probability level of $\alpha = 0.05$ was considered. These analyses were performed using the statistical software R (R Core Team, 2020).

## 3. Results

Physiological descriptors of collected *Phyllospadix torreyi* plants (i.e. field reference values, Table 1) were similar to those measured at the end of the experiment in controls plants (16 C). This indicated (1) that plants were not stressed due to their handling and transplantation, and (2) that the mesocosms growth conditions did not alter the physiological status of experimental plants.

Temperature and irradiance levels had significant effects on the physiology of *P. torreyi* as showed by the multivariate analysis (PERMANOVA, Table 2) that. However, the effect of one factor differed significantly depending on the level of the other factor (significant interaction, Table 2). The pair-wise comparison showed significant differences among all studied treatments (Table 2, PCA biplot in Fig. A1 of Appendix), and SIMPER results showed the highest dissimilarity values between the control and the combined warm and light treatment (16 C vs 25 L, average distance = 52.81). The average distance of the control with warm treatments (16 C vs 25 C, 37.98) was also higher than with the low light treatment (16 C vs 16 L, 28.57). The PCA biplot (Fig. A1, Appendix) distributed temperature treatments along the first axis (PC1), which explained 36.7% of the total variance (Table A2, Appendix). High-temperature treatments were directly related to photobiological descriptors such as $\Phi_{PSII}$, $ETR_{max}$, α, net and gross-$P_{max}$. In contrast, low-temperature treatments were mainly associated with higher pigments content, absorptance, and RGR. The second axis explained 21.5% of the total variance and set a separation among light treatments. Antioxidant capacity, phenolic content and Chl*b*/*a* ratio were directly correlated with low irradiance treatments, while NPQ, $E_c$ and carotenoids content generally presented higher values in the control irradiance treatments.

Values of gross-$P_{max}$, net-$P_{max}$ and α significantly increased in response to warm or low light treatments (Fig. 1A, B, D), and plants treated with both low light and warming (25 L) exhibited the highest values (Table A1). Respiration was only significantly reduced in plants under low irradiance at 16 °C (16 L; Fig. 1B) compared to control plants (16 C). In general, values of $E_c$ declined in response to low irradiance (Fig. 1C), but it was only significantly at 16 °C (Table A1). Similarly, daily net productivity was significantly reduced under low irradiance conditions at both temperatures (Fig. 1E), but the lowest values of productivity were found under the combination of both factors (25 L, Fig. 1E). The content of NSCs decreased in response to low irradiance or temperature treatments (Fig. 1F, Table A1), and the minimum values were detected in 25 L plants.

Values of $ETR_{max}$ and $\Phi_{PSII}$ (Fig. 2A, C) increased at higher temperatures, although differences with the control (16 C) were only significant in 25 L plants (Table A1). The NPQ values only showed a significant reduction with low irradiance at 16 °C, but not at 25 °C (Fig. 2B, Table A1). The experimental treatments did not have any effect on the maximum photochemical efficiency of *P. torreyi*, as $F_v/F_m$ did not vary among treatments (Fig. 2D).

The content in Chl*a* and Chl*b* exhibited lower values in plants at 25 °C with respect to control (Fig. 3A; Table A1). Carotenoids significantly increased in 25 C plants (Fig. 3A; Table A1), while the lowest and highest values of Chl*b*/*a* were found in 25 C and 25 L plants, respectively (Fig. 3B). A significant reduction in leaf absorptance was found in response to warming, regardless of the irradiance level (Table A1, Fig. 4C, D).

Values of leaf phenolic content and antioxidant capacity remained similar in all the treatments (Table 3). A significant decease in RGR was detected only in 25 L plants (Table 3, Table A1).

The activation energy (Table 4) of gross-$P_{max}$ partially described the rise component of thermal breadth in both light treatments, and its value for the plants exposed to control irradiance was about two-fold higher than the calculated for plants under low light. The activation energy for respiration to increased temperature also differed depending on irradiance conditions (Table 4); while at low irradiance, the activation energy ranged between 0.35 eV and 0.79 eV, it was not temperature-dependent in plants under control irradiance. Values of activation energy of $ETR_{max}$ did not show consistent differences between light treatments (Table 4). For its part, the decline in the activation energy of RGR in plants at low irradiance conditions tended to be more abrupt and variable (activation energy: 0.38–1.32 eV) than the increase under control irradiance (0.13–0.17 eV, Table 4).

**Table 2**
Results of permutational multivariate analysis of variance (PERMANOVA) showing the single and interactive effects of temperature (levels: 16 °C, 25 °C) and irradiance (levels: L=low, C=control) on biological descriptors of *P. torreyi*. P (MC) is the p-value based on Monte Carlo approximation. T: temperature, I: Irradiance, T x I: Temperature x Irradiance. Bold numbers indicate significant differences.

| Main test | Source | SS | MS | Pseudo-F | P (perm) |
|---|---|---|---|---|---|
| | T | 90.872 | 90.872 | 9.9611 | **0.0004** |
| | I | 56.207 | 56.207 | 6.1612 | **0.0007** |
| | T x I | 28.449 | 28.449 | 3.1185 | **0.01** |
| **Pair-wise** | **Groups** | **t** | **P(MC)** | | |
| | 16 C x 16 L | 2.4322 | **0.0049** | | |
| | 16 C X 25 L | 3.3029 | **0.0013** | | |
| | 25 C x 25 L | 1.9872 | **0.0171** | | |
| | 25 C x 16 C | 1.9213 | **0.0163** | | |
| | 25 L x 16 L | 3.351 | **0.0018** | | |
| | 25 C x 16 L | 2.4557 | **0.0051** | | |

## 4. Discussion

Our results demonstrated that warming treatments simulating an extreme MHW (+9 °C during ~7 d), applied independently or in combination with low irradiance, had positive effects on the photosynthetic performance of *Phyllospadix torreyi,* reflected as increased values of net and gross-$P_{max}$, α, $ETR_{max}$, $\Phi_{PSII}$ and activation energy for $P_{max}$ and $ETR_{max}$. Plants subjected to both factors (25 L) showed the highest photosynthetic capacities. As far as we know, uniquely one study (i.e., Drew, 1979) examined the photosynthetic response of *P. torreyi* under increasing temperatures. This author also found a positive response of *P. torreyi* to warming (~23 °C), although after much shorter exposure periods (hours). Similarly, Collier et al. (2011) also demonstrated that rising temperature increases photosynthetic rates in the seagrass *Halophila ovalis*. Typically, the photosynthetic rate increase induced by warming has a critical threshold at which metabolic stress starts to occur, eventually resulting in irreversible damage (Koch et al., 2013; Nguyen et al., 2021). For instance, the photosynthetic capabilities of the Mediterranean seagrasses *Posidonia oceanica* and *Cymodocea nodosa* are reduced by warming. This reduction is the result of the existence of

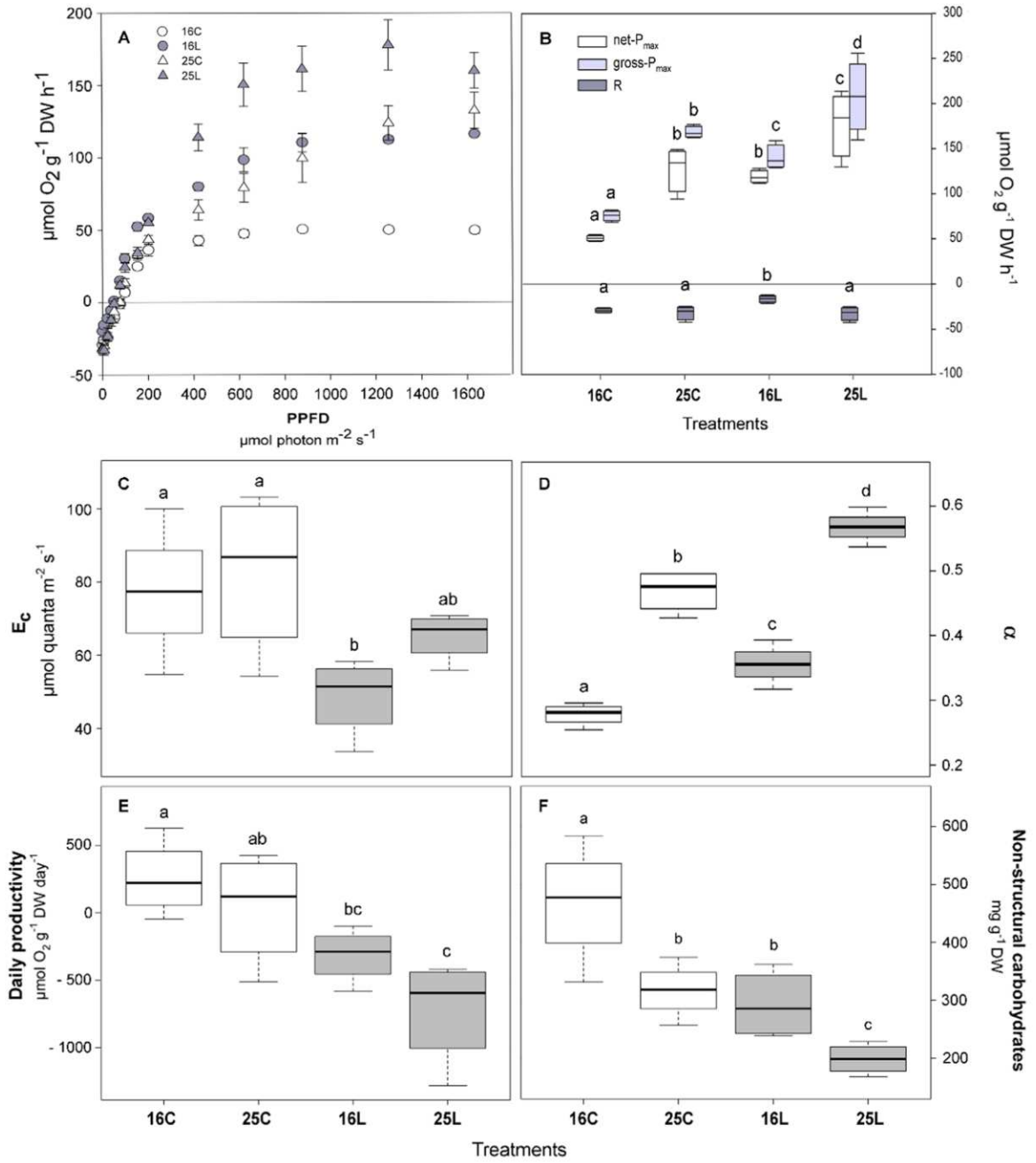


**Fig. 1.** Photosynthesis-Irradiance curves (A), their derived parameters (B, C, D), daily net-productivity (E) and non-structural carbohydrates leaf content (F) determined for *P. torreyi* (n = 4) in response to the experimental treatments of temperature (16 and 25 °C) and light (C= control and L=low irradiance). Different lower-case letters indicate significant differences ($p < 0.05$) between treatments (see Table A1 in the Appendix). Net-$P_{max}$: Net maximum photosynthetic rate, Gross-$P_{max}$: Gross $_{max}$imum photosynthetic rate, R: Respiration rate, $E_c$: Compensation Irradiance, α: Photosynthetic efficiency. Values are means and standard errors.

thermally sensitive components of the photosynthetic apparatus (e.g., reaction centers of photosystems, carbon fixation/assimilation enzymes, thylakoid membranes) (Marín-Guirao et al., 2016, 2017, 2018). Photosynthetic sensitivity to thermal increments is strongly dependent on the adaptation to thermal niches of species and ecotypes (Marín-Guirao et al., 2016; Nguyen et al., 2020). Shallow subtidal (~5 m depth) *P. torreyi* meadows are usually exposed to daily temperature fluctuations (up to 5 °C), following changes in tides and environmental conditions (García-Pantoja et al., 2020). Hence, adaptive properties and acclimation capacities developed under such thermal fluctuation may confer these plants metabolic resistance to cope with increasing temperature (e.g., Franssen et al., 2014). Although not assessed in this study, the thermal stimulation of photosynthetic activity of *P. torreyi* responds to the acceleration of thermally sensitive processes and reactions occurring along the photosynthetic pathway from light-harvesting to carbon fixation (e.g., photophosphorylation, electron transport, plastoquinone diffusion, Rubisco activity) (Davison, 1991), also regulated by heat-stress responsive genes (Marín-Guirao et al., 2017; Nguyen et al., 2021).

Values of $F_v/F_m$ and NPQ remained similar to control in shoots exposed to increasing temperature. Also, the enhanced photosynthetic rates suggests the full functionality of the photosynthetic machinery in *P. torreyi* after the thermal exposure. The lack of an increase of total antioxidant activity and phenolic content suggests the absence of oxidative stress. As documented in other works, warming can cause oxidative stress and photodamage in seagrasses, which might be

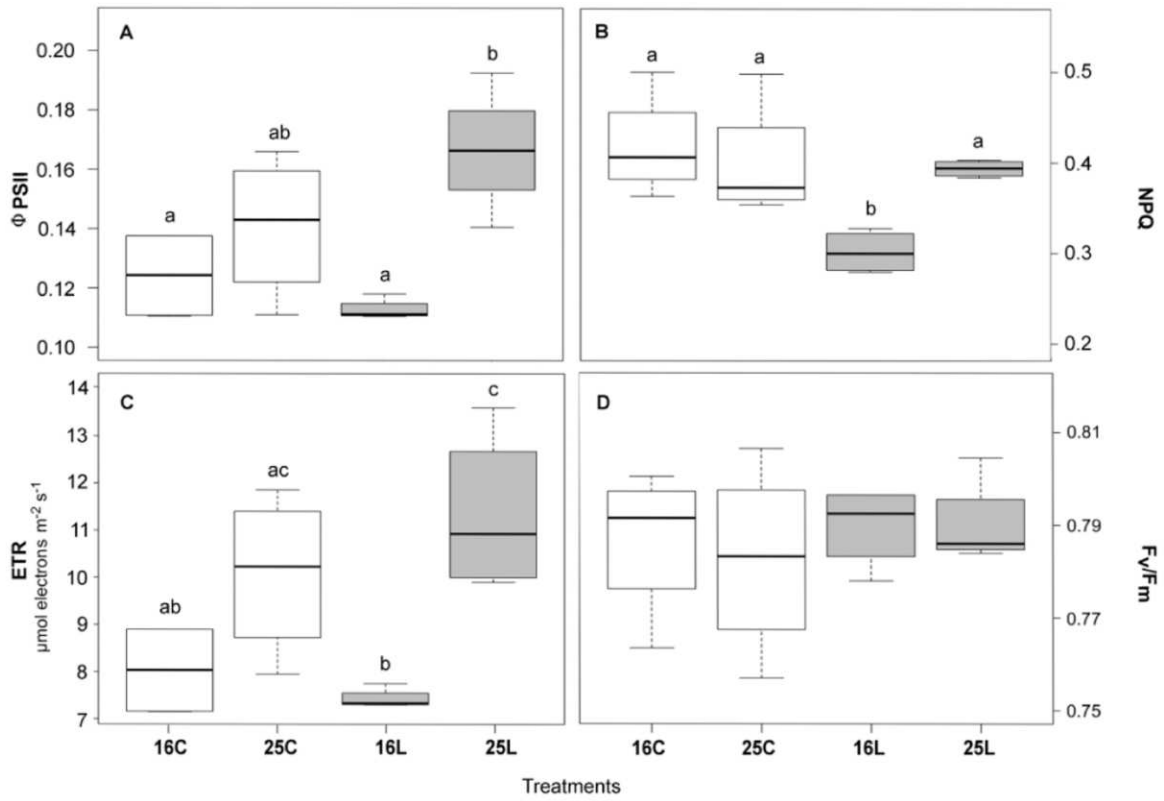


**Fig. 2.** Photochemical descriptors measured in *P. torreyi* leaves (n = 4) in response to the experimental treatments of temperature (16 and 25 °C) and light (C= control and L=low irradiance). Different lower-case letters above bars indicate significant differences ($p < 0.05$) between treatments (see Table A1 in the Appendix). (A) $\Phi_{PSII}$ = Effective quantum yield; (B) NPQ = Non-photochemical quenching; (C) $ETR_{max}$ = Maximum electron transport rate; (D) $F_v/F_m$ = $Maximu_m$ quantum yield. Values are means and standard errors.

minimized by dissipating excess energy as heat via the xanthophyll cycle (XC) in the light-harvesting complexes (LHC), reflected as increments in NPQ (Ralph et al., 2002, Marín-Guirao et al., 2016, Procaccini et al., 2017). In this study, the lowest values of NPQ corresponded to shoots of *P. torreyi* under control temperature, and low-irradiance treatment (i.e., 16 L treatment). Likely, low-light condition prevents the over-energization of the electron transport carriers, and diminishes the production of reactive oxygen species, therefore, alleviating the need to activate alternative electron sinks (Davey et al., 2018). Interestingly, only warming under control irradiance (25 C) lead to a rise in the carotenoids content, which could also be related to activation of the XC, as previously reported in seagrasses when exposed to different stressful conditions (Ralph et al., 2002; York et al., 2013; Sandoval-Gil et al., 2014).

Regardless of the light treatment, shoot respiration (R) was unaffected by the increase in seawater temperature, although it decreased in plants exposed to 16 °C and low light (16 L). In other studies, the behavior of respiration appears to be species- and ecotype-dependent, as well as being influenced by the intensity and duration of the experimental temperature (Collier et al., 2011; Marín-Guirao et al., 2016; Chartrand et al., 2018; Ontoria et al., 2020). The enhancement of respiratory activity is not unusual in seagrasses under increasing water temperature, including *P. torreyi* (Drew, 1979; Bulthuis, 1987; Lee et al., 2007; Koch et al., 2013; Beca-Carretero et al., 2018). It may be necessary to provide catabolic energy required to activate protective and acclimation mechanisms to overcome thermal stress (Marín-Guirao et al., 2017; Nguyen et al., 2020; Costa et al., 2021). Conversely, as observed in this study, the reduction in R has been interpreted as an acclimation mechanism aimed to preserve the whole plant carbon balance under diminished photosynthetic capacities and/or light-limiting conditions (Tanaka, Nakaoka, 2007; Marín-Guirao et al., 2016, 2018). This latter seems to be the case of the 16 L treatment here, since a notable decrease in R, accompanied by an increment in α, resulted in a considerable reduction of $E_c$ compared to control plants. The increased activation energy for R under low irradiance also indicates its strong light dependency. The aggravated effects from MHWs and shading are prone to happen when sub-saturating irradiance prevent seagrasses from offsetting the intensified R caused by warming, which ultimately may result in carbon deficit as previously found in *Zostera muelleri* and *Zostera marina* (Collier et al., 2011; Beca-Carretero et al., 2018; Kim et al., 2020).

*Phyllospadix torreyi* under low-irradiance treatment, and both temperatures notably increased α, and the maximum values were observed in 25 L plants. Seagrasses can regulate functional and structural aspects of photosynthesis to optimize light harvesting under light limitation (Ralph et al., 2007). Notably, increasing α is a typical photo-acclimation mechanism to maximize photosynthetic productivity at sub-saturating light conditions (e.g., Campbell et al., 2003) to maintain positive carbon balances (i.e., Photosynthesis rate > Respiration rate) (Ralph et al., 2007). The subtle increment in the Chl*b:a* molar ratio, representative of the antenna (LHC) size, can be related to increased α, as previously reported for other seagrass species (Longstaff et al., 1999; Campbell et al., 2003; Collier et al., 2009). Additionally, shoots subjected to low light conditions (i.e., 16 L) also showed an increase in $P_{max}$ (but $ETR_{max}$ similar to control). This response seems contradictory to photo-acclimation strategies previously documented in seagrasses exposed to long-term light limitation (weeks to months, e.g., Ruiz and Romero, 2001), and photoadpative properties along the depth gradient (e.g., Marín-Guirao et al., 2016), but shares similarities with other studies based on shorter exposures to reduced light availability. For instance, Bernardeau-Esteller et al. (2015) found a variable response of $P_{max}$ in the green seaweed *Caulerpa cylindracea* subjected to decreasing light

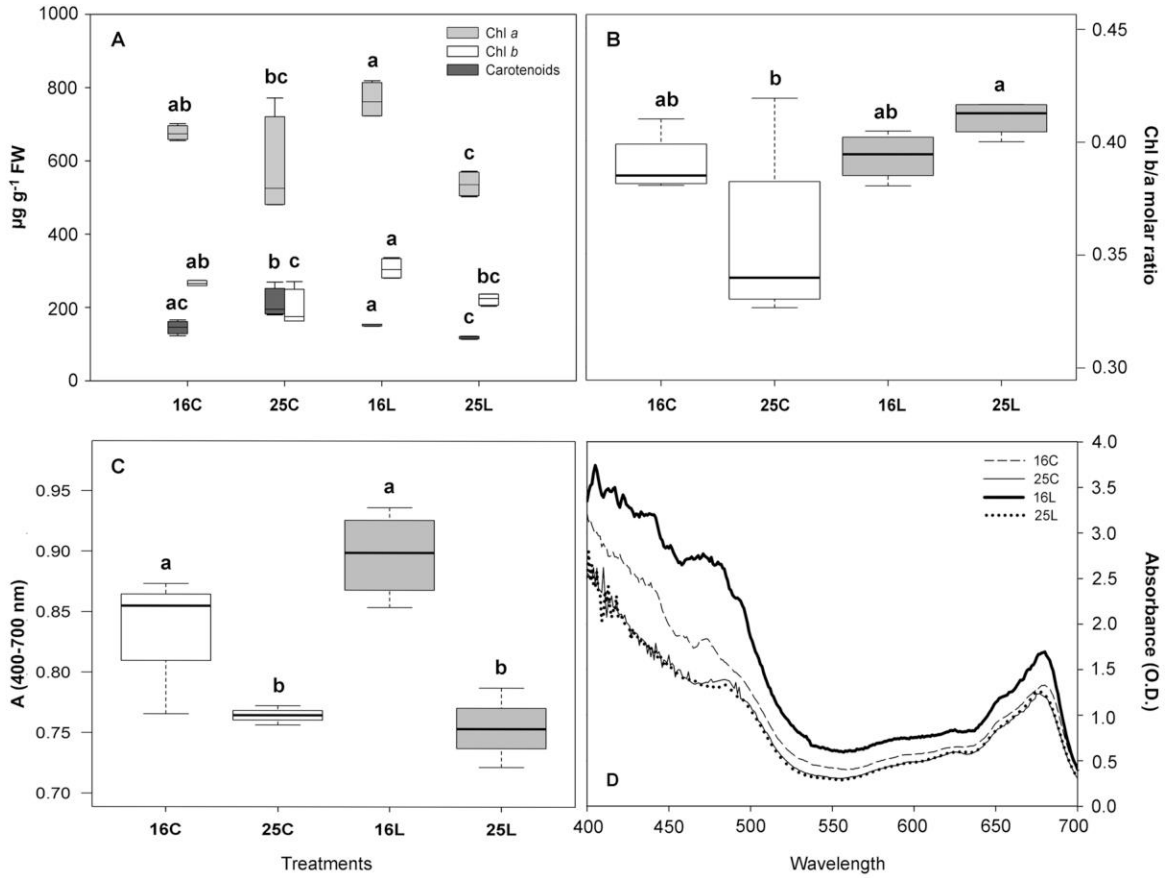


**Fig. 3.** Pigments content and bio-optical properties measured in *P. torreyi* (n = 4) in response to the experimental treatments of temperature (16 and 25 °C) and light (C= control and L=low irradiance). Different lower-case letters above bars indicate significant differences ($p < 0.05$) between treatments (see Table A1 in the Appendix). (A) Chl*a*, Chl*b* and carotenoids; (B) Chl*b*/*a* molar ratio; (C) absorbance (Optical Density) along the PAR range, and (D) integrated absorptance between 400 and 700 nm. Values are means and standard errors.

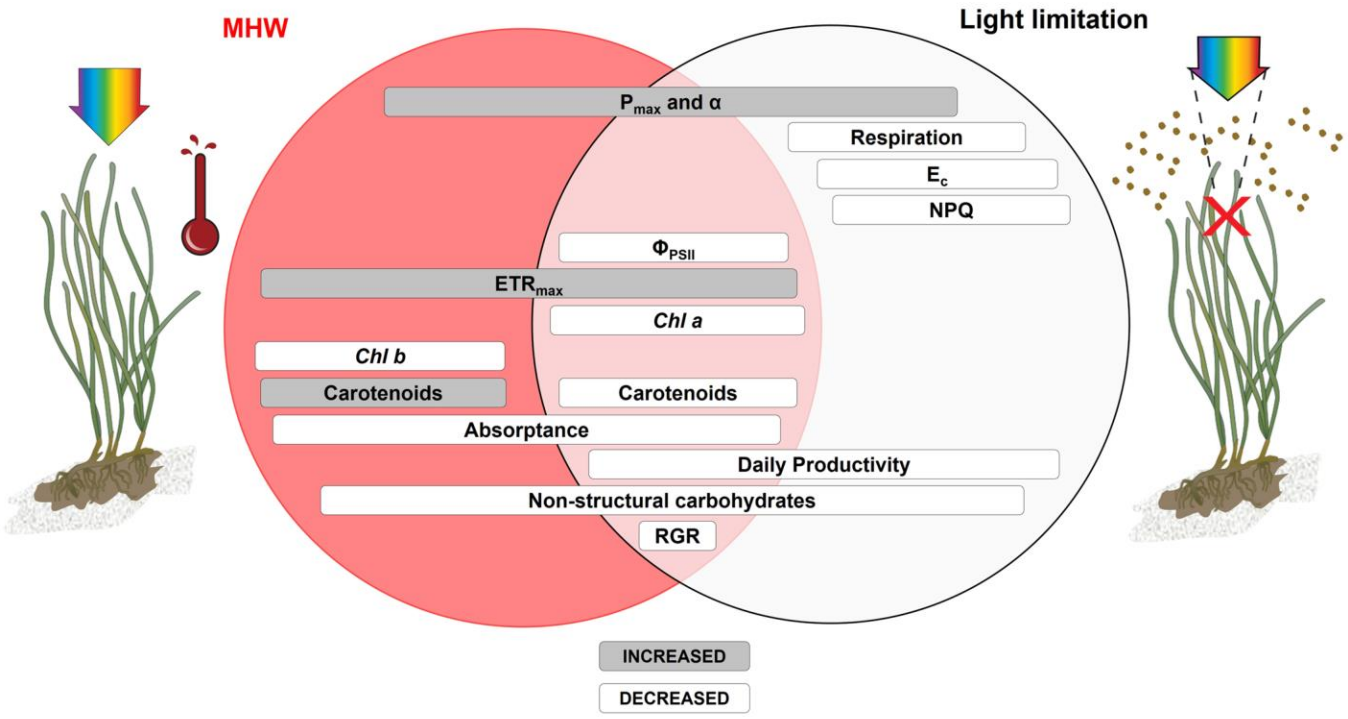


**Fig. 4.** Schematic illustration of the main biological effects showed by *P. torreyi* in response to a simulated MHW (left), light limitation (right) and both factors combined (circles intersection).

**Table 3**
Total phenolic content, total antioxidant capacity and leaf relative growth rate (RGR) measured in *P. torreyi* (n = 4) growing under the different experimental treatments of temperature (16 and 25 °C) and light (C= control and L=low irradiance). Letters indicate significant differences ($p < 0.05$) between treatments according to the two-way ANOVA *post-hoc* tests (see Table A1 in the Appendix). Values are means and standard errors. n.s. not significant.

| Descriptors | Treatments | | | |
|---|---|---|---|---|
| | **16 C** | **25 C** | **16 L** | **25 L** |
| **Total phenolic content** | 16.76 ± 1.14 | 14.64 ± 2.14 | 17.77 ± 1.22 | 17.96 ± 0.93 |
| (mg Eq. GA $g^{-1}$ DW) | ab | a | ab | b |
| **Total antioxidant capacity** | 6.79 ± 0.66 | 6.37 ± 0.93 | 9.27 ± 1.53 | 8.40 ± 2.11 |
| (mg Eq. AA $g^{-1}$ DW) | n.s. | n.s. | n.s. | n.s. |
| **Relative growth rate** | 6.8 ± 0.5 | 7.6 ± 0.1 | 8.2 ± 1.2 | 3.6 ± 0.7 |
| (mg $g^{-1}$ DW $day^{-1}$) | a | a | a | b |

intensities during 7 days. Also, a slight enhancement of $P_{max}$ accompanied by higher α was reported by Umanzor et al. (2020) in kelp juveniles after short-term (7 d) depth acclimation. Attending to these evidences, it is likely that the exposure to low light was too short to promote adjustments of $P_{max}$ in *P. torreyi* under our experimental conditions.

In shoots exposed to increasing seawater temperature, the pigment concentration (mostly Chl*a* and Chl*b*) was slightly reduced, likely caused by their degradation or down-regulation. The effects of warming on photosynthetic pigments are highly variable in seagrasses (Beca-Carretero et al., 2018; Ruocco et al., 2019; Nguyen et al., 2020). In this study, the pigments response pattern of fits well with leaf absorptance but not with photosynthetic parameters. Other studies found similar discrepancies between light acquisition and photosynthetic capacities, likely explained by the regulation of processes at the thylakoid and/or carbon fixation levels, or even by pigments organization determining specific absorption capacities (Sandoval-Gil et al., 2014; Ruocco et al., 2019).

Despite the increment in α and R regulation, a reduced daily net-productivity of photosynthetic tissues was observed in shoots exposed to low irradiance (16 L, 25 L). Under metabolic `energy crisis´, seagrasses may respond by adjusting their clonal structure to acquire or assimilate carbon (e.g., proportion of belowground to aboveground tissues), daily growth rate reduction, or by consuming internal storage reserves to maintain the provision of carbon substrates for vital metabolic processes (Collier et al., 2011; Marín-Guirao et al., 2018; Kim et al., 2020). Accordingly, 16 L and 25 L plants showed lower leaf NSCs than control plants (16 C), although the most severe drop corresponds to the latter (25 L, ~60% lower than control shoots). These responses are consistent with previous studies that report carbohydrates mobilization and/or their consumption among vegetative compartments to maintain metabolic processes to overcome light scarcity (Collier et al., 2009; Statton et al., 2018; Ruocco et al., 2021) or seawater warming (Marín-Guirao et al., 2016, 2018). This ability to alter the plant carbon economy primarily based on fluxes of internal carbon resources, and the respiratory metabolisms of belowground tissues (not quantified in our study), may also be the cause of the significant reduction in carbohydrates detected in plants exposed to seawater warming and saturating irradiances (25 C treatment), even though they exhibited similar daily net-productivity to control plants. Similar patterns have been described in Mediterranean seagrasess in response to warming (Marín-Guirao et al., 2018).

Further, a decrease in leaf growth was only detected in 25 L plants. A previous work with *P. torreyi* reported negative effects of warming and reduced light (independently) on leaf growth, but after a more extended exposure period (20 d) (Drysdale and Barbour, 1975). Venegas (2019) observed massive losses of *P. scouleri* meadows close to its southern distributional limit, likely associated with intense MHWs, hurricanes, and El Nino-Southern Oscillation (ENSO) events, while mesocosm experiments revealed adverse effects by warming on the vegetative productivity of *P. torreyi*. Menge et al. (2020) demonstrated that ocean warming (and also nutrient availability) were the main factors enhancing *P. scouleri* growth along Oregon and California (USA) coastline, while warmer air temperature would have the opposite effect in the intertidal parts of the meadows. Some seagrass species when facing prolonged carbon imbalance, may divert the fixed carbon to storage tissues at the expense of growth, constituting a conservative strategy that prioritizes covering metabolic demands over growth maintenance (Marín-Guirao et al., 2018). Similar findings have been reported for the *genus Zostera*, which despite exhibiting enhanced photosynthetic capacity under low light associated with warm conditions, negative carbon budgets ultimately caused growth reductions (Collier et al., 2011; Beca-Carretero et al., 2018; Kim et al., 2020). In our study, the fall component of activation energy for RGR obtained in the low irradiance treatment is two-fold higher than the average values proposed for marine autotrophs (0.32 ± 0.05 eV; Allen et al., 2005). This suggests that an increasing temperature within the evaluated experimental range may affect the abundance of *P. torreyi* when the competition for light can be a critical factor.

## 5. Conclusions

Overall, our results revealed that short-term increasing temperatures simulating MHWs and the reduction of irradiance to sub-saturating

**Table 4**
Activation energy (Ea) with standard error ( ± SE), coefficient of determination (r2), and significance (p) of fits from Boltzmann–Arrhenius model (central column) for biological rates (left column). Two Sample t-test (right column) was used to evaluate the effect of light-treatments (C= control and L=low irradiance) on the Ea associated to the increment in temperature (from 16° to 25°C). n.s. not significant.

| Biological rates | Light-treatment | Boltzmann–Arrhenius model | | | Two sample t-tests between light-treatments | | |
|---|---|---|---|---|---|---|---|
| | | $E_a$±SE (eV) | $r^2$ | *p* | *t* | *df* | *p-values* |
| **Gross-$P_{max}$** | CI | 0.66 ± 0.02 | 0.981 | < 0.001 | 4.240[b] | 3.229 | < 0.05 |
| | LI | 0.32 ± 0.08 | 0.682 | < 0.05 | | | |
| **R** | CI | n.s. | 0.045 | 0.616 | – | – | – |
| | LI | 0.57 ± 0.09 | 0.752 | < 0.01 | | | |
| **$ETR_{max}$** | CI | 0.18 ± 0.07 | 0.411 | < 0.1 | -1.7459 | 6 | 0.1314 |
| | LI | 0.34 ± 0.06 | 0.807 | < 0.01 | | | |
| **RGR** | CI | 0.14 ± 0.01 | 0.783 | < 0.01 | 4.3587[b] | 3.015 | < 0.05 |
| | LI | 0.71 ± 0.20[a] | 0.589 | < 0.05 | | | |

a Fall component of the thermal response
b Welch two sample *t*-test.

levels produced significant changes in the physiological traits of *Phyllospadix torreyi*. Its photosynthetic machinery was maintained fully functional, and its photosynthetic performance was even enhanced after the experimental exposure to independent and combined treatments, evidenced by higher values of net and gross-$P_{max}$, α, $ETR_{max}$ and $\Phi_{PSII}$. These responses may be related to *P. torreyi's* acclimation to its dynamic environmental niche (i.e. the subtidal and intertidal of exposed shores) where major variations of temperature and irradiance occur. It seems that *P. torreyi* is relatively tolerant to thermal stress compared to other temperate species, which usually have optimal temperatures for photosynthesis below 25 °C (Lee et al., 2007). Also, according to our results *P. torreyi* acclimates to periods of light scarcity by activating different mechanisms to optimize light-harvesting and utilization in photosynthetic processes. On the other hand, we obtained evidence that exposure to a simulated MHW can be harmful to *P. torreyi*, as reflected by a decrease in its internal carbon reserves (i.e. energy status), even when its photostynthetic performance was enhanced. Likely, much of the energy and C-resources acquired through enhanced photosynthetic functioning can be diverted to activate protective and stress responses under warming. Combining this condition with a drastic light reduction can further aggravate the plant's energy status, even at the expense of reduced growth. Overall results support that *P. torreyi* survival could be compromised if MHWs and reduced water transparency persist for more extended periods or more frequently. This claims to maintain optimal coastal water conditions if we aim to preserve this important coastal ecosystem (and its associated socio-ecological services) in the face of climate change.

## CRediT authorship contribution statement

**Manuel Vivanco-Bercovich:** Formal analysis, Writing – original draft, Visualization. **María Dolores Belando-Torrentes:** Formal analysis, Writing – original draft, Visualization. **María Fernanda Figueroa-Burgos:** Conceptualization, Investigation, Formal analysis, Visualization. **Alejandra Ferreira-Arrieta:** Investigation, Formal analysis. **Víctor Macías-Carranza:** Investigation, Formal analysis. **Jessica Anayansi García-Pantoja:** Investigation, Formal analysis. **Alejandro Cabello-Pasini:** Writing – review & editing. **Guillermo Samperio-Ramos:** Formal analysis, Writing – review & editing. **Ricardo Cruz-López:** Writing – review & editing. **Jose Miguel Sandoval-Gil:** Conceptualization, Writing – original draft, Supervision, Project administration, Funding acquisition.

## Declaration of Competing Interest

The authors declare that they have no known competing financial interests or personal relationships that could have appeared to influence the work reported in this paper.

## Acknowledgments

Financial support was provided by the CONACYT-Ciencia Básica Project (A1-S-8382) granted to Sandoval-Gil J.M. Vivanco-Bercovich M. was supported through a CONACYT Doctoral scholarship, and Belando-Torrentes M.D. was granted by a PRODEP postdoctoral fellowship (C.G. I.P. No. 1115/2018–2). We sincerely thank the two anonymous reviewers for their valuable comments that greatly improved this manuscript.

## Appendix A. Supporting information

Supplementary data associated with this article can be found in the online version at doi:10.1016/j.aquabot.2021.103488.

## References

Allen, A.P., Gillooly, J.F., Brown, J.H., 2005. Linking the global carbon cycle to individual metabolism. Funct. Ecol. 19, 202–213. https://doi.org/10.1111/j.1365-2435.2005.00952.x.

Anderson, M.J., Gorley, R.N., Clarke, K.R., 2008, PERMANOVA+ for PRIMER: Guide to Software and Statistical Methods, in: PRIMER-E. Plymouth, UK.

Arafeh-Dalmau, N., Montaño-Moctezuma, G., Martínez, J.A., Beas-Luna, R., Schoeman, D.S., Torres-Moye, G., 2019. Extreme marine heatwaves alter kelp forest community near its equatorward distribution limit. Front. Mar. Sci. 6, 499. https://doi.org/10.3389/fmars.2019.00499.

Beca-Carretero, P., Olesen, B., Marbà, N., Krause-Jensen, D., 2018. Response to experimental warming in northern eelgrass populations: comparison across a range of temperature adaptations. Mar. Ecol. Prog. Ser. 589, 59–72. https://doi.org/10.3354/meps12439.

Beer, S., Bjork, M., Beardall, J., 2014. Photosynthesis in the Marine Environment, Second ed. John Wiley & Sons,.

Bennett, S., Vaquer-Sunyer, R., Jorda, G., Forteza, M., Roca, G., Marbà, N., 2021. Thermal performance reflects evolutionary legacies of seaweeds and seagrasses across a regional climate gradient (preprint). Review. https://doi.org/10.21203/rs.3.rs-228005/v1.

Bernardeau-Esteller, J., Ruiz, J.M., Tomas, F., Sandoval-Gil, J.M., Marín-Guirao, L., 2015. Photoacclimation of *Caulerpa cylindracea*: Light as a limiting factor in the invasion of native Mediterranean seagrass meadows. J. Exp. Mar. Biol. Ecol. 465, 130–141. https://doi.org/10.1016/j.jembe.2014.11.012.

Brown, J.H., Gillooly, J.F., Allen, A.P., Savage, V.M., West, G.B., 2004. Toward a metabolic theory of ecology. Ecology 85, 1771–1789. https://doi.org/10.1890/03-9000.

Bulthuis, D.A., 1987. Effects of temperature on photosynthesis and growth of seagrasses. Aquat. Bot. 27, 27–40. https://doi.org/10.1016/0304-3770(87)90084-2.

Burkholder, J.M., Tomasko, D.A., Touchette, B.W., 2007. Seagrasses and eutrophication. J. Exp. Mar. Biol. Ecol. 350, 46–72. https://doi.org/10.1016/j.jembe.2007.06.024.

Cabello-Pasini, A., Lara-Turrent, C., Zimmerman, R.C., 2002. Effect of storms on photosynthesis, carbohydrate content and survival of eelgrass populations from a coastal lagoon and the adjacent open ocean. Aquat. Bot. 74, 149–164. https://doi.org/10.1016/S0304-3770(02)00076-1.

Campbell, S., Miller, C., Steven, A., Stephens, A., 2003. Photosynthetic responses of two temperate seagrasses across a water quality gradient using chlorophyll fluorescence. J. Exp. Mar. Biol. Ecol. 291, 57–78. https://doi.org/10.1016/S0022-0981(03)00090-X.

Chartrand, K.M., Szabó, Sinutok, M., Rasheed, S., Ralph, M.A., P.J, 2018. Living at the margins – The response of deep-water seagrasses to light and temperature renders them susceptible to acute impacts. Mar. Environ. Res. 136, 126–138. https://doi.org/10.1016/j.marenvres.2018.02.006.

Collier, C.J., Lavery, P.S., Ralph, P.J., Masini, R.J., 2009. Shade-induced response and recovery of the seagrass *Posidonia sinuosa*. J. Exp. Mar. Biol. Ecol. 370, 89–103. https://doi.org/10.1016/j.jembe.2008.12.003.

Collier, C.J., Uthicke, S., Waycott, M., 2011. Thermal tolerance of two seagrass species at contrasting light levels: Implications for future distribution in the Great Barrier Reef. Limnol. Oceanogr. 56, 2200–2210. https://doi.org/10.4319/lo.2011.56.6.2200.

Collier, C.J., Waycott, M., 2014. Temperature extremes reduce seagrass growth and induce mortality. Mar. Pollut. Bull. 83, 483–490. https://doi.org/10.1016/j.marpolbul.2014.03.050.

Collins, M., Knutti, R., Arblaster, J., Dufresne, J.-L., Fichefet, T., Friedlingstein, P., Gao, X., Gutowski, W.J., Johns, T., Krinner, G., Shongwe, M., Tebaldi, C., Weaver, A. J., Wehner, M.F., Allen, M.R., Andrews, T., Beyerle, U., Bitz, C.M., Bony, S., Booth, B. B.B., 2013. Long-term Climate Change: Projections, Commitments and Irreversibility, in: Climate Change 2013 - The Physical Science Basis: Contribution of Working Group I to the Fifth Assessment Report of the Intergovernmental Panel on Climate Change. Cambridge University Press,, pp. 1029–1136.

Cooper, L.W., McRoy, C.P., 1988. Anatomical adaptations to rocky substrates and surf exposure by the seagrass genus *Phyllospadix*. Aquat. Bot. 32, 365–381. https://doi.org/10.1016/0304-3770(88)90108-8.

Costa, M.M., Silva, J., Barrote, I., Santos, R., 2021. Heatwave effects on the photosynthesis and antioxidant activity of the seagrass *Cymodocea nodosa* under contrasting light regimes. Oceans 2, 448–460. https://doi.org/10.3390/oceans2030025.

Davey, P.A., Pernice, M., Ashworth, J., Kuzhiumparambil, U., Szabó, M., Dolferus, R., Ralph, P.J., 2018. A new mechanistic understanding of light-limitation in the seagrass *Zostera muelleri*. Mar. Environ. Res. 134, 55–67. https://doi.org/10.1016/j.marenvres.2017.12.012.

Davison, I.R., 1991. Environmental effects on algal photosynthesis: temperature. J. Phycol. 27, 2–8.

Dean, T., 1985. The temporal and spatial distribution of underwater quantum irradiation in a southern California kelp forest. Estuar. Coast. Shelf Sci. 21, 835–844. https://doi.org/10.1016/0272-7714(85)90077-0.

Delgadillo-Hinojosa, F., Félix-Bermúdez, A., Torres-Delgado, E.V., Durazo, R., Camacho-Ibar, V., Mejía, A., Ruiz, M.C., Linacre, L., 2020. Impacts of the 2014–2015 Warm-Water Anomalies on Nutrients, Chlorophyll-a and Hydrographic Conditions in the Coastal Zone of Northern Baja California. J. Geophys. Res. Oceans 125, e2020JC016473. https://doi.org/10.1029/2020JC016473.

Dell, A.I., Pawar, S., Savage, V.M., 2011. Systematic variation in the temperature dependence of physiological and ecological traits. Proc. Natl. Acad. Sci. 108, 10591–10596. https://doi.org/10.1073/pnas.1015178108.

Den Hartog, C., 1970, The sea-grasses of the world. N.-Holl. Amst.

Dennison, W., 1990. Chlorophyll content. In: Phillips, R.C., McRoy, C.P. (Eds.), Seagrass Research Methods. UNESCO, Paris (France).
Dorantes-Gilardi, M., Rivas, D., 2019. Effects of the 2013–2016 Northeast Pacific warm anomaly on physical and biogeochemical variables off northwestern Baja California, derived from a numerical NPZD ocean model. Deep Sea Res. Part II Top. Stud. Oceano 169–170. https://doi.org/10.1016/j.dsr2.2019.104668.
Drew, E.A., 1979. Physiological aspects of primary production in seagrasses. Aquat. Bot. 7, 139–150. https://doi.org/10.1016/0304-3770(79)90018-4.
Drysdale, F.R., Barbour, M.G., 1975. Response of the marine angiosperm *Phyllospadix torreyi* to certain environmental variables: A preliminary study. Aquat. Bot. 1, 97–106. https://doi.org/10.1016/0304-3770(75)90015-7.
Dubois, M., Gilles, K.A., Hamilton, J.K., Rebers, P.A., Smith, F., 1956. Colorimetric method for determination of sugars and related substances. Anal. Chem. 28, 350–356.
Erftemeijer, P.L.A., Robin Lewis, R.R., 2006. Environmental impacts of dredging on seagrasses: A review. Mar. Pollut. Bull. 52, 1553–1572. https://doi.org/10.1016/j.marpolbul.2006.09.006.
Franssen, S.U., Gu, J., Winters, G., Huylmans, A.-K., Wienpahl, I., Sparwel, M., Coyer, J. A., Olsen, J.L., Reusch, T.B.H., Bornberg-Bauer, E., 2014. Genome-wide transcriptomic responses of the seagrasses *Zostera marina* and *NanoZostera noltii* under a simulated heatwave confirm functional types. Mar. Genomics 15, 65–73. https://doi.org/10.1016/j.margen.2014.03.004.
Fraser, M.W., Kendrick, G.A., Statton, J., Hovey, R.K., Zavala-Perez, A., Walker, D.I., 2014. Extreme climate events lower resilience of foundation seagrass at edge of biogeographical range. J. Ecol. 102, 1528–1536. https://doi.org/10.1111/1365-2745.12300.
García-Pantoja, J.A., Ruiz-Montoya, L., Sandoval-Gil, J.M., Vivanco-Bercovich, M.V., Ferreira-Arrieta, A., Zertuche-González, J.A., Guzmán-Calderón, J.M., Norzagaray-López Orión; Samperio-Ramos, G., Montaño-Moctezuma, G., Hernández-Ayón, M., 2020. Fijación neta de carbono por pastos marinos (*Phyllospadix* spp.) en una isla del Pacífico Mexicano, in: Estado Actual Del Conocimiento Del Ciclo Del Carbono y Sus Interacciones En México: Síntesis a 2020. Síntesis Nac. Programa Mex. Del. Carbon En. Colab. con la Univ. Autónoma Metrop. -Xochim., Texcoco, Estado De. México, México 602.
Gillooly, J.F., Brown, J.H., West, G.B., Savage, V.M., Charnov, E.L., 2001. Effects of size and temperature on metabolic rate. science 293, 2248–2251. https://doi.org/10.1126/science.1061967.
Hammer, O., 2001. PAST: Paleontological statistics software package for education and data analysis palaeontologia electronica. Httppalaeo-Electron 1 (Accessed).
Hobday, A.J., Alexander, L.V., Perkins, S.E., Smale, D.A., Straub, S.C., Oliver, E.C.J., Benthuysen, J.A., Burrows, M.T., Donat, M.G., Feng, M., Holbrook, N.J., Moore, P.J., Scannell, H.A., Sen Gupta, A., Wernberg, T., 2016. A hierarchical approach to defining marine heatwaves. Prog. Oceanogr. 141, 227–238. https://doi.org/10.1016/j.pocean.2015.12.014.
Kendrick, G.A., Nowicki, R.J., Olsen, Y.S., Strydom, S., Fraser, M.W., Sinclair, E.A., Statton, J., Hovey, R.K., Thomson, J.A., Burkholder, D.A., McMahon, K.M., Kilminster, K., Hetzel, Y., Fourqurean, J.W., Heithaus, M.R., Orth, R.J., 2019. A systematic review of how multiple stressors from an extreme event drove ecosystem-wide loss of resilience in an iconic seagrass community. Front. Mar. Sci. 6, 455. https://doi.org/10.3389/fmars.2019.00455.
Kim, M., Qin, L.-Z., Kim, S.H., Song, H.-J., Kim, Y.K., Lee, K.-S., 2020. Influence of Water Temperature Anomalies on the Growth of *Zostera marina* Plants Held Under High and Low Irradiance Levels. Estuaries Coasts 43, 463–476. https://doi.org/10.1007/s12237-019-00578-2.
Koch, M., Bowes, G., Ross, C., Zhang, X.-H., 2013. Climate change and ocean acidification effects on seagrasses and marine macroalgae. Glob. Change Biol. 19, 103–132. https://doi.org/10.1111/j.1365-2486.2012.02791.x.
Lee, K.-S., Park, S.R., Kim, Y.K., 2007. Effects of irradiance, temperature, and nutrients on growth dynamics of seagrasses: A review. J. Exp. Mar. Biol. Ecol. 350, 144–175. https://doi.org/10.1016/j.jembe.2007.06.016.
Lichtenthaler, H.K., Wellburn, A.R., 1983. Determinations of total carotenoids and chlorophylls a and b of leaf extracts in different solvents. Biochem. Soc. Trans. 11, 591–592. https://doi.org/10.1042/bst0110591.
Longstaff, B.J., Loneragan, N.R., O'Donohue, M.J., Dennison, W.C., 1999. Effects of light deprivation on the survival and recovery of the seagrass *Halophila ovalis* (R.Br.) Hook. J. Exp. Mar. Biol. Ecol. 234, 1–27. https://doi.org/10.1016/S0022-0981(98)00137-3.
Marbà, N., Duarte, C.M., 2010. Mediterranean warming triggers seagrass (*Posidonia oceanica*) shoot mortality. Glob. Change Biol. 16, 2366–2375. https://doi.org/10.1111/j.1365-2486.2009.02130.x.
Marín-Guirao, L., Bernardeau-Esteller, J., García-Muñoz, R., Ramos, A., Ontoria, Y., Romero, J., Pérez, M., Ruiz, J.M., Procaccini, G., 2018. Carbon economy of Mediterranean seagrasses in response to thermal stress. Mar. Pollut. Bull. 135, 617–629. https://doi.org/10.1016/j.marpolbul.2018.07.050.
Marín-Guirao, L., Entrambasaguas, L., Dattolo, E., Ruiz, J.M., Procaccini, G., 2017. Molecular mechanisms behind the physiological resistance to intense transient warming in an iconic marine plant. Front. Plant Sci. 8, 1142. https://doi.org/10.3389/fpls.2017.01142.
Marín-Guirao, L., Ruiz, J.M., Dattolo, E., Garcia-Munoz, R., Procaccini, G., 2016. Physiological and molecular evidence of differential short-term heat tolerance in Mediterranean seagrasses. Sci. Rep. 6, 28615. https://doi.org/10.1038/srep28615.
Menge, B.A., Close, S.L., Hacker, S.D., Nielsen, K.J., Chan, F., 2020. Biogeography of macrophyte productivity: Effects of oceanic and climatic regimes across spatiotemporal scales. Limnol. Oceanogr. lno 11635. https://doi.org/10.1002/lno.11635.
Moulton, O.M., Hacker, S.D., 2011. Congeneric variation in surfgrasses and ocean conditions influence macroinvertebrate community structure. Mar. Ecol. Prog. Ser. 433, 53–63. https://doi.org/10.3354/meps09180.
Nguyen, H.M., Kim, M., Ralph, P.J., Marín-Guirao, L., Pernice, M., Procaccini, G., 2020. Stress memory in seagrasses: first insight into the effects of thermal priming and the role of epigenetic modifications. Front. Plant Sci. 11, 494. https://doi.org/10.3389/fpls.2020.00494.
Nguyen, H.M., Ralph, P.J., Marín-Guirao, L., Pernice, M., Procaccini, G., 2021. Seagrasses in an era of ocean warming: a review. Biol. Rev. https://doi.org/10.1111/brv.12736.
Olivé, I., Vergara, J.J., Pérez-Lloréns, J.L., 2013. Photosynthetic and morphological photoacclimation of the seagrass *Cymodocea nodosa* to season, depth and leaf position. Mar. Biol. 160, 285–297. https://doi.org/10.1007/s00227-012-2087-2.
Ontoria, Y., Webster, C., Said, N., Ruiz, J.M., Pérez, M., Romero, J., McMahon, K., 2020. Positive effects of high salinity can buffer the negative effects of experimental warming on functional traits of the seagrass *Halophila ovalis*. Mar. Pollut. Bull. 158, 111404 https://doi.org/10.1016/j.marpolbul.2020.111404.
Padfield, D., 2017. Scaling the effects of warming on metabolism from organisms to ecosystems. Ph.D. thesis, University of Exeter.
Price, C.A., Gilooly, J.F., Allen, A.P., Weitz, J.S., Niklas, K.J., 2010. The metabolic theory of ecology: prospects and challenges for plant biology. N. Phytol. 188, 696–710. https://doi.org/10.1111/j.1469-8137.2010.03442.x.
Procaccini, G., Ruocco, M., Marín-Guirao, L., Dattolo, E., Brunet, C., D'Esposito, D., Lauritano, C., Mazzuca, S., Serra, I.A., Bernardo, L., Piro, A., Beer, S., Björk, M., Gullström, M., Buapet, P., Rasmusson, L.M., Felisberto, P., Gobert, S., Runcie, J.W., Silva, J., Olivé, I., Costa, M.M., Barrote, I., Santos, R., 2017. Depth-specific fluctuations of gene expression and protein abundance modulate the photophysiology in the seagrass *Posidonia oceanica*. Sci. Rep. 7, 42890. https://doi.org/10.1038/srep42890.
Core Team, R., 2020. R: A language and environment for statistical computing. R Found. Stat. Comput.
Ralph, P.J., Durako, M.J., Enríquez, S., Collier, C.J., Doblin, M.A., 2007. Impact of light limitation on seagrasses. J. Exp. Mar. Biol. Ecol. 350, 176–193. https://doi.org/10.1016/j.jembe.2007.06.017.
Ralph, P.J., Polk, S.M., Moore, K.A., Orth, R.J., Smith, W.O., 2002. Operation of the xanthophyll cycle in the seagrass *Zostera marina* in response to variable irradiance. J. Exp. Mar. Biol. Ecol. 271, 189–207. https://doi.org/10.1016/S0022-0981(02)00047-3.
Ramírez-García, P., Lot, A., Duarte, C., Terrados, J., Agawin, N., 1998. Bathymetric distribution, biomass and growth dynamics of intertidal *Phyllospadix scouleri* and *Phyllospadix torreyi* in Baja California (Mexico). Mar. Ecol. Prog. Ser. 173, 13–23. https://doi.org/10.3354/meps173013.
Ramírez-García, P., Terrados, J., Ramos, F., Lot, A., Ocaña, D., Duarte, C.M., 2002. Distribution and nutrient limitation of surfgrass, *Phyllospadix scouleri* and *Phyllospadix torreyi*, along the Pacific coast of Baja California (México). Aquat. Bot. 74, 121–131. https://doi.org/10.1016/S0304-3770(02)00050-5.
Ruiz, J.M., Romero, J., 2001. Effects of in situ experimental shading on the Mediterranean seagrass *Posidonia oceanica*. Mar. Ecol. Prog. Ser. 215, 107–120. https://doi.org/10.3354/meps215107.
Ruiz-Montoya, L., Sandoval-Gil, J.M., Belando-Torrentes, M.D., Vivanco-Bercovich, M., Cabello-Pasini, A., Rangel-Mendoza, L.K., Maldonado-Gutiérrez, A., Ferreira-Arrieta, A., Guzmán-Calderón, J.M., 2021. Ecophysiological responses and self-protective canopy effects of surfgrass (*Phyllospadix torreyi*) in the intertidal. Mar. Environ. Res. 172, 105501 https://doi.org/10.1016/j.marenvres.2021.105501.
Ruocco, M., De Luca, P., Marín-Guirao, L., Procaccini, G., 2019. Differential leaf age-dependent thermal plasticity in the keystone seagrass *Posidonia oceanica*. Front. Plant Sci. 10, 1556. https://doi.org/10.3389/fpls.2019.01556.
Ruocco, M., Entrambasaguas, L., Dattolo, E., Milito, A., Marín-Guirao, L., Procaccini, G., 2021. A king and vassals' tale: Molecular signatures of clonal integration in *Posidonia oceanica* under chronic light shortage. J. Ecol. 109, 294–312. https://doi.org/10.1111/1365-2745.13479.
Rutherford, A., 2001. Introducing ANOVA and ANCOVA: a GLM approach. Sage.
Sabeena Farvin, K.H., Jacobsen, C., 2013. Phenolic compounds and antioxidant activities of selected species of seaweeds from Danish coast. Food Chem. 138, 1670–1681. https://doi.org/10.1016/j.foodchem.2012.10.078.
Samperio-Ramos, G., Olsen, Y.S., Tomas, F., Marbà, N., 2015. Ecophysiological responses of three Mediterranean invasive seaweeds (*Acrothamnion preissii, Lophocladia lallemandii* and *Caulerpa cylindracea*) to experimental warming. Mar. Pollut. Bull. 96, 418–423. https://doi.org/10.1016/j.marpolbul.2015.05.024.
Sandoval-Gil, J.M., Ruiz, J.M., Marín-Guirao, L., Bernardeau-Esteller, J., Sánchez-Lizaso, J.L., 2014. Ecophysiological plasticity of shallow and deep populations of the Mediterranean seagrasses *Posidonia oceanica* and *Cymodocea nodosa* in response to hypersaline stress. Mar. Environ. Res. 95, 39–61. https://doi.org/10.1016/j.marenvres.2013.12.011.
Schlegel, R.W., 2020, Marine Heatwave Tracker. <http://www.marineheatwaves.org/tracker.html>
Sen Gupta, A., Thomsen, M., Benthuysen, J.A., Hobday, A.J., Oliver, E., Alexander, L.V., Burrows, M.T., Donat, M.G., Feng, M., Holbrook, N.J., Perkins-Kirkpatrick, S., Moore, P.J., Rodrigues, R.R., Scannell, H.A., Taschetto, A.S., Ummenhofer, C.C., Wernberg, T., Smale, D.A., 2020. Drivers and impacts of the most extreme marine heatwave events. Sci. Rep. 10, 19359. https://doi.org/10.1038/s41598-020-75445-3.
Serrano, O., Arias-Ortiz, A., Duarte, C.M., Kendrick, G.A., Lavery, P.S., 2021. Impact of marine heatwaves on seagrass ecosystems. In: Ecosystem Collapse and Climate Change. Springer, pp. 345–364.

Shelton, A.O., 2010. Temperature and community consequences of the loss of foundation species: Surfgrass (*Phyllospadix* spp., Hooker) in tidepools. J. Exp. Mar. Biol. Ecol. 391, 35–42. https://doi.org/10.1016/j.jembe.2010.06.003.

Shibata, K., 1959. Spectrophotometry of translucent biological materials-opal glass transmission method. Methods Biochem. Anal. 7, 77–109.

Singleton, V.L., Rossi, J.A., 1965. Colorimetry of total phenolics with phosphomolybdic-phosphotungstic acid reagents. Am. J. Enol. Vitic. 16, 144–158.

Smale, D.A., Wernberg, T., Oliver, E.C.J., Thomsen, M., Harvey, B.P., Straub, S.C., Burrows, M.T., Alexander, L.V., Benthuysen, J.A., Donat, M.G., Feng, M., Hobday, A. J., Holbrook, N.J., Perkins-Kirkpatrick, S.E., Scannell, H.A., Sen Gupta, A., Payne, B. L., Moore, P.J., 2019. Marine heatwaves threaten global biodiversity and the provision of ecosystem services. Nat. Clim. Change 9, 306–312. https://doi.org/10.1038/s41558-019-0412-1.

Statton, J., McMahon, K., Lavery, P., Kendrick, G.A., 2018. Determining light stress responses for a tropical multi-species seagrass assemblage. Mar. Pollut. Bull. 128, 508–518. https://doi.org/10.1016/j.marpolbul.2018.01.060.

Stockbridge, J., Jones, A.R., Gillanders, B.M., 2020. A meta-analysis of multiple stressors on seagrasses in the context of marine spatial cumulative impacts assessment. Sci. Rep. 10, 11934. https://doi.org/10.1038/s41598-020-68801-w.

Tanaka, Y., Nakaoka, M., 2007. Interspecific variation in photosynthesis and respiration balance of three seagrasses in relation to light availability. Mar. Ecol. Prog. Ser. 350, 63–70. https://doi.org/10.3354/meps07103.

Terrados, J., Williams, S., 1997. Leaf versus root nitrogen uptake by the surfgrass *Phyllospadix torreyi*. Mar. Ecol. Prog. Ser. 149, 267–277. https://doi.org/10.3354/meps149267.

Umanzor, S., Ramírez-García, M.M., Sandoval-Gil, J.M., Zertuche-González, J.A., Yarish, C., 2020. Photoacclimation and Photoprotection of Juvenile Sporophytes of *Macrocystis pyrifera* (Laminariales, Phaeophyceae) Under High-light Conditions During Short-term Shallow-water Cultivation1. J. Phycol. 56, 380–392. https://doi.org/10.1111/jpy.12951.

Underwood, A.J., Underwood, A.L., Underwood, A.J., J, W.A., Cambridge, U., 1997. Experiments in Ecology: Their Logical Design and Interpretation Using Analysis Of Variance. Cambridge University Press.

Vásquez-Elizondo, R.M., Legaria-Moreno, L., Pérez-Castro, M.Á., Krämer, W.E., Scheufen, T., Iglesias-Prieto, R., Enríquez, S., 2017. Absorptance determinations on multicellular tissues. Photosynth. Res. 132, 311–324. https://doi.org/10.1007/s11120-017-0395-6.

Venegas, K., 2019, Distribución espacio-temporal y efecto de la temperatura en praderas de Phyllospadix scouleri en tres localidades de B.C.S. PhD thesis. Universidad Autónoma de Baja California Sur.

Wei, X., Li, K., Kilpatrick, T., Wang, M., Xie, S., 2021. Large-scale conditions for the record-setting Southern California marine heatwave of August 2018. Geophys. Res. Lett. 48. https://doi.org/10.1029/2020GL091803.

York, P.H., Gruber, R.K., Hill, R., Ralph, P.J., Booth, D.J., Macreadie, P.I., 2013. Physiological and Morphological Responses of the Temperate Seagrass *Zostera muelleri* to Multiple Stressors: Investigating the Interactive Effects of Light and Temperature. PLoS ONE 8, e76377. https://doi.org/10.1371/journal.pone.0076377.

Zieman, J.C., 1974. Methods for the study of the growth and production of turtle grass, *Thalassia testudinum* König. Aquaculture 4, 139–143. https://doi.org/10.1016/0044-8486(74)90029-5.

# CAPÍTULO II – Respuestas ecofisiológicas, crecimiento y capacidad de recuperación de *Phyllospadix scouleri* frente a la exposición a olas de calor marinas consecutivas

**Increased heatwave recurrence will aggravate thermal stress in the surfgrass *Phyllospadix scouleri***

**Authors:** Manuel Vivanco-Bercovich[a#], Jose Miguel Sandoval-Gil*[a#],

Paula Bonet-Meliá[a], Alejandro Cabello-Pasini[a], Raquel Muñiz-Salazar[a], Leonardo Ruiz Montoya[a], Nadine Schubert[c], Lázaro Marín-Guirao[b], Gabriele Procaccini[d], Alejandra Ferreira-Arrieta[a]

[a]Universidad Autónoma de Baja California (UABC), Instituto de Investigaciones Oceanológicas (IIO), Marine Botany Research Group, Ensenada, Baja California, México

[b]Instituto Español de Oceanografía (IEO), Centro Oceanográfico de Murcia, Seagrass Ecology Group, C/Varadero s/n, 30740 San Pedro del Pinatar, Murcia, Spain.

[c]CCMAR – Center of Marine Sciences, University of Algarve, Faro, Portugal.

[d]Stazione Zoologica Anton Dohrn, Villa Comunale, Naples, Italy.

# These authors contributed equally to the manuscript.

***Corresponding author:** Jose Miguel Sandoval Gil, Universidad Autónoma de Baja California (UABC), Instituto de Investigaciones Oceanológicas,

Carretera Ensenada-Tijuana No. 3917, Fraccionamiento Playitas

C.P. 22860 en Ensenada, Baja California, México. Tel: +52 1 646 138 9598

jmsandovalgil@gmail.com

Orchid ID: **0000-0001-8973-0306**

**ABSTRACT**

The surfgrass *Phyllospadix scouleri*, a scarcely studied species, constitutes highly productive meadows along the intertidal and subtidal rocky shores of the Pacific coast of North America, where marine heatwaves (MHWs) have caused substantial alterations in marine ecosystems. This experimental study assessed the effects of consecutive MHWs and recovery phases on critical ecophysiological descriptors of *P. scouleri*. Our results revealed a progressive deterioration of the plant overall physiological status undergoing repeated warming events. Photosynthetic parameters (Net- and Gross-$P_{max}$, $F_v/F_m$, $\Phi_{PSII}$, ETR) showed negative effects during the recovery phase after the first simulated MHW event and reached minimum values after the second event. These declines were preceded by elevated oxidative damage and coincided with marked peaks of NPQ, evidencing the induction of photoprotective mechanisms. Also, nitrate uptake rates were affected during heatwaves or subsequent recovery period. By contrast, non-structural carbohydrates and relative growth rate did not show significant responses during the experimental period. Our results highlight the importance of recovery periods for physiological recuperation/compensation, and call attention to the accumulative detrimental effects that consecutive intense MHWs may exert in seagrasses, potentially compromising their important ecosystem services.

***Keywords:*** thermal stress, consecutive, recovery, ecophysiology, climate change, surfgrass

**Abbreviations:** MHW: Marine heatwaves, Net-$P_{max}$: Net maximum photosynthetic, Gross-$P_{max}$: Gross maximum photosynthetic, R: dark respiration, α: Photosynthetic efficiency, $E_c$: Compensation Irradiance, $E_k$: Saturating irradiance, $F_v/F_m$: Maximum quantum yield, ETR =

Electron transport rate, $\Phi_{PSII}$: Effective quantum yield, NPQ: Non-photochemical quenching, Chl*a*: Chlorophyll *a* content, Chl*b*: Chlorophyll *b* content, Chlb/a ratio: Chlorophyll *b/a* ratio , Carot.: Carotenoids content, N: Nitrogen content, $\delta^{15}N$: Nitrogen isotopic signal ($^{15}N/^{14}N$), NSC: Non-structural carbohydrates, RGR: Relative growth rate.

## 1. Introduction

Marine ecosystems are being threatened globally by more frequent and intense marine heatwaves (MHWs) (Fox-Kemper et al., 2021). Seagrasses are ranked as one of the most valuable marine biological systems worldwide and have been severely impacted by ocean warming and MHWs globally (de los Santos et al., 2020; Strydom et al., 2020; Garrabou et al., 2022). MHWs have the potential to negatively impact seagrass vitality and community structure, and to cause large die-off events, thus threatening the ecological services and goods they provide (Serrano et al., 2021; Unsworth et al., 2022).

The interaction between seagrasses and raising temperatures has received considerable attention in the last decade (see reviews by Koch et al. (2013), Duarte et al. (2018) and Nguyen et al. (2021a)). The tolerance of seagrasses to warming depends mainly on complex interactions among their stress responses (i.e., phenotypic plasticity) at different organizational levels (e.g., molecular, physiological, morphological, community) (Deguette et al., 2022; Pazzaglia et al., 2021). Interspecifically, the thermal tolerance of seagrasses varies depending on the thermal evolutionary history of the species, with tropical species generally being more tolerant than temperate species (Hyndes et al., 2016). On the other hand, ecotypes and genotypes of a species may also exhibit different capacities for thermal adaptation and acclimation depending on the specific temperature regime they naturally experience in their native environment (e.g., Marín-Guirao et al., 2016, 2018; Nguyen et al., 2021b; Stipcich et al., 2022). In general, symptoms of heat stress that usually occur when warming exceeds the metabolic tolerance of plants are a decrease in photosynthetic performance, depletion of internal carbon stocks and reduced plant growth (e.g., Collier et al., 2011; Collier & Waycott, 2014; Marín-Guirao et al., 2018).

The effects of MHWs on seagrasses have been usually studied in controlled experiments based on the exposure to one single warming event (e.g., Costa et al., 2021; Nguyen et al., 2021a; Deguette et al., 2022; Vivanco-Bercovich et al., 2022). However, these experimental approaches overlook the fact that seagrass meadows can be repeatedly impacted by MHWs, as the frequency of these events is rising globally (Laufkötter et al., 2020; Fox-Kemper et al., 2021). The effects of consecutive warming events have only been addressed in few recent manipulative studies (e.g., DuBois et al., 2020; Nguyen et al., 2020; Saha et al., 2020; Pazzaglia et al., 2022a). Pre-exposure of seagrasses to mild temperature stress could act as `eu-stress´ (*sensu* Lichtenthaler (1998)) promoting physiological strengthening (and/or inducing a stress memory) and thermo-tolerance to successive MHWs, as documented for *Posidonia australis, P. oceanica* and *Zostera muelleri* (Nguyen et al., 2020; Pazzaglia et al., 2022a). Interestingly, these studies revealed that pre-heated plants exhibited better physiological performance and growth under heat stress than shoots not previously exposed to heat. Conversely, three consecutive MHWs with increasing intensity resulted in a cumulative growth weakening in *Zostera marina* (Saha et al., 2020). Possibly, the intensity of the first warming event could determine the magnitude and direction of seagrass responses to subsequent MHWs. Hence, assessing the effects of consecutive and intense MHWs can provide critical knowledge to better understand the resilience of seagrasses to thermal stress associated with the ongoing climate change.

Surfgrasses (*Phyllospadix scouleri* Hooker and *Phyllospadix torreyi* S.Watson) are the only seagrasses able to colonize wave exposed rocky substrates (Cooper & McRoy, 1988), where they regulate important coastal physico-chemical and biological processes, and provide food and shelter for a number of marine organisms (Shelton, 2010; Moulton & Hacker, 2011). Surfgrasses form extensive and highly productive meadows along the Pacific coast of North America, from

Alaska (USA) to Baja California Sur in Mexico (Den Hartog, 1970; Ramírez-García et al., 2002; Garcia-Pantoja et al., 2020). The Baja California Peninsula Pacific coastline, under the southernmost influence of the California Current System (Durazo, 2015), is susceptible to drastic and unpredictable ecological and economic impacts due to climate change (Xiu et al., 2018; Sunday et al., 2022). In this region, episodic thermal anomalies such as ENSO and MHWs (e.g., "the Blob" in 2014-2016, Sen Gupta et al., 2020) have caused major transformations in kelp forest ecosystems deleterious effects at physiological and community levels in kelps species (Arafeh-Dalmau et al., 2019; Michaud et al., 2022), but documented cases for surfgrasses are extremely scarce. For instance, Venegas (2019) reported the disappearance of intertidal *P. scouleri* meadows near its southern distribution limit in Baja California Sur after the incidence of strong MHWs and hurricanes. In contrast, Menge et al. (2020) reported increased growth rates with increasing intertidal water temperature on intertidal *P. scouleri* populations along the Oregon and California (USA) coastline during the period 2008-2013.

Experimentally, only a few studies (Drysdale & Barbour, 1975; Drew 1979; Ruiz-Montoya et al., 2021; Vivanco-Bercovich et al., 2022) have assessed the physiological responses of *P. torreyi* under warming conditions, while the thermal metabolic tolerance of the sister species *P. scouleri* remains largely unknown to date. Furthermore, most studies on surfgrasses have been conducted using intertidal plants, which may respond to warming differently from subtidal plants due to the specific regimes of environmental variables (including temperature) they naturally experience. While intertidal *Phyllospadix* plants can be exposed to a temperature rise from 22 to ~40°C within a few minutes-hours due to periodic tidal cycles (Ruiz-Montoya et al., 2021), subtidal plants are subjected to a much narrower range of daily temperature variation (e.g., usually < 3°C at the donor meadow of this study). Yet, subtidal populations represent the largest and most

dense portion of surfgrass meadows (Garcia-Pantoja et al., 2020) and have been suggested to play a critical role for plant recruitment in the intertidal surfgrass belt (Williams, 1995). Understanding the capacity of subtidal surfgrasses to withstand realistic thermal disturbance regime associated to climate change is therefore critical for anticipating the future of these important foundation species and their related ecosystems.

In this study we have conducted a manipulative mesocosm experiment to assess the ability of subtidal plants of *P. scouleri* to cope with a realistic regime of thermal perturbations associated with climate change. The experiment simulated two consecutive marine heatwaves and studied plant responses using a broad set of ecophysiological descriptors (photobiology, nutrient acquisition, oxidative stress, and growth) at the end of each thermal event and its respective recovery period. In this experiment, we aim to provide the first insights into the effects of anomalous warming events on subtidal *P. scouleri* plants and to determine whether these effects are aggravated or alleviated when the warming event recurs. This information will allow for predictions regarding the potential consequences for the seagrass community and their future trajectories.

## 2. Material and methods

### *Plant collection, field conditions and experimental design*

*Phyllospadix scouleri* was sampled in August 2020 in a meadow located on Todos Santos Island (Ensenada, Baja California, Mexico, 31°48'25.66"N, 116°47'46.41"O), belonging to the Pacific Islands Biosphere Reserve (Fig. 1A-C). The meadow is located in the infralittoral zone (~5 m below MHWL) of a rocky and wave-exposed shoreline, exposed to an annual seawater

temperature range between 15-20ºC (Schlegel, 2020). Plants were detached from their substrate by slowly inserting a plastic spatula between the rock and the plant´s adhesion disc (similar to a holdfast, formed by roots, rhizomes, and adhesive mucilage), while carefully pulling the clump of shoots, which were kept together to maintain the clonal integrity as much as possible.

After collection, plants were transported in coolers (within 2 h) filled with seawater to the experimental facilities of the Instituto de Investigaciones Oceanológicas (Universidad Autónoma de Baja California). Experimental plants were randomly allocated in a mesocosm system consisting of eight independent aquaria (60 L). Each aquarium contained 5-6 shoot clumps, which were formed by approximately 50 shoots each and were attached to one rock each to prevent them from floating. Plants were acclimated during five days at 18°C, 150-180 μmol photon $m^{-2}$ $s^{-1}$ with a photoperiod of 14:10 (dark: light) and a salinity of 33, according to summer average values at the donor meadow. Light was provided by LED lamps (150W), while the temperature was controlled by chillers and submersible quartz heaters. Submersible pumps were installed in each aquarium to allow water circulation and avoid temperature gradients. Light and temperature were monitored throughout the experiment by using submersible light/temperature sensors (Onset-HOBO MX2202), while salinity and pH were monitored using a multiparameter submersible probe (HACH HQd, YSI Professional Plus). Seawater was partially replaced (50%) every two days with filtered (1 μm)-UV treated seawater to maintain water quality.

After the acclimation period, conditions remained unchanged in half of the tanks (Control treatment, n=4), while the other half were subjected to a seawater warming regime consisting of two consecutive MHWs, followed by corresponding recovery periods (MHWs treatment, n=4). The thermal regime of the MHWs treatment was defined according to the characteristics of

historically recorded MHWs in Todos Santos Island (see Fig. SM 1, Supplementary material) during the period 1982-2019, obtained from Marine Heatwave Tracker (Schlegel et al., 2020) and based on Hobday's definition of MHWs (Hobday et al., 2016; seawater temperatures exceeding the 90$^{th}$ percentile for at least 5 consecutive days). The experimental thermal regime included two consecutive MHWs, in which the temperature was increased at a rate of 2°C/day and maintained for five days at the maximum temperature of 24°C, and afterwards returned to 18°C (2°C/day) for a 5-day recovery period. Plant responses were characterized at the end of each simulated MHW and at the end of their respective recovery periods (in chronological order: HW-1, R-1, HW-2, R-2) (Fig. 1D, E). To obtain reference values for the biological status of plants in the field (Table SM 2, Supplementary material), photobiological descriptors were measured immediately after plant collection, and leaf tissues were frozen (-80°C) to perform further biological analysis following the methods described below.

***Physiological traits and growth***

For each biological variable, measurements were performed in two plants per aquarium and averaged to obtain a true replicate (n = 4), except for the P-E curves and leaf growth determination, which were performed on a single plant per aquarium, and nitrate uptake measurements, on three plants per aquarium. All measurements were conducted on the middle section of the second mature leaf to avoid variability of biological descriptors within/among leaves.

***Photosynthesis and Respiration (P vs. E curves)***

Photosynthesis (P) and respiration (R) rates were determined in leaf segments using respirometers composed of 200 mL borosilicate jacketed chambers connected to a temperature-

controlled circulating bath and surrounded by four light sources (LED 10 W) that were automatically controlled by customized software (Fig. SM 3). Oxygen evolution was measured by optodes (DP-PSt3, PreSens, Germany), connected to a fiber-optic oxygen meter (OXY4 SMA, PreSens, Germany) and controlled by software (Measurement Studio 2, PreSens, Germany). A ratio of plant biomass/seawater volume of about 0.03-0.05 g DW $L^{-1}$ was used to ensure accurate measurements of photosynthetic rates. Epiphyte-free leaf segments were initially incubated in darkness for 10 min to determine R and subsequently exposed to nine increasing PAR irradiance steps up to 806 µmol photon $m^{-2}$ $s^{-1}$, each lasting 5 min. Light intensities within the chamber were previously calibrated, using a spherical (4π) quantum sensor (Biospherical Instruments; California, USA). Maximum net photosynthetic rate (Net-$P_{max}$; µmol $O_2$ $g^{-1}$ DW $h^{-1}$) was determined by averaging the maximum values above the saturating irradiance ($E_k$ = net-$P_{max}$/ α; µmol photon $m^{-2}$ $s^{-1}$). Maximum gross photosynthesis (Gross-$P_{max}$; µmol $O_2$ $g^{-1}$ DW $h^{-1}$) was calculated as the sum of Net-$P_{max}$ and R. Photosynthetic efficiency (α) was calculated as the slope of the regression line fitted to the initial linear part of the P *vs*. E curve. The compensation irradiance ($E_c$; µmol photon $m^{-2}$ $s^{-1}$) was determined as the intercept of the initial linear part of the curve on the X-axis.

***Daily productivity***

A proxy of daily net-productivity (DP, µmol $O_2$ $g^{-1}$ DW $day^{-1}$) was calculated, considering the average light availability within plant´s canopy in the aquaria (100 µmol photon $m^{-2}$ $s^{-1}$) and the selected photoperiod (14:10, dark: light). DP was calculated as [(net-$P_{100}$ x 10) - (R x 14)], where net-$P_{100}$ is the net photosynthesis corresponding to the irradiance at 100 µmol photon $m^{-2}$ $s^{-1}$ of P-E curves.

***Chlorophyll a fluorescence and absorptance***

The chlorophyll-*a* fluorescence emission of PSII was measured using a portable Diving-PAM fluorometer (Walz, Germany). The leaf surface was carefully cleaned off epiphytes and held in the fluorometer DCL-8 leaf-clip holder to assure a constant distance between the tissue and the fiber optic of the fluorometer. Maximum quantum yield ($F_v/F_m$), basal ($F_0$) and maximum ($F_m$) fluorescence were obtained from plants kept in darkness overnight. Values of effective quantum yield ($\Phi_{PSII}$), $F_0$' and $F_m$' were obtained at midday from light-acclimated plants and illuminated with the actinic light (175 µmol photon $m^{-2}$ $s^{-1}$) of the fluorometer for 90 seconds. The intensity of the actinic light was adjusted to the light intensity provided by lamps in the aquaria, while the 90 seconds illumination period was selected to ensure photosynthetic steady state at this irradiance according to previous trials. Values of non-photochemical quenching, NPQ, was calculated as $(F_m-F_{m'})/F_{m'}$. Absolute ETR was calculated as $ETR = \Phi_{PSII} \cdot 175 \cdot A \cdot 0.5$, where A is the leaf absorptance (see below), 175 is the actinic-light intensity and 0.5 is a constant assuming that half of the incident photons is absorbed by the PSII (Beer et al., 2014). Leaf absorptance (A) was estimated as A = 1 - (LT / L0) - TW, where LT is the transmitted light trough the leaf tissue, L0 is the total incident light emitted by the lamp and TW is the transmitted light through a bleached leaf (Vásquez-Elizondo et al. 2017). Light transmision was measured using the miniature fiber optics quantum sensor (Diving-F1, Walz, Germany) of the submergible Diving-PAM fluorometer (Walz, Germany). The light sensor was attached to the fluorometer clip holder, entirely covered by the leaf tissue. The actinic light was provided through the fiber optic of the fluorometer, attached to the clip holder.

***Pigment content***

Leaf pigments were extracted from 10 – 15 mg FW leaf tissue, homogenized in 100% acetone, with $MgCO_3$ solution added to prevent acidification of the extract (Dennison, 1990). Extracts were stored at 4°C in the dark for 24 h. After centrifugation (1000 x g, 10 min), absorbance was measured spectrophotometrically at 470, 646, and 663 nm, using 1 mL cuvettes. The Chlorophylls *a*, *b,* and total carotenoid concentration were calculated using the equations described by Lichtenthaler & Wellburn (1983) and expressed as mg $g^{-1}$ FW.

***Lipid peroxidation***

Oxidative damage was evaluated by malondialdehyde (MDA) quantification following the thiobarbituric acid-reactive-substances (TBARS) assay, described by Hodges et al. (1999) and Correia et al. (2006). Ultrafrozen leaf tissue (0.2 g FW) was mechanically ground in 2 ml ethanol 80%, centrifuged for 10 min (3000 x g, 4°C), and the supernatant was added to a solution of trichloroacetic acid (TCA, 20%) and thiobarbituric acid (TBA, 0.5%). Blanks were prepared by adding the supernatant to a solution of TCA 20%. These two solutions were heated at 90°C for 30 min, and then centrifuged again (3000 x g) for 10 min. The supernatants were extracted, and their absorbance (440, 532 and 600 nm) were determined spectrophotometrically. Lipid peroxidation was expressed as equivalents of malonil-dialdehyde (Eq MDA; molar extinction coefficient 155 mM $cm^{-1}$), which were calculated using the equations in Hodges et al. (1999).

***Total phenolic content and antioxidant capacity***

Phenolic and antioxidant compounds were extracted from dried ground leaf tissue (0.02 g DW) in 1 mL 80% methanol in darkness for 24 h. The extract was then centrifuged at 10,000 rpm for 10 min. The phenolic compound content was determined according to a modification of the Folin–

Ciocalteu assay using gallic acid as standard (Singleton & Rossi 1965). The methanolic extract (0.01 mL) was diluted in 1mL distilled water ($dH_2O$), 0.1 mL Folin–Ciocalteu reagent and 0.3 mL $dH_2O$ saturated with $NaCO_3$. This mixture was homogenized, heated (40°C for 3 min), and its absorbance read spectrophotometrically at 765 nm. Total phenolic content was expressed as gallic acid equivalents (mg Eq. GA $g^{-1}$ DW). The radical scavenging activity was quantified according to Sabeena-Farvin & Jacobsen (2013); the reaction mixture was prepared with 0.1 mL of diluted extract (1:10 with 80% methanol) and 1 mL of 60 μM 2,2-diphenyl-1-picrylhydrazyl (DPPH) dissolved in 90% methanol. The absorbance was measured at 517 nm 30 min after DPPH addition. The total antioxidant capacity was expressed as ascorbic acid equivalents (mg Eq. AA $g^{-1}$ DW).

***Nitrate uptake rate, nitrogen content and nitrogen isotopic signal***

The leaves from three shoots per aquarium were incubated for 30 min in independent plastic containers filled with 6 L of filtered (5 μm) and UV-treated seawater supplemented with $^{15}N$ tracer ($K^{15}NO_3$ at 99%, Cambridge Isotope Laboratories) at 20 μM. This nitrate concentration was selected according to maximum values of this nutrient during upwelling near the collection site (Espinosa-Carreón et al., 2001). Incubations were performed in large incubators under constant temperature and irradiance, which corresponded to the conditions of each treatment. Seawater was constantly homogenized by magnetic stirrers to reduce the blade boundary layer. To avoid substantial reduction in nitrate concentration, a plant biomass versus volume of 0.3 g FW $L^{-1}$ was used in each incubation. At the end of the incubations, leaf tissues were rinsed with deionized water to remove the tracer adsorbed to their surfaces, and dried at 60°C until constant weight. Thereafter, samples were ground to a fine powder for isotope enrichment analyses.

Isotopic determinations were carried out at UC-Davis Stable Isotope Facility using an elemental analyzer (EA) interfaced with a continuous flow isotope ratio mass spectrometer (IRMS). Nitrogen content and nitrogen isotopic signal, $\delta^{15}N$, were analyzed similarly, but in leaf tissues not exposed to the tracer. Nitrate uptake rates (expressed as μmol N $g^{-1}$ DW $h^{-1}$) were calculated using the equations shown in Sandoval-Gil et al. (2015).

***Non-structural carbohydrates***

Total soluble non-structural carbohydrates (free sugars and starch) were determined using the colorimetric phenol-sulfuric acid method (Dubois et al., 1956), with glucose as standard. Leaf tissues were oven-dried at 60°C until constant weight and ground to a fine powder. The powder was digested in 0.1 N HCl (60ºC, 3h), centrifuged (4000 x g, 5 min), and the supernatant mixed with 3% phenol and concentrated sulfuric acid. Absorbance was measured spectrophotometrically at 490 nm. Non-structural carbohydrates content was expressed in mg $g^{-1}$ DW.

***Relative leaf growth rate***

At the beginning of each simulated MHW (HW-1 and HW-2) and each recovery phase (R-1 and R-2), the leaves of one shoot per aquarium was marked following the hole punching method adapted from Zieman (1974). Subsequently, all marked shoots were harvested at the end of each experimental period, and leaf segments below the mark (i.e., newly formed tissue) were dried and weighted for all leaves of each shoot. Shoot growth was expressed as relative to the total shoot biomass or relative leaf growth rate (RGR; mg $g^{-1}$ DW $day^{-1}$).

***Statistical analysis***

Two-way Analysis of Variance (ANOVA) was used to test for the main and interactive effects of the factors Treatment ("Trt.", 2 levels: Control and MHWs) and "Time" ("Time", 4 levels: HW-1, R-1, HW-2, R-2) for each biological descriptor. In case of significant interaction ($P < 0.05$), Tukey HSD post-hoc tests were used to compare individual means between Control group and the MHWs group at each sampling time. Data that did not meet the assumptions of normality (Shapiro-Wilk normality test, $p > 0.05$) or homogeneity (Bartlett test, $p > 0.05$) of variance were corrected with logarithmic transformations (i.e., $E_k$, $E_c$, phenolic content, nitrate uptake). If the data still remained heteroscedastic (R, ΦPSII, NPQ, lipid peroxidation and $\delta^{15}N$ content), the model was adjusted with "White-corrected" covariance matrices (Long & Ervin, 2000).

Overall trends in biological responses to experimental treatments and correlations between variables were examined by multivariate analyses. Principal Component Analysis (PCA) and Permutational Multivariate Analysis of Variance (PERMANOVA) were performed based on Euclidean distance matrix of normalized data. For the PCA analysis, correlated variables ($P < 0.05$, data not shown) were grouped into biological meaningful groups to simplify representation (*Photosynthesis*: Gross-$P_{max}$, Net-$P_{max}$, Ek and α; *Respiration*: R and $E_c$; *PSII efficiency*: $F_v/F_m$, $\Phi_{PSII}$ and ETR; *Pigments*: Chl*a*, chl*b* and carotenoids; *Antioxidants*: phenolic content and antioxidant capacity). PERMANOVA tested for the main and interactive effects of the factor "Treatment" ("Trt.", 2 levels: Control vs. MHWs) and the factor "Time" (4 levels: HW-1, R-1, HW-2, R-2). Pair-wise comparisons were performed between different Time levels for each Treatment, where the P-values were corrected by Monte Carlo test and Bonferroni adjustment.

Univariate analyses and the PCA were performed using the statistical software R (R CoreTeam 2020). PERMANOVA was run with PRIMER 6 (Anderson et al., 2008).

## 3. Results

Multivariate analyses indicated that the overall response of *P. scouleri* was different among treatments and sampling times (see PCA plot in Fig. SM 4 and loadings in Table SM 5, and PERMANOVA results in Table SM 6). Plants exposed to warming (i.e., MHWs treatment) presented significant variation in the set of physiological traits among sampling times, while changes in control plants were not significative (Pairwise PERMANOVA tests between sampling times, Table SM 6). Also, significantly different physiological responses between treatments were observed at the end of the experiment (i.e., R-2) (Pairwise PERMANOVA tests between treatments, Table SM 6). Although the PCA did not explain much of the data variance (only 52% with the first two dimensions together), it depicted an overall differentiation between control plants and most of MHW plants (except HW-1) along the PC1 (Fig. SM 4). This axis was positively correlated (loadings > 0.3) with antioxidants, respiration, and with the overall photosynthetic performance, while it was inversely correlated (loadings < -0.3) with NPQ and $^{15}N$ (Table SM 5). Also, observations located at the "most negative" region of the PC1 were MHW plants at recovery sampling times (i.e., R-1 and R-2). Differently, the PC2 evidenced differences not between treatments, but among sampling times (Fig. SM 4). This axis had a positive correlation (loading > 0.5) with nitrate uptake, and an inverse relationship with lipid peroxidation and NSC content (loadings < -0.5) (Table SM 5).

In plants exposed to MHWs, maximum photosynthetic capacities (gross- and net-$P_{max}$; Fig. 2A, B) and $E_k$ (Fig. 2C) progressively decreased by ~50% from HW-1 to R-2 ($p < 0.001$, Table SM 7). Differences in compensation irradiance ($E_c$, Fig. 2D), photosynthetic efficiency ($\alpha$, Fig. 2E) and respiration (R, Fig. 2F) between control and MHW plants were not statistically different (Table SM 7).

Maximum photochemical efficiency ($F_v/F_m$, Fig. 3A), effective quantum yield ($\Phi_{PSII}$, Fig. 3B) and electron transport rate (ETR, Fig. 3C) significantly decreased in plants recovering from experimental warming (Table SM 7, $p < 0.05$), showing the highest reduction at the last recovery period (R-2), when those variables presented values 10, 36 and 31% lower than the control, respectively. Conversely, NPQ in warmed plants nearly doubled in both recovery periods (R-1, R-2), compared to control plants (Fig. 3D, Table SM 7, $p < 0.001$).

Chl*a* and carotenoids significantly increased by 30 and 35%, respectively, in plants exposed to the first heatwave (HW-1), respect to the control (Fig. SM 8A, C; Table SM 7, $p < 0.05$). In contrast, Chl*a* and *b* were in lower concentration in warmed plants at the second heatwave (HW-2), compared to the control (Fig. SM 8A, B, $p < 0.05$). Values of Chl *b/a* ratio in warmed plants were higher than in the control at the first HW, but lower at the second recovery period (Fig. SM 8C, Table SM 7, $p < 0.05$).

Lipid peroxidation was significantly higher in warmed plants (Fig. 4A, Table SM 7, $p < 0.001$). The largest differences occurred during both experimental heatwaves (increase by 22% in HW-1 and by 49% in HW-2) (Fig. 4A). Phenolic content and antioxidant capacity were also significantly affected by treatments, with warmed plants exhibiting overall higher values (Fig. 4B, C, Table SM 7). Phenolic content was lower in warmed plants by 22% in R-2, and by 32% in

HW-2, compared to control (Fig. 4B). Antioxidant capacity was 10 - 30% lower in warmed plants during the entire experiment (Fig. 4C).

Nitrate uptake rates were substantially reduced (Table SM 7, $p < 0.001$) in plants exposed to MHWs respect to the control in all sampling times, but differences were larger in HW-1 and R-2 (down to 80% lower, Fig. 5A). No significant differences between treatments for leaf N-content were found (Fig. 5B). Values of $\delta^{15}N$ progressively increased towards the end of the experiment in warmed plants respect to control values (Fig. 5C, Table SM 7, $p < 0.01$).

The content of non-structural carbohydrates (Fig. 6A) was not different between control and MHW plants (Table SM 7). Differently, the daily productivity was significantly affected by the MHW treatment (Fig. 6B, Table SM 7, $p < 0.001$). Values were lower (by 29 – 52%) in warmed plants compared to control, with the largest differences found for R-2 (Fig. 6B). Relative growth rate was not significantly affected by treatments (Table SM 7), although a considerable - but not significant - decrease (-36%, respect to control) was detected at R-1 in plants previously exposed to warming (Fig. 6C).

## 4. Discussion

The results of this study showed that recurrent and intense MHWs (+6°C) can produce a progressive ecophysiological debilitation of subtidal *Phyllospadix scouleri* plants off the Baja Californian coast, which was especially more evident once the heat exposures were ceased (i.e., recovery phases) (Fig. 7). Nitrogen uptake was strongly impaired during the simulated marine heat waves. Although this did not have an obvious effect on the nitrogen content of leaf tissues, possibly due to their short duration, longer-lasting heatwaves could affect the nutritional status of plants with potential effects on plant´s health and the trophic chains they support. Other obvious

effects from the heatwaves were an increase in oxidative damage (lipid peroxidation) and an exhaustion of antioxidant power, as indicated by reductions in phenol concentration and antioxidant capacity. Negative effects on plant photosynthesis were most evident during the recovery phases, indicating a time lag in the response of *P. scouleri* to increased temperature. These lag-effects, which appear to be more intense during the second heat wave, resulted in decreased seagrass productivity, which together with a lack of recovery of nitrogen uptake rates indicate that an increase in the recurrence of heat waves could overcome the resilience of this species to warming.

*Phyllospadix scouleri* plants did not show signs of physiological stress at the photosynthetic level (Fig. 2, 3) during the first experimental warming (i.e., HW-1). Similarly, Vivanco-Bercovich et al. (2022) found that maximum photosynthetic capacities and photochemical efficiency can be maintained (or even enhanced) in the surfgrass *Phyllospadix torreyi*, while exposed to warming. Within metabolic tolerance ranges, warming can stimulate photosynthesis by enhancing enzymatic activity and facilitating mobility of proteins within the thylakoid membranes (Masini & Manning, 1997; Beca-Carretero et al., 2018). However, the delayed but strong MHW-impact on photosynthesis (Fig. 2 and 3) in *P. scouleri*, together with its seemingly low recovery capacity, led to a progressive reduction in the plants' productivity during the experimental period. Heat stress can directly affect the structure and functionality of the PSII by increasing the fluidity of thylakoid membranes and dislodging key proteins (Mathur et al., 2014). For instance, one primary target of thermal stress is the oxygen evolving complex because heat can induce the dissociation of its manganese cluster (Mathur et al., 2014). These and other potential heat induced alterations on the photosynthetic machinery at thylakoid level (e.g., inhibited D1 repair cycle, unregulated state transitions, disrupted electron transport) and downstream processes (e.g.,

carbon fixation/assimilation) may have contributed to the diminished photosynthetic capacity observed here, as also reported for other seagrasses exposed to warming (e.g., Marín-Guirao et al., 2016; Costa et al., 2021, Deguette et al., 2022). Probably, the drop in $F_v/F_m$ (from ~0.76 in HW-1 to ~0.65 in R-2) reflected the accumulation of heat-induced damage on the PSII. Warming may hamper reaction centers functionality due to the thermolability of the D1 protein (Rokka et al., 2000), and it can reduce the quantum efficiency by separating reaction centers from the light harvesting complexes, thus blocking energy transfer and decelerating electron transport carriers (Briantais et al., 1996; Pospíšil & Tyystjärvi, 1999). On the contrary, MHW impact on the light harvesting capacity seemed to have been of minor importance in the decrease of photosynthetic capacity, since photosynthetic pigments (i.e., Chl*a* and Chl*b*) were lower only after the second heatwave (Fig. SM 8). Slightly higher values of Chl*b/a* ratio, found in plants recovered from HW-2, could be indicative of changes in the thylakoid membrane architecture to increase the efficiency of photoprotective mechanisms (Friedland et al., 2019).

Overall, lowered photosynthetic capacity clearly indicated a progressive deterioration of the photosynthetic apparatus in plants repeatedly exposed to warming, which was manifested specially during recovery periods (Fig. 7). These apparently delayed stress responses are interesting, likely associated with complex trade-offs as plants engage in photoprotection mechanisms, metabolic compensation strategies and photosystem repair cycles (Allakhverdiev et al., 2008). In fact, this seems to be a common response among seagrass species, as similar delayed responses after thermal stress conditions have been reported also in *Cymodocea nodosa* and *Zostera marina* (Franssen et al., 2011; Winters et al., 2011; Jueterbock et al., 2020; Deguette et al., 2022). Likewise, remarkable increments in NPQ were measured in plants recovering from both warming periods (Fig. 7). Increased NPQ during post-heat stress condition, or NPQ

suppressed by elevated temperature, have been also previously found in *Phyllospadix torreyi* (Ruiz-Montoya et al., 2021) and other seagrass species (e.g., Chartrand et al., 2018; Ontoria et al., 2019).

The photosynthetic and photoprotective responses of *P. scouleri* were consistent with the responses in oxidative stress, antioxidant capacity and phenolic content (Fig. 4). Increments in malondialdehyde (MDA) in leaf tissues associated to the peroxidation of membrane phospholipids by ROS, were found in plants at HW-1 and HW-2 respect to control. Similar signs of oxidative damage were recently reported for intertidal *P. torreyi* plants facing extreme warming and desiccation during low tide (Ruiz-Montoya et al., 2021). Surpassing antioxidant responses, accumulation of ROS can produce damage to different cellular components (e.g., proteins, chloroplast membranes, DNA), and inhibit the *de novo* synthesis of D1 protein, which can lead to cellular death (Apel & Hirt, 2004; Sharma et al., 2012). In *P. scouleri*, the repeated thermal stress seemingly exceeded its antioxidant capacity, related to the activation of antioxidant enzymes and the accumulation of antioxidant compounds (Tutar et al., 2017), which declined together with the phenolic concentration at the end of the experiment. This in turn was accompanied by an increase in lipid peroxidation. Likely, the high phenolic concentration and antioxidant capacity found in *P. scouleri*, compared to other seagrass species (e.g., *Cymodocea nodosa*, Silva et al., 2013; *Thalassia hemprichii, Halophila ovata, Syringodium isoetifolium*; Jeyapragash et al., 2016), contributed to limiting the oxidative damage. Rather than their active synthesis, the maintenance of stable high concentration of antioxidant compounds and enzymes could be a more effective (and energy-conservative) strategy of seagrasses and seaweeds to overcome recurring stressful conditions (Wiencke & Bischof, 2012; Ruiz-Montoya et al., 2021).

Nitrate uptake rate was another physiological process strongly affected in *P. scouleri* subjected to warming (Fig. 5A). Nitrate availability fueled by upwelling events (up to ~20 μM) can be a primary source of N for seagrass nutrition (Sandoval-Gil et al., 2019). However, the incorporation and assimilation of nitrate is a highly energy-demanding process, even competing with other metabolic processes for photosynthate C-skeletons (Touchette & Burkeholder, 2000). Hence, diminished photosynthetic capabilities can restrict the potential for nitrate uptake in *P. scouleri*, as documented in the giant kelp (*Macrocystis pyrifera*) exposed to experimental MHWs (Sánchez-Barredo et al., 2020). Other works have reported downregulation of genes related to nitrate uptake and assimilation in seagrasses facing metabolic imbalances caused by stressful conditions, such as warm and fertilized water (Pazzaglia et al., 2022b), and temperature effects in nitrate assimilatory enzymes (such as nitrate reductase and glutamine synthetase) (Touchette & Burkholder, 2000). Apparently, leaf N-content contrasted with the nitrate uptake rates since it remained similar throughout the experiment. Nitrogen isotopic signal, $\delta^{15}N$, was enriched in warmed plants, indicating a lower discrimination against $^{15}N$, or the preferential incorporation of N-compounds with more enriched isotopic signal (Evans, 2001). Warming could alter other processes not assessed in our study, such as the mobilization of N-internal resources, N-exudation rates, or the acquisition of other N forms (ammonium or organic forms), all of which are considered key metabolic components determining whole-plant nitrogen budget for seagrass under stressful conditions (e.g., Alcoverro et al., 2000; Martin et al., 2018; Alexandre et al., 2020).

The reduced photosynthetic performance of plants repeatedly exposed to warming caused a decline in their net productivity, i.e., photosynthetic C-gains vs. respiratory C-losses. However, leaf growth rates and non-structural carbohydrates (assumed as C-internal reserves) did not show

any significant responses to the experimental treatments. This suggests that *P. scouleri* is either capable of maintaining its plant carbon balance during short-term thermal stress events in expense of other than leaf carbon reserves (e.g., NSC from rhizomes), or that the effects of the experienced thermal stress will appear at a later stage (not covered by the experimental period), as growth is a variable that exhibits a longer response time, compared to other physiological processes, such as photosynthesis. Light can be drastically attenuated within seagrass canopies, and photosynthetic efficiency/productivity at low (sub-saturating) irradiances can critically contribute to the whole-plant carbon economy (Enríquez & Pantoja-Reyes, 2005, Enríquez et al., 2019). Because of leaf self-shading, light penetration within surfgrasses canopies can be exceptionally reduced by ~90% (Ruiz-Montoya et al., 2021), forcing a shade-adapted photo-physiology (Garcia-Pantoja et al., 2020). Also, the regulation of leaf respiration is critical for seagrasses facing heat stress (Marín-Guirao et al., 2016; 2018), and it could be especially relevant for those with high above/below biomass ratio, such as surfgrass (Garcia-Pantoja et al., 2020). Our results demonstrate that compensation irradiances ($E_c$), photosynthetic efficiency ($\alpha$), and even respiratory rates, were close to control values in *P. scouleri* shoots exposed to warming, probably contributing to prolong their internal carbon storage capacity and sustain growth during our short experimental timeframe. Yet, compromised photosynthetic capacities, high investment in photoprotection, oxidative stress and impaired nitrogen acquisition would have very likely caused carbon reserves to be exhausted if thermal stress was extended for a longer period.

## 5. Conclusions

An increasing frequency in MHWs, such as predicted for the near future (Laufkötter et al., 2020; Fox-Kemper et al., 2021), will have detrimental effects for seagrass performance, due to the

accumulation of thermal-stress induced effects, as shown here in the case of *Phyllospadix scouleri*, a seagrass species that has been scarcely studied despite its remarkable ecological relevance for coastal marine ecosystems along the Pacific coast of North America. During its experimental exposure to two consecutive MHWs, fast responsive traits, such as those related to photosynthesis, nitrate acquisition and oxidative damage, revealed a progressive deterioration of plant´s overall physiological status. By contrast, variables with slower response time (e.g., internal nutrient resources, leaf growth) remained constant throughout the experiment and indicated that carbon reserves were not exhausted within our experimental timeframe. Furthermore, it was notable that most of stress and acclimatory responses were manifested once heat stress ceased, thus demonstrating the importance of extending the assessments of physiological responses to heat stress towards recovery periods in future experimental approaches.

The more accentuated physiological stress after the second heatwave raised evidence of accumulative detrimental effects that consecutive MHWs may exert on seagrasses. These results contrast with reported responses of other seagrass species, in which plants pre-exposed to temperature increase before facing a second warming exposure presented ameliorated effects (Nguyen et al., 2020; Pazzaglia et al., 2022a). This discrepancy could be associated to species-specific thermal tolerance ranges, but also to different experimental conditions among studies (e.g., intensity of the first warming exposure, rate of temperature increase). Therefore, the direction and magnitude of MHW effects on seagrass performance seem to be defined by the frequency, as well as the intensity (and most likely local acclimation) of the consecutive events. Experimenting with different intensities for the first warming event could help identifying

temperature thresholds between the stimulation of physiological "hardening" (or "stress memory") and the accumulation of stress (or metabolic weakening).

## 6. References


Alcoverro, T., Manzanera, M., Romero, J., 2000. Nutrient mass balance of the seagrass *Posidonia oceanica*: the importance of nutrient retranslocation. Mar. Ecol. Prog. Ser. 194, 13–21.

Alexandre, A., Quintã, R., Hill, P.W., Jones, D.L., Santos, R., 2020. Ocean warming increases the nitrogen demand and the uptake of organic nitrogen of the globally distributed seagrass *Zostera marina*. Funct. Ecol. 34, 1325–1335. https://doi.org/10.1111/1365-2435.13576

Allakhverdiev, S.I., Kreslavski, V.D., Klimov, V.V., Los, D.A., Carpentier, R., Mohanty, P., 2008. Heat stress: an overview of molecular responses in photosynthesis. Photosynth. Res. 98, 541. https://doi.org/10.1007/s11120-008-9331-0

Anderson, M.J., Gorley, R.N., Clarke, K.R., 2008. PERMANOVA+ for PRIMER: Guide to Software and Statistical Methods, in: PRIMER-E. Plymouth, UK.

Apel, K., Hirt, H., 2004. Reactive oxygen species: metabolism, oxidative stress, and signal transduction. Annu. Rev. Plant Biol. 55, 373–399. https://doi.org/10.1146/annurev.arplant.55.031903.141701

Arafeh-Dalmau, N., Montaño-Moctezuma, G., Martínez, J.A., Beas-Luna, R., Schoeman, D.S., Torres-Moye, G., 2019. Extreme marine heatwaves alter kelp forest community near its equatorward distribution limit. Front. Mar. Sci. 6, 499. https://doi.org/10.3389/fmars.2019.00499

Beas-Luna, R., Micheli, F., Woodson, C.B., Carr, M., Malone, D., Torre, J., Boch, C., Caselle, J.E., Edwards, M., Freiwald, J., Hamilton, S.L., Hernandez, A., Konar, B., Kroeker, K.J., Lorda, J., Montaño-Moctezuma, G., Torres-Moye, G., 2020. Geographic variation in responses of kelp forest communities of the California Current to recent climatic changes. Glob. Change Biol. 26, 6457–6473. https://doi.org/10.1111/gcb.15273

Beca-Carretero, P., Olesen, B., Marbà, N., Krause-Jensen, D., 2018. Response to experimental warming in northern eelgrass populations: comparison across a range of temperature adaptations. Mar. Ecol. Prog. Ser. 589, 59–72. https://doi.org/10.3354/meps12439

Beer, S., Björk, M., Beardall, J., 2014. Photosynthesis in the marine environment. John Wiley & Sons.

Briantais, J.-M., Dacosta, J., Goulas, Y., Ducruet, J.-M., Moya, I., 1996. Heat stress induces in leaves an increase of the minimum level of chlorophyll fluorescence, $F_o$: A time-resolved analysis. Photosynth. Res. 48, 189–196. https://doi.org/10.1007/BF00041008

Chartrand, K.M., Szabó, M., Sinutok, S., Rasheed, M.A., Ralph, P.J., 2018. Living at the margins – The response of deep-water seagrasses to light and temperature renders them susceptible to acute impacts. Mar. Environ. Res. 136, 126–138. https://doi.org/10.1016/j.marenvres.2018.02.006

Collier, C.J., Uthicke, S., Waycott, M., 2011. Thermal tolerance of two seagrass species at contrasting light levels: Implications for future distribution in the Great Barrier Reef. Limnol. Oceanogr. 56, 2200–2210.

Collier, C.J., Waycott, M., 2014. Temperature extremes reduce seagrass growth and induce mortality. Mar. Pollut. Bull. 83, 483–490. https://doi.org/10.1016/j.marpolbul.2014.03.050

Cooper, L.W., McRoy, C.P., 1988. Anatomical adaptations to rocky substrates and surf exposure by the seagrass genus *Phyllospadix*. Aquat. Bot. 32, 365–381. https://doi.org/10.1016/0304-3770(88)90108-8

Correia, M.J., Osório, M.L., Osório, J., Barrote, I., Martins, M., David, M.M., 2006. Influence of transient shade periods on the effects of drought on photosynthesis, carbohydrate accumulation and lipid peroxidation in sunflower leaves. Environ. Exp. Bot. 58, 75–84. https://doi.org/10.1016/j.envexpbot.2005.06.015

Costa, M.M., Silva, J., Barrote, I., Santos, R., 2021. Heatwave effects on the photosynthesis and antioxidant activity of the seagrass *Cymodocea nodosa* under contrasting light regimes. Oceans 2, 448–460. https://doi.org/10.3390/oceans2030025

de los Santos, C.B., Scott, A., Arias-Ortiz, A., Jones, B., Kennedy, H., Mazarrasa, I., McKenzie, L., Nordlund, L.M., de la Torre-Castro, M. de la T., Unsworth, R.K.F., Ambo-Rappe, R., 2020. Seagrass ecosystem services: assessment and scale of benefits. Blue Value Seagrasses Environ. People 19–21.

Deguette, A., Barrote, I., Silva, J., 2022. Physiological and morphological effects of a marine heatwave on the seagrass *Cymodocea nodosa*. Sci. Rep. 12, 7950. https://doi.org/10.1038/s41598-022-12102-x

Delgadillo-Hinojosa, F., Félix-Bermúdez, A., Torres-Delgado, E.V., Durazo, R., Camacho-Ibar, V., Mejía, A., Ruiz, M.C., Linacre, L., 2020. Impacts of the 2014–2015 warm-water anomalies on nutrients, *chlorophyll-a* and hydrographic conditions in the coastal zone of Northern Baja California. J. Geophys. Res. Oceans 125, e2020JC016473. https://doi.org/10.1029/2020JC016473

Den Hartog, C., 1970. The sea-grasses of the world. N.-Holl. Amst.

Dennison, W., 1990. Chlorophyll content, in: Seagrass Research Methods. Phillips, R.C.; McRoy, C.P., Paris (France) UNESCO.

Drew, E.A., 1979. Physiological aspects of primary production in seagrasses. Aquat. Bot. 7, 139–150. https://doi.org/10.1016/0304-3770(79)90018-4

Drysdale, F.R., Barbour, M.G., 1975. Response of the marine angiosperm *Phyllospadix torreyi* to certain environmental variables: A preliminary study. Aquat. Bot. 1, 97–106. https://doi.org/10.1016/0304-3770(75)90015-7

Duarte, B., Martins, I., Rosa, R., Matos, A.R., Roleda, M.Y., Reusch, T.B.H., Engelen, A.H., Serrão, E.A., Pearson, G.A., Marques, J.C., Caçador, I., Duarte, C.M., Jueterbock, A., 2018. Climate change impacts on seagrass meadows and macroalgal forests: an integrative perspective on acclimation and adaptation potential. Front. Mar. Sci. 5, 190. https://doi.org/10.3389/fmars.2018.00190

DuBois, K., Williams, S.L., Stachowicz, J.J., 2020. Previous exposure mediates the response of eelgrass to future warming via clonal transgenerational plasticity. Ecology 101. https://doi.org/10.1002/ecy.3169

Dubois, M., Gilles, K.A., Hamilton, J.K., Rebers, P.A., Smith, F., 1956. Colorimetric method for determination of sugars and related substances. Anal. Chem. 28, 350–356.

Durazo, R., 2015. Seasonality of the transitional region of the California Current System off Baja California. J. Geophys. Res. Oceans 120, 1173–1196. https://doi.org/10.1002/2014JC010405

Enríquez, S., Borowitzka, M.A., 2010. The use of the fluorescence signal in studies of seagrasses and macroalgae, in: *Chlorophyll a* Fluorescence in Aquatic Sciences: Methods and Applications. Springer, pp. 187–208.

Enríquez, S., Olivé, I., Cayabyab, N., Hedley, J.D., 2019. Structural complexity governs seagrass acclimatization to depth with relevant consequences for meadow production, macrophyte diversity and habitat carbon storage capacity. Sci. Rep. 9, 14657. https://doi.org/10.1038/s41598-019-51248-z

Enríquez, S., Pantoja-Reyes, N.I., 2005. Form-function analysis of the effect of canopy morphology on leaf self-shading in the seagrass *Thalassia testudinum*. Oecologia 145, 234–242. https://doi.org/10.1007/s00442-005-0111-7

Espinosa-Carreón, T.L., Gaxiola-Castro, G., Robles-Pacheco, J.M., Nájera-Martínez, S., 2001. Temperature, salinity, nutrients and chlorophyll a in coastal waters of the Southern California Bight. Cienc. Mar. 27, 397–422. https://doi.org/10.7773/cm.v27i3.490

Evans, R.D., 2001. Physiological mechanisms influencing plant nitrogen isotope composition. Trends Plant Sci. 6, 121–126. https://doi.org/10.1016/S1360-1385(01)01889-1

Fox-Kemper, B., 2021. Ocean, Cryosphere and Sea Level Change (Ch. 9 of Climate Change 2021: The Physical Science Basis). Contrib. Work. Group Sixth Assess. Rep. Intergov. Panel Clim. Change.

Franssen, S.U., Gu, J., Bergmann, N., Winters, G., Klostermeier, U.C., Rosenstiel, P., Bornberg-Bauer, E., Reusch, T.B.H., 2011. Transcriptomic resilience to global warming in the seagrass *Zostera marina*, a marine foundation species. Proc. Natl. Acad. Sci. 108, 19276–19281. https://doi.org/10.1073/pnas.1107680108

Friedland, N., Negi, S., Vinogradova-Shah, T., Wu, G., Ma, L., Flynn, S., Kumssa, T., Lee, C.-H., Sayre, R.T., 2019. Fine-tuning the photosynthetic light harvesting apparatus for improved photosynthetic efficiency and biomass yield. Sci. Rep. 9, 13028. https://doi.org/10.1038/s41598-019-49545-8

García-Pantoja, J.A., Ruiz-Montoya, L., Sandoval-Gil, J.M., Vivanco-Bercovich, M.V., Ferreira-Arrieta, A., Zertuche-González, J.A., Guzmán-Calderón, J.M., Norzagaray-López Orión; Samperio-Ramos, G., Montaño-Moctezuma, G., Hernández-Ayón, M., 2020. Fijación neta de carbono por pastos marinos (*Phyllospadix* spp.) en una isla del Pacífico Mexicano, in: Estado actual del conocimiento del ciclo del carbono y sus interacciones en México: Síntesis a 2020, Síntesis Nacionales. Programa Mexicano del Carbono en colaboración con la Universidad Autónoma Metropolitana-Xochimilco, Texcoco, Estado de México, México, p. 602.

Garrabou, J., Gómez-Gras, D., Medrano, A., Cerrano, C., Ponti, M., Schlegel, R., Bensoussan, N., Turicchia, E., Sini, M., Gerovasileiou, V., Teixido, N., Mirasole, A., Tamburello, L., Cebrian, E., Rilov, G., Ledoux, J.-B., Souissi, J.B., Khamassi, F., Ghanem, R., Benabdi, M., Grimes, S., Ocaña, O., Bazairi, H., Hereu, B., Linares, C., Kersting, D.K., la Rovira, G., Ortega, J., Casals, D., Pagès-Escolà, M., Margarit, N., Capdevila, P., Verdura, J., Ramos, A., Izquierdo, A., Barbera, C., Rubio-Portillo, E., Anton, I., López-Sendino, P., Díaz, D., Vázquez-Luis, M., Duarte, C., Marbà, N., Aspillaga, E., Espinosa, F., Grech, D., Guala, I., Azzurro, E., Farina, S., Cristina Gambi, M., Chimienti, G., Montefalcone, M., Azzola, A., Mantas, T.P., Fraschetti, S., Ceccherelli, G., Kipson, S., Bakran-Petricioli, T., Petricioli, D., Jimenez, C., Katsanevakis, S., Kizilkaya, I.T., Kizilkaya, Z., Sartoretto, S., Elodie, R., Ruitton, S., Comeau, S., Gattuso, J.-P., Harmelin, J.-G., 2022. Marine heatwaves drive recurrent mass mortalities in the Mediterranean Sea. Glob. Change Biol. 28, 5708–5725. https://doi.org/10.1111/gcb.16301

Hodges, D.M., DeLong, J.M., Forney, C.F., Prange, R.K., 1999. Improving the thiobarbituric acid-reactive-substances assay for estimating lipid peroxidation in plant tissues containing anthocyanin and other interfering compounds. Planta 207, 604–611. https://doi.org/10.1007/s004250050524

Hyndes, G.A., Heck, K.L., Vergés, A., Harvey, E.S., Kendrick, G.A., Lavery, P.S., McMahon, K., Orth, R.J., Pearce, A., Vanderklift, M., Wernberg, T., Whiting, S., Wilson, S., 2016. Accelerating tropicalization and the transformation of temperate seagrass meadows. BioScience 66, 938–948. https://doi.org/10.1093/biosci/biw111

Jeyapragash, D., Subhashini, P., Raja, S., Abirami, K., Thangaradjou, T., 2016. Evaluation of in-vitro antioxidant activity of seagrasses: signals for potential alternate source. Free Radic. Antioxid. 6, 77–89. https://doi.org/10.5530/fra.2016.1.10

Jueterbock, A., Boström, C., Coyer, J.A., Olsen, J.L., Kopp, M., Dhanasiri, A.K.S., Smolina, I., Arnaud-Haond, S., Van de Peer, Y., Hoarau, G., 2020. The seagrass methylome is associated with variation in photosynthetic performance among clonal shoots. Front. Plant Sci. 11.

Koch, M., Bowes, G., Ross, C., Zhang, X.-H., 2013. Climate change and ocean acidification effects on seagrasses and marine macroalgae. Glob. Change Biol. 19, 103–132. https://doi.org/10.1111/j.1365-2486.2012.02791.x

Laufkötter, C., Zscheischler, J., Frölicher, T.L., 2020. High-impact marine heatwaves attributable to human-induced global warming. Science. https://doi.org/10.1126/science.aba0690

Lichtenthaler, H.K., 1998. The Stress Concept in Plants: An Introduction. Ann. N. Y. Acad. Sci. 851, 187–198. https://doi.org/10.1111/j.1749-6632.1998.tb08993.x

Lichtenthaler, H.K., Wellburn, A.R., 1983. Determinations of total carotenoids and *chlorophylls a* and *b* of leaf extracts in different solvents. Biochem. Soc. Trans. 11, 591–592. https://doi.org/10.1042/bst0110591

Marín-Guirao, L., Bernardeau-Esteller, J., García-Muñoz, R., Ramos, A., Ontoria, Y., Romero, J., Pérez, M., Ruiz, J.M., Procaccini, G., 2018. Carbon economy of Mediterranean seagrasses in response to thermal stress. Mar. Pollut. Bull. 135, 617–629. https://doi.org/10.1016/j.marpolbul.2018.07.050

Marín-Guirao, L., Ruiz, J.M., Dattolo, E., Garcia-Munoz, R., Procaccini, G., 2016. Physiological and molecular evidence of differential short-term heat tolerance in Mediterranean seagrasses. Sci. Rep. 6, 28615. https://doi.org/10.1038/srep28615

Martin, B.C., Statton, J., Siebers, A.R., Grierson, P.F., Ryan, M.H., Kendrick, G.A., 2018. Colonizing tropical seagrasses increase root exudation under fluctuating and continuous low light. Limnol. Oceanogr. 63, S381–S391. https://doi.org/10.1002/lno.10746

Masini, R.J., Manning, C.R., 1997. The photosynthetic responses to irradiance and temperature of four meadow-forming seagrasses. Aquat. Bot. 58, 21–36. https://doi.org/10.1016/S0304-3770(97)00008-9

Mathur, S., Agrawal, D., Jajoo, A., 2014. Photosynthesis: Response to high temperature stress. J. Photochem. Photobiol. B, Stress and Photosynthesis 137, 116–126. https://doi.org/10.1016/j.jphotobiol.2014.01.010

Menge, B.A., Close, S.L., Hacker, S.D., Nielsen, K.J., Chan, F., 2020. Biogeography of macrophyte productivity: Effects of oceanic and climatic regimes across spatiotemporal scales. Limnol. Oceanogr. lno.11635. https://doi.org/10.1002/lno.11635

Michaud, K.M., Reed, D.C., Miller, R.J., 2022. The Blob marine heatwave transforms California kelp forest ecosystems. Commun. Biol. 5, 1–8. https://doi.org/10.1038/s42003-022-04107-z

Moulton, O.M., Hacker, S.D., 2011. Congeneric variation in surfgrasses and ocean conditions influence macroinvertebrate community structure. Mar. Ecol. Prog. Ser. 433, 53–63. https://doi.org/10.3354/meps09180

Nguyen, H.M., Bulleri, F., Marín-Guirao, L., Pernice, M., Procaccini, G., 2021a. Photo-physiology and morphology reveal divergent warming responses in northern and southern hemisphere seagrasses. Mar. Biol. 168, 129. https://doi.org/10.1007/s00227-021-03940-w

Nguyen, H.M., Kim, M., Ralph, P.J., Marín-Guirao, L., Pernice, M., Procaccini, G., 2020. Stress memory in seagrasses: first insight into the effects of thermal priming and the role of epigenetic modifications. Front. Plant Sci. 11, 494. https://doi.org/10.3389/fpls.2020.00494

Nguyen, H.M., Ralph, P.J., Marín-Guirao, L., Pernice, M., Procaccini, G., 2021b. Seagrasses in an era of ocean warming: a review. Biol. Rev. 96, 2009–2030. https://doi.org/10.1111/brv.12736

Ontoria, Y., Cuesta-Gracia, A., Ruiz, J.M., Romero, J., Pérez, M., 2019. The negative effects of short-term extreme thermal events on the seagrass *Posidonia oceanica* are exacerbated by ammonium additions. PLOS ONE 14, e0222798. https://doi.org/10.1371/journal.pone.0222798

Pazzaglia, J., Badalamenti, F., Bernardeau-Esteller, J., Ruiz, J.M., Giacalone, V.M., Procaccini, G., Marín-Guirao, L., 2022a. Thermo-priming increases heat-stress tolerance in seedlings of the Mediterranean seagrass *P. oceanica*. Mar. Pollut. Bull. 174, 113164. https://doi.org/10.1016/j.marpolbul.2021.113164

Pazzaglia, J., Reusch, T.B.H., Terlizzi, A., Marín-Guirao, L., Procaccini, G., 2021. Phenotypic plasticity under rapid global changes: The intrinsic force for future seagrasses survival. Evol. Appl. 14, 1181–1201. https://doi.org/10.1111/eva.13212

Pazzaglia, J., Santillán-Sarmiento, A., Ruocco, M., Dattolo, E., Ambrosino, L., Marín-Guirao, L., Procaccini, G., 2022b. Local environment modulates whole-transcriptome expression in the seagrass *Posidonia oceanica* under warming and nutrients excess. Environ. Pollut. 303, 119077. https://doi.org/10.1016/j.envpol.2022.119077

Pospíšil, P., Tyystjärvi, E., 1999. Molecular mechanism of high-temperature-induced inhibition of acceptor side of Photosystem II. Photosynth. Res. 62, 55–66. https://doi.org/10.1023/A:1006369009170

R Core Team, 2020. R: A language and environment for statistical computing. R Found. Stat. Comput.

Ramírez-García, P., Terrados, J., Ramos, F., Lot, A., Ocaña, D., Duarte, C.M., 2002. Distribution and nutrient limitation of surfgrass, *Phyllospadix scouleri* and *Phyllospadix torreyi*, along the Pacific coast of Baja California (México). Aquat. Bot. 74, 121–131. https://doi.org/10.1016/S0304-3770(02)00050-5

Rokka, A., Aro, E.-M., Herrmann, R.G., Andersson, B., Vener, A.V., 2000. Dephosphorylation of photosystem II reaction center proteins in plant photosynthetic membranes as an immediate response to abrupt elevation of temperature. Plant Physiol. 123, 1525–1536. https://doi.org/10.1104/pp.123.4.1525

Ruiz-Montoya, L., Sandoval-Gil, J.M., Belando-Torrentes, M.D., Vivanco-Bercovich, M., Cabello-Pasini, A., Rangel-Mendoza, L.K., Maldonado-Gutiérrez, A., Ferrerira-Arrieta, A., Guzmán-Calderón, J.M., 2021. Ecophysiological responses and self-protective canopy effects of surfgrass (*Phyllospadix torreyi*) in the intertidal. Mar. Environ. Res. 172, 105501. https://doi.org/10.1016/j.marenvres.2021.105501

Sabeena Farvin, K.H., Jacobsen, C., 2013. Phenolic compounds and antioxidant activities of selected species of seaweeds from Danish coast. Food Chem. 138, 1670–1681. https://doi.org/10.1016/j.foodchem.2012.10.078

Saha, M., Barboza, F.R., Somerfield, P.J., Al-Janabi, B., Beck, M., Brakel, J., Ito, M., Pansch, C., Nascimento-Schulze, J.C., Jakobsson Thor, S., Weinberger, F., Sawall, Y., 2020. Response of foundation macrophytes to near-natural simulated marine heatwaves. Glob. Change Biol. 26, 417–430. https://doi.org/10.1111/gcb.14801

Sánchez-Barredo, M., Sandoval-Gil, J.M., Zertuche-González, J.A., Ladah, L.B., Belando-Torrentes, M.D., Beas-Luna, R., Cabello-Pasini, A., 2020. Effects of heat waves and light deprivation on giant kelp juveniles (*Macrocystis pyrifera*, Laminariales, Phaeophyceae). J. Phycol. 56, 880–894.

Sandoval-Gil, J.M., Barrote, I., Silva, J., Olivé, I., Costa, M.M., Ruiz, J.M., Marín-Guirao, L., Sánchez-Lizaso, J.L., Santos, R., 2015. Plant-water relations of intertidal and subtidal seagrasses. Mar. Ecol. 36, 1294–1310. https://doi.org/10.1111/maec.12230

Sandoval-Gil, J.M., del Carmen Ávila-López, M., Camacho-Ibar, V.F., Hernández-Ayón, J.M., Zertuche-González, J.A., Cabello-Pasini, A., 2019. Regulation of nitrate uptake by the seagrass *Zostera marina* during upwelling. Estuaries Coasts 42, 731–742.

Schlegel, R.W., 2020. Marine Heatwave Tracker. URL http://www.marineheatwaves.org/tracker.html

Sen Gupta, A., Thomsen, M., Benthuysen, J.A., Hobday, A.J., Oliver, E., Alexander, L.V., Burrows, M.T., Donat, M.G., Feng, M., Holbrook, N.J., Perkins-Kirkpatrick, S., Moore, P.J., Rodrigues, R.R., Scannell, H.A., Taschetto, A.S., Ummenhofer, C.C., Wernberg, T., Smale, D.A., 2020. Drivers and impacts of the most extreme marine heatwave events. Sci. Rep. 10, 19359. https://doi.org/10.1038/s41598-020-75445-3

Serrano, O., Arias-Ortiz, A., Duarte, C.M., Kendrick, G.A., Lavery, P.S., 2021. Impact of marine heatwaves on seagrass ecosystems, in: Ecosystem Collapse and Climate Change. Springer, pp. 345–364.

Sharma, P., Jha, A.B., Dubey, R.S., Pessarakli, M., 2012. Reactive oxygen species, oxidative damage, and antioxidative defense mechanism in plants under stressful conditions. J. Bot. 2012, e217037. https://doi.org/10.1155/2012/217037

Shelton, A.O., 2010. Temperature and community consequences of the loss of foundation species: Surfgrass (*Phyllospadix* spp., Hooker) in tidepools. J. Exp. Mar. Biol. Ecol. 391, 35–42. https://doi.org/10.1016/j.jembe.2010.06.003

Silva, J., Barrote, I., Costa, M.M., Albano, S., Santos, R., 2013. Physiological Responses of *Zostera marina* and *Cymodocea nodosa* to Light-Limitation Stress. PLOS ONE 8, e81058. https://doi.org/10.1371/journal.pone.0081058

Singleton, V.L., Rossi, J.A., 1965. Colorimetry of total phenolics with phosphomolybdic-phosphotungstic acid reagents. Am. J. Enol. Vitic. 16, 144–158.

Stipcich, P., Marín-Guirao, L., Pansini, A., Pinna, F., Procaccini, G., Pusceddu, A., Soru, S., Ceccherelli, G., 2022. Effects of current and future summer marine heat waves on *Posidonia oceanica*: Plant origin matters? Front. Clim. 4, 844831. https://doi.org/10.3389/fclim.2022.844831

Strydom, S., Murray, K., Wilson, S., Huntley, B., Rule, M., Heithaus, M., Bessey, C., Kendrick, G.A., Burkholder, D., Fraser, M.W., Zdunic, K., 2020. Too hot to handle: Unprecedented seagrass death driven by marine heatwave in a World Heritage Area. Glob. Change Biol. 26, 3525–3538. https://doi.org/10.1111/gcb.15065

Sunday, J.M., Howard, E., Siedlecki, S., Pilcher, D.J., Deutsch, C., MacCready, P., Newton, J., Klinger, T., 2022. Biological sensitivities to high-resolution climate change projections in the California current marine ecosystem. Glob. Change Biol. 28, 5726–5740. https://doi.org/10.1111/gcb.16317

Touchette, B.W., Burkholder, J.M., 2000. Review of nitrogen and phosphorus metabolism in seagrasses. J. Exp. Mar. Biol. Ecol. 250, 133–167. https://doi.org/10.1016/S0022-0981(00)00195-7

Tutar, O., Marín-Guirao, L., Ruiz, J.M., Procaccini, G., 2017. Antioxidant response to heat stress in seagrasses. A gene expression study. Mar. Environ. Res. 132, 94–102. https://doi.org/10.1016/j.marenvres.2017.10.011

Unsworth, R.K., Cullen-Unsworth, L.C., Jones, B.L., Lilley, R.J., 2022. The planetary role of seagrass conservation. Science 377, 609–613.

Vásquez-Elizondo, R.M., Legaria-Moreno, L., Pérez-Castro, M.Á., Krämer, W.E., Scheufen, T., Iglesias-Prieto, R., Enríquez, S., 2017. Absorptance determinations on multicellular tissues. Photosynth. Res. 132, 311–324. https://doi.org/10.1007/s11120-017-0395-6

Venegas, K., 2019. Distribución espacio-temporal y efecto de la temperatura en praderas de *Phyllospadix scouleri* en tres localidades de B.C.S. Universidad Autónoma de Baja California Sur. Tesis de Doctorado. Universidad Autónoma de Baja California Sur.

Vivanco-Bercovich, M., Belando-Torrentes, M.D., Figueroa-Burgos, M.F., Ferreira-Arrieta, A., Macías-Carranza, V., García-Pantoja, J.A., Cabello-Pasini, A., Samperio-Ramos, G., Cruz-López, R., Sandoval-Gil, J.M., 2022. Combined effects of marine heatwaves and reduced light on the physiology and growth of the surfgrass *Phyllospadix torreyi* from Baja California, Mexico. Aquat. Bot. 178, 103488. https://doi.org/10.1016/j.aquabot.2021.103488

Wiencke, C., Bischof, K. (Eds.), 2012. Seaweed Biology: Novel Insights into Ecophysiology, Ecology and Utilization, Ecological Studies. Springer Berlin Heidelberg, Berlin, Heidelberg. https://doi.org/10.1007/978-3-642-28451-9

Williams, S.L., 1995. Surfgrass (*Phyllospadix torreyi*) Reproduction: Reproductive Phenology, Resource Allocation, and Male Rarity. Ecology 76, 1953–1970. https://doi.org/10.2307/1940726

Winters, G., Nelle, P., Fricke, B., Rauch, G., Reusch, T., 2011. Effects of a simulated heat wave on photophysiology and gene expression of high- and low-latitude populations of *Zostera marina*. Mar. Ecol. Prog. Ser. 435, 83–95. https://doi.org/10.3354/meps09213

Xiu, P., Chai, F., Curchitser, E.N., Castruccio, F.S., 2018. Future changes in coastal upwelling ecosystems with global warming: The case of the California Current System. Sci. Rep. 8, 2866. https://doi.org/10.1038/s41598-018-21247-7

Zieman, J.C., 1974. Methods for the study of the growth and production of turtle grass, *Thalassia testudinum* König. Aquaculture 4, 139–143.

## 7. Figure legends

**Figure 1.** The unaltered donor meadow of *Phyllospadix scouleri* is located at Todos Santos Island, Baja California, Mexico (A, B and C, red dot), where seawater temperature was monitored with sensors in situ before and during the experiment (D, black line). Seawater temperature at the mesocosm was also recorded (D, blue and red lines). Below (E), a schematic representation of the experimental design, which consisted in one treatment (MHWs) with two consecutive warm periods (24°C) succeeded by recovery periods (18°C) and a control treatment with constant temperature (C - 18°C). Biological descriptors were determined at the end of each experimental period (HW-1, R-1, HW-2, R-2), as indicated by black or red circles.

**Figure 2. Parameters derived from photosynthesis-irradiance curves** determined for *P. scouleri* in response to two temperature treatments (MHWs in red, Control in black) along four sampling times (HW-1, R-1, HW-2, R-2). The treatment MHWs included two consecutive heatwaves of 24°C (red filled circles, HW-1 and HW-2) and their respective recovery periods at 18°C (red hollow circles, R-1 and R-2). Meanwhile, a reference group of plants (Control) was maintained at constant 18°C during the entire experiment. Values are means and standard errors (n = 4). The significance of the main effects from Treatment (Trt.) and Time and their interaction term (Two-way ANOVA) is indicated at the bottom left corner of each graph. In case of significant interaction, the significance of paired comparisons (Tukey HSD post-hoc test) between treatments at each sampling time is indicated with asterisks on top of the relevant sampling times. *$p<0.05$, **$p<0.01$, ***$p<0.001$, n.s.:$p>0.1$ (For complete results, see Table SM 7). (A) Net-$P_{max}$: Net maximum photosynthetic rate, (B) Gross- $P_{max}$: Gross maximum

photosynthetic rate, (C) $E_k$: Saturation Irradiance, (D) $E_c$: Compensation Irradiance, (E) α: Photosynthetic efficiency, (F) R: Respiration rate.

**Figure 3. Chlorophyll *a* fluorescence parameters** measured in *P. scouleri* in response to two temperature treatments (MHWs in red, Control in black) along four sampling times (HW-1, R-1, HW-2, R-2). The treatment MHWs included two consecutive heatwaves of 24°C (red filled circles, HW-1 and HW-2) and their respective recovery periods at 18°C (red hollow circles, R-1 and R-2). Meanwhile, a reference group of plants (Control) was maintained at constant 18°C during the entire experiment. Values are means and standard errors (n = 4). The significance of the main effects from Treatment (Trt.) and Time and their interaction term (Two-way ANOVA) is indicated at the bottom left corner of each graph. In case of significant interaction, the significance of paired comparisons (Tukey HSD post-hoc test) between treatments at each sampling time is indicated with asterisks on top of the relevant sampling times. *$p<0.05$, **$p<0.01$, ***$p<0.001$, n.s.:$p>0.1$ (For complete results, see Table SM 7). (A) $F_v/F_m$: Maximum photochemical efficiency, (B) $\Phi_{PSII}$: Effective photochemical efficiency, (C) ETR: Electron transport rate, (D) NPQ: Non-photochemical quenching.

**Figure 4. Lipid peroxidation (A), total phenolic content (B) and total antioxidant capacity (C)** determined in *P. scouleri* leaves in response to two temperature treatments (MHWs in red, Control in black) along four sampling times (HW-1, R-1, HW-2, R-2). The treatment MHWs included two consecutive heatwaves of 24°C (red filled circles, HW-1 and HW-2) and their respective recovery periods at 18°C (red hollow circles, R-1 and R-2). Meanwhile, a reference group of plants (Control) was maintained at constant 18°C during the entire experiment. Values

are means and standard errors (n = 4). The significance of the main effects from Treatment (Trt.) and Time and their interaction term (Two-way ANOVA) is indicated at the bottom left corner of each graph. In case of significant interaction, the significance of paired comparisons (Tukey HSD post-hoc test) between treatments at each sampling time is indicated with asterisks on top of the relevant sampling times. *p<0.05, **p<0.01, ***p<0.001, n.s.:p>0.1 (For complete results, see Table SM 7).

**Figure 5. Nitrate uptake rate (A), nitrogen content (B) and isotopic ratio of nitrogen (C)** determined in *P. scouleri* leaves in response to two temperature treatments (MHWs in red, Control in black) along four sampling times (HW-1, R-1, HW-2, R-2). The treatment MHWs included two consecutive heatwaves of 24°C (red filled circles, HW-1 and HW-2) and their respective recovery periods at 18°C (red hollow circles, R-1 and R-2). Meanwhile, a reference group of plants (Control) was maintained at constant 18°C during the entire experiment. Values are means and standard errors (n = 4). The significance of the main effects from Treatment (Trt.) and Time and their interaction term (Two-way ANOVA) is indicated at the bottom left corner of each graph. In case of significant interaction, the significance of paired comparisons (Tukey HSD post-hoc test) between treatments at each sampling time is indicated with asterisks on top of the relevant sampling times. *p<0.05, **p<0.01, ***p<0.001, n.s.:p>0.1 (For complete results, see Table SM 7).

**Figure 6. Non-structural carbohydrates (A), daily productivity (B) and relative growth rate (C)** determined in *P. scouleri* leaves in response to two temperature treatments (MHWs in red, Control in black) along four sampling times (HW-1, R-1, HW-2, R-2). The treatment MHWs

included two consecutive heatwaves of 24°C (red filled circles, HW-1 and HW-2) and their respective recovery periods at 18°C (red hollow circles, R-1 and R-2). Meanwhile, a reference group of plants (Control) was maintained at constant 18°C during the entire experiment. Values are means and standard errors (n = 4). The significance of the main effects from Treatment (Trt.) and Time and their interaction term (Two-way ANOVA) is indicated at the bottom left corner of each graph. In case of significant interaction, the significance of paired comparisons (Tukey HSD post-hoc test) between treatments at each sampling time is indicated with asterisks on top of the relevant sampling times. *p<0.05, **p<0.01, ***p<0.001, n.s.:p>0.1 (For complete results, see Table SM 7).

**Figure 7. Graphical representation** of the main responses observed in *P. scouleri* plants after being exposed to two consecutive heatwaves with recovery periods. The behavior of general physiological processes/features (bold letters and vertical arrows) is based on the measurements of representative biological descriptors (italic letters). Only statistically significant differences were considered (Two-way ANOVA with significant interaction term and post-hoc Tukey-HSD test with $p < 0.05$). Gross-Pmax: Gross maximum photosynthetic capacity, Net-Pmax: Net maximum photosynthetic capacity, $E_k$: Saturation irradiance, $F_v/F_m$: Maximum quantum yield, $\Phi_{PSII}$: Effective quantum yield, ETR: Electron transport rate, NPQ: Non-photochemical quenching, N(%): Nitrogen content, NSC: Non-structural carbohydrates, RGR: Relative growth rate.

## 8. Figures

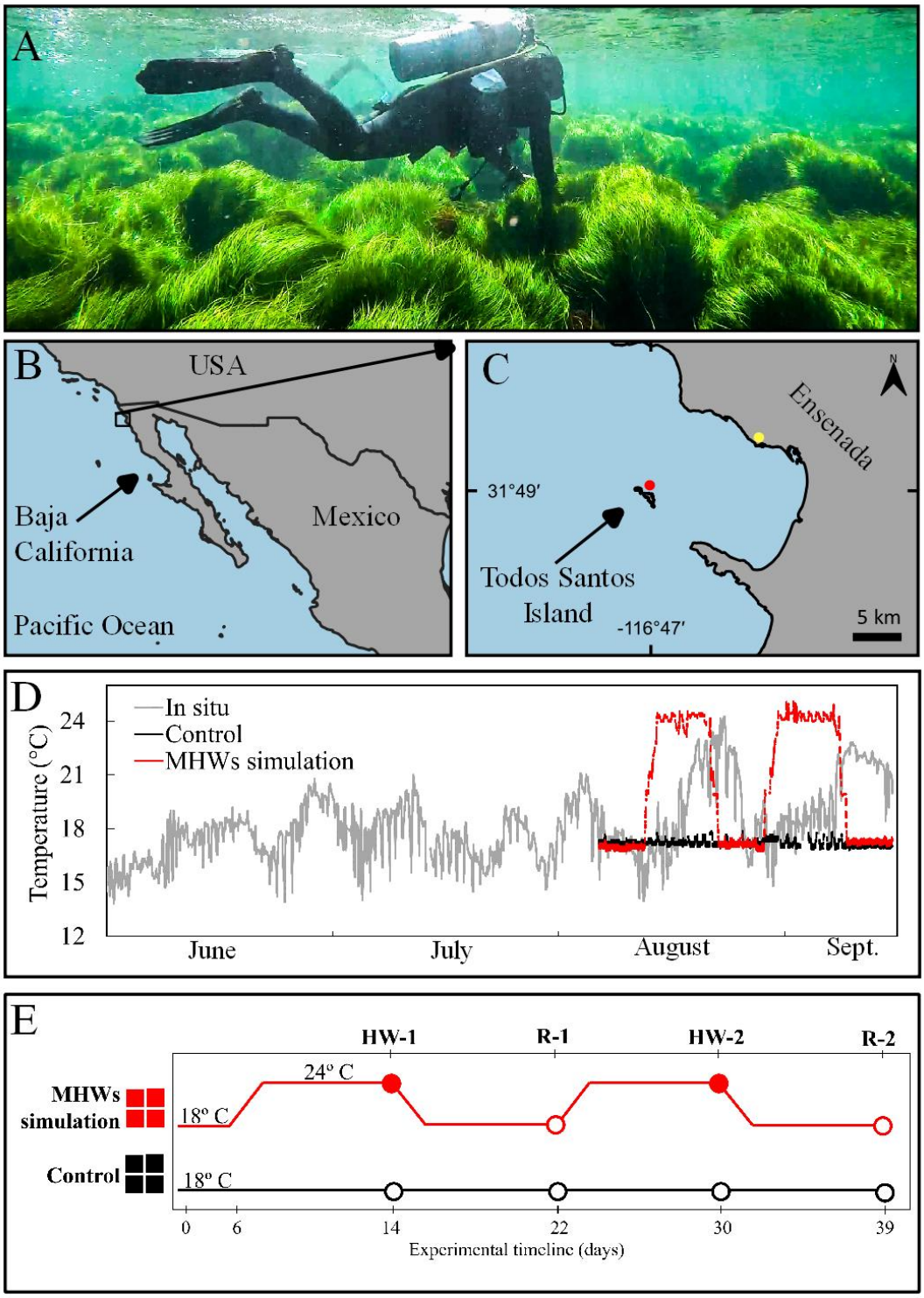
A
B
USA
Baja
California
Mexico
Pacific Ocean
C
N
Ensenada
31°49′
Todos Santos
Island
-116°47′
5 km
D
In situ
Control
MHWs simulation
Temperature (°C)
24
21
18
15
12
June
July
August
Sept.
E
HW-1
R-1
HW-2
R-2
24° C
MHWs
simulation
18° C
Control
18° C
0
6
14
22
30
39
Experimental timeline (days)

Fig. 1.

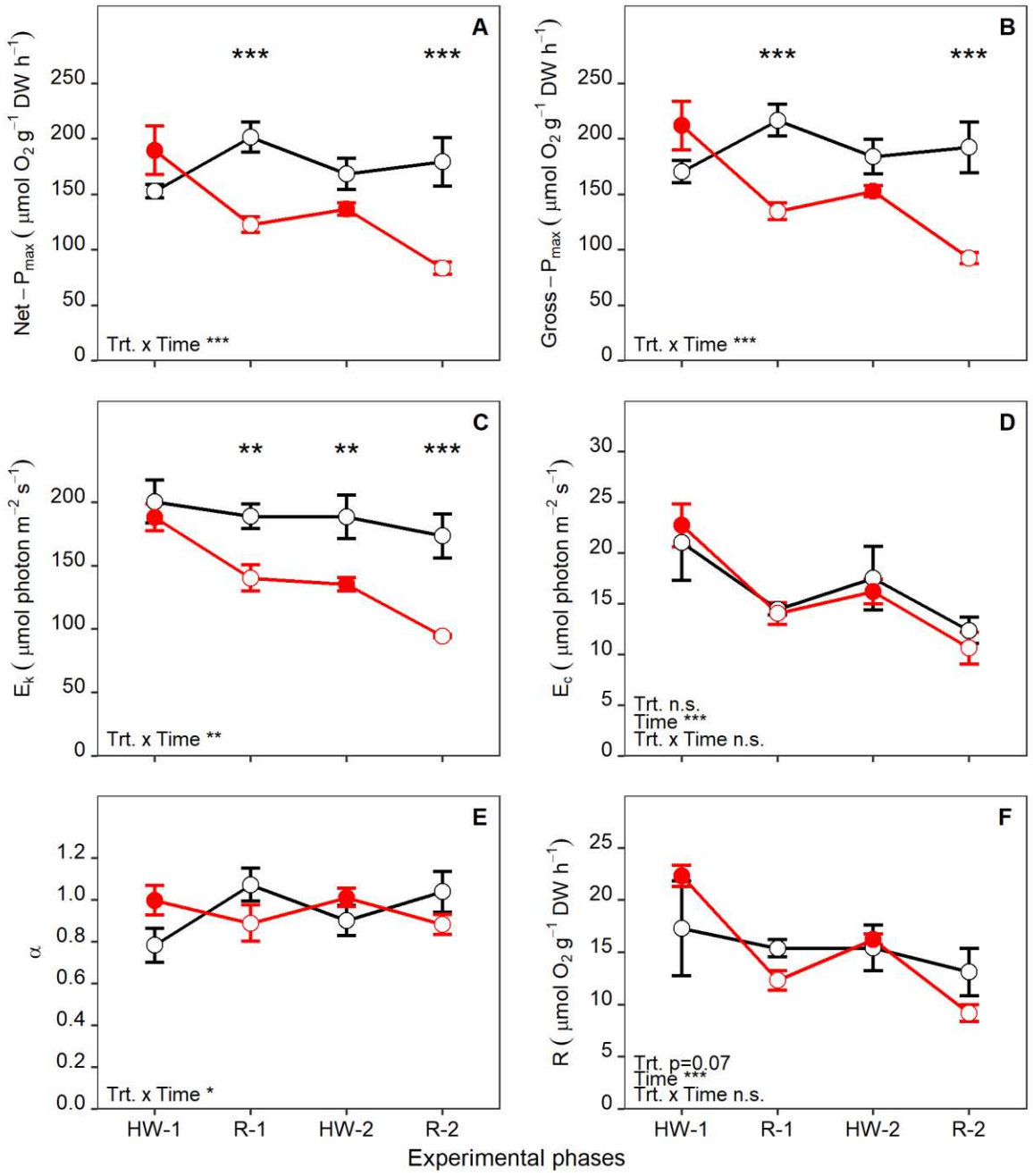
A
B
C
D
E
F
***
**
Net – $P_{max}$ ( µmol $O_2$ $g^{-1}$ DW $h^{-1}$)
Gross – $P_{max}$ ( µmol $O_2$ $g^{-1}$ DW $h^{-1}$)
$E_k$ ( µmol photon $m^{-2}$ $s^{-1}$)
$E_c$ ( µmol photon $m^{-2}$ $s^{-1}$)
α
R ( µmol $O_2$ $g^{-1}$ DW $h^{-1}$)
Trt. x Time ***
Trt. x Time **
Trt. x Time *
Trt. n.s.
Time ***
Trt. x Time n.s.
Trt. p=0.07
Time ***
Trt. x Time n.s.
HW-1
R-1
HW-2
R-2
Experimental phases

Fig. 2.

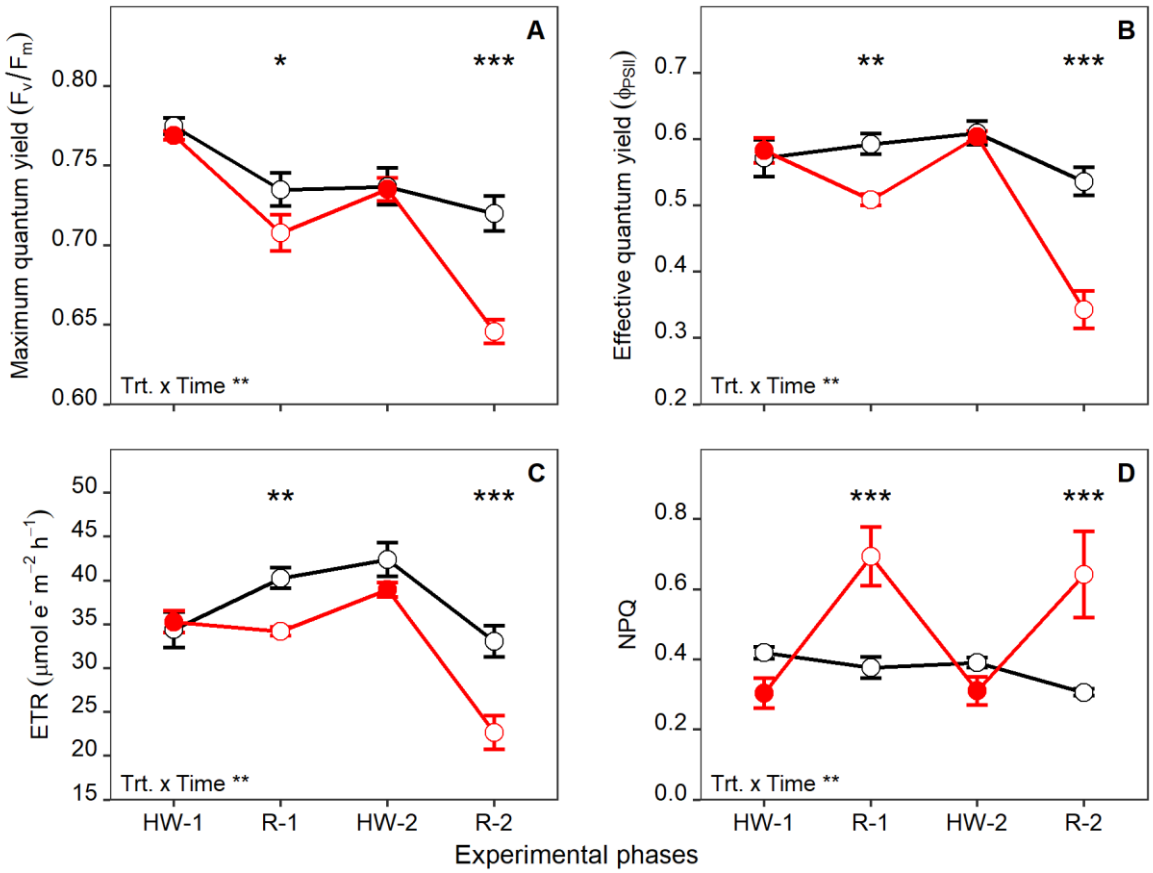
A
B
C
D
Maximum quantum yield ($F_v/F_m$)
Effective quantum yield ($\phi_{PSII}$)
ETR (µmol $e^-$ $m^{-2}$ $h^{-1}$)
NPQ
Trt. x Time **
HW-1
R-1
HW-2
R-2
Experimental phases

Fig. 3

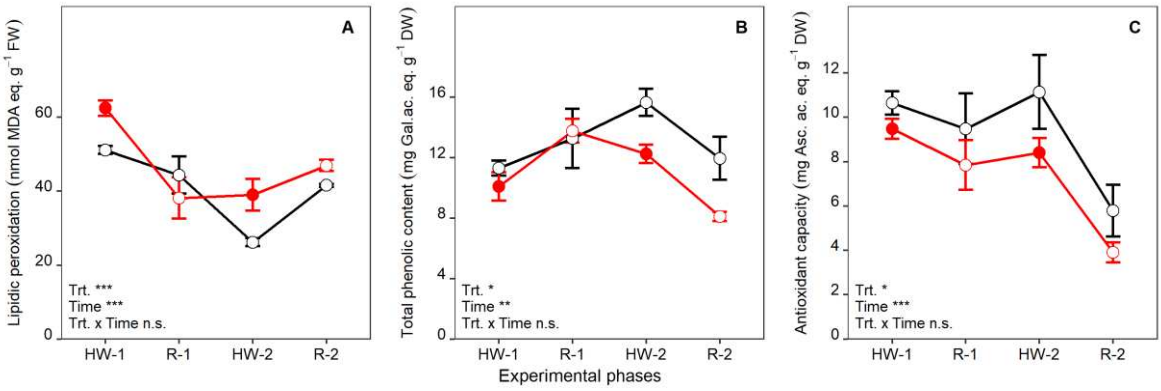
A
Lipidic peroxidation (nmol MDA eq. g-1 FW)
Trt. ***
Time ***
Trt. x Time n.s.
B
Total phenolic content (mg Gal.ac. eq. g-1 DW)
Trt. *
Time **
Trt. x Time n.s.
C
Antioxidant capacity (mg Asc. ac. eq. g-1 DW)
Trt. *
Time ***
Trt. x Time n.s.
HW-1
R-1
HW-2
R-2
Experimental phases

Fig. 4.

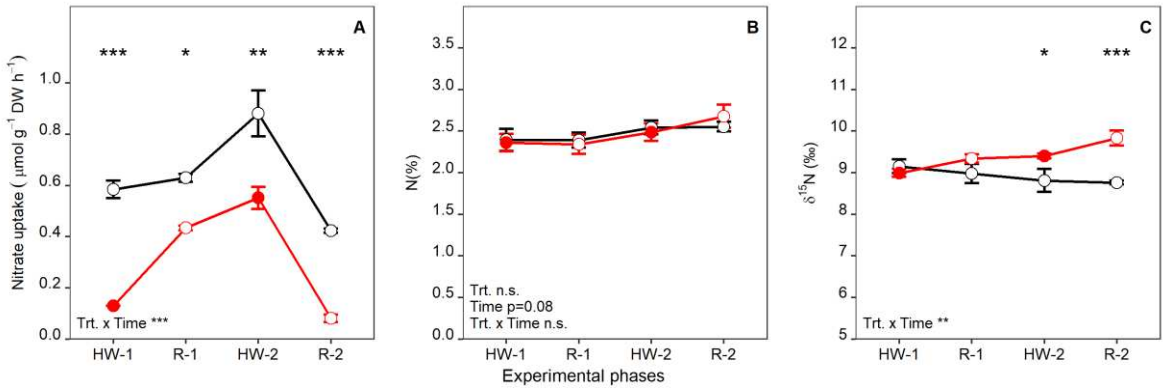
A
B
C
***
*
**
***
*
***
Nitrate uptake ( µmol g⁻¹ DW h⁻¹)
N(%)
δ15N (‰)
Trt. x Time ***
Trt. n.s.
Time p=0.08
Trt. x Time n.s.
Trt. x Time **
HW-1
R-1
HW-2
R-2
Experimental phases

Fig. 5.

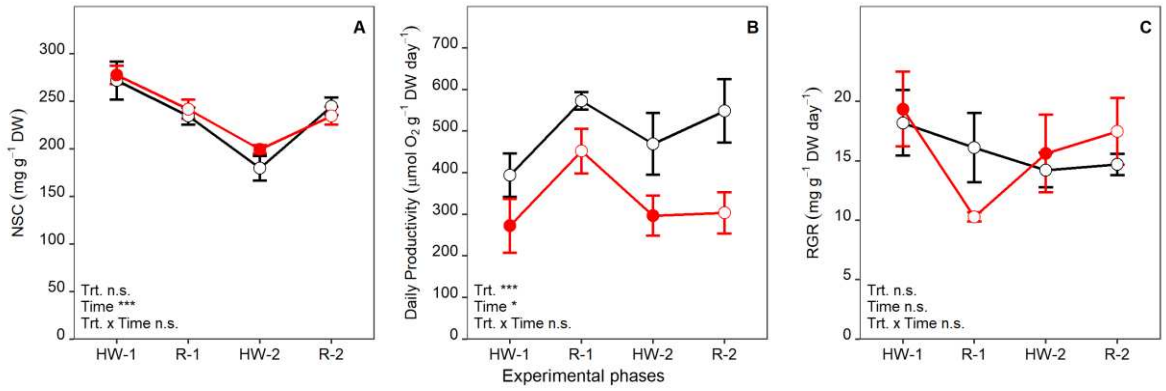
A
NSC (mg g$^{-1}$ DW)
300
250
200
150
100
50
0
Trt. n.s.
Time ***
Trt. x Time n.s.
HW-1
R-1
HW-2
R-2
B
Daily Productivity (µmol $O_2$ g$^{-1}$ DW day$^{-1}$)
700
600
500
400
300
200
100
0
Trt. ***
Time *
Trt. x Time n.s.
HW-1
R-1
HW-2
R-2
Experimental phases
C
RGR (mg g$^{-1}$ DW day$^{-1}$)
20
15
10
5
0
Trt. n.s.
Time n.s.
Trt. x Time n.s.
HW-1
R-1
HW-2
R-2

Fig. 6.

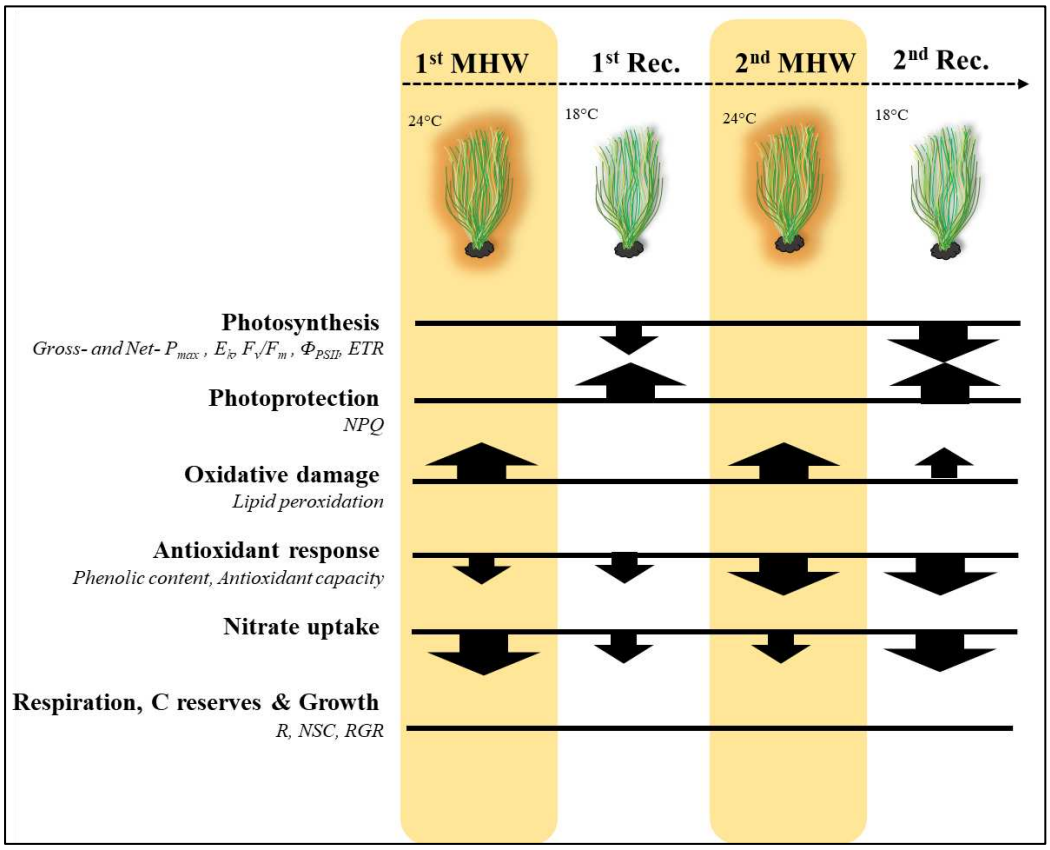
1st MHW
1st Rec.
2nd MHW
2nd Rec.
24°C
18°C
24°C
18°C
Photosynthesis
Gross- and Net- $P_{max}$ , $E_k$, $F_v/F_m$ , $\Phi_{PSII}$, ETR
Photoprotection
NPQ
Oxidative damage
Lipid peroxidation
Antioxidant response
Phenolic content, Antioxidant capacity
Nitrate uptake
Respiration, C reserves & Growth
R, NSC, RGR

Fig. 7.

## *9.* Supplementary material

**Figure SM 1.** Characteristics of the MHWs that were registered at the donor meadow location (Todos Santos Island, B.C., Mexico) between the years 1982 – 2019. A – Monthly distribution of MHWs incidence; B – Maximum intensity of registered MHWs; D - Duration of the registered MHWs; E – Duration of interval periods between consecutive MHWs; F – Number of days per year classified as MHW. Data was extracted from Marine Heatwave Tracker (Schlegel, 2020) and the selected pixel was: Lon. 116,875; Lat. 31,875.

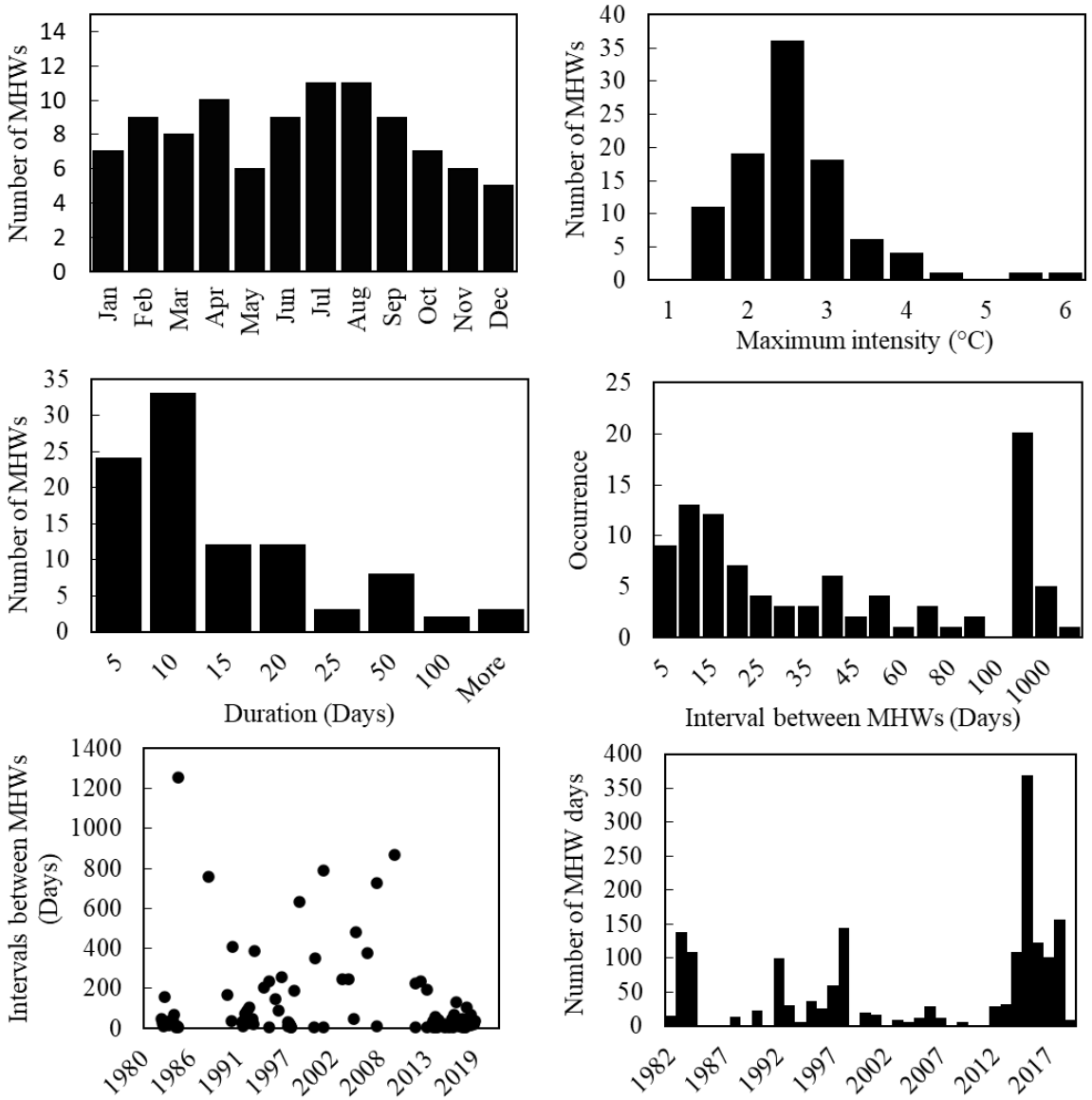

**Table SM 2.** Physiological characterization of *P. scouleri* plants after collection, before the beginning of the experiment. The unit, minimum (Min.), maximum (Max.) and mean values and the standard error (SE) are shown for each descriptor. The number of samples (n) was 6 for all descriptors. Net-$P_{max}$: Net maximum photosynthetic rate, Gross-$P_{max}$: Gross maximum photosynthetic rate, α: Photosynthetic efficiency, $E_c$: Compensation irradiance, $E_k$: Saturation irradiance, R: Respiration rate, $F_v/F_m$: Maximum photochemical yield, NPQ: Non-photochemical quenching, $\Phi_{PSII}$: Effective photochemical efficiency, ETR: Electron transport rate, NSC: Non-structural carbohydrates content.

| **Descriptors** | **n** | **Units** | **Reference values of *P. scouleri*** | | |
|---|---|---|---|---|---|
| | | | **Min.** | **Max.** | **Mean ± SE** |
| Net-$P_{max}$ | 6 | µmol $O_2$ $g^{-1}$ DW $h^{-1}$ | 129.70 | 199.50 | 166.5 ± 9.9 |
| Gross-$P_{max}$ | 6 | µmol $O_2$ $g^{-1}$ DW $h^{-1}$ | 152.00 | 227.50 | 185.6 ± 10.7 |
| α | 6 | µmol $O_2$ $g^{-1}$ DW $h^{-1}$/ µmol quanta $m^{-2}$ $s^{-1}$ | 0.81 | 1.29 | 1.03 ± 0.07 |
| $E_c$ | 6 | µmol quanta $m^{-2}$ $s^{-1}$ | 12.90 | 22.10 | 18.4 ± 1.3 |
| $E_k$ | 6 | µmol quanta $m^{-2}$ $s^{-1}$ | 107.50 | 218.40 | 166.8 ± 14.9 |
| R | 6 | µmol $O_2$ $g^{-1}$ DW $h^{-1}$ | 10.50 | 22.30 | 17.6 ± 1.2 |
| $F_v/F_m$ | 6 | - | 0.78 | 0.79 | 0.79 ± 0.002 |
| NPQ | 6 | - | 0.37 | 1.03 | 0.68 ± 0.09 |
| $\Phi_{PSII}$ | 6 | - | 0.52 | 0.66 | 0.59 ± 0.01 |
| ETR | 6 | µmol $e^-$ $m^{-2}$ $s^{-1}$ | 47.30 | 52.20 | 49.9 ± 0.51 |
| Chlorophyll *a* | 6 | mg $g^{-1}$ FW | 8.67 | 10.42 | 9.7 ± 0.22 |
| Chlorophyll *b* | 6 | mg $g^{-1}$ FW | 3.27 | 3.96 | 3.64 ± 0.07 |
| Chl. *b/a* ratio | 6 | - | 0.36 | 0.37 | 0.37 ± 0.002 |
| Carotenoids | 6 | mg $g^{-1}$ FW | 2.07 | 2.56 | 2.32 ± 0.06 |
| Lipid peroxidation | 6 | MDA Eq. (nmol $g^{-1}$ FW) | 57.70 | 98.10 | 81.3 ± 4.6 |
| Antioxidant capacity | 6 | Asc. Ac. Eq. (mg $g^{-1}$ DW) | 9.69 | 12.34 | 11.1 ± 0.44 |
| Phenolic content | 6 | Gal. Ac. Eq. (mg $g^{-1}$ DW) | 14.40 | 18.00 | 16.1 ± 0.49 |
| NSC | 6 | mg $g^{-1}$ DW | 361.00 | 443.40 | 405.6 ± 8.2 |

**Figure SM 3.** Photosynthesis (P) x Irradiance (E) curves determined by measuring the evolution of dissolved oxygen in respirometers containing leaf segments while gradually increasing the incident irradiance. Curves were performed during the first heatwave (A, "HW-1"), first recovery phase (B, "R-1"), second heatwave (C, "HW-2") and second recovery phase (D, "R-2"). At each sampling time, curves were determined for warmed plants (MHWs, red line) and for control plants (C, black line). An additional curve was determined before starting the experiment (gray line, used as reference in all figures). Bars represent standard error (N=4).

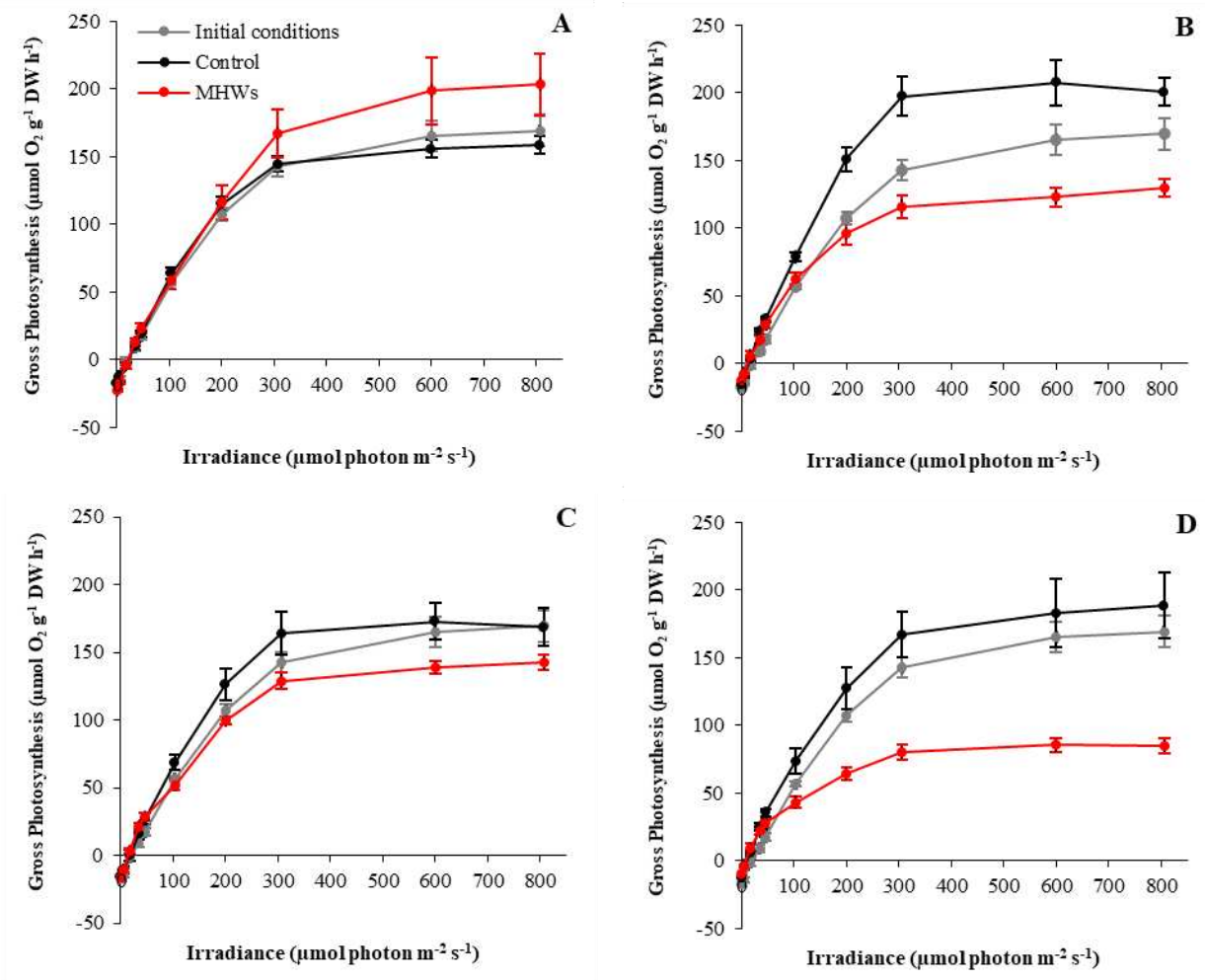

**Figure SM 4.** Ordination diagram of Principal Component Analysis (PCA) performed with all biological descriptors of *Phyllospadix scouleri* exposed to one experimental treatment (MHWs, red symbols) which included two consecutive heatwaves of 24°C (HW-1 and HW-2) and their respective recovery periods at 18°C (R-1 and R-2). A reference group of plants (Control, black symbols) was maintained at constant temperature of 18°C during the entire experiment. Shapes of symbols indicate sampling times. Before running the analysis, highly correlated variables were grouped (which are indicated by asterisks) as follows: Photosynthesis (Gross-$P_{max}$, Net-$P_{max}$, $E_k$, α), Respiration (R, $E_c$), PSII efficiency ($F_v/F_m$, $\Phi_{PSII}$, ETR), Pigments (Chl*a*, chl*b*, carotenoids), Antioxidants (Phenolic content, Antioxidant capacity).

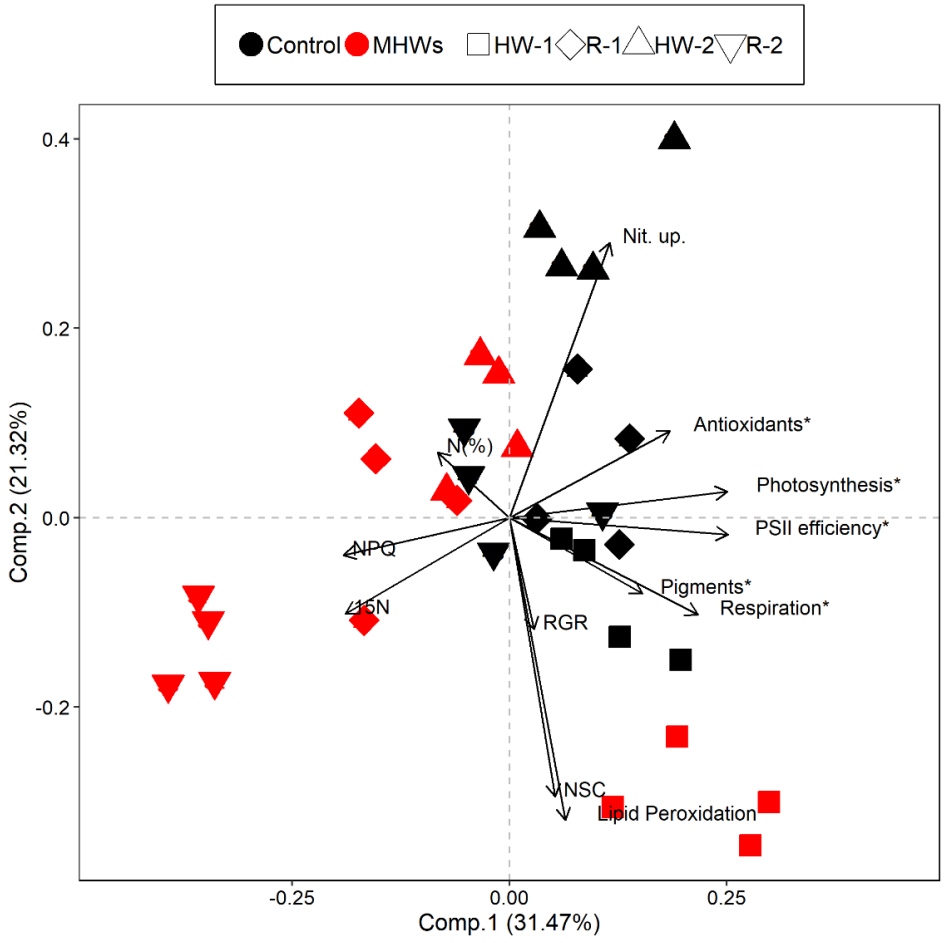


*Abbreviations*: NPQ: Non-photochemical quenching; Lip. peroxidation.: Lipid peroxidation; Nit. up.: Nitrate uptake rate; N (%): Nitrogen content; 15N: Nitrogen isotopic signal; NSC: Non-structural carbohydrates; RGR: Relative growth rate.

**Table SM 5.** Contribution of each variable (i.e., loadings) for the first two axes (PC1 and PC2) of the PCA applied to the complete data set. Before running the analysis, highly correlated variables were grouped (which are indicated by asterisks) as follows: Photosynthesis (Gross-$P_{max}$, Net-$P_{max}$, Ek, α), Respiration (R, $E_c$), PSII efficiency ($F_v/F_m$, $\Phi_{PSII}$, ETR), Pigments (Chl*a*, chl*b*, carotenoids), Antioxidants (phenolic content, antioxidant capacity).

| Variable | PC1 | PC2 |
|---|---|---|
| Photosynthesis* | 0.44 | 0.05 |
| Respiration* | 0.38 | -0.18 |
| PSII efficiency* | 0.44 | -0.03 |
| NPQ | -0.33 | -0.07 |
| Pigments* | 0.27 | -0.14 |
| Antioxidants* | 0.32 | 0.16 |
| Lipid Peroxidation | 0.11 | -0.56 |
| N(%) | -0.14 | 0.12 |
| Nit. up. | 0.20 | 0.51 |
| 15N | -0.33 | -0.18 |
| NSC | 0.09 | -0.51 |
| RGR | 0.05 | -0.21 |

Abbreviations*: NPQ: Non-photochemical quenching; Lip. peroxidation.: Lipid peroxidation; Nit. up.: Nitrate uptake rate; N (%): Nitrogen content; 15N: Nitrogen isotopic signal; NSC: Non-structural carbohydrates; RGR: Relative growth rate.*

**Table SM 6.** Summarized results of permutational analysis of variance (PERMANOVA) applied to the physiological responses of *Phyllospadix scouleri* to two temperature treatments (MHWs and Control), with four sampling times (HW-1, R-1, HW-2, R-2). The treatment MHWs included two consecutive heatwaves of 24°C (HW-1 and HW-2) and their respective recovery periods at 18°C (R-1 and R-2). A reference group of plants (Control) was maintained at constant temperature of 18°C during the entire experiment. The data set included all descriptors used in the PCA, but without grouping (SM 3, 4). The analysis was based on a Euclidean distance matrix derived from normalized data. Apart from the main test (top block), paired comparisons were performed to identify individual differences between treatments and among sampling times (bottom blocks; only P-values are shown). In the case of paired comparisons, the Bonferroni adjustment was applied. P values in bold text indicate statistical significance at $P < 0.05$.

| **Main test** | | | | |
|---|---|---|---|---|
| Source | df | MS | Pseudo-F | P |
| Treatment | 3 | 81 | 6 | **0.001** |
| Time | 1 | 87 | 7 | **0.001** |
| Treatment * Time | 3 | 41 | 3 | **0.001** |
| Residuals | 23 | 12 | | |

| **Pairwise tests** | | | | |
|---|---|---|---|---|
| *Between treatments for each sampling time* | | | | |
| | HW-1 | R-1 | HW-2 | R-2 |
| C x MHWs | 0.256 | 0.092 | 0.176 | **0.048** |

| *Between sampling times for each treatment* | | |
|---|---|---|
| | C | MHWs |
| HW-1 x R-1 | 0.330 | **0.030** |
| HW-1 x HW-2 | 0.186 | **0.036** |
| HW-1 x R-2 | 0.222 | **0.012** |
| R-1 x HW-2 | 0.498 | 0.204 |
| R-1 x R-2 | 2.214 | 0.078 |
| HW-2 x R-2 | 0.228 | **0.018** |

**Table SM 7.** Results of 2-way Anova (left block) where the main and interactive effects of the factors Treatment ("Trt.", 2 levels: Control and MHWs) and Time ("Time", 4 levels: HW-1, R-1, HW-2, R-2) were tested for each biological descriptor. In case of a significant interaction term ($p < 0.05$), Tukey-HSD post-hoc test was used to compare individual means between MHWs and Control at each sampling time. At the right block, individual means and standard error are presented, as well as the significance of the Tukey-HSD test.

| Variable | 2-Way Anova RM | | | | Individual means and paired differences | | | |
|---|---|---|---|---|---|---|---|---|
| | Effect | F | p | | HW-1 | R-1 | HW-2 | R-2 |
| **Net-$P_{max}$** | Trt. | 19.374 | *** | C | 153.05 ± 6.16 | 201.57 ± 13.58 | 168.48 ± 13.97 | 179.37 ± 21.98 |
| | Time | 3.155 | * | MHW | 189.8 ± 21.85 | 122.67 ± 7.06 | 136.75 ± 5.47 | 83.51 ± 5.43 |
| | Trt.*Time | 9.475 | *** | *Tukey HSD* | *0.07* | *** | *n.s.* | *** |
| **Gross-$P_{max}$** | Trt. | 17.595 | *** | C | 170.35 ± 10.11 | 216.96 ± 14.3 | 183.9 ± 15.58 | 192.48 ± 23.01 |
| | Time | 3.982 | * | MHW | 212.09 ± 21.86 | 134.98 ± 7.47 | 153 ± 5.03 | 92.66 ± 4.79 |
| | Trt.*Time | 9.695 | *** | *Tukey HSD* | *0.05* | *** | *n.s.* | *** |
| **α** | Trt. | 0.005 | n.s. | C | 0.78 ± 0.08 | 1.07 ± 0.08 | 0.9 ± 0.07 | 1.04 ± 0.1 |
| | Time | 0.554 | n.s. | MHW | 1 ± 0.07 | 0.89 ± 0.09 | 1.01 ± 0.04 | 0.88 ± 0.05 |
| | Trt.*Time | 3.525 | * | *Tukey HSD* | *0.05* | *0.09* | *n.s.* | *n.s.* |
| **R** | Trt. | 3.647 | p=0.07 | C | 17.29 ± 4.57 | 15.39 ± 0.82 | 15.42 ± 2.2 | 13.1 ± 2.26 |
| | Time | 28.547 | *** | MHW | 22.29 ± 1.02 | 12.32 ± 0.94 | 16.25 ± 0.52 | 9.16 ± 0.8 |
| | Trt.*Time | 1.294 | n.s. | | | | | |
| **$E_k$** | Trt. | 45.182 | *** | C | 200.57 ± 17.02 | 188.86 ± 9.55 | 188.56 ± 17.11 | 173.47 ± 17.4 |
| | Time | 12.993 | *** | MHW | 188.08 ± 10.44 | 140.34 ± 10.3 | 135.4 ± 5.29 | 94.49 ± 1.38 |
| | Trt.*Time | 5.319 | ** | *Tukey HSD* | *n.s.* | ** | ** | *** |
| **$E_c$** | Trt. | 0.117 | n.s. | C | 21.05 ± 3.77 | 14.43 ± 0.55 | 17.53 ± 3.15 | 12.36 ± 1.3 |
| | Time | 9.374 | *** | MHW | 22.71 ± 2.1 | 14.05 ± 1.07 | 16.19 ± 1.2 | 10.62 ± 1.57 |
| | Trt.*Time | 0.419 | n.s. | | | | | |
| **$F_v/F_m$** | Trt. | 18.642 | *** | C | 0.77 ± 0.01 | 0.73 ± 0.01 | 0.74 ± 0.01 | 0.72 ± 0.01 |
| | Time | 34.163 | *** | MHW | 0.77 ± 0 | 0.71 ± 0.01 | 0.74 ± 0.01 | 0.65 ± 0.01 |
| | Trt.*Time | 6.951 | ** | *Tukey HSD* | *n.s.* | * | *n.s.* | *** |
| **NPQ** | Trt. | 0.87 | n.s. | C | 0.42 ± 0.02 | 0.38 ± 0.03 | 0.39 ± 0.01 | 0.31 ± 0.01 |
| | Time | 9.627 | *** | MHW | 0.3 ± 0.04 | 0.69 ± 0.08 | 0.31 ± 0.04 | 0.64 ± 0.12 |
| | Trt.*Time | 7.211 | ** | *Tukey HSD* | *n.s.* | *** | *n.s.* | *** |
| **$\Phi_{PSII}$** | Trt. | 17.914 | *** | C | 0.57 ± 0.03 | 0.59 ± 0.02 | 0.61 ± 0.02 | 0.54 ± 0.02 |
| | Time | 25.493 | *** | MHW | 0.58 ± 0.02 | 0.51 ± 0.01 | 0.6 ± 0.01 | 0.34 ± 0.03 |
| | Trt.*Time | 7.029 | ** | *Tukey HSD* | *n.s.* | ** | *n.s.* | *** |
| **ETR** | Trt. | 19.476 | *** | C | 34.39 ± 2.03 | 40.29 ± 1.2 | 42.38 ± 1.93 | 33.07 ± 1.77 |
| | Time | 25.327 | *** | MHW | 35.31 ± 1.22 | 34.21 ± 0.51 | 38.95 ± 0.84 | 22.68 ± 1.9 |
| | Trt.*Time | 4.862 | ** | *Tukey HSD* | *n.s.* | ** | *n.s.* | *** |
| **Chl*a*** | Trt. | 0.026 | n.s. | C | 7.72 ± 0.38 | 7.36 ± 0.12 | 8.72 ± 0.42 | 6.81 ± 0.94 |
| | Time | 5.474 | ** | MHW | 10.03 ± 0.51 | 7.42 ± 0.47 | 6.23 ± 0.26 | 7.17 ± 0.46 |
| | Trt.*Time | 7.834 | *** | *Tukey HSD* | ** | *n.s.* | ** | *n.s.* |
| **Chl*b*** | Trt. | 0.05 | n.s. | C | 3.69 ± 0.2 | 2.99 ± 0.11 | 3.49 ± 0.25 | 2.77 ± 0.34 |
| | Time | 7.256 | ** | MHW | 3.92 ± 0.27 | 3 ± 0.13 | 2.69 ± 0.07 | 3.2 ± 0.12 |
| | Trt.*Time | 3.432 | * | | | n.s. | n.s. | * |
| **Chl *b/a* ratio** | Trt. | 2.389 | n.s. | C | 0.43 ± 0 | 0.39 ± 0.01 | 0.41 ± 0.01 | 0.4 ± 0.01 |
| | Time | 0.897 | n.s. | MHW | 0.4 ± 0 | 0.42 ± 0.02 | 0.42 ± 0.01 | 0.43 ± 0.01 |
| | Trt.*Time | 4.833 | ** | *Tukey HSD* | * | *0.09* | *n.s.* | * |
| **Carotenoids** | Trt. | 1.919 | n.s. | C | 1.92 ± 0.05 | 1.84 ± 0.04 | 2.14 ± 0.14 | 1.92 ± 0.24 |
| | Time | 3.344 | * | MHW | 2.6 ± 0.2 | 2.6 ± 0.2 | 1.89 ± 0.09 | 1.8 ± 0.06 |
| | Trt.*Time | 5.077 | ** | *Tukey HSD* | ** | *n.s.* | *0.08* | *n.s.* |
| **Phenolic content** | Trt. | 7.187 | * | C | 11.3 ± 0.49 | 13.26 ± 1.96 | 15.65 ± 0.9 | 11.95 ± 1.42 |
| | Time | 7.536 | ** | MHW | 10.1 ± 0.94 | 13.77 ± 0.79 | 12.25 ± 0.61 | 8.09 ± 0.3 |
| | Trt.*Time | 2.212 | n.s. | | | | | |
| **Antioxidant capacity** | Trt. | 6.134 | * | C | 10.65 ± 0.53 | 9.48 ± 1.59 | 11.14 ± 1.66 | 5.79 ± 1.16 |
| | Time | 10.277 | *** | MHW | 9.47 ± 0.45 | 7.85 ± 1.12 | 8.41 ± 0.66 | 3.9 ± 0.45 |
| | Trt.*Time | 0.19 | n.s. | | | | | |
| **Lipid peroxidation** | Trt. | 25.907 | *** | C | 51.14 ± 1.07 | 44.38 ± 4.98 | 26.2 ± 1.11 | 41.59 ± 0.39 |
| | Time | 77.915 | *** | MHW | 62.49 ± 2.1 | 38.16 ± 5.62 | 39.04 ± 4.27 | 46.95 ± 1.53 |
| | Trt.*Time | 2.324 | n.s. | *Tukey HSD* | | | | |

| | | | | | | | | |
|---|---|---|---|---|---|---|---|---|
| **Nitrate uptake** | Trt. | 238.452 | *** | C | 0.58 ± 0.03 | 0.63 ± 0.02 | 0.88 ± 0.09 | 0.42 ± 0.01 |
| | Time | 86.241 | *** | MHW | 0.13 ± 0 | 0.43 ± 0.01 | 0.55 ± 0.04 | 0.08 ± 0.01 |
| | Trt.*Time | 27.647 | *** | *Tukey HSD* | *** | * | ** | *** |
| **N (%)** | Trt. | 0.002 | n.s. | C | 2.4 ± 0.13 | 2.39 ± 0.09 | 2.54 ± 0.08 | 2.55 ± 0.06 |
| | Time | 2.507 | p=0.08 | MHW | 2.36 ± 0.1 | 2.34 ± 0.12 | 2.49 ± 0.11 | 2.68 ± 0.14 |
| | Trt.*Time | 0.326 | n.s. | | | | | |
| **$\delta^{15}N$** | Trt. | 13.785 | ** | C | 9.15 ± 0.16 | 8.99 ± 0.23 | 8.81 ± 0.28 | 8.76 ± 0.04 |
| | Time | 1.451 | n.s. | MHW | 8.99 ± 0.1 | 9.34 ± 0.1 | 9.4 ± 0.06 | 9.84 ± 0.18 |
| | Trt.*Time | 5.573 | ** | *Tukey HSD* | *n.s.* | *n.s.* | * | *** |
| **NSC** | Trt. | 0.496 | n.s. | C | 271.89 ± 19.87 | 234.63 ± 9.06 | 179.66 ± 12.83 | 244.9 ± 9.37 |
| | Time | 19.039 | *** | MHW | 277.63 ± 9.64 | 241.64 ± 10.02 | 199.5 ± 4.42 | 234.9 ± 9.35 |
| | Trt.*Time | 0.58 | n.s. | | | | | |
| **RGR** | Trt. | 16.56 | *** | C | 393.8 ± 52.27 | 572.56 ± 21.33 | 469.1 ± 74.04 | 548.52 ± 76.09 |
| | Time | 3.514 | * | MHW | 272.27 ± 64.58 | 451.89 ± 54.01 | 296.56 ± 47.95 | 303.49 ± 49.41 |
| | Trt.*Time | 0.523 | n.s. | | | | | |

**Abbreviations:** *Net-Pmax: Net maximum photosynthetic capacity; Gross-Pmax: Gross maximum photosynthetic capacity; α: Photosynthetic efficiency; $E_c$: Compensating Irradiance; $E_k$: Saturating irradiance; R: Dark respiration rate; $F_v/F_m$: Maximum photochemical efficiency; NPQ: Non-photochemical quenching; $\Phi_{PSII}$: Effective photochemical efficiency; ETR: Electron transport rate; Chl. a: Chlorophyll a content; Chl. b: Chlorophyll b content; Chl. b/a ratio: Chlorophyll b/a ratio; N(%): Nitrogen content; $\delta^{15}N$: Isotopic ratio of nitrogen ($^{15}N/^{14}N$); NSC: Non-structural carbohydrates; RGR: Relative growth rate.*

**Figure SM 8.** Leaf pigment content determined in *P. scouleri* in response to two temperature treatments (MHWs in red, Control in black) along four sampling times (HW-1, R-1, HW-2, R-2). The treatment MHWs included two consecutive heatwaves of 24°C (red filled circles, HW-1 and HW-2) and their respective recovery periods at 18°C (red hollow circles, R-1 and R-2). Meanwhile, a reference group of plants (Control) was maintained at constant 18°C during the entire experiment. Values are means and standard errors (n = 4). The significance of the main effects from Treatment (Trt.) and Time and their interaction term (Two-way ANOVA) is indicated at the bottom left corner of each graph. In case of significant interaction, the significance of paired comparisons (Tukey HSD post-hoc test) between treatments at each sampling time is indicated with asterisks on top of the relevant sampling times. *$p<0.05$, **$p<0.01$, ***$p<0.001$, n.s.:$p>0.1$ (For complete results, see Table SM 7). (A) Chl. *a*: Chlorophyll *a* content, (B) Chl. *b*: Chlorophyll *b* content, (C) Chl. b/a ratio: Chlorophyll *b/a* ratio,

(D) Carot.: Carotenoids content.

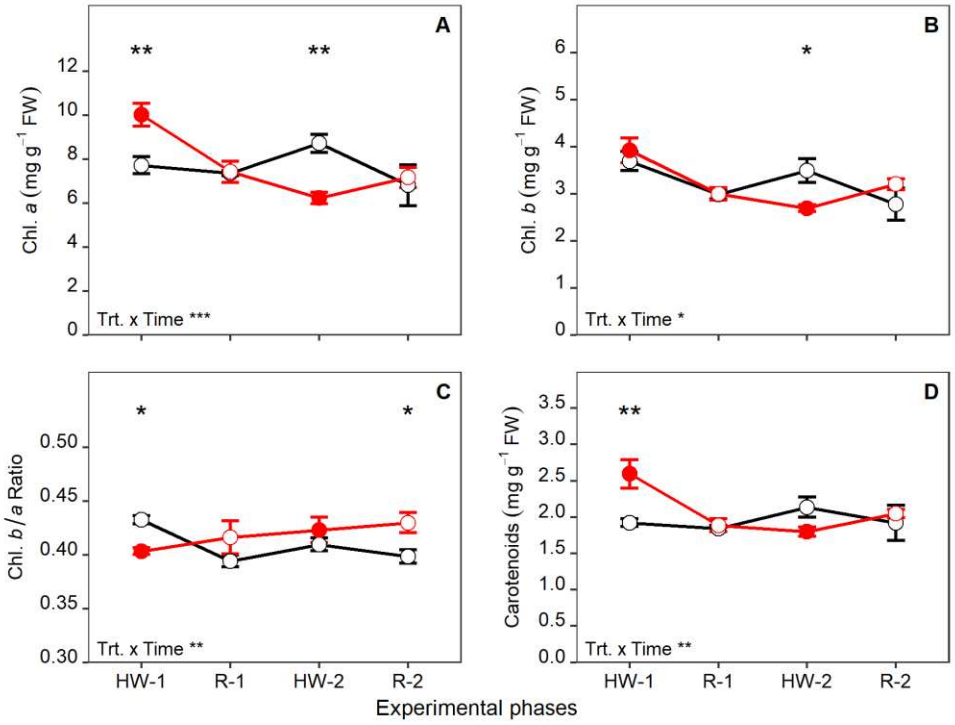

**CAPÍTULO III – Comparación de los efectos de olas de calor marinas de distinta intensidad (severas vs. extremas) en la ecofisiología, crecimiento y capacidad de recuperación de *Phyllospadix scouleri***

**Extreme marine heatwaves could overcome the thermal limit of the surfgrass *Phyllospadix scouleri***


## ABSTRACT

Marine ecosystems' structure and functionality is being challenged by the occurrence of increasingly intense marine heatwaves (MHWs) as consequence of global climate change. Seagrass meadows - and the multiple ecosystem services they provide - are potentially threatened by these extreme warming events. Accurately predicting the thermal tolerance of seagrasses is fundamental to understand and manage potential impacts of climate change. In this study, we conducted an experiment with the surfgrass *Phyllospadix scouleri* - a keystone species for coastal ecosystems along the Pacific coast of North America - to investigate the potential effects of MHWs, as these events have become more intense in present days. We simulated warming events of different intensities under a fluctuating temperature regime (HW-1: 23.5 ± 1.5°C; HW-2: 26.5 ± 1.5°C; Control: 18.5 ± 1.5°C) in an outdoor mesocosm system with thermo-regulated aquariums and determined the ecophysiological responses of *P. scouleri* plants during the exposure to heat and after a recovery period. Our results indicate that the overall physiological status of *P. scouleri* was not affected by the severe MHW (i.e., HW-1), as the photosynthetic performance and carbon balance were preserved, photoprotective mechanisms were activated and no signs of oxidative stress were manifested. Conversely, the extreme MHW (i.e., HW-2) induced meaningful alterations in *P. scouleri* plants, which apart from manifesting more accentuated oxidative pressure, exhibited negative carbon balance (i.e., daily productivity) due to decreased photosynthesis and increased respiration, and presented a significant decline in leaf

growth rate. Overall, our results suggest that the thermo-tolerance capacity of surfgrass in Baja California may be surpassed by future MHWs.

***Keywords:*** thermal stress, ecophysiology, climate change, surfgrass, photosynthesis, respiration, oxidative stress, growth

**Abbreviations:** MHW: Marine heatwaves, Net-$P_{max}$: Net maximum photosynthetic rate, Gross-$P_{max}$: Gross maximum photosynthetic rate, R: Respiration rate, α: Photosynthetic efficiency, $E_c$: Compensation irradiance, $E_k$: Saturation irradiance, $ETR_{max}$: Maximum electron transport rate, $\Phi_{PSII}$: Effective quantum yield, NPQ: Non-photochemical quenching, $F_v/F_m$: Maximum quantum yield, $F_0$: Minimum fluorescence, $F_m$: Maximum fluorescence, NSCs: Non-structural carbohydrates, RGR: Relative growth rate, DP: Daily productivity.

## 1. Introduction

Surfgrasses (*Phyllospadix scouleri* W.J. Hooker, and *Phyllospadix torreyi* S. Watson*)* are among the most important key foundation species which dominate intertidal landscapes throughout the Northeast Pacific coasts, from Vancouver Island (Canada) to Baja California (Mexico) (den Hartog & Kuo, 2006). Because of their high productivity (> 8000 g DW $m^{-2}$ $year^{-1}$; Ramírez-García et al., 1998) and dense canopy architecture (8000 – 12000 shoots $m^{-2}$, Garcia-Pantoja et al., 2020), formed by extremely large leaves (up to 160 cm, Garcia-Pantoja et al., 2020), surfgrasses strongly condition the physico-chemical and biological processes from the upper intertidal and tide-pools, to shallow (~5 m) bottoms (Hori, 2006; Moulton and Hacker, 2011; Tharaldson, 2018; Ruiz-Montoya et al. 2021). Mixed *Phyllospadix* meadows hold similar ecological and socio-economic benefits than those identified for other seagrasses (Tharaldson, 2018; Garcia-Pantoja et al., 2020; Fields & Silbiger, 2022). Also, these plants exhibit particular morphological and ultrastructural properties, which make this species able to grow on rocky substrates in high wave-exposed shores (Cooper & McRoy, 1988; Kuo and Stewart, 1995). This condition sustains the ecological relevance of *Phyllospadix* in these challenging environments and makes it unique among the seagrasses.

Nowadays, *Phyllospadix* are threatened by similar human-induced activities and factors fueled by climate change (such as ocean warming) that have caused a global decline of seagrass meadows during the last decades (Waycott et al., 2009; Dunic et al., 2021). Since seagrass meadows are highly valuable ecosystems in virtue of the multiple services they provide, their loss represents a threat for human well-being and other intrinsically connected coastal ecosystems (Carlson et al., 2021; Unsworth et al., 2022). While these effects are well documented in other temperate regions

(e.g., *Posidonia oceanica* in the Mediterranean Sea; Marbà et al., 2014; McDonald et al., 2023) and in the Northeast Pacific (e.g., *Zostera marina;* Kelly et al., 2019; Munsch et al., 2023; Magel et al., 2023), there is extremely scarce information about the responses of *Phyllospadix* to anthropogenic stressors (Pearse et al., 2015; Honig et al., 2016). Furthermore, and even though ocean warming and marine heatwaves are considered among the major threats to seagrass-dominated systems (Dunic et al., 2021; Serrano et al., 2021), knowledge is practically nil for *Phyllospadix* (Vivanco-Bercovich et al., 2022). Understanding how surfgrasses will respond to future environmental conditions, associated to climate change, could support adaptation and mitigation strategies for the conservation of these important ecosystems (Rilov et al., 2019; Unsworth et al., 2019).

Marine heatwaves have been associated with large alterations in seagrass meadow's structure and functioning, even leading to mass mortality events (e.g., Marbà & Duarte, 2010; Hyndes et al., 2016; Arias-Ortiz et al., 2018). Particularly, the Pacific coasts of EUA and Baja California (Mexico) have been repeatedly impacted by MHWs in the last few years (Bond et al., 2015; Wei et al., 2021), causing large negative impacts on marine biota (Smith et al., 2023), including kelp forests (Arafeh-Dalmau et al., 2019; Michaud et al., 2022). However, knowledge on their potential effects on *Phyllospadix* is extremely scarce, based on only a few studies (Drysdale & Barbour, 1975; Menge et al., 2020). Recent experimental studies have investigated the responses of surfgrasses to warming, particularly addressing variabilities along a latitudinal gradient (Venegas, 2019), the combination of warming with light reduction (Vivanco-Bercovich et al., 2022) and the effects from repeated exposures to MHWs (Vivanco-Bercovich et al., 2023, in preparation).

Global seawater surface temperature is projected to increase up to 4°C by 2100, depending on the pathways that future societies might track in the emission of greenhouse gases (Fox-Kemper et al., 2021). Closely associated with global warming, the intensity of marine heatwaves (MHWs, see definition in Hobday et al., 2016) is expected to increase dramatically over the next decades (Marin et al., 2021). MHWs have rarely reached the "extreme" category (as defined by Hobday et al., 2018) during the last century, but current projections indicate that, depending on emissions scenarios, such events may account for up to 70% of all MHWs globally by 2100 (Oliver et al., 2019). These predictions are alarming since MHWs can cause catastrophic impacts on marine ecosystems, such as seagrasses (Smith et al., 2023), compromising their services and resulting in large socioeconomic repercussions (Sen-Gupta et al., 2020; Smith et al., 2021).

The severity of the effects of MHWs on seagrasses is strongly conditioned to events´ characteristics in terms of intensity, duration, and temperature stability (e.g., Ontoria et al., 2019; Stipcich et al., 2022). For instance, while mild temperature increases (e.g., "moderate" MHWs) may favor some metabolic functions, such as photosynthesis (e.g., Beca-Carretero et al., 2018), intense warming (e.g., "extreme" MHWs) that surpasses plant tolerance thresholds can cause permanent physiological damage, growth reduction and seagrass mortality (e.g., Collier & Waycott, 2014; Beca-Carretero et al., 2021). Biological factors can further condition the plant resistance under high temperature, such as local adaption phenomena to thermal niches (e.g., Bennet et al., 2022), biological seasonal patterns (e.g., Beca-Carretero et al., 2021), plant ontogenic stage (e.g., Guerrero-Meseguer et al., 2017), and age of the plant tissue (e.g., Ruocco et al., 2019).

While most of the knowledge about the ecophysiological responses of seagrasses to warming is originated from experimental studies conducted with *Zostera marina*, *Posidonia oceanica* and

*Cymodocea nodosa* (Nguyen et al. (2021a), this field remains largely unexplored for many other important seagrass species around the world. Only a fraction of these studies simulated warming events with intensity and duration that represent realistic present-day MHWs. Even fewer works have examined the potential effects of MHWs with increased intensity related to future warmer scenarios. Addressing these topics is important to foster contextualized discussions about acclimation capacities and tolerance thresholds of seagrasses in face of current and future warmer scenarios.

In this study, we aimed to understand how surfgrass meadows might respond to MHWs as these events become more intense in the near future due to global warming. Thus, we conducted a 27-day mesocosm experiment, where we exposed subtidal *P. scouleri* plants to two MHW scenarios: a severe MHW with an intensity within the range of contemporary events (maximum intensity of +5°C), and an extreme MHW that could occur in the near future (maximum intensity of +8°C). We analyzed a set of ecophysiological descriptors to identify acclimation and stress responses, which revealed the potential effects of extreme MHWs on the ecophysiological performance and recovery capacity of *P. scouleri*, as well as a likely thermal threshold for this species.

## 2. Material and methods

### *Donor meadow and thermal history*

The donor meadow is located at the Todos Santos Island (31°48'25.66"N, 116°47'46.41"O), which is situated ~19 km off Ensenada city (Baja California, México) and belongs to the Biosphere Reserve Pacific Islands (Fig. 1A, B). The donor meadow covers an area of >32000 $m^2$

and is distributed over the intertidal and subtidal zones (down to ~ 7 m depth) of a rocky and wave-exposed shore (Garcia-Pantoja et al., 2020).

Based on historical satellite sea surface temperature (SST) data (Fig SM 1), more than a hundred MHWs have been identified for this region since 1982 (data analysis: Marine Heatwave Tracker platform, Schlegel et al., 2020, Pixel: 116.875°W 31.875°N). Among those events, the majority did not exceed 3°C of intensity and 10 days of duration (Fig SM 2). According to the MHW classification framework proposed by Hobday et al. (2018), 88% of all the registered events were "moderate", 18% were "strong", and there were only two "severe", and one "extreme" MHWs since 1982.

Previous studies have detected significant differences between satellite SST data and seawater temperature measured *in situ* (e.g., Smit et al., 2013; Schlegel et al., 2017). To address this issue, submersible sensors (Onset-HOBO MX2202) were maintained during two years within the donor meadow to evaluate the thermal regime with higher accuracy (Fig. 1C). We found that SST data (NOAA High Resolution SST data, http://www.esrl.noaa.gov/psd/) was strongly correlated with the daily average from our *in situ* measurements, and especially with the daily maximum record (Fig. SM 2). Even so, SST under- and overestimations exceeded 3°C. For instance, the maximum temperature recorded by our sensors (24.3°C) during this period was underestimated in SST records by nearly 2°C (Fig. 1C). In addition, the sensor data revealed large daily variation in seawater temperature (Fig. SM 3), probably related to the upwelling of cold water forced by afternoon alongshore winds and other local processes (e.g., Woodson et al., 2007; Aristizával et al., 2017).

***Plant collection and experimental design***

*Phyllospadix scouleri* plants were collected in September 2023 by divers at the subtidal zone (~5 m below MHWL) of the meadow, where plants are presumably less tolerant to warming than their intertidal counterparts (Marín-Guirao et al., 2016). Plants were carefully detached from the rocks preserving connection among ramets, to maintain the clonal integrity of shoot clumps. Plants were transported in coolers (within 2 h) to the facilities at the Instituto de Investigaciones Oceanológicas (University of Baja California) and placed in the outdoor experimental system for acclimation during five days prior to the experiment. To obtain field reference values of plant biological status (Table 1), the day after collection photobiological descriptors were measured and leaf tissues were frozen (-80°C) to perform pigment and non-structural carbohydrate analysis. The acclimation seawater temperature was adjusted to the averaged field conditions before the start of the experiment (18.5 ± 1.5°C) (Fig 1C). Natural solar irradiance was adjusted by placing shader screens over the tanks to maintain averaged maximum light intensity and daily PAR dose similar to field conditions (~200 μmol photon $m^{-2}$ $s^{-1}$ and 4.5 mol photon $m^{-2}$ $day^{-1}$, respectively).

Plants were exposed to simulated MHWs with different intensities (Fig 1D). One MHW (HW-1) was set to an average temperature of 23.5°C, and the other (HW-2) to an average temperature of 26.5°C. Warm periods lasted ten days (seven days at maximum temperature and three days for transitions) and were succeeded by recovery periods of the same duration. For the recovery period, temperature was returned to 18.5°C, which was the same temperature at which another group of plants was maintained during the entire experiment (C - Control). Attending to the temperature fluctuations observed *in situ*, temperature was adjusted for ± 1.5°C daily variation

over the mentioned averages in all three treatments (i.e., C, HW-1, HW-2). According to the classification proposed by Hobday et al. (2018), daily peaks of HW-1 (25°C, +5°C above local climatology) and HW-2 (28°C, +8°C above local climatology) would characterize them as "severe" (category III) and "extreme" (category IV) events, respectively. For the physiological characterization, samples were taken at the end of the MHWs (T-1), and at the end of the recovery period (T-2).

The experimental system consisted of 12 independent aquaria (1000 L), each considered as the experimental unit (EU). Four EU were disposed for each treatment (n = 4). Each EU contained 6-8 shoot clumps with approximately 200 connected shoots each, which were attached to rocks at the bottom of the aquaria. A water pump (AQUAPAK SUPRA 15/1230, flow: 100-390 l/min) permanently recirculated water between one chiller (Aqua Logic Multi-temp Chiller MT-4, 3HP), a water reservoir containing submersible heaters and the four EUs of each treatment. Positioning of water inlets and outlets and the permanent and intense aeration assured water homogenization within EUs. Before the start of warming and recovery periods, the seawater in the system was completely exchanged and posteriorly fertilized with nitrate and phosphate (5μM) to ensure optimal seawater quality for plants growth.

***Physiological traits and growth***

Random shoots from the EUs were sampled at the end of MHWs (T-1) and after recovery periods (T-2) for the physiological analysis and growth determination. For each descriptor, measurements were averaged for two samples per EU to obtain the true replicate (n = 4 per treatment), except for P-E curves, which were performed in only one sample per EU. All samples were taken from

the middle section of the second mature leaf to reduce the variability of biological descriptors within/among leaves.

***Photosynthesis and Respiration (P vs. E curves)***

Photosynthesis (P) and respiration (R) rates were determined in leaf segments using a respirometer (see PE curves in Fig. SM 6). This respirometer consisted of 200 mL borosilicate jacketed chambers connected to a controlled temperature circulating bath and surrounded by four light sources (LED 10 W) automatically controlled by customized software. Oxygen evolution was measured by optodes (dipping probe DP-PSt3, PreSens, Germany) connected to a fiber-optic oxygen meter (OXY4 SMA, PreSens, Germany) controlled by software (Measurement Studio 2, PreSens, Germany). A ratio of plant biomass/seawater volume of about 0.03-0.05 g DW $L^{-1}$ was used to ensure accurate measurements of photosynthetic rates, avoiding the underestimation of photosynthesis due to oxygen over-saturation and carbon limitation. Leaf segments were initially incubated in darkness for 10 min to determine R. Subsequently, tissues were exposed to increasing PAR irradiance levels (0 – 801 µmol photon $m^{-2}$ $s^{-1}$) for 5 min at each irradiance level. Light intensities within the chamber were previously calibrated using a spherical (4π) quantum sensor (Biospherical Instruments; California, USA). Maximum net photosynthetic rate (net-$P_{max}$; µmol $O_2$ $g^{-1}$ DW $h^{-1}$) was determined by averaging the maximum values above the saturating irradiance ($E_k$ = net-$P_{max}$/ α; µmol photon $m^{-2}$ $s^{-1}$). Maximum gross photosynthesis (gross-$P_{max}$; µmol $O_2$ $g^{-1}$ DW $h^{-1}$) was calculated as the sum of net-$P_{max}$ and R. Photosynthetic efficiency (α) was calculated as the slope of the regression line fitted to the initial linear part of the P *vs*. E curve. The compensation irradiance ($E_c$; µmol photon $m^{-2}$ $s^{-1}$) was determined as the intercept of the initial linear part of the curve on the X-axis.

***Chlorophyll a fluorescence and absorptance***

The chlorophyll-*a* fluorescence emission of PSII was measured using a portable Diving-PAM fluorometer (Walz, Germany). The leaf surface was carefully cleaned off epiphytes and held in the fluorometer DCL-8 leaf-clip holder to assure a constant distance between the tissue and the fiber optic of the fluorometer. To standardize data collection among plants, photochemistry measurements were performed in the middle section of the leaf where maximum values of maximum quantum yield ($F_v/F_m$) were measured in previous trials. $F_v/F_m$, $F_0$ and $F_m$ were obtained from plants maintained in darkness overnight, while effective quantum yield ($\Phi_{PSII}$), $F_0$' and $F_m$' were obtained from light acclimated plants illuminated with actinic-light (60 s, 247 µmol photon $m^{-2}$ $s^{-1}$). Absolute ETR was calculated as $ETR = \Phi_{PSII} \cdot 247 \cdot A \cdot 0.5$, where A is the leaf absorptance (see below), 247 is the actinic-light intensity and 0.5 is a constant assuming that half of the incident photons go through PSII (Beer et al. 2014). Leaf absorptance (A) was calculated as A = 1 - (LT / L0) – TW, where LT is the transmitted light trough the tissue, L0 is the total incident light emitted by the lamp and TW is the transmitted light through a bleached leaf. Light transmision through the tissue was measured using the miniature fiber optics quantum sensor (Diving-F1, Walz, Germany) of the submergible Diving-PAM fluorometer (Walz, Germany). The light sensor was attached to the leaf clip to maintain a constant geometry among leaves, lamp and light sensor (Vásquez-Elizondo et al. 2017). Finally, the NPQ was calculated as $(F_m-F_{m'})/F_{m'}$, where $F_m$ is the maximum fluorescence obtained in plants adapted to darkness overnight, and $F_{m'}$ the fluorescence measured under actinic-light illumination.

***Pigment content***

Leaf pigments were extracted from ~15 mg FW leaf tissue homogenized in 100% acetone, with $MgCO_3$ solution added to prevent acidification of the extract (Dennison, 1990). Extracts were stored at 4°C in the dark for 24 h. After centrifugation (1000 x g, 10 min) absorbance was measured spectrophotometrically at 470, 646, and 663 nm, using 1 mL cuvettes. The Chl *a*, *b,* and total carotenoid concentration were calculated using the equations described by Lichtenthaler & Wellburn (1983) and expressed as mg $g^{-1}$ FW.

***Non-structural carbohydrates***

Total soluble non-structural carbohydrates (free sugars and starch) were determined using the colorimetric phenol-sulfuric acid method (Dubois et al. 1956) using glucose as standard. Leaf tissues were oven-dried at 60°C until constant weight and ground to a fine powder. The powder was digested in 0.1 N HCl (60º C, 3h), centrifuged (4000 x g, 5 min), and the supernatant mixed with 3% phenol and concentrated sulphuric acid. Absorbance was measured spectrophotometrically at 490 nm. Non-structural carbohydrates content (NSCs) was expressed in mg $g^{-1}$ DW.

***Total phenolic content and antioxidant capacity***

Phenolic and antioxidant compounds were extracted from dried ground leaf tissue (0.02 g DW) in 1 mL 80 % methanol in darkness for 24 h. The extract was then centrifuged at 10,000 rpm for 10 min. The methanolic extracts were used to quantify phenolic compounds and antioxidant capacity. The phenolic compound content was determined according to a modification of the Folin–Ciocalteu assay using gallic acid as standard (Singleton & Rossi 1965). The methanolic extract (0.01 mL) was diluted in 1mL distilled water ($dH_2O$), 0.1 mL Folin–Ciocalteu reagent,

and 0.3 mL $dH_2O$ saturated with $NaCO_3$. This mixture was homogenized, heated (40°C for 3 min), and its absorbance read spectrophotometrically at 765 nm. Total phenolic content was expressed as gallic acid equivalents (mg Eq. GA $g^{-1}$ DW). The same methanolic extracts were used to quantify the radical scavenging activity according to Sabeena-Farvin & Jacobsen (2013); the reaction mixture was prepared with 0.1 mL of diluted extract (1:10 with 80 % methanol) and 1 mL of 60 μM 2,2-diphenyl-1-picrylhydrazyl (DPPH) dissolved in 90% methanol. The absorbance was measured at 517 nm 30 min after DPPH addition. The total antioxidant capacity was expressed as ascorbic acid equivalents (mg Eq. AA $g^{-1}$ DW).

***Lipidic peroxidation***

Oxidative damage was evaluated by malondialdehyde (MDA) quantification. Lipid peroxidation was measured following the thiobarbituric acid-reactive-substances (TBARS) assay described by Hodges et al. (1999) and Correia et al. (2006). Ultrafrozen leaf tissue (0.2 g FW) was mechanically ground in 2 ml ethanol 80%. Tissue homogenate was then centrifuged for 10 min (3000 x g, 4°C) and supernatant was added to a solution of trichloroacetic acid (TCA, 20%) and thiobarbituric acid (TBA, 0.5%). Blanks were prepared by adding the supernatant to a solution of TCA 20%. These solutions two were heated at 90°C for 30 min, and then centrifuged again (3000 x g) for 10 min. The supernatants were extracted and their absorbances (440, 532 and 600 nm) were determined spectrophotometrically. Lipid peroxidation was expressed as equivalents of malonil-dialdehyde (Eq MDA; molar extinction coefficient 155 mM-1 cm-1), which were calculated using the equations in Hodges et al. (1999).

***Daily Productivity***

The daily productivity (DP) was calculated using the equation of a polynomial curve ($3^{rd}$ or $4^{th}$ degree) fitted over the P vs. E curves from each EU (n = 4). The y-intercept of these curves were fixed to the respective value of R. Each fitted equation was integrated through a general daily cycle of irradiance to obtain a value of daily productivity (μmol O2 $g^{-1}$ DW $day^{-1}$). The irradiance cycle was obtained by averaging the data from sensors (Onset-HOBO MX2202) maintained in aquariums (n = 3) during the entire experiment. Sensors were attached in pairs and maintained in mid water to capture irradiance coming from up (direct sunlight) and down (reflection from the aquarium).

***Relative leaf growth rate***

At the beginning of the heatwave and recovery periods, leaves were marked following the punching hole method adapted from Zieman (1974). At the end of each experimental period, all marked shoots were harvested, and leaf segments below the mark (i.e., newly formed tissue) were dried and weighted for all leaves of each shoot. Shoot growth was expressed as relative to the total shoot biomass or relative leaf growth rate (RGR; mg $g^{-1}$ DW $day^{-1}$).

***Statistical analysis***

Two-way ANOVAs were used to test for the main and interactive effects of treatments ("Trt.", 3 levels: C, HW-1, and HW-2) and sampling time ("Time", 2 levels: T-1, T-2) on each biological descriptor. Tukey´s HSD post-hoc test was used to compare individual means in case of a significant main effect from Treatment, or in case of significant interaction term ($P < 0.05$). Departures from normality (Shapiro-Wilk normality test, $p > 0.05$) were corrected *a priori* with logarithmic transformations (i.e., Chl. *b* content). The analysis of variance for variables that

presented heteroscedastic data (i.e., $F_0$, $F_m$, Chl. *b/a* ratio, phenolic content and NSC) was corrected with White´s adjustment, and the non-parametric Games-Howell test was applied as post-hoc. All analyses were performed using the statistical software R (R CoreTeam 2020).

## 3. Results

Gross- and Net-$P_{max}$ remained similar to initial conditions during T-1 in control plants and those exposed to HW-1 (Table 1, Fig 2A, B). However, there was a general reduction in these parameters, and in saturation irradiance ($E_k$), from T-1 to T-2 (Fig 2A, B, E). Treatments had important effects on Gross-$P_{max}$, Net-$P_{max}$ ($p = 0.07$), and $E_k$. Plants exposed to HW-2 presented significantly lower photosynthetic capacity and saturation irradiance than the other treatments. The minimum values of Gross- and Net -$P_{max}$ and $E_k$ were achieved during the recovery period (i.e., T-2) when HW-2 plants had 39%, 19%, and 19%, less than control, respectively.

Although the photosynthetic efficiency (α) presented a meaningful reduction in all treatments compared to initial conditions (~30% lower), it did not vary significantly among treatments, nor in the course of the experiment (Fig. 2C). Plants exposed to HW-2 presented the highest α among treatments at T-1, and the lowest α at T-2 (25% lower than C), but these differences were not statistically significant (Fig. 2C). Respiration rates (R) and compensation irradiance ($E_c$) were strongly affected by warming treatments (Fig. 2D, F). Compared to control, plants exposed to HW-2 presented higher R by 77% and 113% at T-1 and T-2, respectively. Similarly, $E_c$ was 53% and 181% higher than control in HW-2 plants at T-1 and T-2, respectively. Plants exposed to HW-1 also presented elevated R and $E_c$, but these increases were approximately half of those observed for HW-2. Both variables also showed a slight increase in C plants, at T-1, compared to initial conditions (Table 1), but this difference was offset during T-2 (Fig. 2D, F).

Maximum photochemical efficiency ($F_v/F_m$) was significantly affected by experimental treatments (Fig. 3A). Plants exposed to HW-2 exhibited $F_v/F_m$ 5% and 10% lower than control, in T-1 and T-2, respectively. The $F_v/F_m$ in initial conditions was similar to control and HW-1 plants in T-1 (0.76 - 0.77), and both decreased during T-2 (0.73-0.74). The NPQ was very variable in control plants: at T-1 it decreased by as much as 47% (NPQ = 0.29) compared to initial conditions (NPQ = 0.55, Table 1), and then at T-2 it increased by more than two-fold (NPQ = 0.64) compared to T-1 (Fig. 3B). On the other hand, plants exposed to HW-1 and HW-2 showed more stable NPQ (ranging between 0.4 and 0.5), which was always lower than initial conditions. The basal fluorescence ($F_0$) was significantly affected by treatments (Fig. 3C). While control plants maintained $F_0$ values similar to initial conditions (~ 485), HW-2 plants had higher $F_0$ than control by 11 and 6%, at T-1 and T-2, respectively. Maximum fluorescence ($F_m$) was slightly enhanced in HW-1 plants at T-1 (6% higher than initial conditions), but at T-2 all treatments showed a considerable decrease (Fig. 3D). The effective quantum yield ($\Phi_{PSII}$) in control plants was lower than in initial conditions at both T-1 and T-2 by about 30%. HW-1 plants showed enhanced $\Phi_{PSII}$ at T-1, and HW-2 plants had significantly lower $\Phi_{PSII}$ at T-2 (44% lower than control) (Fig. 3E). The electron transport rate (ETR) also decreased substantially in control plants at T-1 (38% lower) compared to initial conditions. Plants exposed to HW-1 also showed enhanced ETR at T-1 (20% higher than control). All treatments had decreased ETR at T-2, particularly HW-2 plants reached the minimum value, which was 30% lower than the control (Fig. 3F).

The experimental treatments did not significantly affect the contents of chlorophylls *a* and *b* (Fig. 4A, B). For both chlorophylls, and also for carotenoids, the highest content was presented by HW-1 at T-1, and by HW-2 at T-2, although without statistical significance (Fig. 4A, B, D).

When compared to initial conditions, control plants, and those exposed to HW-2 showed a substantial decrease in the content of chlorophylls at T-1 (-28% for both). Differently, the ratio chl *b/a* varied significantly among treatments (Fig. 4C), and only HW-1 plants maintained values similar to initial conditions. The ratio chl *b/a* in HW-1 plants was 0.41 at both periods (T-1 and T-2), while it ranged between 0.44 and 0.45 in control and HW-2 plants (Fig. 4C).

Leaf phenolic content in control plants was maintained similar to initial conditions (~ 6 mg Gal. ac. Eq. $g^{-1}$ DW). Differently, HW-1 and HW-2 plants showed a significant reduction of about 27% and 21% at T-1 compared to the control, respectively (Fig. 5A). At T-2, leaf phenolic content was raised in HW-1 and HW-2, but remained lower than control by 5% and 17%, respectively. Total antioxidant capacity was significantly affected by treatments (Fig. 5B). At T-1, plants exposed to HW-1 and HW-2 presented nearly 40% lower values than control plants, which in turn exhibited similar values to initial conditions. Both warming treatments had increased antioxidant capacity at T-2, but while HW-1 plants matched control levels, HW-2 remained 30% lower than the control. Although the lipid peroxidation in control plants did not vary from T-1 to T-2, it was reduced by half from initial conditions. Plants exposed to HW-1 exhibited a significant reduction in lipid peroxidation at T-1 (31% lower than control) but increased to near control levels at T-2 (Fig. 5C). In HW-2 plants lipid peroxidation did not vary significantly, presenting values slightly higher than control at T-1 and slightly lower at T-2.

Leaf non-structural carbohydrates (NSC) content was decreased by 25% in control plants compared to initial conditions. All treatments were similar at T-1, but at T-2 HW-1 plants showed significantly higher NSC content (+52%) than control plants, while HW-2 plants remained undifferentiated (Fig. 6A). Leaf relative growth rate (RGR) was strongly affected by treatments (Fig. 6B). While control and HW-1 plants showed similar values during the whole

experiment, RGR in plants exposed to HW-2 was reduced by 45% and 62% compared to control at T-1 and T-2, respectively. Daily productivity (DP) was also significantly affected by treatments (Fig. 6C), and there was a substantial reduction in DP from initial conditions, with 58% lower values in control plants at T-1. Plants exposed to HW-1 showed slightly lower DP than control, but without statistical significance. On the other hand, HW-2 plants presented significantly lower values than control and HW-1, with negative DP at both warming and recovery periods.

## 4. Discussion

The intensity of marine heatwaves is increasing with climate change, potentially exceeding the physiological capacity of seagrasses to cope with those events and threatening their related marine ecosystems. Here we compared the effects of severe ($T_{max}$ = 25°C) and extreme ($T_{max}$ = 28°C) MHWs on *P. scouleri* ecophysiology. Our results show that MHWs could represent a major threat to surfgrass meadows from northern Baja California depending on their intensity. While *P. scouleri* coped with the severe event, the extreme MHW caused major physiological alterations that ultimately lead to growth impairment (Fig. 7).

The exposition to a severe heatwave (HW-1) did not cause any detrimental effects on the photosynthetic performance of *P. scouleri*. These plants had their photosynthetic capacity (Net- and Gross-$P_{max}$) preserved, and PSII photochemical efficiency (i.e., ETR and $\Phi_{PSII}$) was even enhanced. The temperature regime simulated in the severe heatwave ($T_{mean}$ = 23.5°C, $T_{max}$ = 25°C) is not novel for *P. scouleri* at this location since summer temperatures have repeatedly reached such temperatures in the last few years (Fig. 7). Within the plants' tolerance range, temperature can favor photosynthesis due to enhanced enzymatic activity and protein mobility

within the thylakoid membrane, as also observed in other seagrass species (e.g., Beca-Carretero et al., 2018; Lawrence & Bolton, 2022). In fact, *Phyllospadix torreyi* plants from a close meadow (<15 km) had their photosynthetic capacity stimulated, and photochemical efficiency unaltered after one week of continuous exposition to 25°C (Vivanco-Bercovich et al., 2022). Our results also evidenced signs of photoacclimatory/photoprotective mechanisms in HW-1 plants, which may have contributed to equilibrating the incident photonic energy with PSII capacity to transport electrons, thus minimizing potential formation of ROS (discussed below) and damage to PSII. For instance, there was an induction of NPQ during the warming period (also in HW-2 plants), which is a form of dissipating the excess photonic energy as heat before it reaches the reaction centers (Murchie & Ruben, 2020), and is commonly observed in seagrasses exposed to warming (e.g., Ruocco et al., 2019), including *P. scouleri* (Vivanco-Bercovich et al., 2023, in preparation). Also, HW-1 plants showed an slight reduction in Chl*b/a* ratio, which is considered a proxy for antenna size and may indicate a reduction in the amount of energy being harvested, thus reducing the reducing power over reaction centers.

Conversely, the photosynthetic performance of *P. scouleri* plants exposed to the extreme heatwave (i.e., HW-2) was severely affected, as evidenced by reduced photosynthetic capacity (Net-$P_{max}$, Gross-$P_{max}$, $E_k$) and photochemical efficiency (i.e., $F_v/F_m$, $\Phi_{PSII}$, ETR). Similar responses have been previously repported for other seagrasses exposed to warming (e.g., Costa et al., 2021; Nguyen et al., 2021b; Deguette et al., 2022) and may indicate heat induced disruption of key PSII components, such as light harvesting complexes, reaction centers and oxygen evolving complexes (Mathur et al., 2014). The strong association between $F_v/F_m$ decline and incremented basal fluorescence (i.e., $F_0$, Fig. 3) suggests potential heat-induced damage of the PSII core protein D1 (Allakhverdiev et al., 2008). Particularly, unaltered leaf pigmentation (Chl*a*

and Chl*b*) in these plants (i.e., HW-2) could indicate that the photosynthetic depression was mostly related to limiting processes at the thylakoid and/or carbon fixation levels, rather than to light acquisition structures (Sandoval-Gil et al., 2014; Ruocco et al., 2019).

On the other hand, the content of malondialdehyde (MDA) in leaf tissues was maintained stable in both warming treatments (HW-1 and HW-2). This result is especially surprising in the case of HW-2 plants because the loss of PSII functionality is often associated with oxidative damage on the photosynthetic apparatus (Gururani et al., 2015), and it also contrasts with a previous work that reported increased MDA levels in plants warmed to 26°C (Vivanco-Bercovich et al., 2023, *in preparation*). Overall, we may hypothesize that the antioxydant system of *P. scouleri* was able to restrict oxidative damage from warming.

Our results show that the concentrations of antioxidant compounds (i.e., leaf phenolic content and total antioxidant capacity) were reduced during both heatwaves (HW-1 and HW-2). Similar behaviours that have been previously noted in recent studies on surfgrasses (Ruiz-Montoya et al., 2021; Vivanco-Bercovich et al., 2022; Vivanco-Bercovich et al., 2023, *in preparation*). The strategies to neutralize excessive ROS produced under stressful conditions can vary widely between seagrass species and ecotypes (e.g., Tutar et al., 2017). Altough the activation of antioxidant mechanisms is generaly related to the active synthesis and accumulation of antioxidant compounds (e.g., Costa et al., 2021), maintaining stable levels of antioxidant compounds may comprise a convenient strategy for macrophytes to cope with the variable environmental conditions found in shallow waters (Dring, 2005; Bischof & Rautenberger, 2012). Relatively constant levels of phenolic content over seasons has also been reported for *Phyllospadix torreyi* (Grignon-Dubois et al., 2022). Plants exposed to the extreme heatwave (i.e., HW-2) seemed to be under a more accentuated oxidative pressure, since leaf phenolic content

and total antioxidant capacity did not return to control levels during the recovery period, differently to HW-1 plants. Possibly, the slight accumulation of carotenoids in HW-2 plants during the recovery period may reflect an additional antioxidant response (e.g., Repolho et al., 2017), as these compounds can detoxify various forms of ROS (Sharma et al., 2012). Apart from the antioxidant compounds measured here, there is a variety of other important non-enzymatic and enzymatic antioxidant mechanisms that could have been involved in antioxidant strategy employed against thermal stress (Mehla et al, 2017).

Despite not causing evident oxidative damage, our results indicate that when exceeding a certain treshold, MHWs could severely affected the balance between carbon gains (photosynthesis) and losses (respiration) in *P. scouleri*. Plant respiration is usually highly sensible to temperature, and the ability to stabilize it (or to counter balance it) is a key acclimation asset for seagrasses facing abnormally warm conditions (Marín-Guirao et al., 2016; Beca-Carretero et al., 2018). As evidenced here by plants exposed to HW-1, and in previous works (Vivanco-Bercovich et al., 2022, Vivanco-Bercovich et al., 2023, *in preparation*), surfgrasses can withstand certain degree of warming without raising respiratory rates (i.e., up to ~25-26°C). Nevertheless, the extreme heatwave (HW-2, $T_{mean}$ = 26.5°C, $T_{max}$ = 28°C) apparently exceeded this tolerance treshold and respiration rates in these plants rose significantly. This condition, in combination with compromised photosynthetic performance, possibly created a metabolic imbalance in HW-2 plants, as evidenced by our estimation of daily produtivity falling into negative values.

Seagrasses can employ different carbon economy strategies to meet metabolic demands during situations of unfavorable carbon balance (Marín-Guirao et al., 2018). Altough HW-2 plants did not present lower NSC content in leaves, we can not discard that the increased respiratory demand was attained in expense of starch reserves from rizomes, as generally this is the main

storage tissue in seagrasses and is more suscetible to environmental fluctuations (Burke 1996, Alcoverro et al., 2001). Previous works have found contradictory responses of leaf NSC in response to warming (Marín-Guirao et al., 2018; Stipcich et al., 2022), also among surfgrasses (Vivanco-Bercovich et al., 2022; Vivanco-Bercovich et al., 2022, in preparation), which may be related to complex dynamics in temporal (seasonality; Alcoverro et al., 2001) and spatial (translocation among the different pools within the clonal structure; Marín-Guirao et al., 2018; Ruocco et al., 2021) scales. Apart from consuming internal storage reserves, seagrasses may adjust their clonal structure (e.g., proportion of belowground to aboveground tissues) to maintain the provision of carbon substrates (Collier et al., 2011). For instance, the reduction of growth rate observed in HW-2 plants could represent a crisis strategy in response to the scarcing energy and its redirection towards vital metabolic processes related to celular maintenance, repair and protection (Ruocco et al., 2019).

While one simulated heatwave of 24°C caused various physiological alterations in *P. scouleri* without affecting its productivity or growth (Vivanco-Bercovich et al., 2023, *in preparation*), the extreme heatwave simulated in this study (i.e., HW-2; $T_{mean}$ = 26.5°C; $T_{max}$ = 28°C) resulted in major photosynthetic impairment and carbon deficit that compromised leaf growth, possibly anticipating shoot mortality (e.g., Massa et al., 2009; Collier & Waycott, 2014). In conjunction, the available evidence indicates that 26.5°C (as daily average temperature for at least seven days) may represent a tipping point ($T_{lim}$) for surfgrass thermal resistance in northern Baja California Peninsula (Fig. 7), which is also similar to the average thermal limit reported for temperate seagrasses survival globally (i.e., ~27°C; Marbà et al., 2022).

The mean maximum summer temperature ($T_{max}$, warmest month average temperature) in the study region for the period 1990-2019 was ~20.5°C, and during the period 2014-2019 $T_{max}$ was

21.5°C, thus the current "thermal safety margin" (i.e., TSM = $T_{max}$ – $T_{lim}$) for *P. scouleri* populations in northern the Baja California Peninsula is around 5 - 6°C, which is within the range of values reported for most of seagrass meadows worldwide (Marbà et al., 2022). But the elevation of $T_{max}$ associated with oceans warming trend and stronger MHWs might cause a reduction of the TSM in the future. For instance, sea surface temperature in the study region has repeatedly exceeded 23°C in the last few years, including records of 25°C during recent MHWs (Fig. SM 1), which is close to the $T_{lim}$ of these populations. Mass mortality events driven by anomalous warming events have been reported for temperate (*Posidonia oceanica* in the west Mediterranean, *Amphibolis antartica* in Sharks Bay) and tropical (*Thalassia testudinum* in Florida Bay, *Zostera marina* and *Ruppia maritima* in Chesapeak Bay) seagrass populations with similar TSM (Marbà and Duarte, 2010; Moore et al., 2014; Thomson et al., 2015; Carlson et al., 2018).

In this study we focused in examining the physiological responses of *P. scouleri* plants exposed to temperatures resembling predicted more intentense future MHWs. Our results illustrate the current vulnerability of these populations due to seawater temperature elevation associated with ongoing ocean warming and marine heatwaves. However, there are multiple factors beyond the scope of this study that may determine *P. scouleri* thriving in the complex context of the real life. For example, tolerance to warming can vary seasonally (Beca-Carretero et al., 2021), or among life stages (i.e., higher vulnerability of seedlings, Olsen et al., 2012; Guerrero-Meseguer et al., 2017). Another important aspect to consider is that seagrasses can rapidly acclimate/adapt to novel environmental conditions through epigenetic processes that enhance their phenotypic plasticity (Pazzaglia et al., 2021). In other words, the formation of "stress memory" could result in a progressive elevation of the $T_{lim}$ of these populations as they experience repeated MHWs

(e.g., Nguyen et al., 2020; Pazzaglia et al., 2022; Stipcich et al., 2022). Local acclimation can result in differential warming tolerance among same species populations (Bennet et al., 2021). On the other hand, there are other factors that may intensify the stress associated with warming and MHWs, such as overlapping environmental stressors (e.g., eutrophication, Mvungi & Pillay, 2019; light reduction, Vivanco-Bercovich et al., 2022), or altered ecological processes (e.g., shifts in trophic interactions increasing herbivory, Hernán et al., 2017).

## 5. Conclusions

The aim of this study was to examine and compare the physiological performance of *P. scouleri* when exposed to two MHWs with different intensities: one within the contemporary range, and other resembling a future warmer scenario. The two simulated MHWs induced very different responses. Plants exposed to the severe heatwave (i.e., HW-1) did not show large differences relative to control plants, while the extreme heatwave (i.e., HW-2) caused major physiological stress, including photosynthetic impairment, negative carbon balance and growth reduction.

Thus, this study demonstrates that future, more intense MHWs are a potential threat to subtidal *P. scouleri* meadows in the northern Baja California Peninsula. Our results indicate 26.5°C (daily mean) as a likely temperature threshold for *P. scouleri* thermal tolerance. Past MHWs in the region have reached 25°C and are predicted to increase in intensity in the near future, which could result in severe consequences for this species, also compromising the functionality of the important ecosystem it sustains.

In future works, it would be relevant to investigate the genetic diversity and population structure of *P. scouleri* (and *P. torreyi*) to identify more thermo-resistant genotypes to use in restoration

initiatives (i.e., assisted evolution, Pazzaglia et al., 2021). Also, it would be fundamental to initiate and maintain monitoring programs in surfgrass meadows to capture field-based evidence of future MHWs effects, and to gain understanding on indirect effects from warming on surfgrass meadows.

## 6. References

Alcoverro, T., Manzanera, M., Romero, J., 2001. Annual metabolic carbon balance of the seagrass *Posidonia oceanica*: the importance of carbohydrate reserves. Mar. Ecol. Prog. Ser. 211, 105–116. https://doi.org/10.3354/meps211105

Allakhverdiev, S.I., Kreslavski, V.D., Klimov, V.V., Los, D.A., Carpentier, R., Mohanty, P., 2008. Heat stress: an overview of molecular responses in photosynthesis. Photosynth. Res. 98, 541. https://doi.org/10.1007/s11120-008-9331-0

Arafeh-Dalmau, N., Montaño-Moctezuma, G., Martínez, J.A., Beas-Luna, R., Schoeman, D.S., Torres-Moye, G., 2019. Extreme marine heatwaves alter kelp forest community near its equatorward distribution limit. Front. Mar. Sci. 6, 499. https://doi.org/10.3389/fmars.2019.00499

Arias-Ortiz, A., Serrano, O., Masqué, P., Lavery, P.S., Mueller, U., Kendrick, G.A., Rozaimi, M., Esteban, A., Fourqurean, J.W., Marbà, N., Mateo, M.A., Murray, K., Rule, M.J., Duarte, C.M., 2018. A marine heatwave drives massive losses from the world's largest seagrass carbon stocks. Nat. Clim. Change 8, 338–344. https://doi.org/10.1038/s41558-018-0096-y

Aristizábal, M.F., Fewings, M.R., Washburn, L., 2017. Effects of the relaxation of upwelling-favorable winds on the diurnal and semidiurnal water temperature fluctuations in the Santa Barbara Channel, California. J. Geophys. Res. Oceans 122, 7958–7977. https://doi.org/10.1002/2017JC013199

Beca-Carretero, P., Azcárate-García, T., Julia-Miralles, M., Stanschewski, C.S., Guihéneuf, F., Stengel, D.B., 2021. Seasonal acclimation modulates the impacts of simulated warming and light reduction on temperate seagrass productivity and biochemical composition. Front. Mar. Sci. 8.

Beca-Carretero, P., Olesen, B., Marbà, N., Krause-Jensen, D., 2018. Response to experimental warming in northern eelgrass populations: comparison across a range of temperature adaptations. Mar. Ecol. Prog. Ser. 589, 59–72. https://doi.org/10.3354/meps12439

Beer, S., Björk, M., Beardall, J., 2014. Photosynthesis in the marine environment. John Wiley & Sons.

Bennett, S., Alcoverro, T., Kletou, D., Antoniou, C., Boada, J., Buñuel, X., Cucala, L., Jorda, G., Kleitou, P., Roca, G., Santana-Garcon, J., Savva, I., Vergés, A., Marbà, N., 2022. Resilience of seagrass populations to thermal stress does not reflect regional differences in ocean climate. New Phytol. 233, 1657–1666. https://doi.org/10.1111/nph.17885

Bennett, S., Vaquer-Sunyer, R., Jorda, G., Forteza, M., Roca, G., Marbà, N., 2021. Thermal performance reflects evolutionary legacies of seaweeds and seagrasses across a regional climate gradient (preprint). In Review. https://doi.org/10.21203/rs.3.rs-228005/v1

Bischof, K., Rautenberger, R., 2012. Seaweed responses to environmental stress: reactive oxygen and antioxidative strategies, in: Seaweed Biology. Springer, pp. 109–132.

Bond, N.A., Cronin, M.F., Freeland, H., Mantua, N., 2015. Causes and impacts of the 2014 warm anomaly in the NE Pacific. Geophys. Res. Lett. 42, 3414–3420. https://doi.org/10.1002/2015GL063306

Burke, M., Dennison, W., Moore, K., 1996. Non-structural carbohydrate reserves of eelgrass *Zostera marina*. Mar. Ecol. Prog. Ser. 137, 195–201. https://doi.org/10.3354/meps137195

Carlson, D.F., Yarbro, L.A., Scolaro, S., Poniatowski, M., McGee-Absten, V., Carlson, P.R., 2018. Sea surface temperatures and seagrass mortality in Florida Bay: Spatial and temporal patterns discerned from MODIS and AVHRR data. Remote Sens. Environ. 208, 171–188. https://doi.org/10.1016/j.rse.2018.02.014

Carlson, R.R., Evans, L.J., Foo, S.A., Grady, B.W., Li, J., Seeley, M., Xu, Y., Asner, G.P., 2021. Synergistic benefits of conserving land-sea ecosystems. Glob. Ecol. Conserv. 28, e01684. https://doi.org/10.1016/j.gecco.2021.e01684

Collier, C.J., Uthicke, S., Waycott, M., 2011. Thermal tolerance of two seagrass species at contrasting light levels: Implications for future distribution in the Great Barrier Reef. Limnol. Oceanogr. 56, 2200–2210.

Collier, C.J., Waycott, M., 2014. Temperature extremes reduce seagrass growth and induce mortality. Mar. Pollut. Bull. 83, 483–490. https://doi.org/10.1016/j.marpolbul.2014.03.050

Cooper, L.W., McRoy, C.P., 1988. Anatomical adaptations to rocky substrates and surf exposure by the seagrass genus *Phyllospadix*. Aquat. Bot. 32, 365–381. https://doi.org/10.1016/0304-3770(88)90108-8

Correia, M.J., Osório, M.L., Osório, J., Barrote, I., Martins, M., David, M.M., 2006. Influence of transient shade periods on the effects of drought on photosynthesis, carbohydrate accumulation and lipid peroxidation in sunflower leaves. Environ. Exp. Bot. 58, 75–84. https://doi.org/10.1016/j.envexpbot.2005.06.015

Costa, M.M., Silva, J., Barrote, I., Santos, R., 2021. Heatwave effects on the photosynthesis and antioxidant activity of the seagrass *Cymodocea nodosa* under contrasting light regimes. Oceans 2, 448–460. https://doi.org/10.3390/oceans2030025

Deguette, A., Barrote, I., Silva, J., 2022. Physiological and morphological effects of a marine heatwave on the seagrass *Cymodocea nodosa*. Sci. Rep. 12, 7950. https://doi.org/10.1038/s41598-022-12102-x

Dennison, W., 1990. Chlorophyll content, in: Seagrass Research Methods. Phillips, R.C.; McRoy, C.P., Paris (France) UNESCO.

Dring, M.J., 2005. Stress resistance and disease resistance in seaweeds: the role of reactive oxygen metabolism, in: Advances in Botanical Research, Incorporating Advances in Plant Pathology. Academic Press, pp. 175–207. https://doi.org/10.1016/S0065-2296(05)43004-9

Drysdale, F.R., Barbour, M.G., 1975. Response of the marine angiosperm *Phyllospadix torreyi* to certain environmental variables: A preliminary study. Aquat. Bot. 1, 97–106. https://doi.org/10.1016/0304-3770(75)90015-7

Dubois, M., Gilles, K.A., Hamilton, J.K., Rebers, P.A., Smith, F., 1956. Colorimetric method for determination of sugars and related substances. Anal. Chem. 28, 350–356.

Dunic, J.C., Brown, C.J., Connolly, R.M., Turschwell, M.P., Côté, I.M., 2021. Long-term declines and recovery of meadow area across the world's seagrass bioregions. Glob. Change Biol. 27, 4096–4109. https://doi.org/10.1111/gcb.15684

Fields, J.B., Silbiger, N.J., 2022. Foundation species loss alters multiple ecosystem functions within temperate tidepool communities. Mar. Ecol. Prog. Ser. 683, 1–19. https://doi.org/10.3354/meps13978

Fox-Kemper, B., 2021. Ocean, Cryosphere and Sea Level Change (Ch. 9 of Climate Change 2021: The Physical Science Basis). Contrib. Work. Group Sixth Assess. Rep. Intergov. Panel Clim. Change.

García-Pantoja, J.A., Ruiz-Montoya, L., Sandoval-Gil, J.M., Vivanco-Bercovich, M.V., Ferreira-Arrieta, A., Zertuche-González, J.A., Guzmán-Calderón, J.M., Norzagaray-López Orión; Samperio-Ramos, G., Montaño-Moctezuma, G., Hernández-Ayón, M., 2020. Fijación neta de carbono por pastos marinos (*Phyllospadix* spp.) en una isla del Pacífico Mexicano, in: Estado actual del conocimiento del ciclo del carbono y sus interacciones en México: Síntesis a 2020, Síntesis Nacionales. Programa Mexicano del Carbono en colaboración con la Universidad Autónoma Metropolitana-Xochimilco, Texcoco, Estado de México, México, p. 602.

Grignon-Dubois, M., Rezzonico, B., Blanchet, H., 2022. Phenolic fingerprints of the Pacific seagrass *Phyllospadix torreyi* - Structural characterization and quantification of undescribed flavonoid sulfates. Phytochemistry 201, 113256. https://doi.org/10.1016/j.phytochem.2022.113256

Guerrero-Meseguer, L., Marín, A., Sanz-Lázaro, C., 2017. Future heat waves due to climate change threaten the survival of *Posidonia oceanica* seedlings. Environ. Pollut. 230, 40–45. https://doi.org/10.1016/j.envpol.2017.06.039

Gururani, M.A., Venkatesh, J., Tran, L.S.P., 2015. Regulation of photosynthesis during abiotic stress-induced photoinhibition. Mol. Plant 8, 1304–1320. https://doi.org/10.1016/j.molp.2015.05.005

Hartog, C. den, Kuo, J., 2006. Taxonomy and Biogeography of Seagrasses, in: Seagrasses: Biology, Ecology and Conservation. Springer Netherlands, Dordrecht, pp. 1–23. https://doi.org/10.1007/978-1-4020-2983-7_1

Hernán, G., Ortega, M.J., Gándara, A.M., Castejón, I., Terrados, J., Tomas, F., 2017. Future warmer seas: increased stress and susceptibility to grazing in seedlings of a marine habitat-forming species. Glob. Change Biol. 23, 4530–4543. https://doi.org/10.1111/gcb.13768

Hobday, A.J., Alexander, L.V., Perkins, S.E., Smale, D.A., Straub, S.C., Oliver, E.C.J., Benthuysen, J.A., Burrows, M.T., Donat, M.G., Feng, M., Holbrook, N.J., Moore, P.J., Scannell, H.A., Sen Gupta, A., Wernberg, T., 2016. A hierarchical approach to defining marine heatwaves. Prog. Oceanogr. 141, 227–238. https://doi.org/10.1016/j.pocean.2015.12.014

Hobday, A.J., Oliver, E.C., Gupta, A.S., Benthuysen, J.A., Burrows, M.T., Donat, M.G., Holbrook, N.J., Moore, P.J., Thomsen, M.S., Wernberg, T., 2018. Categorizing and naming marine heatwaves. Oceanography 31, 162–173.

Hodges, D.M., DeLong, J.M., Forney, C.F., Prange, R.K., 1999. Improving the thiobarbituric acid-reactive-substances assay for estimating lipid peroxidation in plant tissues containing anthocyanin and other interfering compounds. Planta 207, 604–611. https://doi.org/10.1007/s004250050524

Honig, S.E., Mahoney, B., Glanz, J.S., Hughes, B.B., 2016. Are seagrass beds indicators of anthropogenic nutrient stress in the rocky intertidal? Mar. Pollut. 8.

Hori, M., 2006. Intertidal surfgrass as an allochthonous resource trap from the subtidal habitat. Mar. Ecol. Prog. Ser. 314, 89–96. https://doi.org/10.3354/meps314089

Hyndes, G.A., Heck, K.L., Vergés, A., Harvey, E.S., Kendrick, G.A., Lavery, P.S., McMahon, K., Orth, R.J., Pearce, A., Vanderklift, M., Wernberg, T., Whiting, S., Wilson, S., 2016. Accelerating tropicalization and the transformation of temperate seagrass meadows. BioScience 66, 938–948. https://doi.org/10.1093/biosci/biw111

Kelly, J.J., Orr, D., Takekawa, J.Y., 2019. Quantification of damage to eelgrass (*Zostera marina*) beds and evidence-based management strategies for boats anchoring in San Francisco Bay. Environ. Manage. 64, 20–26.

Kuo, J., Stewart, J.G., 1995. Leaf anatomy and ultrastructure of the North American marine angiosperm *Phyllospadix* (Zosteraceae). Can. J. Bot. 73, 827–842. https://doi.org/10.1139/b95-091

Lawrence, C.M., Bolton, J.J., 2022. Experimental effects of warming and epiphyte grazing on the ecophysiology of two seagrass morphotypes. J. Exp. Mar. Biol. Ecol. 151834. https://doi.org/10.1016/j.jembe.2022.151834

Lichtenthaler, H.K., Wellburn, A.R., 1983. Determinations of total carotenoids and *chlorophylls a* and *b* of leaf extracts in different solvents. Biochem. Soc. Trans. 11, 591–592. https://doi.org/10.1042/bst0110591

Magel, C.L., Chan, F., Hessing-Lewis, M., Hacker, S.D., 2023. Differential responses of eelgrass and macroalgae in Pacific Northwest estuaries following an unprecedented NE Pacific Ocean marine heatwave. Consequences Glob. Change Coast. Ecosyst. Multidiscip. Perspect. 16648714, 69.

Marbà, N., Díaz-Almela, E., Duarte, C.M., 2014. Mediterranean seagrass (*Posidonia oceanica*) loss between 1842 and 2009. Biol. Conserv. 176, 183–190. https://doi.org/10.1016/j.biocon.2014.05.024

Marbà, N., Duarte, C.M., 2010. Mediterranean warming triggers seagrass (*Posidonia oceanica*) shoot mortality. Glob. Change Biol. 16, 2366–2375. https://doi.org/10.1111/j.1365-2486.2009.02130.x

Marbà, N., Jordà, G., Bennett, S., Duarte, C.M., 2022. Seagrass thermal limits and vulnerability to future warming. Front. Mar. Sci. 9.

Marin, M., Feng, M., Phillips, H.E., Bindoff, N.L., 2021. A global, multiproduct analysis of coastal marine heatwaves: distribution, characteristics, and long-term trends. J. Geophys. Res. Oceans 126, e2020JC016708. https://doi.org/10.1029/2020JC016708

Marín-Guirao, L., Bernardeau-Esteller, J., García-Muñoz, R., Ramos, A., Ontoria, Y., Romero, J., Pérez, M., Ruiz, J.M., Procaccini, G., 2018. Carbon economy of Mediterranean seagrasses in response to thermal stress. Mar. Pollut. Bull. 135, 617–629. https://doi.org/10.1016/j.marpolbul.2018.07.050

Marín-Guirao, L., Ruiz, J.M., Dattolo, E., Garcia-Munoz, R., Procaccini, G., 2016. Physiological and molecular evidence of differential short-term heat tolerance in Mediterranean seagrasses. Sci. Rep. 6, 28615. https://doi.org/10.1038/srep28615

Massa, S.I., Arnaud-Haond, S., Pearson, G.A., Serrão, E.A., 2009. Temperature tolerance and survival of intertidal populations of the seagrass *Zostera noltii* (Hornemann) in Southern Europe (Ria Formosa, Portugal). Hydrobiologia 619, 195–201. https://doi.org/10.1007/s10750-008-9609-4

Mathur, S., Agrawal, D., Jajoo, A., 2014. Photosynthesis: Response to high temperature stress. J. Photochem. Photobiol. B, Stress and Photosynthesis 137, 116–126. https://doi.org/10.1016/j.jphotobiol.2014.01.010

McDonald, A.M., McDonald, R.B., Cebrian, J., Sánchez Lizaso, J.L., 2023. Reconstructed life history metrics of the iconic seagrass *Posidonia oceanica* (L.) detect localized anthropogenic disturbance signatures. Mar. Environ. Res. 186, 105901. https://doi.org/10.1016/j.marenvres.2023.105901

Mehla, N., Sindhi, V., Josula, D., Bisht, P., Wani, S.H., 2017. An introduction to antioxidants and their roles in plant stress tolerance, in: Khan, M.I.R., Khan, N.A. (Eds.), Reactive oxygen species and antioxidant systems in plants: role and regulation under abiotic stress. Springer Singapore, Singapore, pp. 1–23. https://doi.org/10.1007/978-981-10-5254-5_1

Menge, B.A., Close, S.L., Hacker, S.D., Nielsen, K.J., Chan, F., 2020. Biogeography of macrophyte productivity: Effects of oceanic and climatic regimes across spatiotemporal scales. Limnol. Oceanogr. lno.11635. https://doi.org/10.1002/lno.11635

Michaud, K.M., Reed, D.C., Miller, R.J., 2022. The Blob marine heatwave transforms California kelp forest ecosystems. Commun. Biol. 5, 1–8. https://doi.org/10.1038/s42003-022-04107-z

Moore, K.A., Shields, E.C., Parrish, D.B., 2014. Impacts of varying estuarine temperature and light conditions on *Zostera marina* (eelgrass) and its interactions with *Ruppia maritima* (widgeongrass). Estuaries Coasts 37, 20–30. https://doi.org/10.1007/s12237-013-9667-3

Moulton, O.M., Hacker, S.D., 2011. Congeneric variation in surfgrasses and ocean conditions influence macroinvertebrate community structure. Mar. Ecol. Prog. Ser. 433, 53–63. https://doi.org/10.3354/meps09180

Munsch, S.H., Beaty, F.L., Beheshti, K.M., Chesney, W.B., Endris, C.A., Gerwing, T.G., Hessing-Lewis, M., Kiffney, P.M., O'Leary, J.K., Reshitnyk, L., Sanderson, B.L., Walter, R.K., 2023. Northeast Pacific eelgrass dynamics: interannual expansion distances and meadow area variation over time. Mar. Ecol. Prog. Ser. 705, 61–75. https://doi.org/10.3354/meps14248

Murchie, E.H., Ruban, A.V., 2020. Dynamic non-photochemical quenching in plants: from molecular mechanism to productivity. Plant J. 101, 885–896. https://doi.org/10.1111/tpj.14601

Mvungi, E.F., Pillay, D., 2019. Eutrophication overrides warming as a stressor for a temperate African seagrass (*Zostera capensis*). PLOS ONE 14, e0215129. https://doi.org/10.1371/journal.pone.0215129

Nguyen, H.M., Bulleri, F., Marín-Guirao, L., Pernice, M., Procaccini, G., 2021b. Photo-physiology and morphology reveal divergent warming responses in northern and southern hemisphere seagrasses. Mar. Biol. 168, 129. https://doi.org/10.1007/s00227-021-03940-w

Nguyen, H.M., Kim, M., Ralph, P.J., Marín-Guirao, L., Pernice, M., Procaccini, G., 2020. Stress memory in seagrasses: first insight into the effects of thermal priming and the role of epigenetic modifications. Front. Plant Sci. 11, 494. https://doi.org/10.3389/fpls.2020.00494

Nguyen, H.M., Ralph, P.J., Marín-Guirao, L., Pernice, M., Procaccini, G., 2021a. Seagrasses in an era of ocean warming: a review. Biol. Rev. 96, 2009–2030. https://doi.org/10.1111/brv.12736

Oliver, E.C.J., Burrows, M.T., Donat, M.G., Sen Gupta, A., Alexander, L.V., Perkins-Kirkpatrick, S.E., Benthuysen, J.A., Hobday, A.J., Holbrook, N.J., Moore, P.J., Thomsen, M.S., Wernberg, T., Smale, D.A., 2019. Projected marine heatwaves in the 21st century and the potential for ecological impact. Front. Mar. Sci. 6.

Olsen, Y.S., Sánchez-Camacho, M., Marbà, N., Duarte, C.M., 2012. Mediterranean seagrass growth and demography responses to experimental warming. Estuaries Coasts 35, 1205–1213. https://doi.org/10.1007/s12237-012-9521-z

Ontoria, Y., Cuesta-Gracia, A., Ruiz, J.M., Romero, J., Pérez, M., 2019. The negative effects of short-term extreme thermal events on the seagrass *Posidonia oceanica* are exacerbated by ammonium additions. PLOS ONE 14, e0222798. https://doi.org/10.1371/journal.pone.0222798

Pazzaglia, J., Badalamenti, F., Bernardeau-Esteller, J., Ruiz, J.M., Giacalone, V.M., Procaccini, G., Marín-Guirao, L., 2022. Thermo-priming increases heat-stress tolerance in seedlings of the Mediterranean seagrass *P. oceanica*. Mar. Pollut. Bull. 174, 113164. https://doi.org/10.1016/j.marpolbul.2021.113164

Pazzaglia, J., Nguyen, H.M., Santillán-Sarmiento, A., Ruocco, M., Dattolo, E., Marín-Guirao, L., Procaccini, G., 2021. The genetic component of seagrass restoration: what we know and the way forwards. Water 13, 829. https://doi.org/10.3390/w13060829

Pearse, J.S., Doyle, W.T., Pearse, V., Gowing, M.M., Pennington, J.T., Danner, E., Wasser, A., 2015. Long-term monitoring of surfgrass meadows in the Monterey Bay National Marine Sanctuary: Recovery followed by stability after the termination of a domestic sewage discharge.

R Core Team, 2020. R: A language and environment for statistical computing. R Found. Stat. Comput.

Ramírez-García, P., Lot, A., Duarte, C., Terrados, J., Agawin, N., 1998. Bathymetric distribution, biomass and growth dynamics of intertidal *Phyllospadix scouleri* and *Phyllospadix torreyi* in Baja California (Mexico). Mar. Ecol. Prog. Ser. 173, 13–23. https://doi.org/10.3354/meps173013

Repolho, T., Duarte, B., Dionísio, G., Paula, J.R., Lopes, A.R., Rosa, I.C., Grilo, T.F., Caçador, I., Calado, R., Rosa, R., 2017. Seagrass ecophysiological performance under ocean warming and acidification. Sci. Rep. 7, 41443. https://doi.org/10.1038/srep41443

Rilov, G., Mazaris, A.D., Stelzenmüller, V., Helmuth, B., Wahl, M., Guy-Haim, T., Mieszkowska, N., Ledoux, J.-B., Katsanevakis, S., 2019. Adaptive marine conservation planning

in the face of climate change: What can we learn from physiological, ecological and genetic studies? Glob. Ecol. Conserv. 17, e00566. https://doi.org/10.1016/j.gecco.2019.e00566

Ruiz-Montoya, L., Sandoval-Gil, J.M., Belando-Torrentes, M.D., Vivanco-Bercovich, M., Cabello-Pasini, A., Rangel-Mendoza, L.K., Maldonado-Gutiérrez, A., Ferrerira-Arrieta, A., Guzmán-Calderón, J.M., 2021. Ecophysiological responses and self-protective canopy effects of surfgrass (*Phyllospadix torreyi*) in the intertidal. Mar. Environ. Res. 172, 105501. https://doi.org/10.1016/j.marenvres.2021.105501

Ruocco, M., De Luca, P., Marín-Guirao, L., Procaccini, G., 2019. Differential Leaf Age-Dependent Thermal Plasticity in the Keystone Seagrass *Posidonia oceanica*. Front. Plant Sci. 10, 1556. https://doi.org/10.3389/fpls.2019.01556

Ruocco, M., Entrambasaguas, L., Dattolo, E., Milito, A., Marín-Guirao, L., Procaccini, G., 2021. A king and vassals' tale: Molecular signatures of clonal integration in *Posidonia oceanica* under chronic light shortage. J. Ecol. 109, 294–312. https://doi.org/10.1111/1365-2745.13479

Sabeena Farvin, K.H., Jacobsen, C., 2013. Phenolic compounds and antioxidant activities of selected species of seaweeds from Danish coast. Food Chem. 138, 1670–1681. https://doi.org/10.1016/j.foodchem.2012.10.078

Sandoval-Gil, J.M., Ruiz, J.M., Marín-Guirao, L., Bernardeau-Esteller, J., Sánchez-Lizaso, J.L., 2014. Ecophysiological plasticity of shallow and deep populations of the Mediterranean seagrasses *Posidonia oceanica* and *Cymodocea nodosa* in response to hypersaline stress. Mar. Environ. Res. 95, 39–61. https://doi.org/10.1016/j.marenvres.2013.12.011

Schlegel, R.W., 2020. Marine Heatwave Tracker. URL http://www.marineheatwaves.org/tracker.html

Schlegel, R.W., Oliver, E.C.J., Wernberg, T., Smit, A.J., 2017. Nearshore and offshore co-occurrence of marine heatwaves and cold-spells. Prog. Oceanogr. 151, 189–205. https://doi.org/10.1016/j.pocean.2017.01.004

Sen Gupta, A., Thomsen, M., Benthuysen, J.A., Hobday, A.J., Oliver, E., Alexander, L.V., Burrows, M.T., Donat, M.G., Feng, M., Holbrook, N.J., Perkins-Kirkpatrick, S., Moore, P.J., Rodrigues, R.R., Scannell, H.A., Taschetto, A.S., Ummenhofer, C.C., Wernberg, T., Smale, D.A., 2020. Drivers and impacts of the most extreme marine heatwave events. Sci. Rep. 10, 19359. https://doi.org/10.1038/s41598-020-75445-3

Serrano, O., Arias-Ortiz, A., Duarte, C.M., Kendrick, G.A., Lavery, P.S., 2021. Impact of marine heatwaves on seagrass ecosystems, in: Ecosystem Collapse and Climate Change. Springer, pp. 345–364.

Sharma, P., Jha, A.B., Dubey, R.S., Pessarakli, M., 2012. Reactive oxygen species, oxidative damage, and antioxidative defense mechanism in plants under stressful conditions. J. Bot. 2012, e217037. https://doi.org/10.1155/2012/217037

Singleton, V.L., Rossi, J.A., 1965. Colorimetry of total phenolics with phosphomolybdic-phosphotungstic acid reagents. Am. J. Enol. Vitic. 16, 144–158.

Smit, A.J., Roberts, M., Anderson, R.J., Dufois, F., Dudley, S.F.J., Bornman, T.G., Olbers, J., Bolton, J.J., 2013. A coastal seawater temperature dataset for biogeographical studies: large biases between in situ and remotely-sensed data sets around the coast of South Africa. PLOS ONE 8, e81944. https://doi.org/10.1371/journal.pone.0081944

Smith, K.E., Burrows, M.T., Hobday, A.J., Gupta, A.S., Moore, P.J., Thomsen, M., Wernberg, T., Smale, D.A., 2021. Socioeconomic impacts of marine heatwaves: Global issues and opportunities. Science. https://doi.org/10.1126/science.abj3593

Smith, K.E., Burrows, M.T., Hobday, A.J., King, N.G., Moore, P.J., Sen Gupta, A., Thomsen, M.S., Wernberg, T., Smale, D.A., 2023. Biological impacts of marine heatwaves. Annu. Rev. Mar. Sci. 15, null. https://doi.org/10.1146/annurev-marine-032122-121437

Stipcich, P., Marín-Guirao, L., Pansini, A., Pinna, F., Procaccini, G., Pusceddu, A., Soru, S., Ceccherelli, G., 2022a. Effects of current and future summer marine heat waves on *Posidonia oceanica*: Plant origin matters? Front. Clim. 4, 844831. https://doi.org/10.3389/fclim.2022.844831

Stipcich, P., Pansini, A., Beca-Carretero, P., Stengel, D.B., Ceccherelli, G., 2022b. Field thermo acclimation increases the resilience of *Posidonia oceanica* seedlings to marine heat waves. Mar. Pollut. Bull. 184, 114230. https://doi.org/10.1016/j.marpolbul.2022.114230

Tharaldson, T., 2018. The ability of *Phyllospadix* spp., a pair of intertidal foundation species, to maintain biodiversity and ameliorate $CO_2$ stress in rocky shore tidepools. Cal Poly Humboldt Theses Proj.

Thomson, J.A., Burkholder, D.A., Heithaus, M.R., Fourqurean, J.W., Fraser, M.W., Statton, J., Kendrick, G.A., 2015. Extreme temperatures, foundation species, and abrupt ecosystem change: an example from an iconic seagrass ecosystem. Glob. Change Biol. 21, 1463–1474. https://doi.org/10.1111/gcb.12694

Tutar, O., Marín-Guirao, L., Ruiz, J.M., Procaccini, G., 2017. Antioxidant response to heat stress in seagrasses. A gene expression study. Mar. Environ. Res. 132, 94–102. https://doi.org/10.1016/j.marenvres.2017.10.011

Unsworth, R.K., Cullen-Unsworth, L.C., Jones, B.L., Lilley, R.J., 2022. The planetary role of seagrass conservation. Science 377, 609–613.

Unsworth, R.K.F., McKenzie, L.J., Collier, C.J., Cullen-Unsworth, L.C., Duarte, C.M., Eklöf, J.S., Jarvis, J.C., Jones, B.L., Nordlund, L.M., 2019. Global challenges for seagrass conservation. Ambio 48, 801–815. https://doi.org/10.1007/s13280-018-1115-y

Vásquez-Elizondo, R.M., Legaria-Moreno, L., Pérez-Castro, M.Á., Krämer, W.E., Scheufen, T., Iglesias-Prieto, R., Enríquez, S., 2017. Absorptance determinations on multicellular tissues. Photosynth. Res. 132, 311–324. https://doi.org/10.1007/s11120-017-0395-6

Venegas, K., 2019. Distribución espacio-temporal y efecto de la temperatura en praderas de P*hyllospadix scouleri* en tres localidades de B.C.S. Tesis de Doctorado. Universidad Autónoma de Baja California Sur.

Vivanco-Bercovich, M., Belando-Torrentes, M.D., Figueroa-Burgos, M.F., Ferreira-Arrieta, A., Macías-Carranza, V., García-Pantoja, J.A., Cabello-Pasini, A., Samperio-Ramos, G., Cruz-López, R., Sandoval-Gil, J.M., 2022. Combined effects of marine heatwaves and reduced light on the physiology and growth of the surfgrass *Phyllospadix torreyi* from Baja California, Mexico. Aquat. Bot. 178, 103488. https://doi.org/10.1016/j.aquabot.2021.103488

Waycott, M., Duarte, C.M., Carruthers, T.J.B., Orth, R.J., Dennison, W.C., Olyarnik, S., Calladine, A., Fourqurean, J.W., Heck, K.L., Hughes, A.R., Kendrick, G.A., Kenworthy, W.J., Short, F.T., Williams, S.L., 2009. Accelerating loss of seagrasses across the globe threatens coastal ecosystems. Proc. Natl. Acad. Sci. 106, 12377–12381. https://doi.org/10.1073/pnas.0905620106

Wei, X., Li, K., Kilpatrick, T., Wang, M., Xie, S., 2021. Large-scale conditions for the record-setting southern california marine heatwave of August 2018. Geophys. Res. Lett. 48. https://doi.org/10.1029/2020GL091803

Woodson, C.B., Eerkes-Medrano, D.I., Flores-Morales, A., Foley, M.M., Henkel, S.K., Hessing-Lewis, M., Jacinto, D., Needles, L., Nishizaki, M.T., O'Leary, J., Ostrander, C.E., Pespeni, M., Schwager, K.B., Tyburczy, J.A., Weersing, K.A., Kirincich, A.R., Barth, J.A., McManus, M.A., Washburn, L., 2007. Local diurnal upwelling driven by sea breezes in northern Monterey Bay. Cont. Shelf Res. 27, 2289–2302. https://doi.org/10.1016/j.csr.2007.05.014

Zieman, J.C., 1974. Methods for the study of the growth and production of turtle grass, *Thalassia testudinum* König. Aquaculture 4, 139–143.

## 7. Figure legends

**Figure 1.** The donor meadow of *Phyllospadix scouleri* is located at Todos Santos Island, Baja California, Mexico (A, B), where the seawater temperature was monitored during two years prior to the experiment using submergible sensors with logging intervals of 15 minutes. The figure C presents the daily mean (black line), daily minimum (blue line) and daily maximum (red line) temperatures from sensors data, as well as the satellite SST data (dotted line), and the marine heatwave periods (black stripes) for the same site. SST data was retrieved from NOAA (High Resolution SST data, http://www.esrl.noaa.gov/psd/), and MHWs data from the "Marine heatwave tracker" (Schegel, et al., 2020). Figure D represents the seawater temperature recorded at each experimental treatment (i.e., Control, HW-1, and HW-2) along the acclimation, heatwave, and recovery periods. Biological descriptors were determined before the acclimation (initial conditions), and at the end of the heatwave and recovery periods (T-1 and T-2, respectively), as indicated by the white dots. Shades of gray on the background indicate MHW classification according to Hobday et al. (2018), which is based on the seawater temperature climatology (dotted gray line).

**Figure 2. Parameters derived from photosynthesis-irradiance curves** determined for *P. scouleri* in response to three temperature treatments: two simulated MHWs with different intensities (i.e., HW-1: $T_{mean}$ = 23.5°C, $T_{max}$ = 25°C; and HW-2: $T_{mean}$ = 26.5°C, $T_{max}$ = 28°C) and one control treatment (i.e., C: $T_{mean}$ = 18.5°C, $T_{max}$ = 20°C). Descriptors were determined at the end of the heatwaves (i.e., T-1), and after recovery periods (i.e., T-2). Values are means and standard errors (n = 4). The significance of the main effects from Treatment (Trt., levels: HW-1,

HW-2) and Time (levels: T-1, T-2) and their interaction term (Two-way ANOVA) is indicated at the top-left corner of each graph. In case of significant effect from Treatment (Trt., $p < 0.05$), upper case letters at the base of the left bars indicate significant differences between treatments. For complete results, see Table SM 5. (A) Net-$P_{max}$: Net maximum photosynthetic rate, (B) Gross- $P_{max}$: Gross maximum photosynthetic rate, (C) α: Photosynthetic efficiency, (D) R: Respiration rate, (E) $E_k$: Saturation Irradiance, (F) $E_c$: Compensation Irradiance.

**Figure 3. Chlorophyll *a* fluorescence parameters** measured in *P. scouleri* in response to three temperature treatments: two simulated MHWs with different intensities (i.e., HW-1: $T_{mean}$ = 23.5°C, $T_{max}$ = 25°C; and HW-2: $T_{mean}$ = 26.5°C, $T_{max}$ = 28°C) and one control treatment (i.e., C: $T_{mean}$ = 18.5°C, $T_{max}$ = 20°C). Descriptors were determined at the end of the heatwaves (i.e., T-1), and after recovery periods (i.e., T-2). Values are means and standard errors (n = 4). The significance of the main effects from Treatment (Trt., levels: HW-1, HW-2) and Time (levels: T-1, T-2) and their interaction term (Two-way ANOVA) is indicated at the top-left corner of each graph. In case of significant effect from Treatment (Trt., $p < 0.05$), upper case letters at the base of the left bars indicate significant differences between each treatment. In case of significant interaction term (Time X Trt., $p < 0.05$), lower case letters over the bars indicate significant differences from paired comparisons (Tukey´s HSD post-hoc test). For complete results, see Table SM 5. (A) $F_v/F_m$: Maximum quantum yield, (B) NPQ: Non-photochemical quenching, (C) Basal fluorescence, (D) Maximum fluorescence, (E) $\Phi_{PSII}$: Effective quantum yield, (F) ETR: Electron transport rate.

**Figure 4. Leaf pigment content** determined in *P. scouleri* in response to three temperature treatments: two simulated MHWs with different intensities (i.e., HW-1: $T_{mean}$ = 23.5°C, $T_{max}$ = 25°C; and HW-2: $T_{mean}$ = 26.5°C, $T_{max}$ = 28°C) and one control treatment (i.e., C: $T_{mean}$ = 18.5°C, $T_{max}$ = 20°C). Descriptors were determined at the end of the heatwaves (i.e., T-1), and after recovery periods (i.e., T-2). Values are means and standard errors (n = 4). The significance of the main effects from Treatment (Trt., levels: HW-1, HW-2) and Time (levels: T-1, T-2) and their interaction term (Two-way ANOVA) is indicated at the top-left corner of each graph. In case of significant effect from Treatment (Trt., $p < 0.05$), upper case letters at the base of the left bars indicate significant differences between each treatment. In case of significant interaction term (Time X Trt., $p < 0.05$), lower case letters over the bars indicate significant differences from paired comparisons (Tukey´s HSD post-hoc test). For complete results, see Table SM 5. (A) Chl. *a*: Chlorophyll *a* content, (B) Chl. *b*: Chlorophyll *b* content, (C) Chl. b/a ratio: Chlorophyll *b/a* ratio, (D) Carot.: Carotenoids content.

**Figure 5. Total phenolic content (A), Total antioxidant capacity (B) and Lipid peroxidation (C)** determined in *P. scouleri* leaves in response to three temperature treatments: two simulated MHWs with different intensities (i.e., HW-1: $T_{mean}$ = 23.5°C, $T_{max}$ = 25°C; and HW-2: $T_{mean}$ = 26.5°C, $T_{max}$ = 28°C) and one control treatment (i.e., C: $T_{mean}$ = 18.5°C, $T_{max}$ = 20°C). Descriptors were determined at the end of the heatwaves (i.e., T-1), and after recovery periods (i.e., T-2). Values are means and standard errors (n = 4). The significance of the main effects from Treatment (Trt., levels: HW-1, HW-2) and Time (levels: T-1, T-2) and their interaction term (Two-way ANOVA) is indicated at the top-left corner of each graph. In case of significant effect from Treatment (Trt., $p < 0.05$), upper case letters at the base of the left bars indicate significant

differences between each treatment. In case of significant interaction term (Time X Trt., $p < 0.05$), lower case letters over the bars indicate significant differences from paired comparisons (Tukey´s HSD post-hoc test). For complete results, see Table SM 5.

**Figure 6. Non-structural carbohydrates (A), relative growth rate (B) and daily productivity (C)** determined in *P. scouleri* leaves in response to three temperature treatments: two simulated MHWs with different intensities (i.e., HW-1: $T_{mean}$ = 23.5°C, $T_{max}$ = 25°C; and HW-2: $T_{mean}$ = 26.5°C, $T_{max}$ = 28°C) and one control treatment (i.e., C: $T_{mean}$ = 18.5°C, $T_{max}$ = 20°C). Descriptors were determined at the end of the heatwaves (i.e., T-1), and after recovery periods (i.e., T-2). Values are means and standard errors (n = 4). The significance of the main effects from Treatment (Trt., levels: HW-1, HW-2) and Time (levels: T-1, T-2) and their interaction term (Two-way ANOVA) is indicated at the top-left corner of each graph. In case of significant effect from Treatment (Trt., $p < 0.05$), upper case letters at the base of the left bars indicate significant differences between each treatment. In case of significant interaction term (Time X Trt., $p < 0.05$), lower case letters over the bars indicate significant differences from paired comparisons (Tukey´s HSD post-hoc test). For complete results, see Table SM 5.

**Figure 7.** Main physiological responses of surfgrasses experimentally exposed to different levels of warming. The data originates from this study (HW-1: 22 - 25°C, HW-2: 25 - 28°C) and two other experimental studies conducted in the same region (Todos Santos Bay, B.C., Mexico). The responses enclosed in the dotted rectangle refer to *P. torreyi* plants exposed to a 25°C MHW (Vivanco-Bercovich et al., 2022). The dashed line contours the responses from *P. scouleri* to a

24°C MHW reported in Vivanco-Bercovich et al. (2023, *in preparation*). The temperature scale is tagged with different marks related to the regional thermal regime.

## 8. Figures

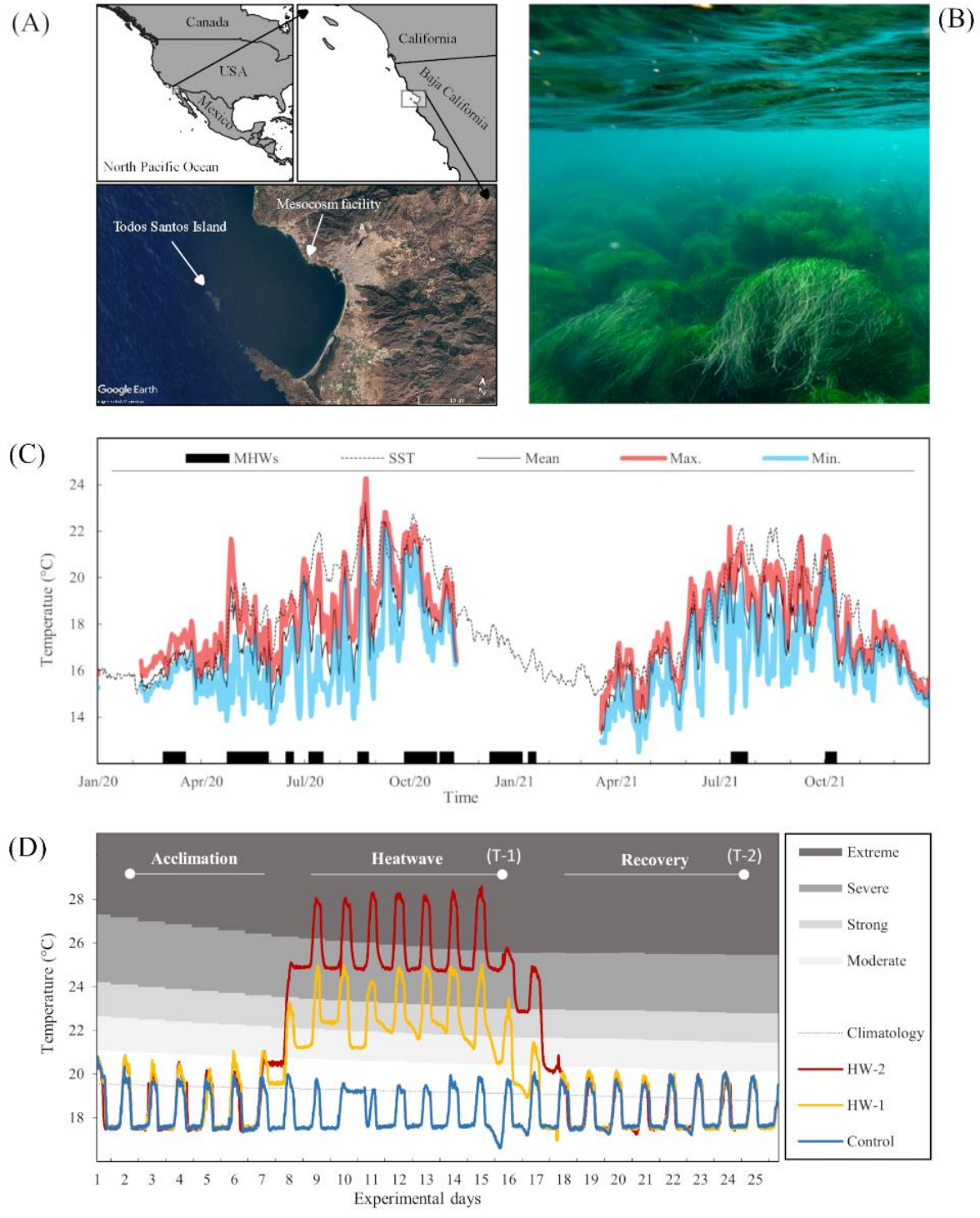
(A)
Canada
USA
Mexico
North Pacific Ocean
California
Baja California
Mesocosm facility
Todos Santos Island
Google Earth
(B)
(C)
MHWs
SST
Mean
Max.
Min.
Temperatue (°C)
Jan/20
Apr/20
Jul/20
Oct/20
Jan/21
Apr/21
Jul/21
Oct/21
Time
(D)
Acclimation
Heatwave
(T-1)
Recovery
(T-2)
Temperature (°C)
Experimental days
Extreme
Severe
Strong
Moderate
Climatology
HW-2
HW-1
Control

Figure 1

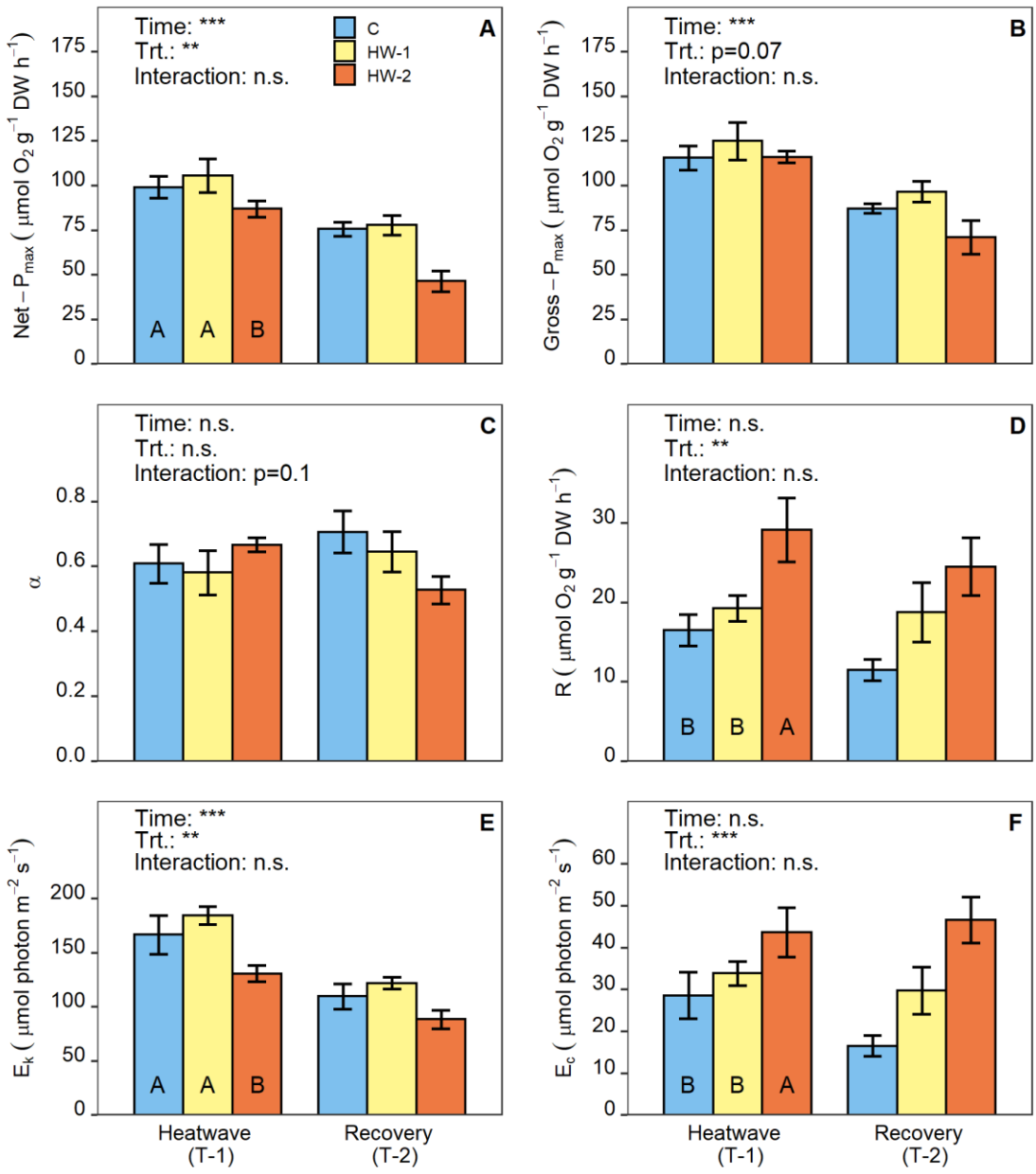


Figure 2

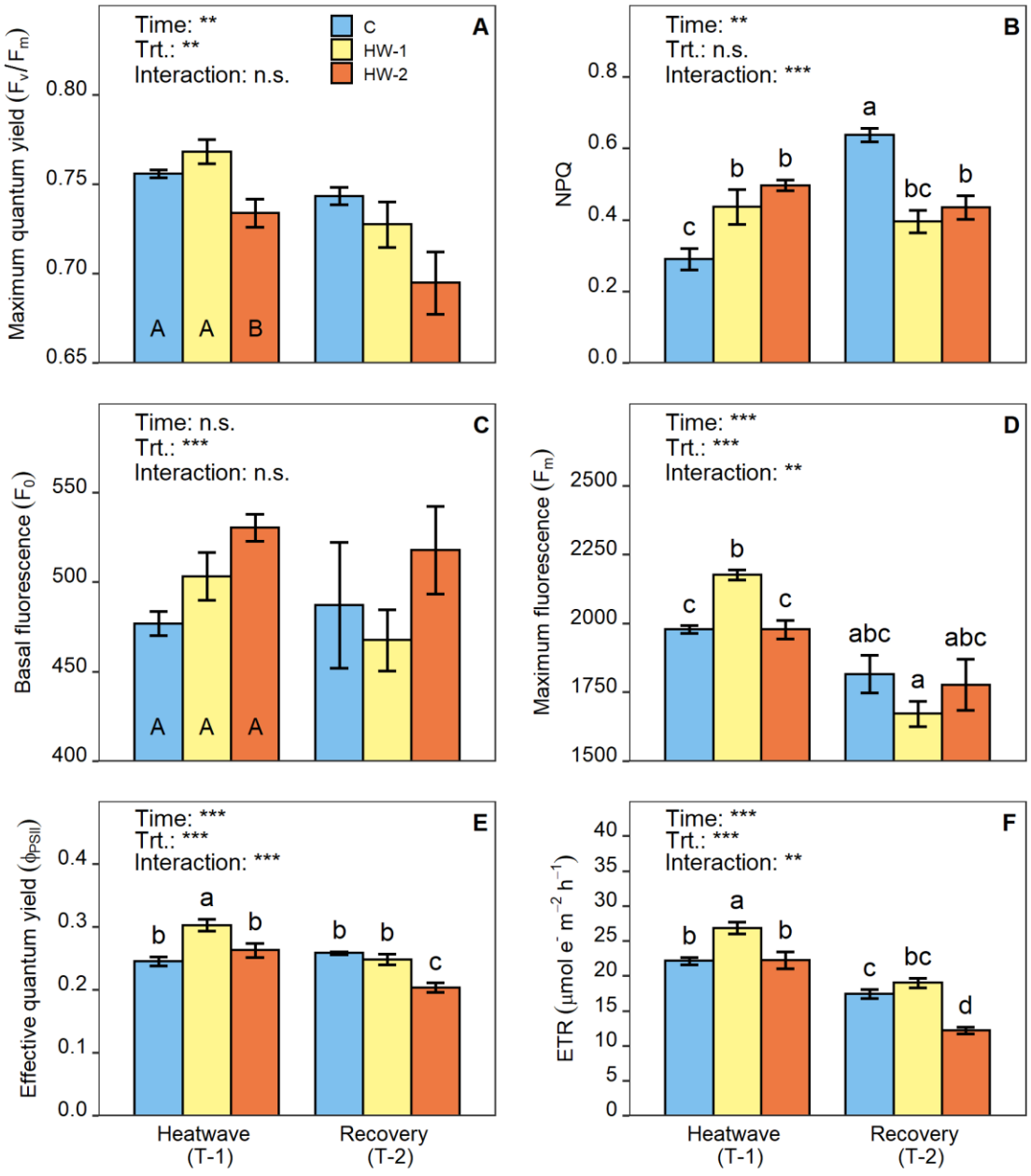
Time: **
Trt.: **
Interaction: n.s.
C
HW-1
HW-2
A
Maximum quantum yield ($F_v/F_m$)
0.80
0.75
0.70
0.65
A A B
Time: **
Trt.: n.s.
Interaction: ***
B
NPQ
0.8
0.6
0.4
0.2
0.0
c b b a bc b
Time: n.s.
Trt.: ***
Interaction: n.s.
C
Basal fluorescence ($F_0$)
550
500
450
400
A A A
Time: ***
Trt.: ***
Interaction: **
D
Maximum fluorescence ($F_m$)
2500
2250
2000
1750
1500
c b c abc a abc
Time: ***
Trt.: ***
Interaction: ***
E
Effective quantum yield ($\phi_{PSII}$)
0.4
0.3
0.2
0.1
0.0
b a b b b c
Time: ***
Trt.: ***
Interaction: **
F
ETR (µmol $e^-$ $m^{-2}$ $h^{-1}$)
40
35
30
25
20
15
10
5
0
b a b c bc d
Heatwave (T-1)
Recovery (T-2)
Heatwave (T-1)
Recovery (T-2)

Figure 3

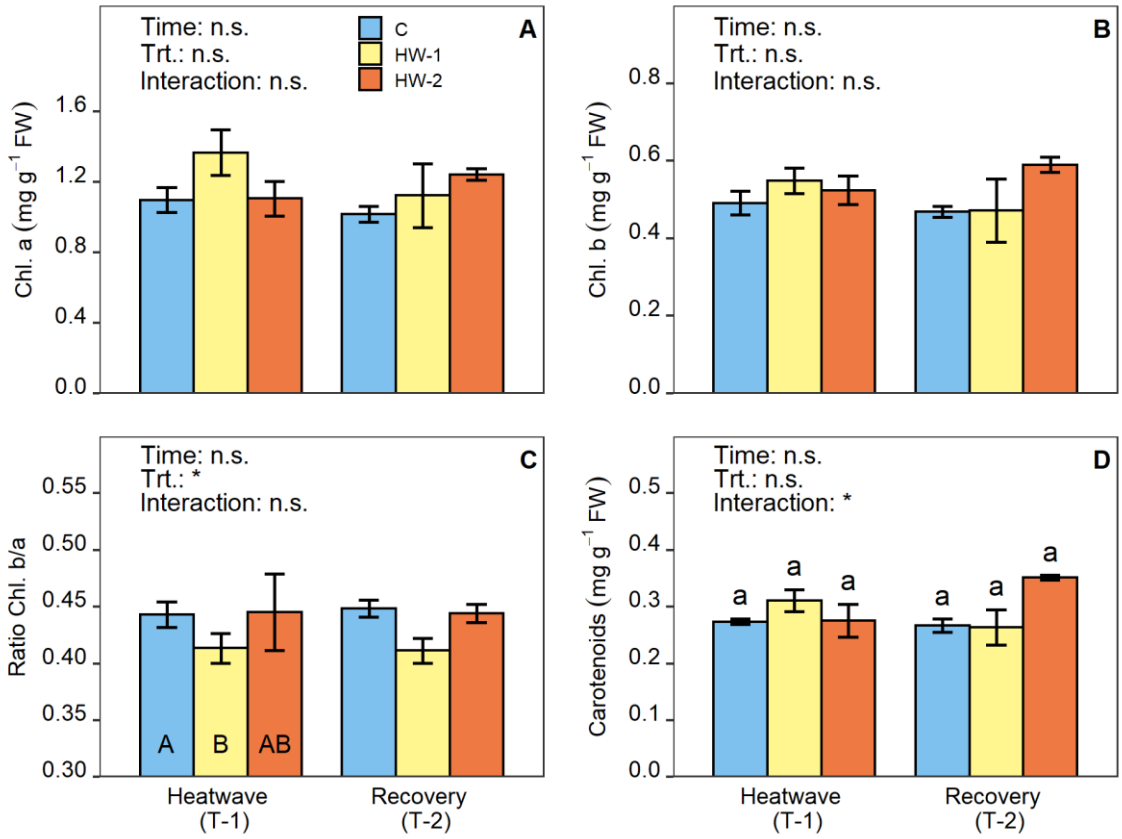
Time: n.s.
Trt.: n.s.
Interaction: n.s.
C
HW-1
HW-2
A
Chl. a (mg g$^{-1}$ FW)
1.6
1.2
0.8
0.4
0.0
B
Chl. b (mg g$^{-1}$ FW)
0.8
0.6
0.4
0.2
0.0
Time: n.s.
Trt.: *
Interaction: n.s.
C
Ratio Chl. b/a
0.55
0.50
0.45
0.40
0.35
0.30
A
B
AB
Time: n.s.
Trt.: n.s.
Interaction: *
D
Carotenoids (mg g$^{-1}$ FW)
0.5
0.4
0.3
0.2
0.1
0.0
a
a
a
a
a
a
Heatwave
(T-1)
Recovery
(T-2)

Figure 4.

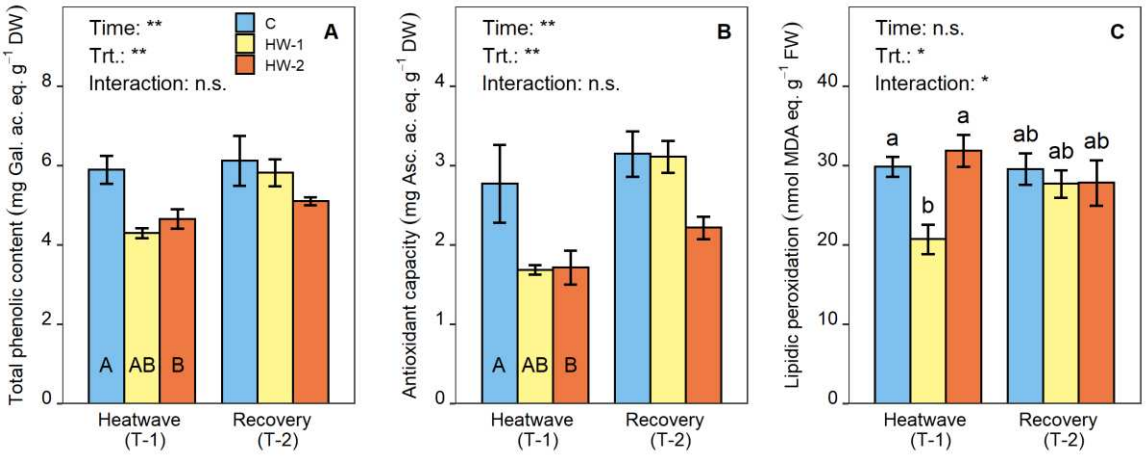
Time: **
Trt.: **
Interaction: n.s.
C
HW-1
HW-2
A
Total phenolic content (mg Gal. ac. eq. g$^{-1}$ DW)
A AB B
Heatwave (T-1)
Recovery (T-2)
Time: **
Trt.: **
Interaction: n.s.
B
Antioxidant capacity (mg Asc. ac. eq. g$^{-1}$ DW)
A AB B
Heatwave (T-1)
Recovery (T-2)
Time: n.s.
Trt.: *
Interaction: *
C
Lipidic peroxidation (nmol MDA eq. g$^{-1}$ FW)
a b a ab ab ab
Heatwave (T-1)
Recovery (T-2)

Figure 5.

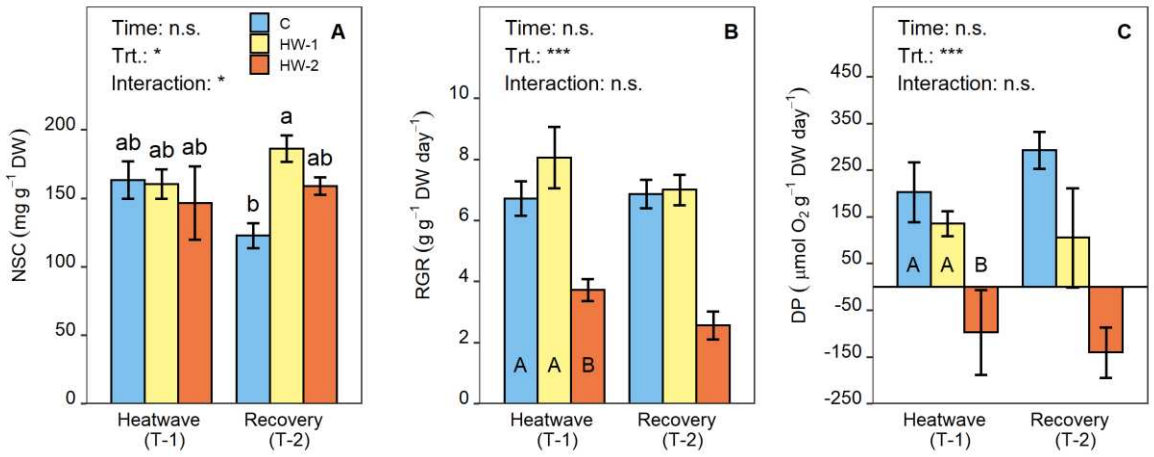
Time: n.s.
Trt.: *
Interaction: *
C
HW-1
HW-2
A
NSC (mg g$^{-1}$ DW)
ab ab ab
b
a
ab
Heatwave (T-1)
Recovery (T-2)
Time: n.s.
Trt.: ***
Interaction: n.s.
B
RGR (g g$^{-1}$ DW day$^{-1}$)
A A B
Heatwave (T-1)
Recovery (T-2)
Time: n.s.
Trt.: ***
Interaction: n.s.
C
DP ( µmol $O_2$ g$^{-1}$ DW day$^{-1}$)
A A B
Heatwave (T-1)
Recovery (T-2)

Figure 6.

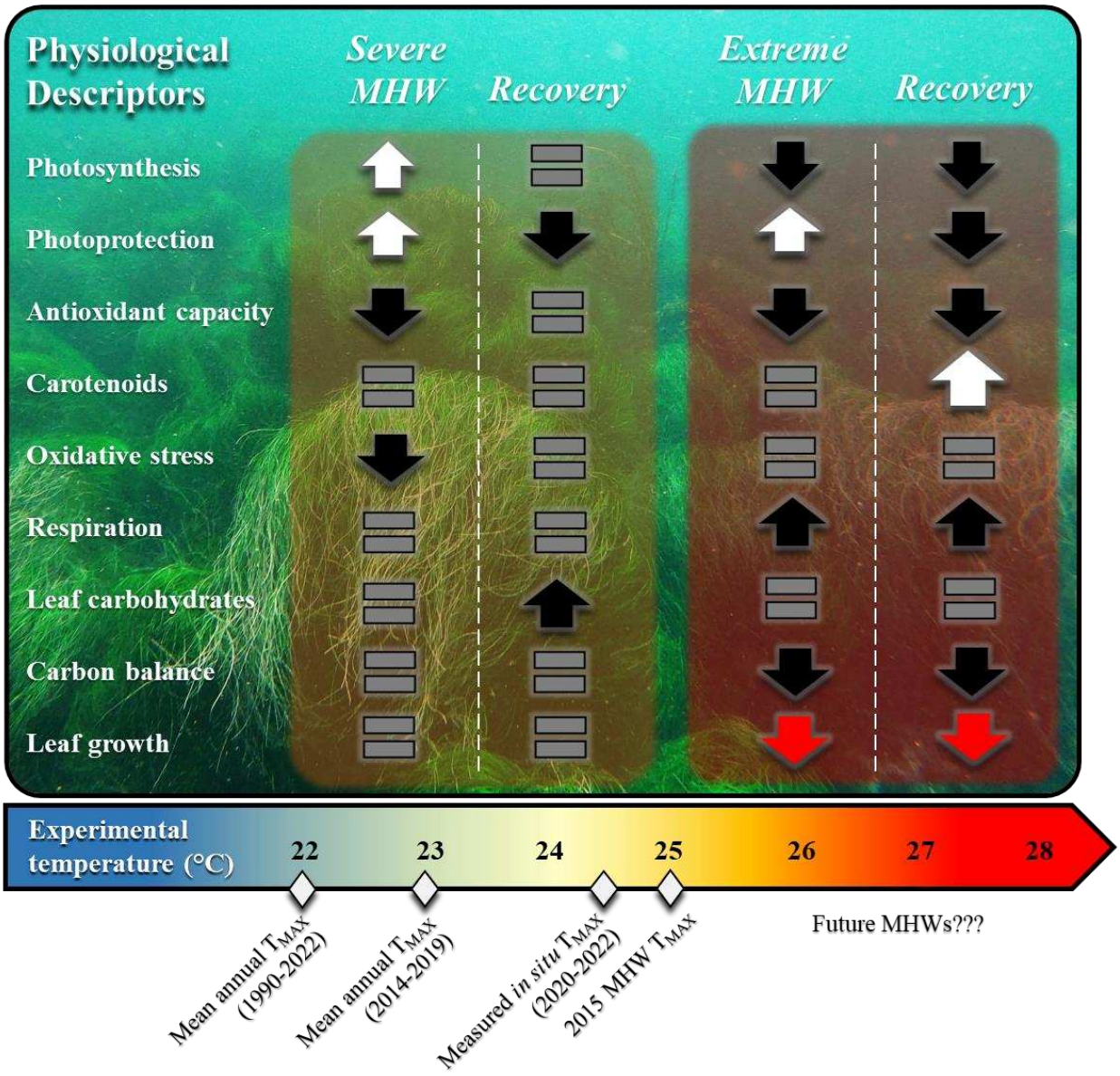
Physiological Descriptors
Severe MHW
Recovery
Extreme MHW
Recovery
Photosynthesis
Photoprotection
Antioxidant capacity
Carotenoids
Oxidative stress
Respiration
Leaf carbohydrates
Carbon balance
Leaf growth
Experimental temperature (°C)
22
23
24
25
26
27
28
Mean annual TMAX (1990-2022)
Mean annual TMAX (2014-2019)
Measured in situ TMAX (2020-2022)
2015 MHW TMAX
Future MHWs???

Figure. 7

## *9.* Supplementary material

Figure SM 1. Sea surface temperature data from 1990 to 2021 at Todos Santos Island region (Baja California, Mexico). Data retrieved from NOAA (High Resolution SST data, http://www.esrl.noaa.gov/psd/).

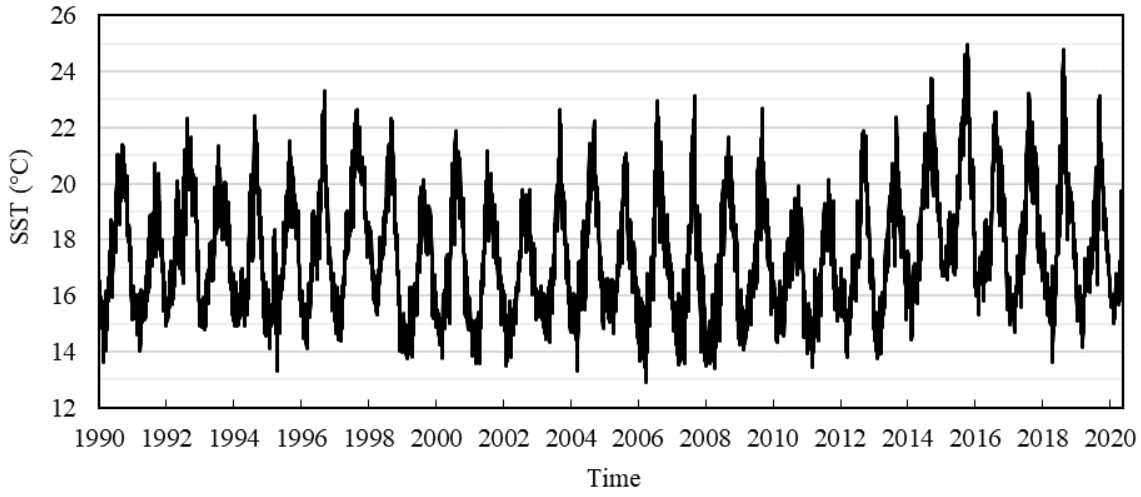

Figure SM 2. Characteristics of the MHWs that were registered at the donor meadow location (Todos Santos Island, Baja California, Mexico) for this study between the years 1982 – 2020. (A) Frequency histogram of MHWs maximum intensity; (B) Frequency histogram of MHWs duration. Data were extracted from Marine Heatwave Tracker (Schlegel, 2020) and the selected pixel was: Lon. 116,875; Lat. 31,875.

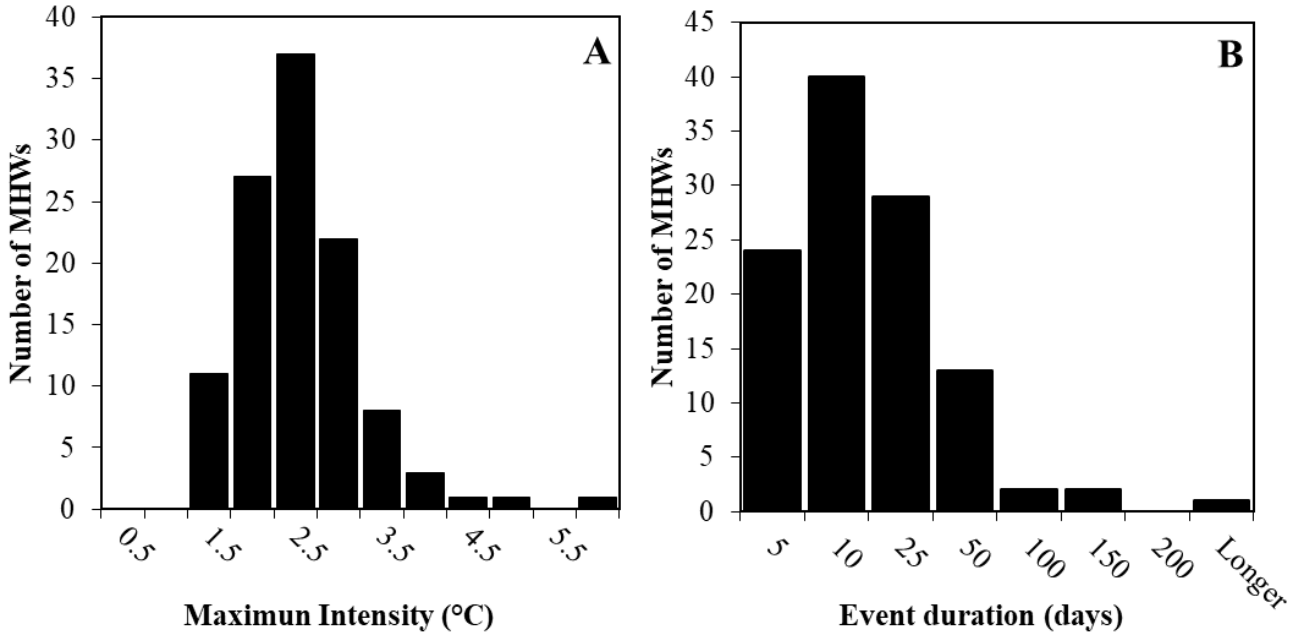

Figure SM 3. Correlation plots between seawater surface temperature SST (from NOAA High Resolution SST data, http://www.esrl.noaa.gov/psd/) and (A) daily minimum temperature, (B) mean temperature and (C) maximum temperature measured *in situ* using submersible sensors (Onset-HOBO MX2202) in the donor surfgrass meadow for this study (Todos Santos Island, Baja California, Mexico).

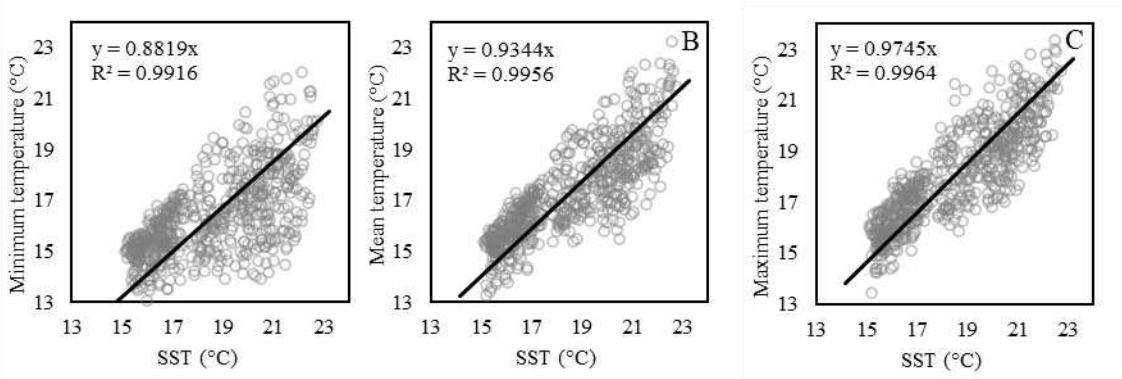

Figure SM 4. Frequency histogram for the daily variation of temperature (i.e., $T_{max} - T_{min}$) measured *in situ* with submersible sensors (Onset-HOBO MX2202) in the donor surfgrass meadow for this study (Todos Santos Island, Baja California, Mexico) during the period 2020-2021.

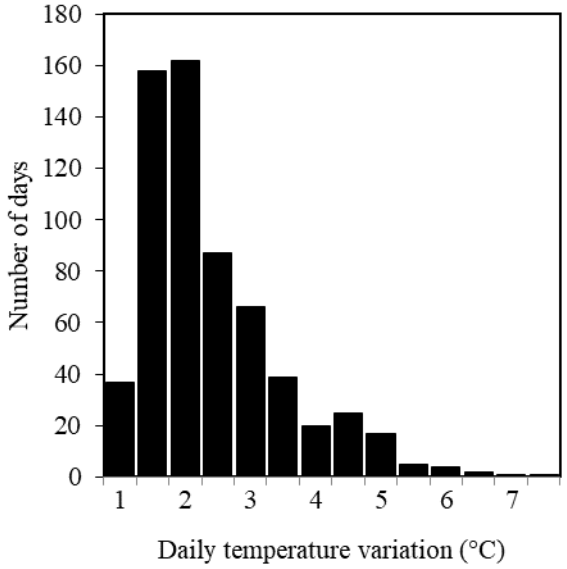

Table SM 5. Results of 2-way Anova (left block) where the main and interactive effects of the factors Treatment ("Trt.", 3 levels: C-Control, HW-1 and HW-2) and Time ("Time", 2 levels: T-1 Heatwave and T-2 Recovery) were tested for each biological descriptor. The individual means ± standard errors, and the significant differences ($p < 0.05$, Tukey`s HSD post-hoc tests) are presented in the right block. Significant individual differences among treatments (in case of significant main effect from trt.) are expressed by uppercase letters beside treatment names. Individual differences among all means (in case of significant interaction term) are expressed by lowercase letters beside individual means. Superscripted "Het." beside variables names indicates heteroscedastic data, for which the White´s adjustment was applied to the analysis of variance, and the Games-Howell test substituted Tukey´s HSD test. * $p < 0.05$, ** $p < 0.01$, *** $p < 0.001$.

| **Variables** | **2-Way Anova** | | | **Individual means and paired differences** | | |
|---|---|---|---|---|---|---|
| | Effect | F | p | | T-1 (Heatwave) | T-2 (Recovery) |
| **Net-$P_{max}$** | Trt. | 37.07 | *** | C (A) | 99.06 ± 6.14 | 75.69 ± 3.87 |
| | Time | 9.464 | ** | HW-1 (A) | 105.7 ± 9.36 | 77.89 ± 5.52 |
| | Trt.*Time | 1.04 | n.s. | HW-2 (B) | 86.98 ± 4.62 | 46.54 ± 5.86 |
| **Gross-$P_{max}$** | Trt. | 34.927 | *** | C | 115.57 ± 6.78 | 87.19 ± 2.7 |
| | Time | 3.007 | 0.07 | HW-1 | 124.96 ± 10.48 | 96.67 ± 5.77 |
| | Trt.*Time | 0.947 | n.s. | HW-2 | 116.15 ± 3.17 | 71.06 ± 9.48 |
| **α** | Trt. | 0.029 | n.s. | C | 0.61 ± 0.06 | 0.71 ± 0.06 |
| | Time | 0.635 | n.s. | HW-1 | 0.58 ± 0.07 | 0.65 ± 0.06 |
| | Trt.*Time | 2.661 | 0.1 | HW-2 | 0.67 ± 0.02 | 0.53 ± 0.04 |
| **R** | Trt. | 2.005 | n.s. | C (B) | 16.51 ± 1.99 | 11.5 ± 1.35 |
| | Time | 9.78 | ** | HW-1 (B) | 19.27 ± 1.63 | 18.78 ± 3.71 |
| | Trt.*Time | 0.368 | n.s. | HW-2 (A) | 29.17 ± 4 | 24.52 ± 3.63 |
| **$E_k$** | Trt. | 38.006 | *** | C (A) | 166.68 ± 17.97 | 109.78 ± 11.5 |
| | Time | 8.573 | ** | HW-1 (A) | 184.26 ± 8.26 | 122.07 ± 5.63 |
| | Trt.*Time | 0.464 | n.s. | HW-2 (B) | 130.78 ± 7.63 | 88.47 ± 8.48 |
| **$E_c$** | Trt. | 1.24 | n.s. | C (B) | 28.59 ± 5.56 | 16.58 ± 2.43 |
| | Time | 10.971 | *** | HW-1 (B) | 33.85 ± 2.91 | 29.76 ± 5.56 |
| | Trt.*Time | 1.182 | n.s. | HW-2 (A) | 43.72 ± 5.91 | 46.6 ± 5.47 |
| **$F_v/F_m$** | Trt. | 14.279 | ** | C (A) | 0.76 ± 0 | 0.74 ± 0 |
| | Time | 7.898 | ** | HW-1 (A) | 0.77 ± 0.01 | 0.73 ± 0.01 |

| | | | | | | |
|---|---|---|---|---|---|---|
| | Trt.*Time | 1.272 | n.s. | HW-2 (B) | 0.73 ± 0.01 | 0.69 ± 0.02 |
| **NPQ** | Trt. | 10.199 | ** | C | 0.29 ± 0.03 (c) | 0.64 ± 0.02 (a) |
| | Time | 1.628 | n.s. | HW-1 | 0.44 ± 0.05 (b) | 0.4 ± 0.03 (bc) |
| | Trt.*Time | 27.076 | *** | HW-2 | 0.5 ± 0.02 (b) | 0.44 ± 0.03 (b) |
| **$F_0$ Het.** | Trt. | 1.263 | n.s. | C (A) | 476.89 ± 6.77 | 487.25 ± 35.28 |
| | Time | 11.092 | *** | HW-1 (A) | 503.27 ± 13.35 | 467.7 ± 17.15 |
| | Trt.*Time | 0.492 | n.s. | HW-2 (A) | 530.53 ± 7.54 | 518.05 ± 24.58 |
| **$F_m$ Het.** | Trt. | 70.167 | *** | C | 1978.5 ± 13.93 (c) | 1816.66 ± 68.98 (abc) |
| | Time | 24.62 | *** | HW-1 | 2176.75 ± 17.82 (b) | 1672.55 ± 46.35 (a) |
| | Trt.*Time | 7.109 | ** | HW-2 | 1978.33 ± 34.1 (c) | 1777.73 ± 92.74 (abc) |
| **$\Phi_{PSII}$** | Trt. | 25.243 | *** | C | 0.25 ± 0.01 (b) | 0.26 ± 0 (b) |
| | Time | 13.306 | *** | HW-1 | 0.3 ± 0.01 (a) | 0.25 ± 0.01 (b) |
| | Trt.*Time | 12.045 | *** | HW-2 | 0.26 ± 0.01 (b) | 0.2 ± 0.01 (c) |
| **ETR** | Trt. | 148.013 | *** | C | 22.17 ± 0.5 (b) | 17.46 ± 0.63 (c) |
| | Time | 28.368 | *** | HW-1 | 26.89 ± 0.84 (a) | 19.03 ± 0.68 (bc) |
| | Trt.*Time | 6.212 | ** | HW-2 | 22.27 ± 1.19 (b) | 12.25 ± 0.47 (d) |
| **Chl. *a*** | Trt. | 0.526 | n.s. | C | 1.1 ± 0.07 | 1.02 ± 0.04 |
| | Time | 1.599 | n.s. | HW-1 | 1.37 ± 0.13 | 1.12 ± 0.18 |
| | Trt.*Time | 1.628 | n.s. | HW-2 | 1.11 ± 0.1 | 1.24 ± 0.03 |
| **Chl. *b*** | Trt. | 0.269 | n.s. | C | 0.49 ± 0.03 | 0.47 ± 0.01 |
| | Time | 1.751 | n.s. | HW-1 | 0.55 ± 0.03 | 0.47 ± 0.08 |
| | Trt.*Time | 1.848 | n.s. | HW-2 | 0.52 ± 0.04 | 0.59 ± 0.02 |
| **Chl. *b/a* ratio Het.** | Trt. | 0.031 | n.s. | C (A) | 0.44 ± 0.01 | 0.45 ± 0.01 |
| | Time | 4.254 | * | HW-1 (B) | 0.41 ± 0.01 | 0.41 ± 0.01 |
| | Trt.*Time | 0.047 | n.s. | HW-2 (AB) | 0.45 ± 0.03 | 0.44 ± 0.01 |
| **Carotenoids** | Trt. | 0.182 | n.s. | C | 0.27 ± 0 (a) | 0.27 ± 0.01 (a) |
| | Time | 2.436 | n.s. | HW-1 | 0.31 ± 0.02 (a) | 0.26 ± 0.03 (a) |
| | Trt.*Time | 5.016 | * | HW-2 | 0.28 ± 0.03 (a) | 0.35 ± 0 (a) |
| **Phenolic content Het.** | Trt. | 10.576 | ** | C (A) | 5.9 ± 0.35 | 6.12 ± 0.63 |
| | Time | 6.947 | ** | HW-1 (AB) | 4.3 ± 0.13 | 5.82 ± 0.34 |
| | Trt.*Time | 2.398 | n.s. | HW-2 (B) | 4.66 ± 0.24 | 5.1 ± 0.1 |
| **Antioxidant capacity** | Trt. | 12.276 | ** | C (A) | 2.77 ± 0.49 | 3.15 ± 0.29 |
| | Time | 6.898 | ** | HW-1 (AB) | 1.69 ± 0.06 | 3.11 ± 0.2 |
| | Trt.*Time | 2.283 | n.s. | HW-2 (B) | 1.72 ± 0.21 | 2.22 ± 0.14 |
| **Lipid peroxidation** | Trt. | 0.292 | n.s. | C | 29.86 ± 1.24 (a) | 29.58 ± 1.98 (ab) |
| | Time | 5.111 | * | HW-1 | 20.75 ± 1.85 (b) | 27.71 ± 1.72 (ab) |
| | Trt.*Time | 3.875 | * | HW-2 | 31.86 ± 2.02 (a) | 27.84 ± 2.86 (ab) |
| **NSCs Het.** | Trt. | 0.015 | n.s. | C | 163.52 ± 13.53 (ab) | 122.9 ± 9.07 (b) |
| | Time | 5.323 | * | HW-1 | 160.63 ± 10.83 (ab) | 186.49 ± 9.69 (a) |
| | Trt.*Time | 3.588 | * | HW-2 | 146.75 ± 26.75 (ab) | 159.09 ± 6.36 (ab) |
| **Daily Productivity** | Trt. | 1.979 | n.s. | C (A) | 6.73 ± 0.56 | 6.87 ± 0.47 |
| | Time | 30.962 | *** | HW-1 (A) | 8.06 ± 1.01 | 7.01 ± 0.5 |

| | | | | | | |
|---|---|---|---|---|---|---|
| | Trt.*Time | 0.726 | n.s. | HW-2 (B) | 3.72 ± 0.36 | 2.58 ± 0.46 |
| **RGR** | Trt. | 0.009 | n.s. | C (A) | 203.35 ± 64.35 | 292.93 ± 39.37 |
| | Time | 14.39 | *** | HW-1 (A) | 135.88 ± 27.13 | 105.52 ± 105.85 |
| | Trt.*Time | 0.557 | n.s. | HW-2 (B) | -96.8 ± 91.15 | -139.83 ± 54.06 |

**Abbreviations:** *Net-Pmax: Net maximum photosynthetic capacity; Gross-Pmax: Gross maximum photosynthetic capacity; α: Photosynthetic efficiency; $E_c$: Compensating Irradiance; $E_k$: Saturating irradiance; R: Dark respiration rate; $F_v/F_m$: Maximum photochemical efficiency; NPQ: Non-photochemical quenching; $F_0$: Basal fluorescence; $F_m$: Maximum fluorescence; $\Phi_{PSII}$: Effective photochemical efficiency; ETR: Electron transport rate; Chl. a: Chlorophyll a content; Chl. b: Chlorophyll b content; Chl. b/a ratio: Chlorophyll b/a ratio; NSC: Non-structural carbohydrates; RGR: Relative growth rate;*

Figure SM 6. Photosynthesis (P) x Irradiance (E) curves determined by measuring the evolution of dissolved oxygen in respirometers containing leaf segments while gradually increasing the incident irradiance. Curves were performed for Control, HW-1 and H-2 treatments at two moments: at the end of the warming period (A) and after a recovery phase (B). An additional curve was determined before starting the experiment (gray dotted line, used as reference in both figures). Bars represent standard error (N=4).

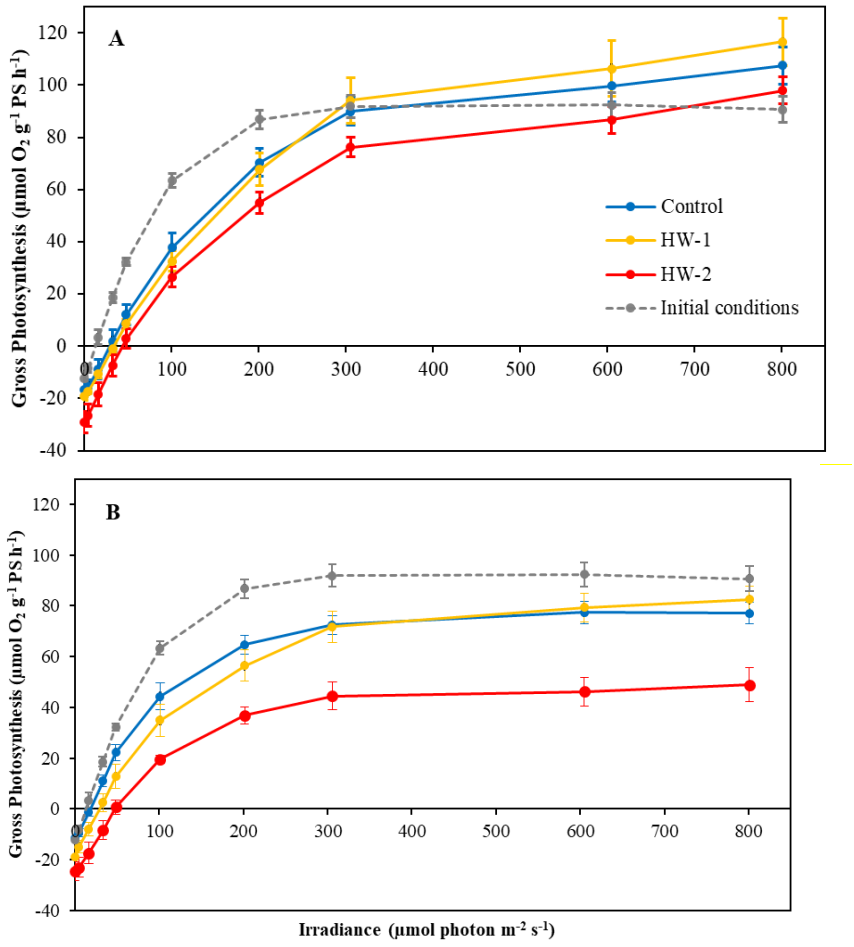

## CONCLUSIONES

- ✓ Los efectos negativos de las OCMs en *Phyllospadix* podrían ser intensificados si su ocurrencia coincide con condiciones de reducción de irradiancia, circunstancias que son comunes en la costa de Baja California a causa de florecimientos fitoplanctónicos o por la suspensión de sedimentos debido a tormentas o huracanes.
- ✓ La exposición a OCMs consecutivas – un escenario cada vez más probable debido a los efectos del cambio climático - podría generar un debilitamiento fisiológico progresivo en *Phyllospadix*.
- ✓ Algunos de efectos de estrés observados en *Phyllospadix* bajo OCMs se presentaron cuando se restablecieron las condiciones de temperatura, y no durante la exposición misma a la OCM. Por lo tanto, la inclusión de fases experimentales de recuperación en trabajos de experimentación es crucial para obtener un conocimiento más robusto acerca de la termo-tolerancia y resiliencia de la planta.
- ✓ Durante la exposición de *Phyllospadix* a una OCM de hasta 25°C (catalogada como "severa"), es posible que no se observen alteraciones mayores en sus tasas fotosintéticas y respiratorias, ni en su balance de carbono. Sin embargo, por lo dicho en el punto anterior, esto no significa que no esté ocurriendo un debilitamiento fisiológico.
- ✓ Una OCM con temperatura promedio de 26.5°C (catalogada como "extrema") podría afectar la fisiología de *Phyllospadix* a tal punto de comprometer su crecimiento. Por lo tanto, las OCMs más intensas pronosticadas para el futuro escenario de cambio climático pueden representar una amenaza para la supervivencia de *Phyllospadix* y los ecosistemas que sustentan.

**Futuras direcciones de investigación**

A lo largo de la ejecución de este proyecto se identificaron diversas lagunas del conocimiento acerca de *Phyllospadix*, las cuales escapan del enfoque de este estudio y podrían ser abordadas en trabajos futuros.

- ✓ En mi perspectiva, lo más urgente seria iniciar y mantener programas de monitoreos en praderas de *Phyllospadix* para registrar e investigar los efectos de la incidencia de OCMs *in situ*. Sería especialmente importante enfocar en poblaciones en el límite de distribución latitudinal de estas especies (para identificar posibles retracciones de su distribución) y en praderas ya expuestas a otros estresores, como vertidos urbanos.
- ✓ También son muy escasos – y necesarios - los trabajos que identifiquen y cuantifiquen los diversos servicios ecosistémicos brindados por las praderas de *Phyllospadix*, y que examinen la susceptibilidad de estos al cambio climático, y a otros estresores naturales y antropogénicos.
- ✓ Para sustentar posibles estrategias de adaptación al cambio climático, sería interesante realizar comparaciones, con respecto a la termo-tolerancia fisiológica, entre *P. scouleri* y *P. torreyi*, y entre poblaciones a lo largo de gradientes batimétricos y latitudinales.
- ✓ En este sentido, también sería relevante investigar la diversidad genética y la estructura de las poblaciones de *Phyllospadix* con el fin de identificar genotipos más termo-tolerantes para utilizar en futuras iniciativas de restauración (p. ej., evolución asistida).